

BMR JOURNAL of Australian Geology & Geophysics



VOLUME 1, NUMBER 1

MARCH 1976



Department of National Resources, Australia

Minister: The Rt Hon. J. D. Anthony, M.P.

Secretary: J. Scully

Bureau of Mineral Resources, Geology and Geophysics

Director: L. C. Noakes

Editor, BMR Journal: J. F. Truswell

The BMR Journal of Australian Geology and Geophysics is a quarterly journal of research and related activities. Contributions are from officers of the BMR, from BMR officers working in collaboration with others, or requested work sponsored by the BMR. In addition to articles the Journal may include shorter notes and discussion of papers published in it. Discussion of papers is invited from anyone.

Annual subscription to the Journal is at the rate of \$10 (Australian). Individual numbers, if available, cost \$3. Subscriptions, etc., made payable to the Receiver of Public Moneys in Australian dollars, should be sent to the Director, Bureau of Mineral Resources, Geology & Geophysics, P. O. Box 378, Canberra, A.C.T. 2601, Australia. The Journal can also be obtained from the offices of the Department of National Resources in Sydney and Melbourne.

Other matters concerning the Journal should be sent to the Director, marked for the attention of the Editor, BMR Journal.



B M R JOURNAL

of Australian Geology and Geophysics

Volume 1, Number 1

March, 1976

AUSTRALIAN GOVERNMENT PUBLISHING SERVICE
CANBERRA 1976

Front cover: The Bureau of Mineral Resources, Geology and Geophysics at Canberra

Photograph: J. E. Zawartko

ISSN 0312-9608

Printed by Kerton Bros (S.A.) Pty Ltd, Edwardstown, S.A.

Preface

This is the first number of a new publication, the BMR Journal of Australian Geology and Geophysics.

Publications of the BMR are all intended to record and present the results of geological and geophysical field, laboratory and observatory investigations, or to provide data on minerals and the mineral industry. Present publications of the organization include Bulletins, usually compiled on completion of major investigations; Reports, in which important preliminary investigations or phases of such investigations, are recorded; and Records, which are the first reporting phase, mostly placed on open file, and available for reference in the State capitals as well as at BMR. Reports are also produced from geophysical observatories. BMR also produces an Annual Review of the Australian Mineral Industry, a Quarterly Review of that industry—in conjunction with the Australian Bureau of Statistics—and a quarterly Petroleum Newsletter. It has also published in summary form a number of company reports resulting from surveys subsidized under the Petroleum Search Subsidy Act.

The Bureau's field activities, in many cases carried out in conjunction with State Geological Surveys, result in the publication of 1:250 000 scale regional geological maps, with Explanatory Notes, and maps at a scale of 1:100 000 for areas mapped in more detail. Maps are also produced to present magnetic, radiometric, seismic and gravity data and both geological and geophysical data contribute to the compilation of regional maps of the continent and the continental margin.

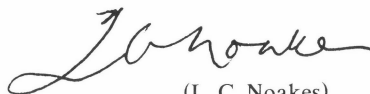
BMR is reviewing aspects of its publication policy; it is, for example, considering micro-publishing, in microfiche form, some of the material currently in the Report and Record series. The introduction of the BMR Journal stems from this review. The Journal is essentially to be a research outlet, but will also chronicle some of the discoveries and developments in the organization; it will reflect in some measure the varying roles and functions of the BMR. The aims of the Journal are clear: to provide a rapid means of publication for important results in a publication for wide distribution. A refereeing system has been established to ensure a high standard.

The Journal will appear quarterly, and will contain articles, shorter notes and discussion. There is provision for news items of significance to be included. Articles and notes will be accepted from: officers of the BMR; co-authors, one of whom is an officer of BMR; and other authors, whose work has been commissioned or sponsored by BMR. Discussion on the other hand is welcome from anybody. It follows that material for the Journal will come principally from those areas where BMR officers are active; mostly these lie in and around Australia, but the Bureau is also active in Antarctica, has officers on secondment to Papua New Guinea and carries out other foreign aid assignments from time to time.

This inaugural number contains articles on earthquake risk in Australia, involving zoning concepts; an account of Cambrian fossils from the Arafura Basin, which revise the Late Proterozoic age attributed to this basin over the last decade; a review of the Cretaceous in the Eromanga and Surat Basins, emphasizing the palaeoenvironments occurring at this time; a report of the use of transient electromagnetism, in which this method is compared with others used in the search for conductive bodies. Also presented are age determination data from The Granites-Tanami region, data of significance in the Precambrian geochronology of north-western Australia; carbonate petrography, and statistical techniques used to distinguish two limestones from the Lennard Shelf in the Canning Basin; and the development of methods for density profiling across elongate topographic features.

The Journal will be an integral part of the BMR's exchange system. It can also be obtained on subscription or, if available, as single numbers.

I feel confident that this Journal will warrant wide recognition as a record of achievement in earth science under the auspices of BMR.



(L. C. Noakes)
Director

Geochronology and related aspects of acid volcanics, associated granites, and other Proterozoic rocks in The Granites-Tanami region, northwestern Australia

R. W. Page, D. H. Blake and M. W. Mahon

Isotopic ages of Proterozoic acid volcanics and associated granitic intrusions in the northeast and southwest part of The Granites-Tanami region are reported and discussed. In the northwest, within The Granites-Tanami Block, the Mount Winnecke Formation, which includes acid volcanics that were probably erupted underwater, is intruded and weakly metamorphosed by the high-level Winnecke Granophyre. The acid volcanics and intrusives have similar major element compositions, and this, together with the field evidence, indicates that they are probably comagmatic. Rb-Sr total rock and mineral data for the Winnecke Granophyre yield an isochron indicating an age of 1802 ± 15 m.y. and an initial $\text{Sr}^{87}/\text{Sr}^{86}$ of 0.7074 ± 0.0036 . Isotopic data for the lavas of the Mount Winnecke Formation give a preferred age of 1808 ± 15 m.y. and an initial $\text{Sr}^{87}/\text{Sr}^{86}$ of 0.7052 ± 0.0038 .

In the southwest, at the western extremity of the Arunta Block, another acid volcanic suite, belonging to the Pollock Hills Formation, is intruded and weakly metamorphosed by the Mount Webb Granite. As in the northeast, the volcanics and intrusives have similar major element compositions, and are considered to be comagmatic. Combining Rb-Sr isotopic data from both the volcanics and intrusives yields an isochron indicating an age of 1526 ± 25 m.y. and an initial $\text{Sr}^{87}/\text{Sr}^{86}$ of 0.711 ± 0.004 . These rocks are appreciably younger than those in the northeast.

The acid igneous rocks in the southwest also postdate three other newly dated granitic units in The Granites-Tanami Block—the Lewis Granite, 1720 ± 8 m.y.; the Slaty Creek Granite, 1770 ± 55 m.y.; and The Granites Granite, 1780 ± 24 m.y.—and are younger than the Gardiner Sandstone, the basal unit of the Birrindudu Group, which unconformably overlies The Granites-Tanami Block.

K-Ar and Rb-Sr ages determined on glauconite from the Gardiner Sandstone show little consistency, due evidently to partial loss of radiogenic daughter products, but a preferred K-Ar age of 1560 ± 20 m.y. is considered a reasonable minimum estimate for the age of sedimentation and diagenesis in the unit.

The Granites-Tanami region was mapped by the Bureau of Mineral Resources and the Geological Survey of Western Australia in the period 1971 to 1973 (Blake, Hodgson & Smith, 1975; Blake, Hodgson & Muhling, 1973; Blake & Towner, 1974; Hodgson, 1974). The region straddles the Northern Territory/Western Australia border northwest of Alice Springs, and is a semi-desert area in which mainly Precambrian rocks are largely covered by superficial Cainozoic deposits. It lies between the Halls Creek Mobile Zone of the Kimberley region to the northwest, the Victoria River Basin to the north and the Arunta Block to the south, which are Precambrian, and is bounded to the west and east respectively by the Phanerozoic Canning and Wiso Basins (Fig. 1).

The oldest rocks exposed in The Granites-Tanami region are metamorphosed sedimentary and volcanic rocks mapped as the Tanami complex. These are correlated with the Halls Creek Group, which crops out in the Halls Creek Mobile Zone (Dow & Gemuts, 1969) and is probably Lower Proterozoic* (Page, 1976, this issue). The Tanami complex is overlain unconformably by Lower Proterozoic sediments and volcanics, and is intruded by granites, some of which are as young as early Carpentarian. The granites and older rocks together make up The Granites-Tanami Block, the basement on which the mainly clastic sediments of the Birrindudu Basin were deposited. The Birrindudu Basin sediments belong to the Birrindudu Group (Blake et al., 1975), the unconformably overlying Redcliff Pound Group (Blake et al., 1973) and their probable correlatives. In the southern part of the area mapped The Granites-Tanami

Block grades into the metamorphics and granites of the Arunta Block.

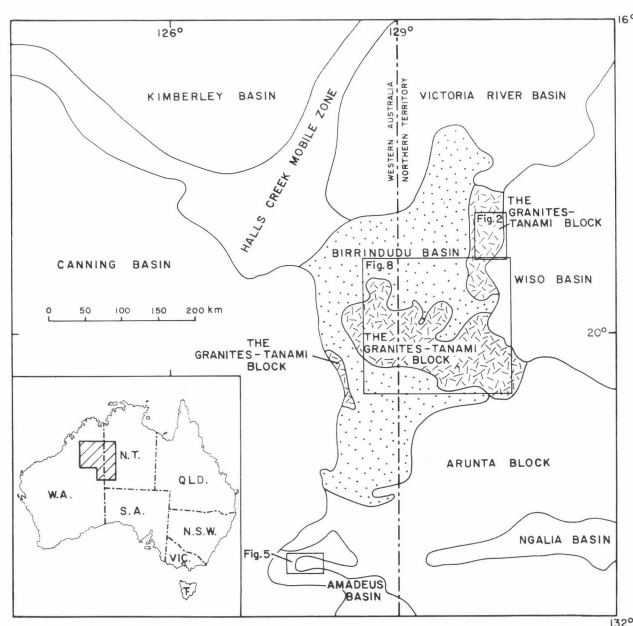


Figure 1. Regional tectonic setting

This paper reports isotopic ages and related aspects of rocks from the area surveyed, and deals firstly with acid volcanics and associated granitic rocks in the northeast and southwest. Those in the northeast are within The Granites-Tanami Block: the volcanics form part of the Mount Winnecke Formation (Blake et al., 1975), previously named the Mount Winnecke Sandstone (Traves, 1955), and the

* The time boundary between the Lower Proterozoic and the Carpentarian is taken to be 1700 ± 20 m.y., and between the Archaean and the Lower Proterozoic to be about 2300 m.y. (Plumb & Derrick, 1975).

associated granitic unit which intrudes the formation is the Winnecke Granophyre (Traves, op. cit.). The acid volcanics in the southwest belong to the Pollock Hills Formation and are intruded by the Mount Webb Granite: definitions of these two units are given by Blake & Towner (1974). In both the northeast and southwest the geological setting, petrographic data and chemical features indicate that the volcanics and associated granitic rocks may be comagmatic and of more or less similar age. The Rb-Sr study of these rocks was undertaken to test this hypothesis, and also to determine the initial $\text{Sr}^{87}/\text{Sr}^{86}$ of the volcanic and plutonic units. Also presented in the paper are isotopic data for three other granitic units in The Granites-Tanami Block—the Lewis, Slaty Creek and The Granites Granites—and the results of Rb-Sr and K-Ar studies on glauconite from the Gardiner Sandstone, the basal formation of the Birrindudu Group. Average chemical analyses of the acid volcanics and granites are shown in Table 1. Petrographic details are given in the Appendix.

Sampling and Geochronological Methods

The chief criterion for choosing sample sites for the granitic and volcanic rocks was the availability of exposed fresh rock, as over much of their outcrop areas these rocks are either intensely weathered or covered by superficial sediments. Where possible, several samples of visibly different rock types were collected from a site, either by hammer or by drilling and blasting, to give a maximum dispersion in Rb/Sr values.

The Rb-Sr total-rock isochron technique has been employed in the acid volcanics and granite geochronology, and both the K-Ar and Rb-Sr methods have been used in the glauconite age determinations. The K-Ar measurements were made by Dr A. W. Webb (AMDL Report 3473) using the following constants:

$$\lambda_p = 4.72 \times 10^{-10} \text{ yr}^{-1}$$

$$\lambda_c = 0.584 \times 10^{-10} \text{ yr}^{-1}$$

$$\text{K}^{40} = 0.0119 \text{ atom per cent}$$

The $\text{Rb}^{85}/\text{Rb}^{87}$ in natural Rb was taken as 2.600, Sr measurements were normalized to 8.3752 for $\text{Sr}^{88}/\text{Sr}^{86}$, and the value of $1.39 \times 10^{-11} \text{ yr}^{-1}$ was used for the decay constant of Rb^{87} . Statistical regression of the Rb-Sr isochron was carried out using the computer programme of McIntyre *et al.* (1966). The coefficients of variation for $\text{Rb}^{87}/\text{Sr}^{86}$ and $\text{Sr}^{87}/\text{Sr}^{86}$ have been taken as 0.5 percent and 0.01 percent, respectively. Errors quoted for the isotopic data are at the 95 percent confidence level.

Rubidium and strontium were determined using a modified version of the isotope dilution technique described by Compston *et al.* (1965). A mixed $\text{Rb}^{85} \text{Sr}^{84}$ spike was used to eliminate the effects of weighing errors in the subsequent determination of $\text{Rb}^{87}/\text{Sr}^{86}$ for the isochron analyses (de Laeter *et al.*, 1973). Rb^{85} was used instead of Rb^{87} , as the former is more easily monitored during the strontium isotopic analysis. Between 0.05 and 0.1 g aliquots of powdered total rock (–200 mesh) or mineral concentrate, depending on their Rb and Sr contents, were dissolved in HF and HClO_4 , spiked, and homogenized in 6N HCl. A preliminary separation of the rubidium and strontium was achieved by washing the sample with HCl through a cation-exchange column containing 4g Dowex resin (AG 50 W, 8 percent cross linkage, 200–400 mesh size and 50–56 percent moisture), and a final concentration was made with smaller columns using 2 g of the same resin. Processing blanks used were $0.007 \mu\text{g}$ for strontium and $0.008 \mu\text{g}$ for rubidium. The ion exchange procedure ensures that spiked rubidium is normally completely separated from strontium. However, if spiked or common rubidium is observed at the beginning of

the strontium run, it is either entirely evaporated from the sample before the isotopes are measured or an appropriate correction is made to the measured $\text{Sr}^{87}/\text{Sr}^{86}$ ratio.

Rubidium isotopic measurements were taken on a 15.25 cm (6-inch)-radius, 90° -sector, mass spectrometer; strontium analyses were made with a Nuclide Analysis Associates (NAA) 30.5 cm (12-inch) radius, 60° -sector, machine. Rhenium triple-filament sources were used. Both mass spectrometers employed 6 kV accelerating voltage, Faraday cup collector, and Cary electrometer model 31, and were operated on-line to a HP-2116B computer which also controlled the magnetic-field peak-switching.

Maximum tail corrections required under the Sr^{87} peak were 0.015 percent, and under the Sr^{86} peak were 0.006 percent. The $\text{Sr}^{87}/\text{Sr}^{86}$ ratio for the Eimer and Amend standard on the NAA machine is 0.70813 ± 0.00004 (1 sigma, Page & Johnson, 1974), normalized to 8.3752 for the $\text{Sr}^{88}/\text{Sr}^{86}$ ratio. Further recent measurements of $\text{Sr}^{87}/\text{Sr}^{86}$ in the standard NBS 987 strontium carbonate give a mean value of 0.71035 ± 0.00006 (1 sigma).

Mount Winnecke Formation and Winnecke Granophyre

The Mount Winnecke Formation and the Winnecke Granophyre which intrudes it are confined to the northeast of The Granites-Tanami region (Fig. 2). Contact metamorphic effects are only minor, and indicate, together with the types of intrusives rocks present, that the Winnecke Granophyre is a high-level intrusion. Both units are inferred to be overlain unconformably by the Carpentarian Birrindudu Group which crops out to the west, but contacts are concealed by superficial sediments.

The **Mount Winnecke Formation** is at least 4800 m thick, and consists of interbedded lithic to sublithic sandstone, tuffaceous sandstone and siltstone, acid lava flows, minor conglomerate and tuff, and rare agglomerate. These rocks have been folded into major anticlines and synclines with moderately to steeply dipping limbs. The lava flows and tuffs are generally less resistant to erosion than the sandstones, and commonly form depressions between steep-sided sandstone ridges and plateaux that are up to 50 m high. The sandstones commonly show cross-bedding, and some show ripple marks.

The acid lava flows tend to be dome-shaped in cross-section, and some are probably over 200 m thick. They occur both singly and in groups, and interfinger laterally with water-laid tuff, tuffaceous sediments, sandstone, and conglomerate. The interiors of the flows appear structureless, but the margins are autobrecciated, commonly scoriaceous, and at several localities show contorted flow-banding. Exposures are generally weathered, and as a result are friable and iron-stained to bleached. Relatively fresh lava is restricted to where the massive interiors of the thickest flows crop out.

The tuffs within the Mount Winnecke Formation are mainly laminated to thin-bedded and medium to very fine-grained, and are closely associated spatially with acid lavas. Some lapilli tuff, made up of angular non-porphyrific acid lava fragments, is also present, 6 km south-southwest of Mount Winnecke. It was laid down in water, probably close to the vent from which it was derived.

Most, if not all, of the acid volcanicity probably took place under water. This is indicated by the intimate association of lava flows with water-laid tuffaceous and non-tuffaceous sediments, and by the absence of air-fall pyroclastics. Eruption under water could also account for the lack of ignimbritic deposits, in spite of the abundance of fragmentary volcanic material, and would partly explain the

highly altered nature of most of the acid lava; acid magma erupted into water chills rapidly, and abundant hydrous volcanic glass is formed which is especially susceptible to contemporaneous hydrothermal alteration, to any subsequent thermal and regional metamorphism, and to weathering.

The Mount Winnecke Formation is intruded by Winnecke Granophyre at several localities. For example, an irregular roof contact is exposed at site A, where altered granophyre is overlain by sandstone that has been thermally metamorphosed to tourmaline-bearing hornfels, and at sites B and C granophyre is exposed in contact with weakly

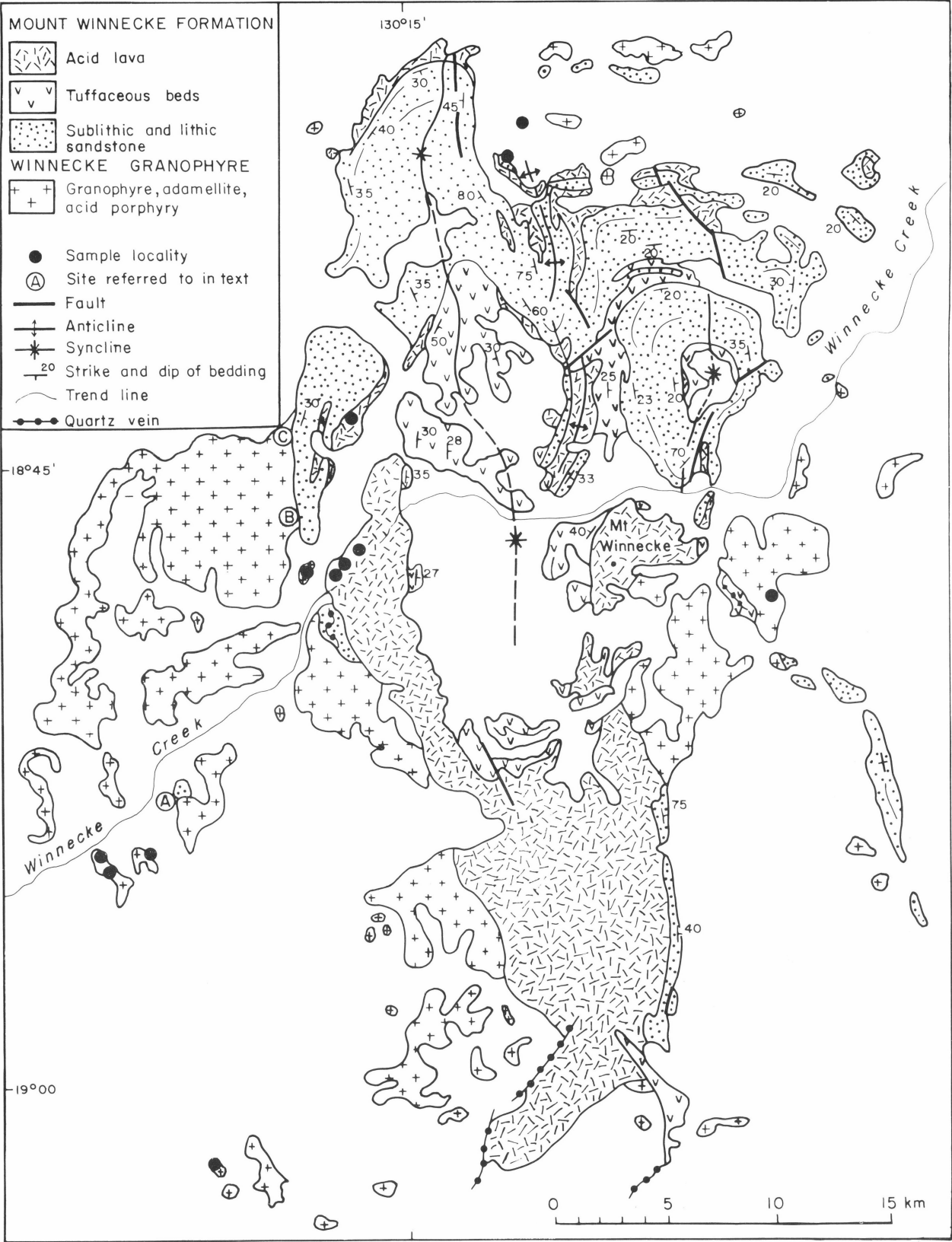


Figure 2. Geological map of the Mount Winnecke area, The Granites-Tanami Block

AUS1/419

TABLE 1 AVERAGE CHEMICAL COMPOSITIONS OF GRANITIC AND VOLCANIC ROCKS

Rock Unit	Lewis Granite	Slatey Creek Granite	The Granites Granite	Winnecke Granophyre	Mount Winnecke Formation	Pollock Hills Formation	Mount Webb Granite
No. of Samples	4	2	3	7	6	5	5
SiO ₂	74.2	71.8	73.3	74.9	71.7	69.4	74.1
TiO ₂	0.18	0.22	0.32	0.26	0.40	0.82	0.21
Al ₂ O ₃	13.6	15.1	13.7	12.8	13.1	12.9	13.0
Fe ₂ O ₃	0.34	0.40	0.35	0.64	0.65	2.70	0.84
FeO	1.48	1.70	1.52	1.32	2.87	2.35	1.63
MnO	0.04	0.05	0.05	0.04	0.08	0.08	0.04
MgO	0.43	0.72	0.40	0.22	0.48	0.73	0.36
CaO	1.05	1.87	1.67	0.86	1.14	2.57	1.75
Na ₂ O	3.29	3.50	3.32	2.69	2.46	2.60	2.70
K ₂ O	3.86	3.93	4.45	5.69	5.45	4.28	5.27
P ₂ O ₅	0.10	0.04	0.01	0.10	0.15	0.19	0.06
H ₂ O ⁺	0.71	0.51	0.43	0.24	0.78	0.60	0.36
H ₂ O ⁻	0.20	0.02	0.02	0.34	0.36	0.22	0.20
CO ₂	—	—	—	<0.05	<0.05	0.38	0.08
S	—	—	—	—	—	0.02	0.03
Total	99.5	99.9	99.5	100.1	99.6	99.8	100.6

Analyst: The Australian Mineral Development Laboratories, Adelaide.

hornfelsed sandstone (Fig. 2). At these localities only sandstone within a few metres of the intrusive contact has been thermally metamorphosed; at site C apparently unaffected acid lava crops out less than 10 m from granophyre.

Neither the base nor top of the Mount Winnecke Formation are exposed. However, the formation is inferred to be unconformable on metamorphic rocks of the basement Tanami complex, and to be overlain unconformably by Carpentarian sediments of the Birrindudu Group to the west and by Cambrian sediments of the Wiso Basin succession to the east.

The **Winnecke Granophyre** is commonly exposed in breakaways up to 10 m high, where it is strongly weathered and capped by laterite. However, in several places the weathered rock has been stripped off by erosion, and spheroidal boulders and tors of fresh granophyre, adamellite, and acid porphyry are revealed. Consequently, exposures of unweathered Winnecke Granophyre are much more numerous than those of unweathered acid lava of the Mount Winnecke Formation.

Both the granophyre and adamellite of the Winnecke Granophyre are pinkish where fresh, and contain biotite as the main ferromagnesian mineral; the granophyre commonly contains phenocrysts up to 1 cm long, and also small drusy cavities containing quartz, chlorite, epidote, and, in one specimen, prehnite. The adamellite is generally non-porphyritic, but some contains poikilitic feldspar crystals up to 3 cm across. Acid porphyry, the least widespread of the main intrusive rocks, contains up to 30 percent phenocrysts which are generally less than 1 cm long.

Small fine-grained xenoliths and cross-cutting quartz veins are common within the Winnecke Granophyre, and greisen is present locally at intrusive contacts. Dykes of pink aplitic microgranite and dark aphyric 'andesite' cut the granophyre and adamellite at some localities. In places the intrusive rocks are strongly sheared, and resemble schist.

Petrographic variations within the outcrop area indicate that the Winnecke Granophyre is probably made up of several separate high-level stocks derived from a common magma chamber. These stocks intrude the Tanami complex as well as the Mount Winnecke Formation.

Chemistry

Chemical analyses (Table 1) show that the acid lavas of the Mount Winnecke Formation and the intrusive Winnecke Granophyre are similar in composition, lending support to the hypothesis that they are comagmatic. Most of the analyses are of samples that were used in the Rb-Sr geochronological work. The lavas analysed show little variation in silica content, and are rhyolites. They have an average K/Na value of 2.2, virtually identical to the average value of 2.1 for the granophyre samples.

Six of the seven samples of Winnecke Granophyre analysed have micrographic textures. All except the most basic sample, which has 71.4 percent SiO₂ and contains hornblende as well as biotite, are richer in silica than the volcanics. In general the samples have lower Sr and higher Rb contents (Table 2), and lower K/Rb values, than the volcanics, indicating that they are later fractionation products than the lavas which they intrude.

Rb-Sr geochronology

Mount Winnecke Formation. Ten rhyolitic lava samples were used in the Rb-Sr isotopic study, of which eight were collected from 3 sites 12 km west of Mount Winnecke (Fig. 2). The lavas analysed have well preserved igneous textures, but all show some sericitic and chloritic alteration which is probable deuteric.

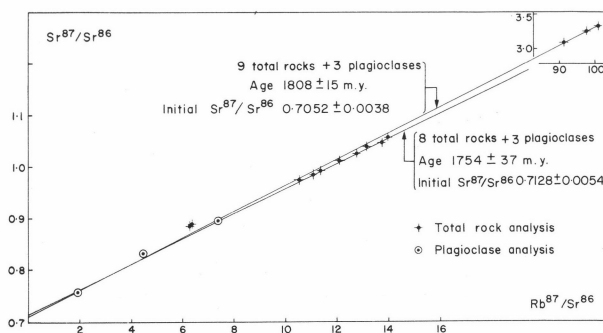


Figure 3. Rb-Sr isochron for the Mount Winnecke Formation

Rb-Sr isotopic analyses of the ten total rocks are given in

Table 2, together with analyses of deuterically altered plagioclase separated from three of the rocks. The data are plotted on a conventional isochron diagram in Figure 3. Regression of all the total rock and mineral data gives an isochron age of 1807 ± 18 m.y. at the 95 percent confidence level and an initial $\text{Sr}^{87}/\text{Sr}^{86}$ of 0.7070 ± 0.0056 . A similar result, 1809 ± 21 m.y., is obtained when only the total rock points are used in the regression. The data do not fit the isochron to within experimental error (Mean square of weighted deviates, $\text{MSWD} = 53.8$), and both regressions assume a model of calculation in which there was some primary variation in initial $\text{Sr}^{87}/\text{Sr}^{86}$ in the samples (Model 3). The most aberrant point is that of 5033, and its deletion from the combined total rock and mineral data results in a Model 3 isochron with a significantly lower MSWD of 14.7, but essentially the same resultant age (1808 ± 15 m.y.) and initial $\text{Sr}^{87}/\text{Sr}^{86}$ (0.7052 ± 0.0038). Another sample, 5034, is much more radiogenically enriched than the others, and thus has a major influence on the slope of the 1808 m.y. isochron. Because of this and because it is the most strongly altered of the samples analysed, it was analysed three times. The triplicate analyses of the sample, with respect to the 1808 m.y. isochron, are consistent and virtually concordant, although because of the small amount of sample used in the isotope dilution procedure, there is up to ten percent variation in the $\text{Rb}^{87}/\text{Sr}^{86}$ and $\text{Sr}^{87}/\text{Sr}^{86}$ values between the three runs. In the statistical regression of the data the mean value of the three isotopic analyses of 5034 has been used.

For the above reasons the data were again regressed, omitting the most radiogenically enriched sample, 5034. The regression involving the eight remaining total rocks and three plagioclase mineral separates again resulted in a Model 3 isochron (Fig. 3), with a similar MSWD of 13.5.

However, a somewhat younger age, 1754 ± 37 m.y., is indicated.

It is difficult to judge from the isotopic data whether the younger (1754 ± 37 m.y.) or older (1808 ± 15 m.y.) isochron result is the more realistic. As sample 5034 is the most altered of those analysed, its inclusion in the regression would be expected to result in an isochron giving a minimum age. Instead, its deletion from the regression leads to an isochron giving the younger age. The eight samples that make up the latter isochron come from the one relatively restricted area west of Mount Winnecke (Fig. 2). Sample 5034, however, comes from a site 19 km to the north-northeast, and it could be argued that its isotopic relationships to the main group of samples are therefore uncertain, and consequently the younger age of 1754 ± 37 m.y. (initial $\text{Sr}^{87}/\text{Sr}^{86}$ 0.7128 ± 0.0054) should be preferred. Nevertheless, the triplicate analyses of sample 5034 indicate an age of a little over 1800 m.y. which is independent of any initial $\text{Sr}^{87}/\text{Sr}^{86}$ up to 0.725; a most unlikely high initial ratio of 0.79 would be required to develop a 1754 m.y. isochron incorporating the 5034 analyses. We therefore conclude from the above data that the rhyolite lavas of the Mount Winnecke Formation are at least as old as 1754 ± 37 m.y., and there is evidence from at least one part of the formation that their age may be slightly over 1800 m.y.

Winnecke Granophyre. The relatively abundant exposures of fresh unaltered Winnecke Granophyre make this unit much more suitable for isotopic analysis than the acid lavas of the Mount Winnecke Formation. The Rb-Sr data given in Table 3 were obtained on 14 samples from seven sites (Fig. 2). Samples of several different varieties of granophyric rocks were collected, nine (5023A to 5025D)

TABLE 2 Rb-Sr DATA FOR THE MOUNT WINNECKE FORMATION AND WINNECKE GRANOPHYRE

Rock Unit	Sample No. (Prefix 7249 unless stated)	Locality		Rock Type/ Mineral Separate	Rb (ppm)	Sr (ppm)	Rb ⁸⁷ /Sr ⁸⁶	Sr ⁸⁷ /Sr ⁸⁶
		Latitude	Longitude					
Mount Winnecke Formation	5029A	18°47' 50"	130°13' 10"	Porphyritic acid lava	307.5	80.5	11.344	0.99363
	5029C			Porphyritic acid lava	312.7	73.1	12.748	1.02740
	5029D			Porphyritic acid lava	309.4	76.0	12.108	1.0111
	5029D			Plagioclase	120.5	178.5	1.959	0.75842
	5029E			Porphyritic acid lava	275.3	59.9	13.719	1.04699
	5029H			Porphyritic acid lava	301.6	80.7	11.084	0.98342
	5029H			Plagioclase	256.3	101.9	7.394	0.89399
	5029K			Porphyritic acid lava	308.8	86.8	10.541	0.97627
	5030	18°47' 30"	130°13' 30"	Porphyritic acid lava	309.6	66.1	13.983	1.05783
	5031	18°47' 10"	130°13' 40"	Porphyritic acid lava	309.2	70.3	13.114	1.03996
	5031	18°44' 05"	130°13' 40"	Plagioclase	315.5	203.9	4.518	0.82832
	5033			Sparsely porphyritic acid lava	38.2	17.9	6.294	0.88617
	5034			18°37' 55"	130°17' 40"	Sparsely porphyritic acid lava	240.1	9.3
		234.2	8.6				97.992	3.22332
		237.3	8.5				101.087	3.29054
Winnecke Granophyre	5022B	19°02' 18"	130°10' 12"	Acid porphyry	256.6	98.9	7.637	0.90337
	5022B			Biotite	1255.9	17.0	455.61	12.3078
	5022B			Plagioclase	57.9	147.4	1.137	0.73666
	5023A	18°54' 30"	130°08' 30"	Granophyre	379.8	28.8	42.116	1.77971
	5023C			Granophyre	433.7	13.2	124.63	3.86991
	5023D			Granophyre	389.5	10.7	141.09	4.21569
	5023F			Granophyre	440.8	18.0	85.600	2.85097
	5024B	18°55' 00"	130°07' 30"	Porphyritic granophyre	391.2	24.1	53.070	2.06778
	5024C			Biotite adamellite	384.4	71.5	14.592	1.08366
	5025A				387.4	77.0	15.075	1.09444
	5025B	18°54' 45"	130°07' 10"	Aplite	483.1	12.4	156.33	4.71973
	5025B			Biotite	1614.1	16.5	930.16	24.0544
	5025B			Plagioclase	314.0	186.5	4.917	0.82476
	5025D			Acid porphyry	365.5	41.4	27.239	1.40280
	5028	18°47' 40"	130°12' 30"	Granophyre	479.8	28.3	55.535	2.08922
	5035A	18°36' 50"	130°18' 10"	Porphyritic granophyre	305.9	79.8	11.382	0.99715
	5035A			Biotite	1132.6	19.5	289.23	8.11884
	5035B			Porphyritic granophyre	302.2	83.8	10.693	0.97918
	71490156	18°48' 20"	130°24' 20"	Acid porphyry	252.1	97.4	7.619	0.90083

coming from one small outcrop area, and these give a suitable broad dispersion in Rb/Sr values. Isotopic analysis of the 14 total rocks yields a Model 2 isochron age of 1797 ± 18 m.y., and an initial $\text{Sr}^{87}/\text{Sr}^{86}$ of 0.7098 ± 0.0037 . The slight scatter of the data points about the line (MSWD = 4.9) may be due to some isotopic disturbance after the time of cooling. Analyses of three biotite and two plagioclase mineral separates from the Winnecke Granophyre are also given in Table 2. The biotite ages range from 1784 to 1818 m.y., and are virtually independent of initial $\text{Sr}^{87}/\text{Sr}^{86}$.

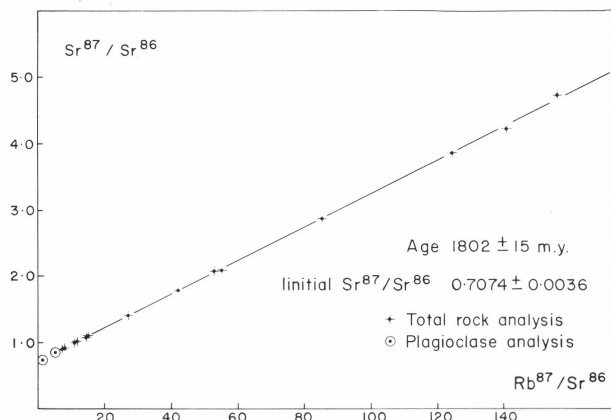


Figure 4. Rb-Sr isochron for the Winnecke Granophyre

These ages are the same as the total rock isochron age, to within experimental error, indicating that there has been little post-emplacement disturbance. Hence the ages obtained correspond to the time of cooling of the Winnecke Granophyre. Regression of the total-rock and mineral data from one small area (5023A to 5025D) is again in agreement, giving an age of 1813 ± 27 m.y. and an initial $\text{Sr}^{87}/\text{Sr}^{86}$ value of 0.7014 ± 0.0054 . Combining all the mineral and total-rock data is thus justified, and this gives an overall preferred age of 1802 ± 15 m.y. and an initial $\text{Sr}^{87}/\text{Sr}^{86}$ value of 0.7074 ± 0.0036 (Fig. 4). Although the 95 percent uncertainties are low, there is more scatter (MSWD = 13.1) about the isochron than can be expected from experimental error alone, and the statistical treatment assumes a Model 4 fit. This indicates a variation in initial $\text{Sr}^{87}/\text{Sr}^{86}$ for the samples, as well as some minor post-crystallization isotopic disturbance.

Discussion. The close affinity between the Mount Winnecke Formation rhyolitic lavas and their probable high-level intrusive equivalents that make up the Winnecke Granophyre is indicated by field evidence and petrographic and chemical data. As the Winnecke Granophyre intrudes the Mount Winnecke Formation, and its age is unequivocally determined, it is clear that the older of the two alternative isochrons for the Mount Winnecke Formation rhyolites, which indicates an age of 1808 ± 15 m.y. and an initial $\text{Sr}^{87}/\text{Sr}^{86}$ of 0.7052 ± 0.0038 (Fig. 3), is preferable.

The significance of the anomalously younger isochron for the rhyolitic lavas, giving an age of 1754 ± 37 m.y., is uncertain. It seems unlikely that this age is due to updating through tectonic disturbance, as both the mica and total rock data for the Winnecke Granophyre are internally consistent at about 1800 m.y. An alternative explanation is that the young apparent age can be attributed to partial open-system behaviour of the Rb and/or radiogenic Sr for some tens of millions of years after extrusion and cooling of the lavas. Such could have been the case if the acid volcanism took place beneath the sea. Under these conditions some exchange of alkalis between the lavas and sea water could take place during deuteric alteration and

any subsequent devitrification processes. Such migration of Rb into the lavas, or loss of radiogenic Sr from them, would be enhanced by even the mildest conditions of hydrothermal alteration. A number of examples in which dating of extrusive acid volcanics by the Rb-Sr whole rock methods provides anomalously young ages have been cited by Fairbairn & Hurley (1969), showing that the Mount Winnecke Formation lavas are not unique in this respect. It is considered that the special susceptibility of submarine acid volcanic rocks to alteration and incomplete chemical and isotopic closure could sometimes be the prime cause of non-adherence to true isochron relationships. Clearly, unless independent age control is available, such as the dating of high-level intrusives equivalent to the extrusives as in the Winnecke area, the interpretation of Rb-Sr whole rock isochrons on acid volcanic rocks must be approached with caution.

The initial $\text{Sr}^{87}/\text{Sr}^{86}$ values for the Mount Winnecke Formation lavas and the Winnecke Granophyre are 0.7052 and 0.7074, respectively, and are experimentally indistinguishable. This and the other isotopic data, together with the field, petrographic, and major element evidence, are consistent with the view that the extrusive and intrusive rocks were comagmatic, and crystallized about 1800 m.y. ago, late in the Lower Proterozoic.

Pollock Hills Formation and Mount Webb Granite

The geological setting in the southwest, where the Pollock Hills Formation and Mount Webb Granite crop out (Fig. 5), is somewhat similar to that in the Mount Winnecke area to the northeast. The Pollock Hills Formation, like the Mount Winnecke Formation, includes acid lava flows and pyroclastics, and it is intruded by the Mount Webb Granite which, like the Winnecke Granophyre, is considered to have been emplaced at a high structural level (Blake & Towner, 1974). The Pollock Hills Formation and Mount Webb Granite are both overlain unconformably by the Heavittree Quartzite, the oldest unit of the Amadeus Basin sequence, which from evidence further east is known to be younger than 1076 ± 50 m.y. (Marjoribanks & Black, 1974).

The **Pollock Hills Formation** is probably over 1000 m thick, and is made up of acid lava overlain by tuffaceous and non-tuffaceous sandstone, and minor lapilli tuff and agglomerate. The sandstone forms a series of cuestas and hogback ridges, whereas the lava mainly forms rounded, undulating to hilly terrain. The base of the formation is concealed, but is presumed to be unconformable on metamorphic rocks of the Arunta Block.

Differences in petrography indicate that several flows may be present, although no contacts between flows have been identified. At several localities, mainly in or near scarp faces, the tops of lava flows are exposed, overlain directly by either sandstone or pyroclastics. The flow tops consist of much altered flow-banded and brecciated pale lava, in places over 10 m thick. The altered lava passes down into much harder dark greyish massive lava. The dark lava has a prominent close steep jointing trending north to west-northwest, and is exposed as low tors and rocky outcrops consisting of angular to rounded blocks.

The upper part of the Pollock Hills Formation consists of a succession of lithic, sublithic, and tuffaceous sandstones similar to those of the Mount Winnecke Formation. In the type section of the formation these sediments are 600 m thick (Blake & Towner, 1975). The sandstones contain clasts of acid lava, some of which have shard-like forms, and also clasts of both plagioclase and alkali feldspar. They are water-laid sediments, and their close association with

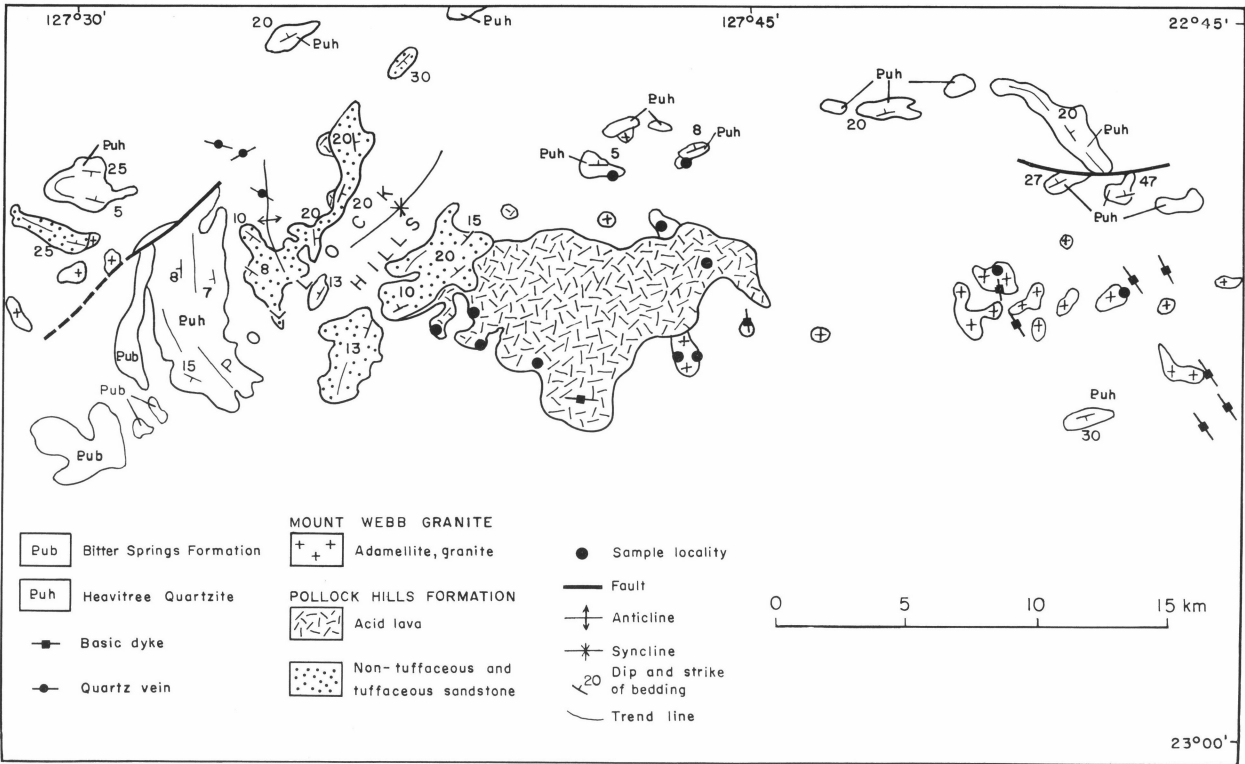


Figure 5. Geological map of the Pollock Hills area, Arunta Block

TABLE 3 Rb-Sr DATA FOR THE POLLOCK HILLS FORMATION AND MOUNT WEBB GRANITE

Rock Unit	Sample No. (Prefix 73490)	Locality		Rock type	Rb (ppm)	Sr (ppm)	Rb ⁸⁷ /Sr ⁸⁶	Sr ⁸⁷ /Sr ⁸⁶
		Latitude	Longitude					
Pollock Hills Formation	115A	22°48' 05"	127°42' 00"	Porphyritic acid lava	163.7	83.5	5.7251	0.82644
	120C	22°47' 50"	127°43' 30"	" (highly altered)	113.4	36.2	9.1557	0.83993
	122	22°50' 00"	127°44' 00"	"	178.9	140.9	3.6974	0.79274
	097	22°51' 00"	127°38' 50"	"	208.3	135.9	4.4705	0.80831
	088	22°51' 25"	127°38' 10"	"	206.1	98.7	6.1074	0.84132
	098	22°51' 40"	127°39' 00"	"	184.7	128.3	4.1939	0.80269
	099	22°52' 00"	127°40' 20"	"	122.0	115.9	3.0573	0.77225
	103	22°51' 20"	127°43' 30"	"	176.7	175.8	2.9205	0.77298
Mount Webb Granite	121	22°49' 10"	127°43' 00"	Biotite adamellite	246.7	84.3	8.6183	0.90563
	101	22°52' 00"	127°43' 30"	Strongly foliated biotite adamellite	239.0	98.5	7.1185	0.86960
	102A	22°52' 00"	127°43' 50"	Aplite	279.6	20.5	42.9682	1.62849
	102B	22°52' 00"	127°43' 50"	Biotite adamellite	260.1	94.5	8.0888	0.88786
	276	22°50' 00"	127°50' 35"	Aplite	259.6	36.4	21.5081	1.17222
	274A	22°50' 30"	127°53' 25"	Foliated hornblende-augite- albite granite	7.3	172.7	0.1226	0.70879

acid lavas and tuffs indicates that the acid volcanics of the Pollock Hills Formation, like those of the Mount Winnecke Formation, may have been erupted under water.

The Pollock Hills Formation is intruded by the Mount Webb Granite whose emplacement, like that of the Winnecke Granophyre, was accompanied by only minor thermal metamorphism, indicating emplacement at a high structural level. Within a few metres of the intrusive contacts, acid lava and sandstone have become mottled, dense, and hornfelsic, and at one locality acid lava is cut by veins of granite.

The Mount Webb Granite crops out mainly to the east of the Pollock Hills, where unweathered granitic rocks are exposed as scattered spheroidal boulders and as tors up to 30 m high. It also crops out west of the Pollock Hills, where it is generally somewhat weathered. The granite is mainly pinkish to pale grey, medium to coarse, and non-por-

phyritic. It commonly shows a moderately to steeply dipping foliation which locally is sufficiently intense to give the rock a gneissic appearance. The foliation generally trends west to north-northwest. The granite is cut by quartz and sparse aplite veins generally less than 1 m thick, and by post-foliation basic dykes, most of which trend northwest.

The foliation of the granite, and straining and local granulation of the quartz, are presumed to have taken place at or near the time of intrusion: if the foliation was a regional, post-crystallization feature, constituents other than quartz should also be affected, and the Pollock Hills Formation would show obvious signs of deformation.

Chemistry

The analysed lava samples from the Pollock Hills Formation are slightly less rich in silica than the analysed samples of Mount Webb Granite, and are rhyodacites, but

otherwise the lavas and granite are closely similar in chemical composition (Table 1), at least as far as major elements are concerned. They are also chemically similar to the Mount Winnecke Formation acid volcanics and the Winnecke Granophyre.

Rb-Sr geochronology

Rb-Sr data for the Pollock Hills lavas and the intrusive granite are given in Table 3 and the data are plotted separately in Figures 10 and 11.

Pollock Hills Formation. Eight lava samples from eight separate sites (Fig. 5) were selected for Rb-Sr isotopic analysis; all show some deuteric alteration, such as sericitization of feldspar. The samples have only a moderate dispersion in $\text{Rb}^{87}/\text{Sr}^{86}$, and show considerable scatter about the fitted isochron (MSWD = 66.3, Model 4 fit). Consequently the 95 percent uncertainty limit on the age obtained, 1510 ± 240 m.y. (Fig. 6), is rather high. It is therefore appropriate to examine once again the probable high-level intrusive equivalents of the volcanics in order to possibly substantiate the age and improve the precision.

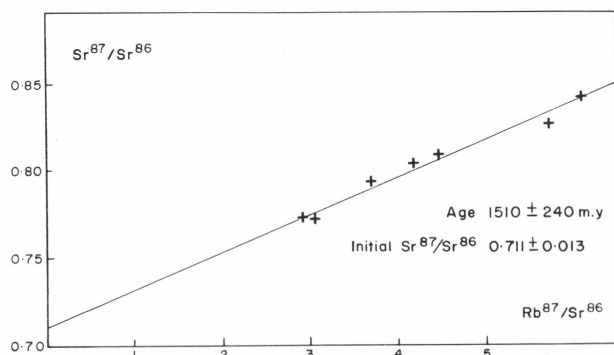


Figure 6. Rb-Sr isochron for the Pollock Hills Formation

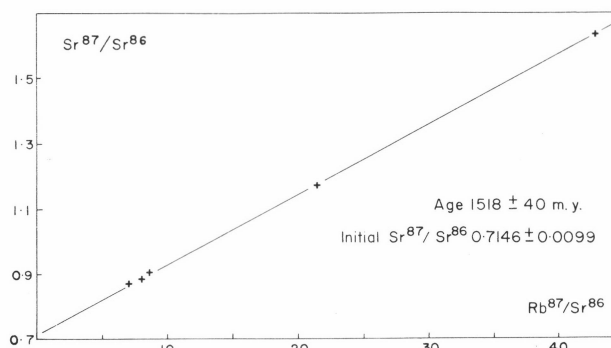


Figure 7. Rb-Sr isochron for the Mount Webb Granite

Mount Webb Granite. The isochron plot of six samples of Mount Webb Granite (Fig. 7) is a Model 3 regression with an age of 1518 ± 40 m.y. and initial $\text{Sr}^{87}/\text{Sr}^{86}$ of 0.7146 ± 0.009 ; the slope of the isochron is not very different from that given by the lava samples (Fig. 6). The granitic samples come from five different sites up to 10 km apart (Fig. 5). Given this sampling limitation, the fit of the data is as good as can be expected, and indicates some variation in initial $\text{Sr}^{87}/\text{Sr}^{86}$ values between samples. Three of the analysed samples are of medium-grained biotite adamellite, and two (102A, 276) are from cross-cutting veins of leucocratic biotite adamellite (aplite) a few centimetres thick. The remaining sample (274A) differs from the others in containing only minor alkali feldspar and no biotite, the main constituents being quartz, sodic plagioclase, augite, and pale green amphibole; epidote and sphene are abundant accessories. If this last sample is deleted from the

regression analysis, the MSWD is markedly lowered, from 45.5 to 9.6, but the resultant age, 1504 ± 33 m.y. and initial $\text{Sr}^{87}/\text{Sr}^{86}$ of 0.7197 ± 0.008 , are not much changed.

Discussion. Both field and isotopic evidence indicate that it is probably justifiable to group the Rb-Sr data from the volcanics of the Pollock Hills Formation with those from the Mount Webb Granite. When this is done the combined regression gives an age of 1526 ± 25 m.y. and an initial $\text{Sr}^{87}/\text{Sr}^{86}$ of 0.7114 ± 0.004 . This date is considered the best estimate for the age of crystallization of both the intrusive and extrusive rocks. The close jointing of the acid lava and the foliation and partial recrystallization of the granite do not appear to have had a major influence on the determined age, indicating that they probable took place close to the time of the primary igneous event. The slightly high indicated initial $\text{Sr}^{87}/\text{Sr}^{86}$ values for the dated rocks are not sufficiently precise to warrant detailed interpretations, but it is clear that this igneous suite did not have any significant crystal prehistory, as the maximum age that can reasonably be derived by averaging the $\text{Rb}^{87}/\text{Sr}^{86}$ values, and assuming a low initial $\text{Sr}^{87}/\text{Sr}^{86}$, is about 1650 m.y. This rules out any notion that the Pollock Hills-Mount Webb igneous suite could represent the metamorphosed equivalent of the 1800 m.y. Winnecke igneous rocks in the northeast of The Granites-Tanami area.

Other granites in The Granites-Tanami Block

Lewis Granite

The Lewis Granite (Blake et al., 1973) crops out along the Lewis Range and to the northeast (Fig. 9). It intrudes the Tanami complex and is overlain by the Lewis Range Sandstone, a basal formation of the Redcliff Pound Group.

The Rb-Sr data for nine samples from five sites are given in Table 4 and plotted on a conventional isochron diagram in Figure 8. There is an excellent dispersion in $\text{Rb}^{87}/\text{Sr}^{86}$ for the samples, and the nine data points are aligned on an isochron in which all error can be effectively regarded as due to experimental uncertainties. The indicated age is 1720 ± 8 m.y. and the initial $\text{Sr}^{87}/\text{Sr}^{86}$ is 0.7091 ± 0.0010 . In view of the broad sampling involved, the Model 1 fit of the data is surprisingly good. Four of the samples (5001 to 5003BB) come from a single site, and the isotopic data from these again yield a Model 1 regression fit, with an age of 1695 ± 30 m.y. and an initial $\text{Sr}^{87}/\text{Sr}^{86}$ of 0.7128 ± 0.0163 . The higher errors in this result are due to the smaller number of samples considered.

It is concluded that the Lewis Granite samples and associated pegmatites and aplites were emplaced in early Carpentarian time, 1720 ± 8 m.y. ago. The moderately high initial $\text{Sr}^{87}/\text{Sr}^{86}$ ratio of 0.7091 ± 0.0010 indicates some crustal contamination during the genesis of the granite magma.

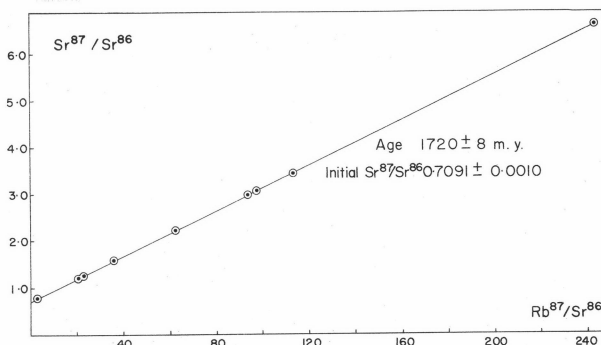


Figure 8. Rb-Sr isochron for the Lewis Granite

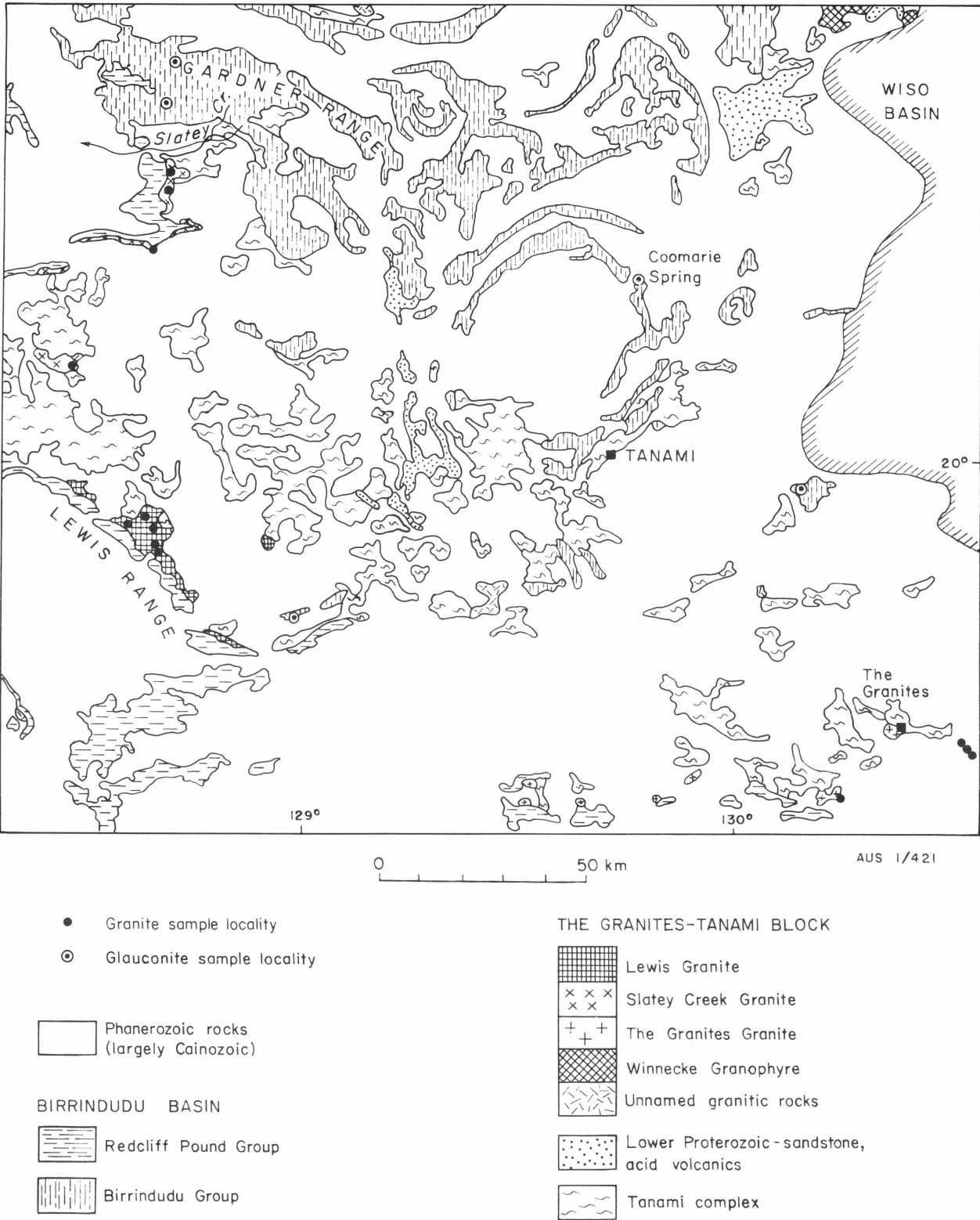


Figure 9. Geological map of the central part of The Granites- Tanami region

TABLE 4 Rb-Sr DATA FOR THE LEWIS, SLATEY CREEK AND THE GRANITES GRANITES

Rock Unit	Sample No. (Prefix 7249)	Locality		Rock Type	Rb (ppm)	Sr (ppm)	Rb ⁸⁷ /Sr ⁸⁶	Sr ⁸⁷ /Sr ⁸⁶
		Latitude	Longitude					
Lewis Granite	0003	20°09'00"	128°40'00"	Muscovite-biotite adamellite	600.2	11.2	243.646	6.61438
	0003C	20°09'00"	128°40'00"	Aplite	691.0	25.9	94.168	2.98831
	2071	20°08'00"	128°35'00"	Biotite adamellite	147.6	147.7	2.905	0.77919
	2663	20°07'40"	128°38'00"	Biotite-muscovite adamellite	511.1	44.4	36.098	1.59123
	5001	20°12'40"	128°40'35"	Microadamellite	520.3	16.7	113.675	3.43336
	5002	20°12'40"	128°40'35"	Microadamellite	533.3	28.3	62.427	2.21575
	5003B	20°12'40"	128°40'35"	Muscovite-biotite adamellite	453.3	65.3	21.066	1.22359
	5003BB	20°12'40"	128°40'35"	Aplite	706.5	25.8	96.972	3.02305
	5005	20°12'00"	128°40'00"	Muscovite-biotite adamellite	311.3	42.7	22.164	1.24754
Slatey Creek Granite	0306	19°48'00"	128°28'00"	Biotite granodiorite	135.7	405.3	0.9691	0.72889
	1022	19°22'00"	128°41'15"	Muscovite-biotite adamellite	226.8	95.3	6.988	0.80046
	5011A	19°32'00"	128°39'15"	Muscovite- adamellite	248.9	14.7	55.405	2.08720
					249.0	14.4	56.660	2.11644
	5014B	19°24'20"	128°41'30"	Aplite	155.7	42.8	10.775	0.98502
The Granites Granite	1492	20°36'40"	130°31'20"	Biotite adamellite	258.7	148.3	5.100	0.83600
	1493	20°36'30"	130°31'10"	Biotite adamellite	254.7	138.3	5.388	0.84197
	1494	20°37'00"	130°31'30"	Biotite adamellite	272.7	56.2	14.517	1.06955
	4150A	20°43'50"	130°14'30"	Biotite adamellite	141.0	199.6	2.050	0.75790
	4150AA	20°43'50"	130°14'30"	Aplite	167.5	41.3	12.060	1.00801
	4150B	20°43'50"	130°14'30"	Biotite adamellite	115.9	188.2	1.786	0.75088
	4210	20°35'45"	130°30'10"	Biotite adamellite	250.2	144.0	5.078	0.83214

Slatey Creek Granite

The Slatey Creek Granite forms scattered outcrops southwest of the Gardner Range, mainly to the south of Slatey Creek after which it is named (Fig. 9). It was mapped as part of the Lewis Granite by Casey & Wells (1964), but is now regarded as a separate granite. It intrudes the Tanami complex, and is overlain by both the Gardiner Sandstone of the Birrindudu Group and the Lewis Range Sandstone of the Redcliff Pound Group.

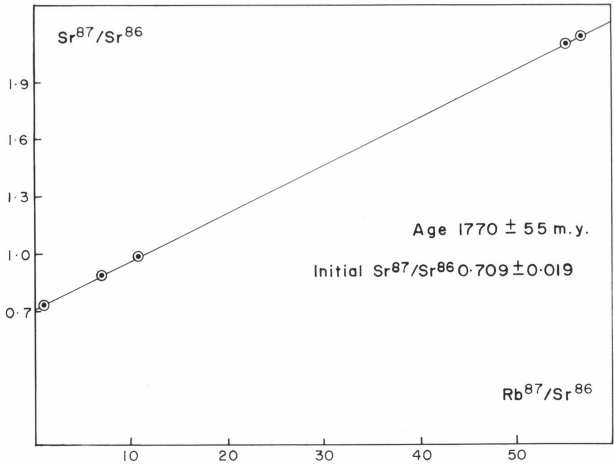


Figure 10. Rb-Sr isochron for the Slatey Creek Granite

Although many exposures were visited, at only four was there granite fresh enough for dating purposes, and only one sample was collected at each site. The four samples analysed come from widely separated localities and represent an inferred area of granite over 50 km across. As might be expected, the four samples do not fit a Model 1 isochron to within experimental uncertainties (MSWD 25.7); instead a Model 3 solution, with an age of 1770 ± 55 m.y. and an initial Sr⁸⁷/Sr⁸⁶ of 0.709 ± 0.019, is obtained (Fig. 10). This result is largely controlled by the duplicated analysis of the most enriched sample (5011A). Because of the reconnaissance nature of the sampling it is not possible

to draw firm conclusions from the data, other than that the Slatey Creek Granite is an early Carpentarian or late Lower Proterozoic intrusion. It may be older than the Lewis Granite to the south, but the available data are not good enough to check this.

The Granites Granite

The Granites Granite forms scattered outcrops near the abandoned gold mining settlement of The Granites (Fig. 8), where it intrudes the Tanami complex.

Seven samples from two outcrop areas, 16 km east-southeast and 23 km south-southwest of The Granites, have been analysed. The samples show a reasonable spread in Rb⁸⁷/Sr⁸⁶ and define a Model 3 isochron (MSWD = 3.1) with an age of 1780 ± 24 m.y. and an initial Sr⁸⁷/Sr⁸⁶ of 0.7066 ± 0.0019 (Fig. 11). The Model 3 solution could be due to small initial variations in the Sr⁸⁷/Sr⁸⁶ between the samples.

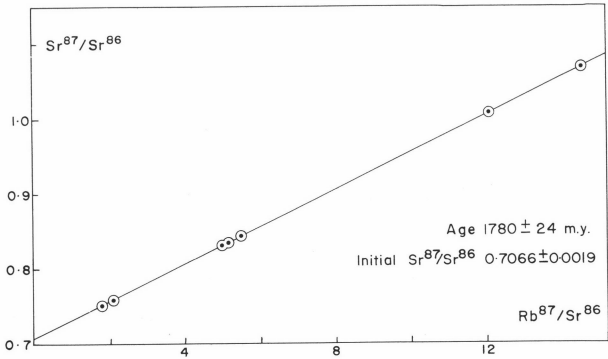


Figure 11. Rb-Sr isochron for The Granites Granite

Gardiner Sandstone

The Gardiner Sandstone, the basal formation of the Birrindudu Group (Blake et al., 1975), has a maximum thickness of about 3000 m. It rests with strong unconformity on the rocks of The Granites-Tanami Block, and is overlain conformably by the Talbot Well Formation, above

TABLE 5 Rb-Sr AND K-Ar DATA FOR GLAUCONITES FROM THE GARDINER SANDSTONE

Sample No. (Prefix 7249)	Locality		Rb ppm	Sr ppm	Rb ⁸⁷ /Sr ⁸⁶	Sr ⁸⁷ /Sr ⁸⁶	K%	Rad. Ar ⁴⁰ /K ⁴⁰	100 × Rad. Ar ⁴⁰ Total Ar ⁴⁰	Age m.y. ± 2 s.d.
	Latitude	Longitude								
0087B	20°20'40"	128°58'30"	347.1	62.9	16.471	1.06978	6.144 6.168	0.14120	99.8	1556 ± 20
0476A	20°20'30"	128°58'50"	319.8	168.4	5.559	0.84941	5.759 5.791	0.15108	99.8	1628 ± 20
0764	20°03'00"	130°09'20"	—	—	—	—	4.511 4.526	0.14265	99.4	1566 ± 30
1127	19°07'15"	128°40'00"	294.6	13.4	73.132	2.26256	5.821 5.844	0.12942	99.6	1465 ± 20
1135	19°12'50"	128°41'10"	372	9.7	144.822	3.84788	6.563 6.575	0.14221	99.7	1563 ± 20
1500	19°40'45"	129°46'40"	344.3	13.4	87.096	2.48664	6.607 6.594	0.13643	99.6	1519 ± 20
5021	19°40'45"	129°46'40"	278.5	26.5	32.206	1.33522	4.735 4.753 4.880	0.13513 0.13583	99.2 99.1	1509 ± 30 1515 ± 30

which comes the Coomarie Sandstone, the youngest formation of the Group.

At most outcrops the Gardiner Sandstone has low dips, and it commonly forms cuestas and plateaus bounded by scarps up to 100 m high. The main rock type exposed is sub-lithic arenite, but quartz arenite, conglomerate, shale and siltstone are also present. Stratigraphic drilling indicates that shale underlies much of the superficial cover between ridges of resistant sandstone. Glauconitic sandstone about 10 m thick is commonly present at two stratigraphic levels in the top 500 m of the formation.

Geochronology

K-Ar. Seven samples were chosen for isotopic dating: two from separate localities in the Gardner Range, two from Coomarie Spring north of Tanami, two from a low range southeast of the Lewis Range, and one from a low range north of The Granites (Fig. 8). The K-Ar ages (Table 5) range from 1465 to 1628 m.y. Interpretation of these results is made difficult by the fact that some of the concentrates used in the K-Ar work contained less than 95 percent glauconite. This is certainly the case for 0476A, in which inherited radiogenic argon in feldspathic impurities may have contributed to its much older age. Three of the glauconite K-Ar ages are, however, closely grouped at around 1560 m.y. and as there is some 40 percent variation in K content, it is probable that this age is geologically significant. The youngest K-Ar age, 1465 m.y., probably reflects some loss of radiogenic argon. The two glauconites from Coomarie Spring (1500, 5021) are also younger, but are in good agreement at 1519 m.y. and 1512 m.y. Because the two Coomarie Spring samples again have quite different K contents, their K-Ar ages may be geologically meaningful. On the other hand, however, they may reflect partial differential outgassing of argon.

On the basis of these limited K-Ar data the two groupings of ages, at around 1560 ± 20 m.y. and 1516 ± 20 m.y., are tentatively regarded as minimum estimates for the age of the glauconite.

Rb-Sr. Six of the seven glauconite samples were subsequently hand-picked to 100 percent purity and analysed by the Rb-Sr isotope dilution procedure (Table 5). The data obtained are plotted on a conventional isochron, diagram (Fig. 12). The glauconite points do not lie on a

single isochron, as the two samples from Coomarie Spring (1500, 5021) both fall markedly below the isochron which joins the other four samples. This isochron indicates an age of 1500 ± 108 m.y. (initial Sr⁸⁷/Sr⁸⁶ = 0.731 ± 0.016) and is consistent with the preferred K-Ar age of 1560 ± 20 m.y. given by some of the same samples. Model Rb-Sr ages calculated for the two Coomarie Spring glauconites are internally discordant at 1461 m.y. and 1405 m.y., and are significantly younger than the respective K-Ar ages, indicating that the two Coomarie Spring glauconites have probably suffered partial loss of radiogenic strontium. If such is the case, radiogenic argon was also probably lost from the two glauconites, and the two apparently concordant K-Ar ages of 1519 m.y. and 1512 m.y. must now be considered as younger than the actual age of glauconite formation.

From the above evidence, the preferred minimum age for the Gardiner Sandstone is considered to be 1560 ± 20 m.y.; this is the K-Ar age of three of the glauconite samples and is consistent with the Rb-Sr isochron age of four of the samples. Of the other samples, three are thought to show a loss in radiogenic argon and two a loss in radiogenic strontium, giving ages which are too young. One sample used for the K-Ar dating contained impurities of feldspathic material which are considered to be responsible for giving a K-Ar age thought to be too old.

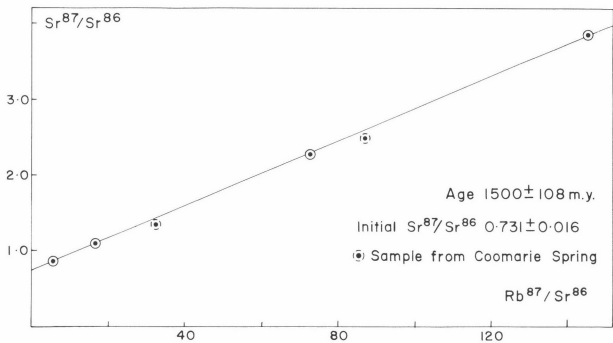


Figure 12. Rb-Sr isochron for glauconite from the Gardiner Sandstone.

Summary of Conclusions

Field, chemical, and isotopic evidence indicate that two groups of igneous rocks in the northeast part of The Granites-Tanami Block are comagmatic. These are acid volcanics of the Mount Winnecke Formation, dated at 1809 ± 15 m.y. (preferred age), with an initial $\text{Sr}^{87}/\text{Sr}^{86}$ of 0.7052 ± 0.0038 , and the high-level Winnecke Granophyre, dated at $1802 \pm$ m.y. with an initial $\text{Sr}^{87}/\text{Sr}^{86}$ of 0.7074 ± 0.0036 . The volcanic and intrusive rocks crystallized at about the same time, late in the Lower Proterozoic.

Similarly, two groups of igneous rocks in the Arunta Block in the southwest are also considered to be comagmatic—acid lava of the Pollock Hills Formation, dated at 1510 ± 240 m.y., and the Mount Webb Granite dated at 1518 ± 40 m.y., initial $\text{Sr}^{87}/\text{Sr}^{86}$ 0.7146 ± 0.0099 . When the Rb-Sr data for these rocks are grouped together, the combined regression gives a mid-Carpentarian age of 1526 ± 25 m.y. and an initial $\text{Sr}^{87}/\text{Sr}^{86}$ 0.7114 ± 0.004 . This age fits in between two metamorphic events which affected the Arunta Block to the east—a regional metamorphism dated at 1719 ± 24 m.y. (Armstrong & Stewart, 1975) and a late migmatitic event dated at 1076 ± 50 m.y. (Marjoribanks & Black, 1974).

In addition to the Winnecke Granophyre, three other granitic units in The Granites-Tanami Block have been isotopically dated—The Lewis Granite, dated at 1720 ± 8 m.y., initial $\text{Sr}^{87}/\text{Sr}^{86}$ 0.7091 ± 0.0010 ; the Slatey Creek Granite, 1770 ± 55 m.y., initial $\text{Sr}^{87}/\text{Sr}^{86}$ 0.709 ± 0.019 ; and The Granites Granite at 1780 ± 24 m.y., initial $\text{Sr}^{87}/\text{Sr}^{86}$ 0.7066 ± 0.0019 . The ages obtained indicate that in this Block, granites were emplaced in the period 1820–1700 m.y., straddling the boundary between the Lower Proterozoic and Carpentarian.

A Carpentarian K-Ar age of 1560 ± 20 m.y., obtained on three glauconite samples from the Gardiner Sandstone, is considered to be the best estimate (minimum) for the age of the deposition of the Birrindudu Group. This Group unconformably overlies The Granites-Tanami Block and comprises the oldest sediments of the Birrindudu Basin.

Acknowledgements

We are indebted to J. Pollard who assisted in the field work. The rocks and mineral separates were prepared by M. Cowan and R. Rudowski. On-line reduction of the isotopic data was computer-programmed by P. A. Arriens whose assistance in this matter is greatly appreciated.

We are grateful to W. B. Dallwitz, K. R. Walker, and L. P. Black for their comments and criticism of earlier versions of the text.

References

- ARMSTRONG, R. L., & STEWART, A. J., 1975—Rubidium-strontium dates and extraneous argon in the Arltunga Nappe Complex, Northern Territory. *Journal of the Geological Society of Australia*, **22**, 103–115.
- BLAKE, D. H., HODGSON, I. M., & MUHLING, P. C. 1973—Geology of The Granites and Precambrian parts of the Billiluna, Lucas and Stansmore 1:250 000 Sheet areas, Northern Territory and Western Australia. *Bureau of Mineral Resources, Australia—Record 1973/171* (unpublished).
- BLAKE, D. H., HODGSON, I. M., & SMITH, P. A., 1975—Geology of The Birrindudu and Tanami 1:250 000 Sheet areas, Northern Territory. *Bureau of Mineral Resources, Australia—Report 174*.
- BLAKE, D. H. & TOWNER, R. R., 1974—Geology of the Webb 1:250 000 Sheet area, Western Australia. *Bureau of Mineral Resources, Australia—Record 1974/53* (unpublished).
- CASEY, J. N. & WELLS, A. T., 1964—The geology of the north-east Canning Basin, Western Australia. *Bureau of Mineral Resources, Australia—Report 49*.
- COMPSTON, W., LOVERING, J. F., & VERNON, M. J., 1965—The Rb-Sr age of the Bishopville aubrite and its component enstatite and feldspar. *Geochimica et Cosmochimica Acta*, **29**, 1085–99.
- DE LAETER, J. R., VERNON, M. J., & COMPSTON, W., 1973—Revision of lunar Rb-Sr ages. *Geochimica et Cosmochimica Acta*, **37**, 700–702.
- DOW, D. B., & GEMUTS, I., 1969—Geology of the Kimberley region, Western Australia: the east Kimberley. *Bureau of Mineral Resources, Australia—Bulletin 106*.
- FAIRBAIRN, H. W., & HURLEY, P. M., 1969—Northern Appalachian geochronology as a model for interpreting ages in older orogens. *M.I.T. 17th Annual Progress Report to the US Atomic Energy Commission—Contract At (30-1)—1381*, 11–17.
- HODGSON, I. M., 1974—Geology of the Highland Rocks 1:250 000 Sheet area, Northern Territory. *Bureau of Mineral Resources, Australia—Record 1974/120* (unpublished).
- MARJORIBANKS, R. W., & BLACK, L. P., 1974—Geology and geochronology of the Arunta Complex north of Ormiston Gorge, central Australia. *Journal of the Geological Society of Australia*, **21**, 291–299.
- MCINTYRE, G. A., BROOKS, C., COMPSTON, W. & TUREK, A., 1966—The statistical assessment of Rb-Sr isochrons. *Journal of Geophysical Research*, **71**, 5459–5468.
- PAGE, R. W., 1976—Reinterpretation of isotopic ages from the Halls Creek Mobile Zone, northwest Australia. *BMR Journal of Australian Geology and Geophysics*, **1**, 79–81.
- PLUMB, K. A., & DERRICK, G. M., 1975—Geology of the Proterozoic rocks of Northern Australia; in KNIGHT, C. L., Editor, ECONOMIC GEOLOGY OF AUSTRALIA AND PAPUA NEW GUINEA. *Australasian Institute of Mining and Metallurgy, Melbourne*.
- TRAVES, D. M., 1955—The geology of the Ord—Victoria region, northern Australia. *Bureau of Mineral Resources, Australia—Bulletin, 27*.

Appendix

Petrography

Mount Winnecke Formation

Most of the lavas of the Mount Winnecke Formation contain phenocrysts of feldspar (sodic plagioclase or alkali feldspar or both), quartz and ferromagnesian minerals, and microphenocrysts of opaque minerals. The phenocrysts constitute up to 20 percent of the total rock, and are generally less than 1 cm across. Most phenocrysts of feldspar and all those of ferromagnesian minerals are completely altered, mainly to clay and sericitic material. Quartz and alkali feldspar phenocrysts show resorption features. The ground mass, which in the least altered parts of the lava flows is a medium to fine-grained mosaic of quartz and alkali feldspar with some chlorite, probably consisted originally of either microlites and glass or microcrystalline quartz and feldspar. Outlines of original microlites are commonly indicated by dust particles and opaque granules. Vesicles in scoriaceous lava are filled with quartz, celadonite and, at one locality, diaspore and pyrophyllite.

Winnecke Granophyre

Three main rock types are present: granophyre, adamellite and acid porphyry. The granophyre commonly contains phenocrysts and is made up essentially of quartz, alkali feldspar, sodic plagioclase, brown biotite and, in one sample examined, green hornblende. The quartz is confined mainly to the groundmass but also forms euhedral to partly resorbed anhedral phenocrysts. The alkali feldspar appears to be orthoclase in some specimens and microcline in others; it is variably turbid but otherwise unaltered, and forms both phenocrysts and micrographic intergrowths with quartz. Plagioclase is present as phenocrysts of oligoclase-andesine composition, partly altered to sericite and kaolin, and appears to be generally subordinate to alkali feldspar. Biotite forms phenocrysts, fine-grained crystal aggregates which may be xenolithic, and small flakes in the groundmass; it shows some alteration, mainly to chlorite. The granophyre also contains minor amounts of allanite, apatite, clinozoisite, epidote, fluorite, leucoxene, sphene, zircon, and metamict and opaque minerals. The adamellite is similar mineralogically to the granophyre, but is coarser and mainly non-porphyrific, and has a general granitic rather than graphic texture. In the acid porphyry phenocrysts of quartz, plagioclase normally zoned from albite to labradorite, orthoclase, biotite, and in some cases blue tourmaline and orthopyroxene are present. They are enclosed in a very fine to fine-grained granitic to patchily graphic mosaic of quartz and alkali feldspar, with flakes of biotite (commonly replaced by chlorite), opaque granules, and microphenocrysts of plagioclase.

Pollock Hills Formation

The acid lava of the Pollock Hills Formation contains 10 to 20 percent phenocrysts, less than 5 mm across, of feldspar and commonly quartz. Pseudomorphed ferromagnesian phenocrysts and microphenocrysts of apatite and opaque minerals are also commonly present. The groundmass is fine to very fine-grained, and consists mainly of felsitic to microgranitic and patchily micrographic quartz and alkali feldspar, and opaque granules. Most feldspar phenocrysts are sodic plagioclase showing alteration to clay minerals, epidote, sericite, and calcite. Sparse alkali feldspar phenocrysts have been identified in a few specimens. Quartz phenocrysts are commonly partly resorbed. Ferromagnesian phenocrysts are pseudomorphed by aggregates of chlorite, iron oxide, greenish biotite, pale green amphibole, and sphene.

Mount Webb Granite

The main rock type of this unit is adamellite consisting essentially of quartz, plagioclase, alkali feldspar, and in most cases biotite, locally accompanied by green to greenish-blue hornblende. Some augite-bearing granite is also present, mainly in the east. The quartz in the adamellite is strained and locally granulated, but the other minerals show evidence of shearing only in gneissic samples. The plagioclase is oligoclase-andesine showing weak normal zoning and partial alteration to epidote, white mica, clay minerals, and chlorite. The alkali feldspar is mainly slightly perthitic microcline, and is generally unaltered. Biotite is commonly partly altered to chlorite and epidote. Augite, where present, is partly unaltered. Apatite, sphene, zircon, and metamict and opaque minerals are common accessory minerals, and minor allanite and tourmaline are present in some specimens.

Lewis Granite

This unit consists mainly of pinkish to pale grey, medium to coarse-grained, muscovite and muscovite-biotite adamellite which commonly contains abundant feldspar phenocrysts. Close to intrusive contacts the phenocrysts are aligned parallel to the margin of the granite, but away from such contacts the flow alignment is generally irregular and less well defined. Cross-cutting sheets of aplite and quartz-alkali feldspar-muscovite pegmatite are widespread, and xenoliths are present locally. In the adamellite the quartz is commonly strained to partly granulated. The sodic plagioclase shows some alteration to sericite, muscovite and clay. The alkali feldspar, mainly microcline, is variably turbid. Muscovite appears fresh but biotite is commonly partly altered to chlorite and epidote. Apatite, fluorite, zircon, and metamict and opaque minerals are common accessories.

Slatey Creek Granite

Rock types exposed are muscovite, biotite-muscovite, and biotite adamellite, and minor biotite granodiorite. The adamellite is similar petrographically to that of the Lewis Granite. Veins of aplite and muscovite-quartz-feldspar pegmatite are common, and dark fine-grained xenoliths are present in places. A weak foliation is developed locally.

The Granites Granite

Pink and grey biotite adamellite, the main rock type, is cut by veins of aplite and pegmatite. Most of the adamellite contains feldspar phenocrysts, and some contains poikilitic crystals of alkali feldspar over 1 cm across. It is generally similar to that of the Lewis and Slatey Creek Granites, but differs in commonly containing myrmekite and abundant accessory sphene, but only small amounts of muscovite.

Gardiner Sandstone

The glauconitic sandstone of the Gardiner Sandstone is generally medium-grained, and consists predominantly of quartz grains cemented by authigenic overgrowths of quartz. Mild deformation is indicated by slight undulose extinction in both detrital and authigenic quartz. The glauconite is a minor constituent in most samples, although it is abundant in one sample (1135), in which there is also some patchy glauconite cement. Other minor constituents include feldspar, lithic fragments, clay, and tourmaline.

Earthquake Risk in Australia

A. McEwin, R. Underwood*, and D. Denham

Earthquake risk maps of Australia were prepared using a computer program which selected events from a regional earthquake file and calculated maximum values of acceleration, velocity and intensity at the nodes of a half degree grid, using a scaling rule of the Kanai form $Y = ae^{bm}R^{-c}$. The parameters a, b and c determined by Esteva and Rosenblueth for the Western United States of America were used.

For each node on the grid the Y values were plotted against the return period (years) on logarithmic scales. The results, which were compiled from the period 1960-1972, were extrapolated to give expected values of ground acceleration, ground velocity and intensity for a fifty-year return period.

These values were plotted and contoured at the following zone boundaries:

Zone	0/1	1/2
Ground Acceleration	1 m/s ²	3m/s ²
Ground velocity	0.05m/s	0.15m/s
Intensity (MM)	6.5	8.0

The following nine Zone-2 areas together with the maximum expected ground accelerations for a fifty-year return period were delineated: Meckering (12m/s²); Gippsland (5m/s²); Picton (4.9m/s²); Cape Otway (4.5m/s²); Broome (4.2m/s²); Lower Eyre Peninsula (3.8m/s², excludes Port Lincoln); east of Carnarvon (3.2m/s²), and the Simpson Desert (4.0m/s²).

This paper gives the results of the application of one seismic zoning technique to Australia; it is however not a critical examination of zoning methods as such.

This collaborative work was undertaken following a recommendation by the National Committee on Earthquake Engineering (NCEE). One major objective of the NCEE is the preparation of building codes for the design of earthquake resistant structures. A sub-committee on seismicity was formed to examine in further detail the collation, co-ordination and assessment of information with the ultimate aim of producing a zoning map for engineering purposes. It recommended the preparation of contour maps of acceleration, velocity and intensity for the Australian mainland and Tasmania as an initial step toward preparing a zone map.

Compared with countries situated in tectonically active regions, like Japan, Australia is relatively aseismic, but there are regions where the earthquake risk is significant and can be quantified. With the growth of population in some of the regions of higher risk it is important that risk parameters are available to structural engineers, town planners, the Civil Defence and other interested bodies.

This is the first attempt to zone Australia, and follows the seismic zoning of North America (Milne & Davenport, 1969; Whitham, Milne & Smith, 1970; Davenport 1972; Stevens & Milne 1973). As such it should be regarded as preliminary.

Method

Data were taken from the BMR Earthquake Data File for the period 1/1/60 to 31/12/72 (Denham & Small, 1973). Before 1960 only six stations operated in Australia (Doyle & Underwood, 1965). These were generally insensitive instruments sited in coastal metropolitan areas and many small earthquakes were not detected. Since 1960 the seismic coverage of Australia has increased. More earthquakes are being recorded and more accurate magnitudes and hypocentres can be assigned. Currently about 500 earthquakes are located reliably each year in the continent. The post-1972 earthquakes had not been processed at the time of this project and were not used in the calculations.

The scaling rule used ($Y = ae^{bm}R^{-c}$) is of the Kanai form,

after Esteva and Rosenblueth (1964) where:

$$R = \sqrt{\Delta^2 + H^2 + Co^2} \text{ (km)}$$

$$\Delta = \text{Epicentral distance (km)}$$

$$H = \text{Depth to focus (km)}$$

$$Co = \text{Depth adjusting constant (20 km)}$$

$$M = \text{Magnitude}$$

Y represents either the maximum ground acceleration, ground velocity, or Modified Mercalli intensity at the given site (for M.M. Intensity $Y_i = \log_e Y$).

The constants a, b, c, were obtained by Esteva and Rosenblueth (*op. cit.*) in America and are given below.

Esteva and Rosenblueth Constants

		a	b	c
Ground	Acceleration	2000.0	0.8	2.0
	Velocity	16.0	1.0	1.7
Intensity		2980.0	1.5	2.5

They are probably not suited for use in Australia owing to different site, source and propagation path conditions. New values of the constants should be determined from Australian isoseismal maps and accelerograph triggerings when these become available. We are of the opinion that the values given by Esteva and Rosenblueth are too high for Australian conditions. Furthermore, as more data come to hand, regional differences may become apparent. We suspect for example that values for Western Australia are different from those for Eastern Australia. Nevertheless the results give a good indication of the relative earthquake risk from region to region.

The program RISK3, developed by R.U., was used to select the earthquakes and calculate and plot the values for each site. From the plots, the expected ground motions and felt intensities for particular return periods were determined, plotted at half degree intervals of latitude and longitude, and contoured to give a zone map (Figures 2, 3 & 4).

The criteria used for the zone boundaries are given below. They were adopted from recommendations by Bubb (1971) and McCue (1973).

* R. Underwood publishes with the permission of the Commissioner, Hydro-Electric Commission, Tasmania.

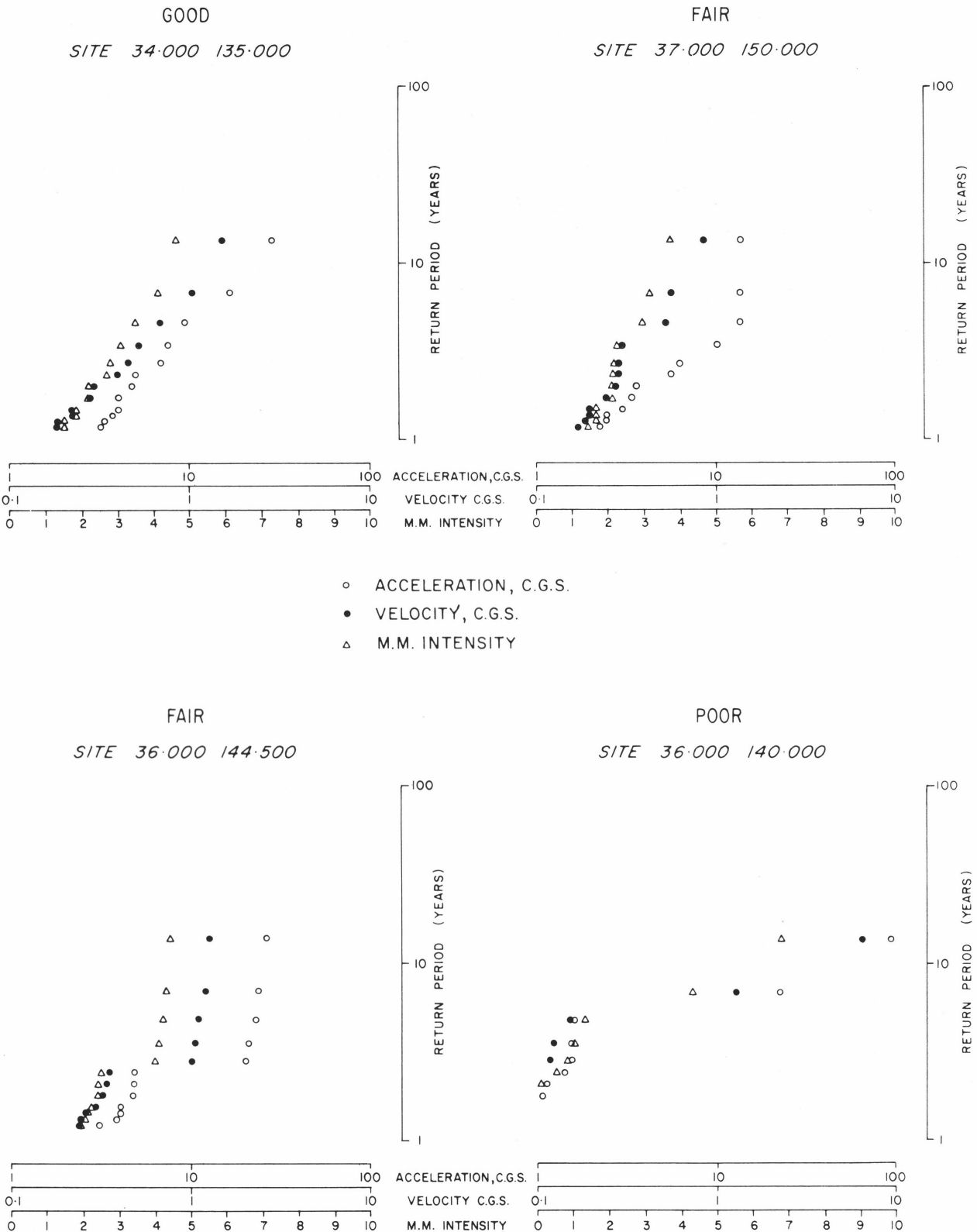


Figure 1. Examples of computer plots. The 12 highest values of acceleration, velocity and intensity are plotted against return period in years for each site. The data are extrapolated to obtain values for 50 year return periods.

Seismic Zoning Contours			
Criteria: 50-year Return Period			
Zone boundary	0/1	1/2	
Ground Acceleration	1 m/s ²	3m/s ²	
Velocity	0.05 m/s	0.15 m/s	
Intensity M.M.	6.5	8.0	

The area selected is traversed at a given increment (0.5 degrees was used in most of this work) on successive latitude lines separated by one increment.

If the event had no recorded depth, a depth of 5 km was assigned. The data file was searched for earthquakes: (a) magnitude 6 or greater occurring anywhere in the area covered by the date file, and (b) magnitude 1.0 or greater

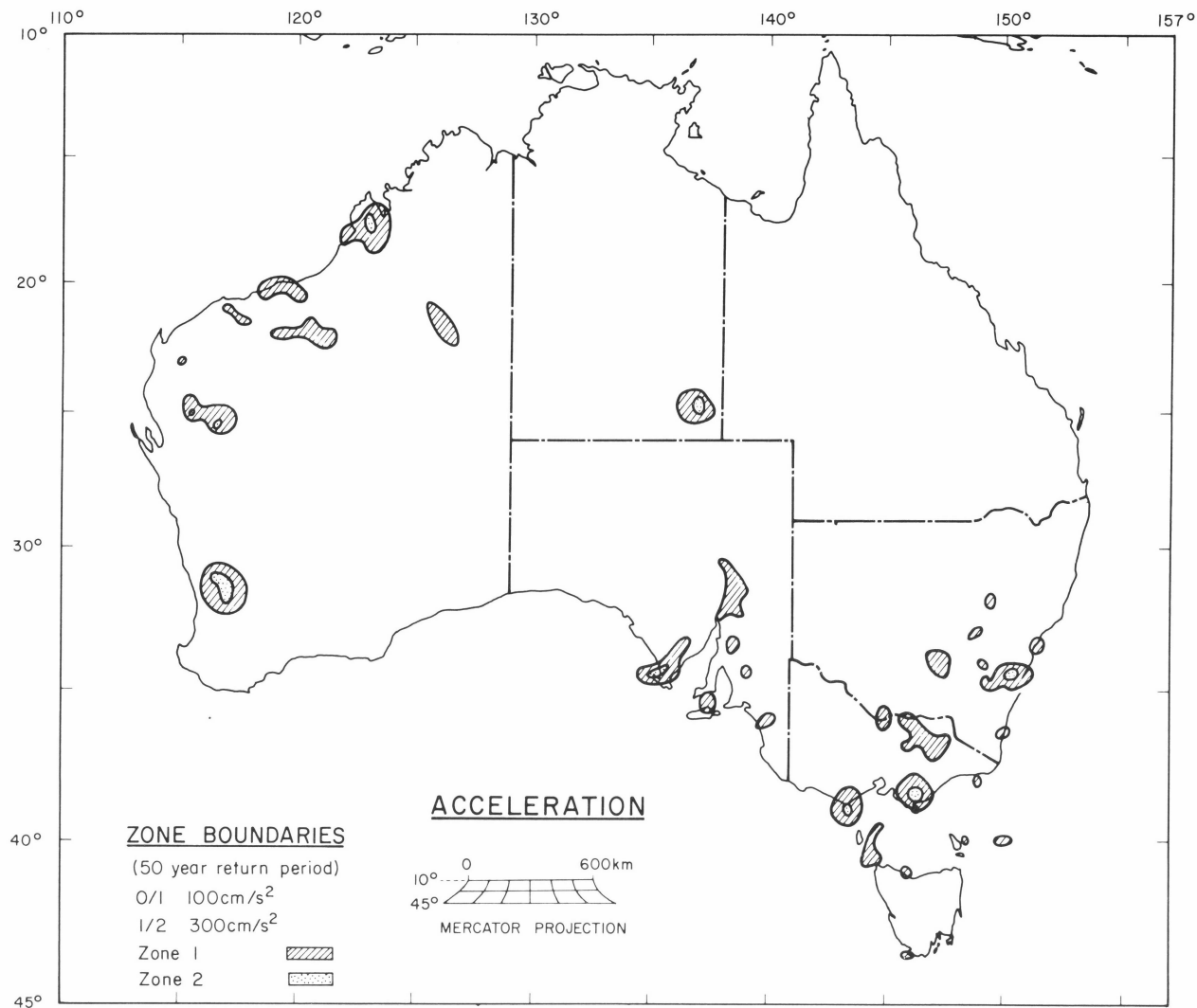


Figure 2. Acceleration (50 year return period)

and within 5 degrees in latitude or longitude from the site. For each earthquake in this subset, the peak ground acceleration was calculated at the selected site. Only if this was at least as large as a preset limit of 0.01 m/s² were the velocity and intensity values calculated. The above provisions economized on computer time, by avoiding the calculation of negligibly small site motions.

The peak ground acceleration values at each site were then sorted in order from largest to smallest and an empirical risk relation between log acceleration values and log return period was plotted. The return period (in years) of the *i*-th largest acceleration was given by

$$\frac{n + 1}{i}$$

where *n* is the number of years covered by the catalogue, in this case 13. The peak ground velocity and intensity values were treated separately, in parallel with the acceleration, except that the intensity was plotted on a linear scale. The twelve highest values of each parameter are plotted on graphs similar to those shown in Fig. 1. The data are extrapolated to obtain estimate of values for 50 year return periods. In regions such as southeastern Australia, where several hundred earthquakes are included in the data sets, the values lie closely on straight lines and it is assumed that the 50 year return period values are reliable. However when the data are patchy and only a few earthquakes are in the

data set the points do not lie close to straight lines and it is difficult to estimate reliable 50 year values. Fig. 1 shows typical plots ranging in quality from poor to good.

A straight line was drawn through the points, giving consideration to their distribution and trend to obtain extrapolations to 50-year return periods. A least-squares method was not used because of the small samples and the correlation between points. The larger ground motions were given greater weight in order to make conservative extrapolations. The values of the expected 50-year ground acceleration, velocity and felt intensity were plotted and contoured for zoning. A complete list of expected ground motions and felt intensities at the 10- and 50-year return periods for each site has been compiled.*

Results

A number of the small areas described hereunder which barely attain the Zone-1 criteria owe their existence to a bias towards high values of the 50 year ground motion introduced by the incompleteness of the data. This is especially so where a few large shocks have been reported but no close study has been made of minor seismicity. All results quoted are for a 50-year return period.

* Available on request from the Director, Bureau of Mineral Resources.

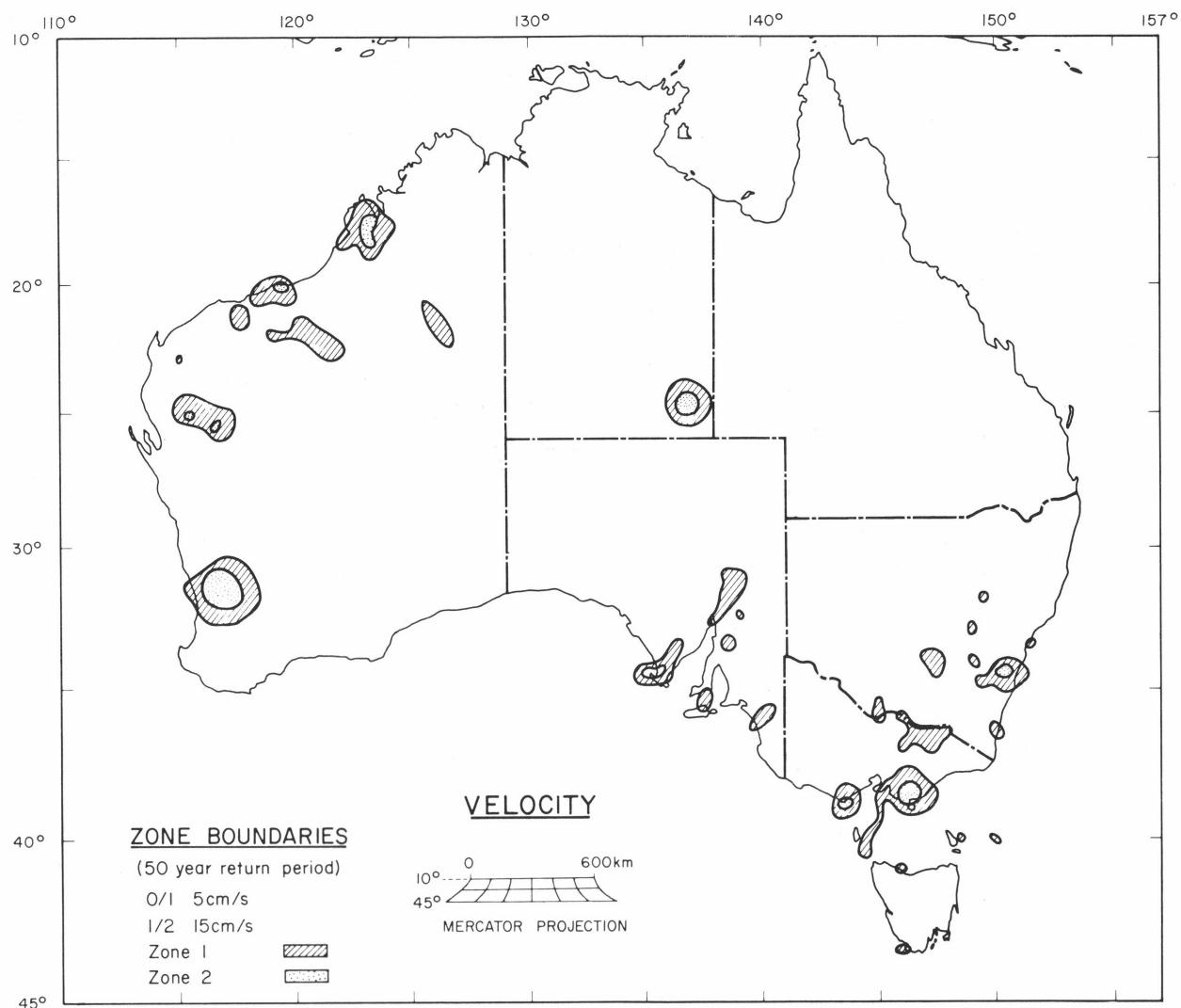


Figure 3. Velocity (50 year return period)

Western Australia

(a) Meckering 29S to 33S, 115E to 119E

The map of earthquake epicentres shows an elongate area in the southwest seismic belt (Fig. 5). A similar shape was expected for the risk map. On processing, a slightly elliptical northwest-southeast Zone-2, with maximum ground acceleration 12 m/s^2 at Meckering (31.6S, 117.0E) was delineated; it has a similar orientation but is not as narrow, nor does it extend as far south as the epicentre plot of the southwest seismic belt. The Zone-2 is centred on Meckering and includes Northam (31.6S, 116.6E), York (31.9S, 116.7E), Cunderdin (31.7S, 117.2E), and extends close to but does not include Wongan Hills (30.9S, 116.7E). The shapes of the zones have obviously been influenced by the Meckering sequence of October 1968, in their tendency to follow the shape of the Meckering isoseismal map.

The Zone-1 includes Brookton (32.4S, 117.0E), Beverley (32.1S, 116.9E), Kellerberrin (31.6S, 117.7E) and New Norcia (31.0S, 116.2E). Perth lies outside the Zone-1.

(b) Carnarvon 22.5S to 26S, 114.5E to 119E

Two Zone-1 areas were contoured. The larger begins 100 km east of Carnarvon (24.9S, 113.6E) and continues another 250 km eastward. It is dumb-bell shaped with two Zone-2 areas centred in the 'eyes' of the dumb-bell (maximum ground accelerations 3.2 and 3.0 m/s^2). The smaller

zone is 150 km south of Onslow (21.6S, 115.1E).

(c) Pilbara 17S to 23S, 117E to 122E

The three irregularly shaped Zone-1 areas in this region trend east-west. The first includes Port Hedland (20.3S, 118.6E) and Mt Goldsworthy (20.3S, 119.5E); the second Bamboo Springs (22.1S, 119.6E) and Nullagine (21.9S, 120.1E), and extends 150 km east of Nullagine; the third is southeast of Roebourne (20.7S, 117.1E).

(d) Broome 16.5S to 19S, 122E to 124E

A Zone-2 is centred between Broome (18.02S, 122.2E) and Derby (17.3S, 123.6E) (maximum ground acceleration 4.2 m/s^2). The Zone-1 contains Broome and Derby.

(e) Canning Basin 21S to 23S, 125.5E to 127E

The area contains a swarm of activity on the epicentral map but only one event survived sorting. No zoning is possible by the method used, so a Zone-1 was drawn subjectively to delineate the area of activity shown on the epicentre map.

Northern Territory

24S to 27S, 137E to 138E

In the period 1960 to 1972 only one earthquake greater than 5.9 occurred. This was in the Simpson Desert.

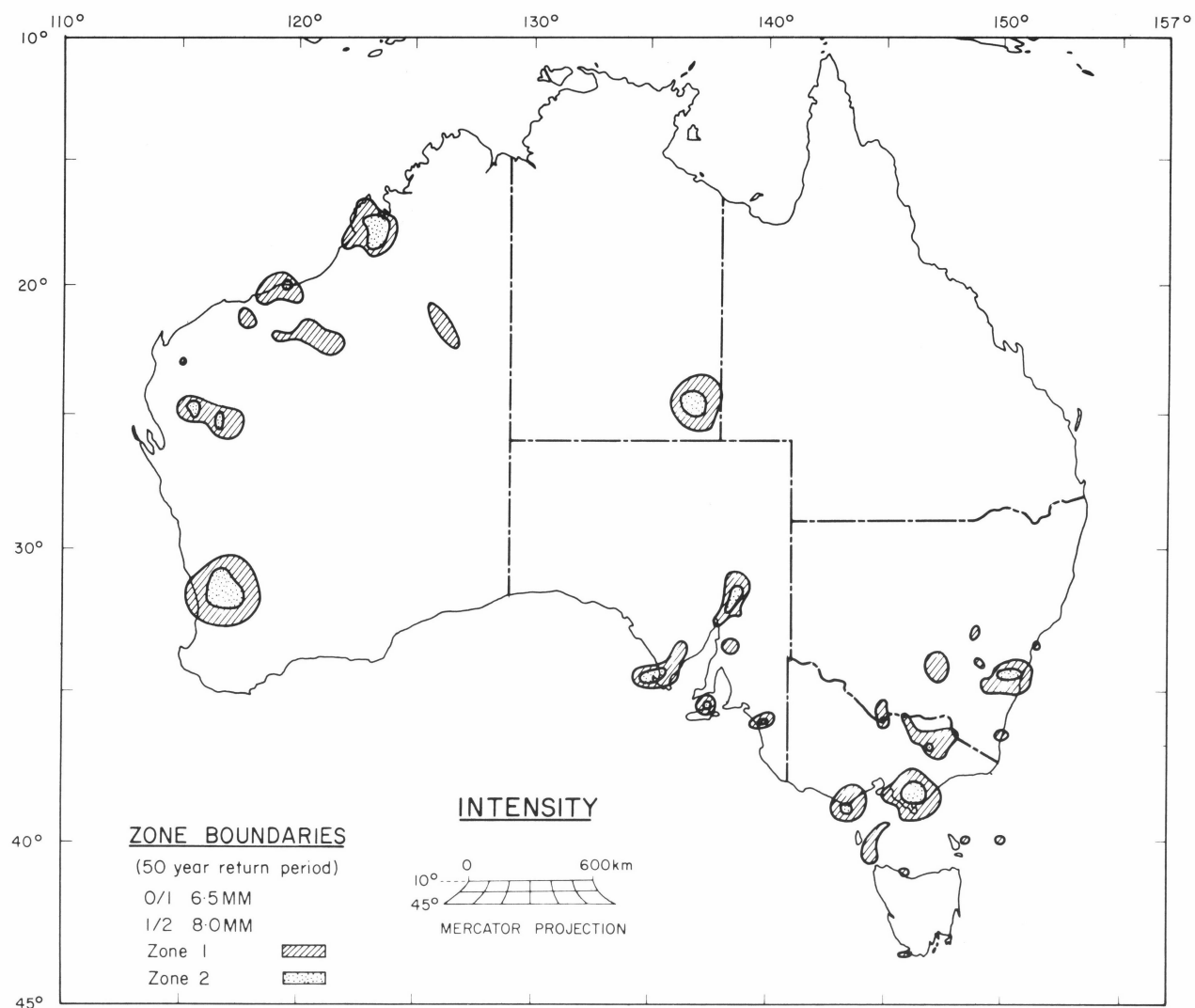


Figure 4. Intensity (50 year return period)

However, between 1937 and 1941 five events greater than 5.9 took place. Although these are not included in the analysis they confirm the Zone-2 designation (maximum ground acceleration 4 m/s^2) and if included in the study would give rise to a circular zone extending slightly farther south than the one shown.

South Australia

30S to 36S, 135E to 140E

Six areas of Zone-1, one with an associated Zone-2, are delineated.

The southern part of Eyre Peninsula has a small Zone-2, with a maximum ground acceleration 3.8 m/s^2 , which includes Cummins (34.3S, 135.7E) and Coffin Bay (34.5S, 135.3E). The zone-1 lies outside this area and includes Port Lincoln (34.7S, 135.9E), and Cleve (33.7S, 136.5E) and extends almost to Kimba (33.1S, 136.4E).

An irregular elongate Zone-1, centred on Hawker (31.9S, 138.4E), follows the Flinders Ranges from Parachilna (31.1S, 138.4E) to Mt Remarkable (32.8S, 138.2E) and Carrieton (32.4S, 138.5E).

The other Zone-1 areas are: centred on Spalding (33.5S, 138.6E), including Georgetown (33.4S, 138.4E), Jamestown (33.2S, 138.6E), Crystal Brook (33.4S, 138.2E), Brinkworth (33.7S, 138.4E) and Clare (33.8S, 138.6E); Tanunda (34.5S, 138.9E) and Truro (34.4S, 139.1E) extending north to the east of Hamley Bridge (34.4S, 138.7E); overlapping the

northern coast of Kangaroo Island (excluding Kingscote) (35.7S, 137.6E); and in the upper southeast extending, from the coast to Keith (36.1S, 140.3E) and Tintinara (35.9S, 140.0E).

Adelaide is not included in any zones. However, if the Adelaide 1954 earthquake had been included in the analysis the Zone-1 boundary would possibly extend to the south to include Adelaide.

Conservative zoning would probably include all these isolated areas in one general South Australian zone.

New South Wales

Eight Zone-1 areas, one of which includes a Zone-2, were delineated.

The Zone-2 area (maximum ground acceleration 4.1 m/s^2) is west of Wollongong (34.4S, 150.9E) and contains Mittagong (34.4S, 150.4E), Bowral (34.4S, 150.4E), Moss Vale (34.6S, 150.4E) and Picton (34.2S, 150.6E) (Verified by the Picton earthquake on 9/3/73). The surrounding Zone-1 includes Nowra (34.9S, 150.6E), Wollongong, Campbelltown (34.1S, 150.7E), Camden (34.0S, 150.7E) and the Dalton (34.7S, 149.2E)—Gunning (34.8S, 149.3E) region.

The following are seven minor local Zone-1 areas: Dunedoo (32.0S, 149.4E); Molong (33.1S, 148.9E); Gosford (33.4S, 151.3E) and Wyong (33.3S, 151.3E); West Wyalong (33.9S, 147.2E) and Temora (34.4S, 147.5E); between Crookwell (34.5S, 149.5E) and Cowra (38.8S, 148.7E);

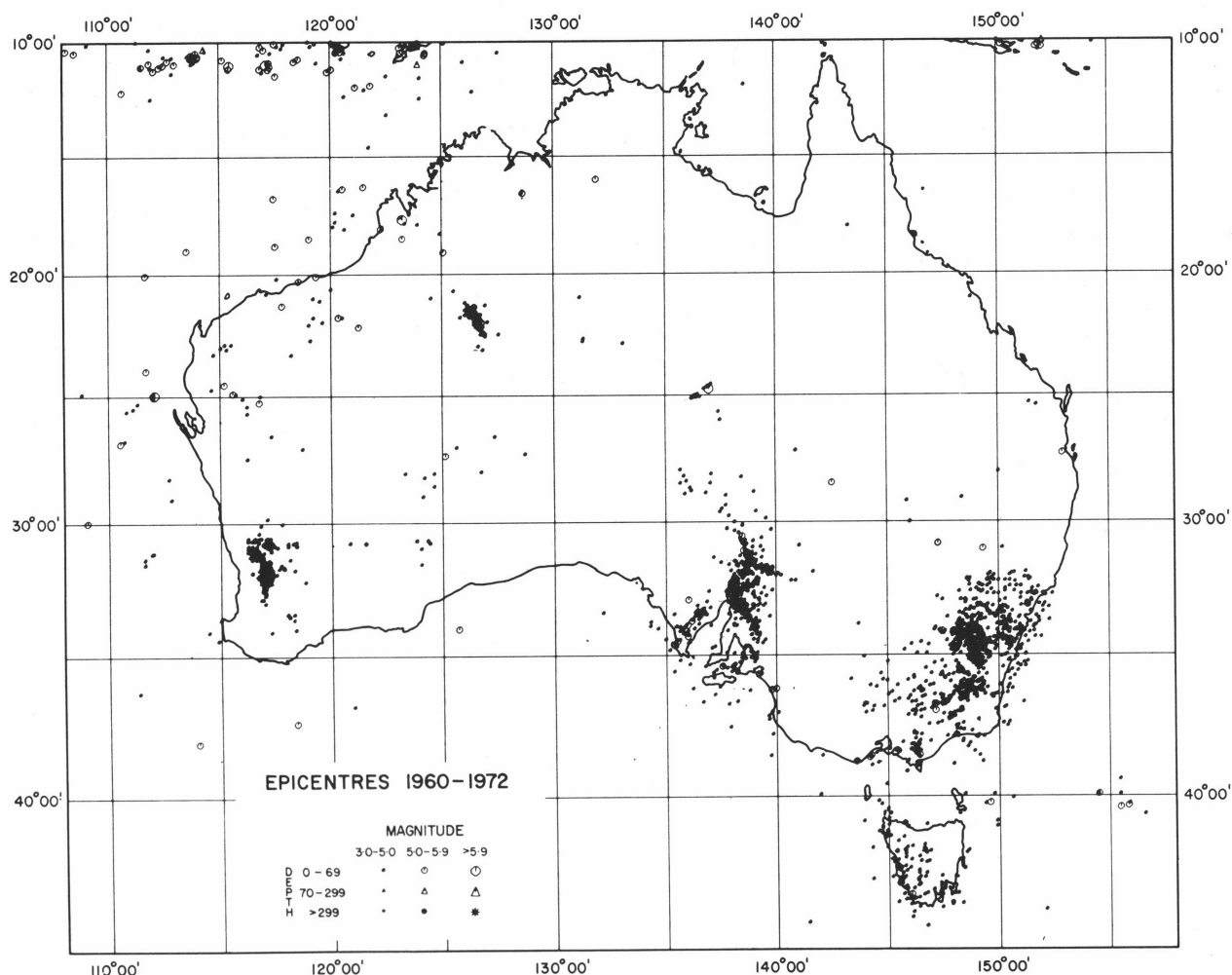


Figure 5. Earthquake epicentres (1960-1972)

Bega (36.7S, 149.8E) and Narooma (36.2S, 150.0E); the final one overlapping the Victorian-NSW border, includes Echuca (36.1S, 144.7E) and Deniliquin (35.5S, 145.0E).

The Dalton-Gunning region as originally zoned on a half-degree grid was below the Zone-0/1 boundary. Re-zoning on a quarter degree grid delineated the zone.

Victoria

Four areas, of which two attain the criterion for Zone-2, were delineated.

The larger Zone-2, with a maximum ground acceleration 5 m/s^2 , is centred in Gippsland containing Yarram (38.6S, 146.7E), Foster (38.6S, 146.2E), Morwell (38.2S, 146.4E) and Traralgon (38.2S, 146.5E). Wilson's Promontory (39.0S, 146.4E), Warragul (38.2S, 145.9E), Moe (38.2S, 146.2E) and Sale (38.1S, 147.1E) lie in the surrounding Zone-1.

The other Zone is centred on Cape Otway (38.9S, 143.5E), with a maximum ground acceleration 4.5 m/s^2 . The associated Zone 1 includes Cobden (38.3S, 143.1E), Colac (38.3S, 143.6E) and Lorne (38.5S, 144.0E). An irregular Zone 1 includes Benalla (36.5S, 146.0E), Euroa (36.7S, 145.6E), Mounts Buller (37.1S, 146.4E), Bogong (36.8S, 147.3E) and Buffalo (36.8S, 146.8E). The fourth is a minor Zone-1 offshore south of Cann River (37.4S, 149.1E).

Melbourne and Geelong (38.1S, 144.3E) lie outside the zoned areas.

Tasmania

Two of the five Zone-1 areas delineated encroach onto the main island. The first is at Southwest Cape (43.6S, 146.0E) and the second smaller one at Burnie (41.1S, 145.9E).

The other three lie in Bass Strait, two east of the Furneaux Group (40.2S, 148.1E), and the third an elongate north-south area east of King Island (39.7S, 144.0E) and extending south to the northwest coast of Tasmania.

Conclusions

This report describes one approach to seismic zoning. The size and shape of the zones are determined strictly from the input data: grid size, constants used in the Kanai formula, and the completeness of the seismic data input all have an influence, as does the judgement of the seismologist. No geological data have been taken into consideration.

As evidence in the Dalton-Gunning region the dimensions of the zoning grid have an effect on the contoured output. A larger grid spacing may miss zoned areas. It is doubtful whether a smaller spacing would give more meaningful results considering the other approximations involved. Owing to the spacing used, the error in fixing the zone boundaries is about 25 km.

The constants used in the Kanai formula are characteristic of the area for which they were derived. New constants should be derived for Australian conditions.

The contoured maps show the expected ground acceleration, velocity and felt intensity for a fifty-year return period. Attention is drawn to the unreliability of extrapolation to a fifty-year return period with only 13 years' data. However, the relative magnitudes of expected ground motions and felt intensity are indicated.

Many areas had insufficient data to consider zoning, e.g. Queensland, and large parts of Western Australia.

References

- BUBB, C. T. J., 1971—On the seismicity of Australia. *Commonwealth Department of Works Report*.
- DAVENPORT, A. G., 1972—A statistical relationship between shock amplitude, magnitude and epicentral distance and its application to seismic zoning. *University of Western Ontario, Canada—Engineering Science Research Report BLWT-4-72*.
- DENHAM, D., & SMALL, G. R., 1973—A new look at Australian earthquakes. *ANZAAS, 45th Congress*, **3**, 118-9 (Abstract).
- DOYLE, H. A. & UNDERWOOD, R., 1965—Seismological stations in Australia. *Australian Journal of Science*, **28**, 40-43.
- ESTEVA, R. L., & ROSENBLUETH, E., 1964—Expectos de temblores distancias moderadas y grandes. *Sociedad Mexicana de Ingerieria Seismica*, **2**, 1-18.
- MCCUE, K. R., 1973—Relative seismicity of Western Australia, Parts I & II. *Report to the Western Australia Public Works Department and the Commonwealth Department of Works*.
- MILNE, W. G., & DAVENPORT, A. G., 1969—Distribution of earthquake risk in Canada. *Seismological Society of America—Bulletin* 729-754.
- STEVENS, A. E., & MILNE, W. G., 1973—Seismic risk in the northern Yukon and adjacent areas. *Environmental-Social Committee Northern Pipelines, Task Force on Northern Oil Development, Government of Canada—Report* 73-7.
- WHITHAM, K., MILNE, W. G., & SMITH, W. E. T., 1970—Earthquake risks in Canada. *Canadian Underwriter*, **28**, 17-26.

The Transient Electromagnetic Method in Australia

B. R. Spies

Transient electromagnetic (TEM) test surveys have been made at various localities in Australia to evaluate the method. The test surveys described in this paper were made in the Rum Jungle, Mary River and Tennant Creek areas, Northern Territory. Good agreement was generally obtained between TEM results and those observed with other electromagnetic methods, and good correlation was obtained with geology. The theoretical advantages inherent in the method make it attractive under Australian conditions of conductive overburden, and field test results demonstrate these advantages. It was found that the TEM equipment could be used in areas where topography or highly conductive surface conditions severely limit the effectiveness of other geophysical methods. The use of large loops with sides 100-150 m enable large areas to be surveyed quickly, while smaller loops proved useful in delineating anomalies accurately. Different loop sizes with loop-overlap were used to assist quantitative interpretation.

Transient electromagnetic scale modelling programs have also been made and two examples are given which demonstrate how interpretation can be improved by such programs. A model study of the Woodlawn copper-lead-zinc deposit indicated that the orebody would have been detected at depths of up to 200 m. Modelling an area known as the Gubberah Gossan in the Northern Territory demonstrated that the anomaly pattern could be caused by resistive quartz-sphalerite mineralization in a conductive carbonaceous shale unit.

Electromagnetic (EM) methods have been used in mineral exploration for more than fifty years and have been particularly successful in the search for sulphide ore deposits. These methods provide the possibility of detecting subsurface electrical conductors by the use of ungrounded loops and can be used in either a reconnaissance or detailed mapping mode. Most electromagnetic systems operate in the frequency domain involving continuous transmission at a fixed frequency. A more recent development is that of time domain electromagnetic systems in which pulses are transmitted and the transient decay of any resultant secondary field is recorded during the interval between the pulses. The name commonly applied to such systems is transient EM or TEM.

The concept of using electromagnetic transient signals in prospecting for conductive orebodies was advanced upon theoretical grounds by Wait in 1951. Since then, Russian investigators have been particularly active in the development and application of the method (Velikin & Bulgakov, 1967). In addition an airborne version of the method developed by Barringer Research and known as Input, has been used successfully (Boniwell, 1967).

The transient electromagnetic method has been used in Australia for a number of years. The Input system was first flown in Queensland in 1964 and has been used in other parts of Australia since then. The first Russian-built ground transient electromagnetic system came to Australia in 1970 and several are now in operation. Several companies have now developed their own ground systems which overcome some of the instrumental problems present in the earlier equipment.

This paper presents some aspects of experimental investigations made by the Bureau of Mineral Resources (BMR) as part of a program to evaluate the application of the transient electromagnetic method in Australian conditions, and deals with field results and scale model studies using the Russian-built MPPO-1 equipment. Areas for field tests (Fig. 1) were chosen on the basis of geophysical and geological controls being available. The field results are compared with those of other geophysical methods commonly used, such as Turam, Slingram, VLF, self-potential and induced polarization.

Basic Theory

Any transient electromagnetic system basically operates on the principle of inducing eddy currents in the ground and analysing their decay to provide information on subsurface conductors. The changing current in the transmitting loop generates a magnetic field in the surrounding environment which in turn induces electric fields in any nearby conductors, producing eddy currents. These induced electric fields depend on the conductivity, shape and size of the conductor and its position with respect to the loop. After their initial establishment, the eddy currents in the conductor tend to diffuse inwards towards the centre of the body, being gradually dissipated by resistive heat losses. With a highly conducting body, the currents tend to circulate on the boundary of the body and to decay more slowly.

The eddy currents, and accordingly the secondary magnetic field, decay within a relatively short time depending on the physical and geometrical properties of the conductor. The receiving coil obtains an output voltage proportional to the time derivative (rate of decay) of the vertical component of the secondary field. In general, the



Figure 1. Locality map

resistivities of rocks and mineralization encountered produce transient decays lasting from a fraction of a millisecond to more than 20 milliseconds.

Electromagnetic methods in general have met with varied success in Australia; intensely weathered conductive near-surface rocks and saline water commonly make it difficult to produce and record a response from an underlying conductor. The transient electromagnetic method offers the opportunity to overcome this problem. An analysis of the shape of the received waveform is equivalent to analysing the response at a number of frequencies for a harmonically varying source. Although the transient curve involves the whole frequency spectrum, different elements contain differing proportions of high and low frequency components. Morrison, Phillips & O'Brien (1969) point out that at early times the response is due to both low and high frequency groups whilst at later times only the low frequency response remains. They also point out that this hypothesis, coupled with the fact that skin depth varies inversely as the square root of the frequency, suggests that the early part of the transient is governed by rapid decay of high frequency energy which has penetrated to only shallow depths, whereas the later part of the response is due to lower frequency energy which has penetrated to greater depths. This result has been verified by Velikin & Bulgakov (1967) and proved theoretically by Wait (1956), Negi & Verma (1972) and others.

Field Results

Rum Jungle

The first example is an area near the Rum Jungle mine, 8 km south of Batchelor, Northern Territory. The geology of the area has been described by Walpole et al. (1968) and consists essentially of rocks of the Lower Proterozoic Golden Dyke Formation. The dominant lithologies are dolomitic and carbonaceous siltstone, quartz siltstone, chert, and dolomite. The carbonaceous siltstone is in part pyritic.

Previous geophysical surveys in the area revealed strong electrical and electromagnetic anomalies over a highly conducting graphitic pyritic black shale bed (Shatwell & Duckworth, 1966; Farrow, 1967; and Duckworth, 1968). The rocks adjacent to the bed are resistive. Laboratory measurements show that the black shale has conductivities greater than 0.1 S/m below the oxidized zone (15 m) and is less conductive in the oxidized zone.

The results of a TEM survey and a comparison with other methods are shown in Figures 2 and 3. The TEM results are presented in the form of profiles of response $e(t)/I$; that is, the induced voltage $e(t)$ in the loop normalized with respect to the primary current I , measured at a particular sample time t . The fact that the anomaly persists for all sample times indicates that the bed is a strong conductor. A useful parameter is the decay time constant, τ , which tends to a limiting value, τ_0 , at late times, and is related to the conductivity and size of the body. In this case τ_0 is 6.3 ms.

From Figure 2 it can be seen that all methods used give a strong anomaly over the conducting black shale bed, in agreement with the TEM results. The asymmetry of the TEM anomaly in Figure 3 reflects the dip of the bed. The profile for 1.1 ms peaks to the right hand side of the profile shown, whereas for late sample times the maximum occurs further to the left. The response at early sample times is due to the less conducting weathered near-surface shale and to the upper parts of the unweathered conducting shale beds. At later sample times it is due to the deeper, more conducting section of the shale bed. Thus by examining the shape of the profiles at different sample times it is possible to infer the dip of the body. It is also possible to infer the dip from the Turam results, in which the peak of the anomaly using 220 Hz is offset from that of the 660 Hz anomaly.

Mary River

This area lies 130 km southeast of Darwin, Northern Territory. Rocks exposed belong to the Lower Proterozoic Masson Formation and consist of interbedded quartzite, greywacke, sandstone, siltstone and carbonaceous shale. However outcrop is poor and most of the area surveyed is flat and covered by up to two metres of alluvium and seven metres of ferricrete. Cullin Granite crops out to the south of the area.

A grid of 2.5 km² was surveyed with a variety of geophysical methods in a reconnaissance survey of the area (Michail, 1974), and the results were used for comparison with a subsequent TEM survey. The TEM survey using 150 m loops was completed in 3½ days which demonstrates that the method can be used for rapid reconnaissance. Contours of TEM response for $t = 1.1$ and 15.3 ms are presented in Figure 4. At early sample times, high values of $e(t)/I$ occur over the entire area which indicates that a large amount of conductive material is present. Examination of the transient decay curves in Figure 5 at locations C and D reveals that they can be approximated by a straight line with a slope of -2.5 . The curves are drawn on a log-log scale so that power relations are evident.

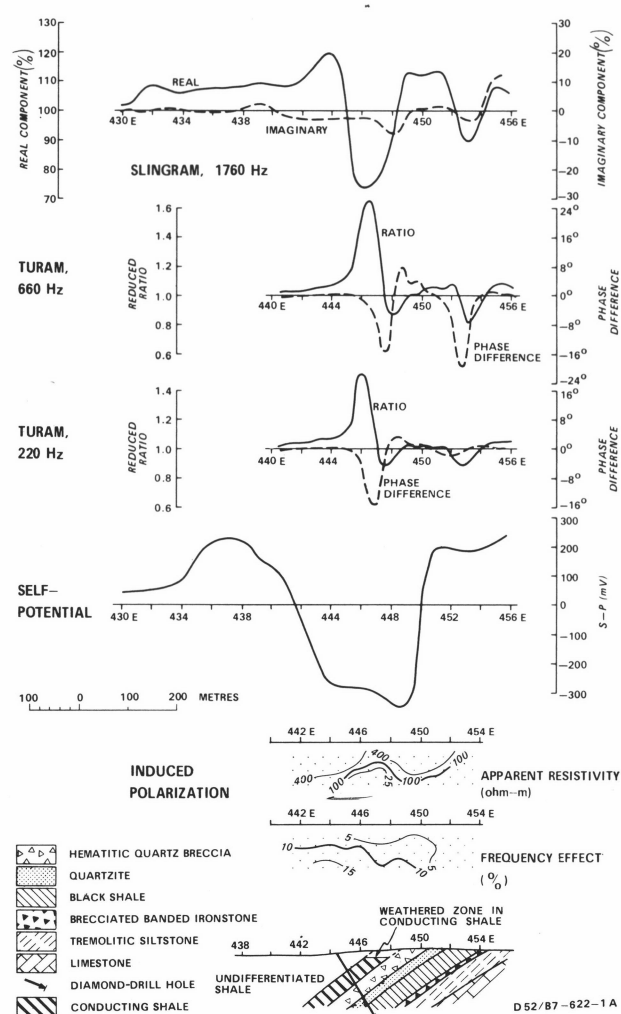


Figure 2. Rum Jungle, comparison of geophysical methods

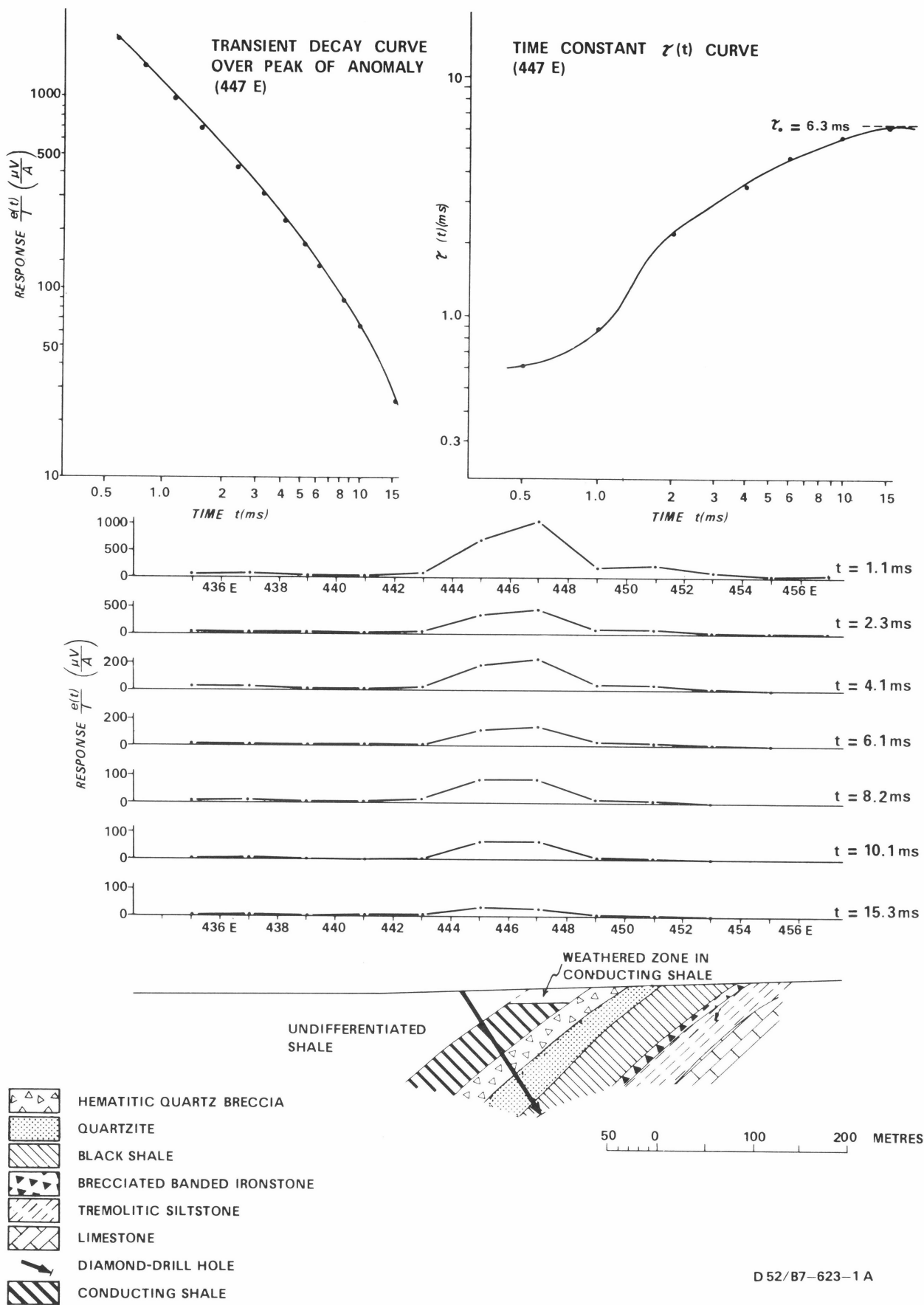


Figure 3. Rum Jungle, TEM profiles and geological section

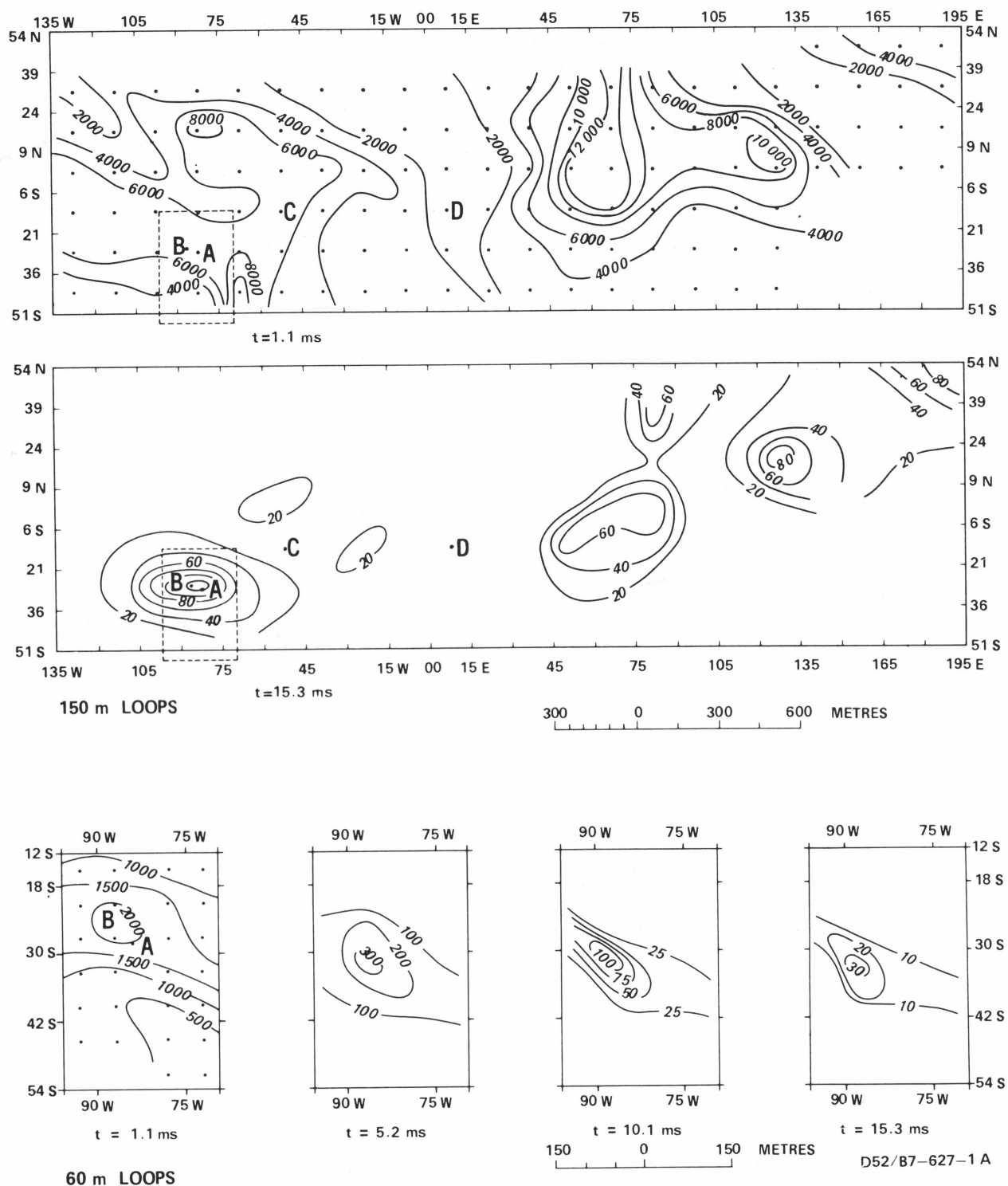


Figure 4. Mary River, TEM contours

The asymptotic expression for the response of a homogeneous half-space at late times derived by Lee & Lewis (1974) is given by the formula

$$E(t) \approx \frac{-bI\mu\sqrt{\pi}}{20t} \left(\frac{\sigma\mu b^2}{t} \right)^{3/2} \dots (1)$$

where

σ = conductivity of the half-space, S/m

μ = magnetic permeability, H/m

b = radius of circular loop, m

t = time, seconds

I = current in loop, amp

When using a square loop of side, d , $b = d / \sqrt{\pi}$ is used.

This expression is of the form $E(t) \propto t^{-2.5}$, so that when the decay curve is plotted on a log-log scale a slope of -2.5 is obtained. Thus the responses at the two locations C and D fit the theoretical expression for a homogeneous half-space, and substituting values the conductivity is calculated as 0.5 S/m at C, and 0.01 S/m at D. These results are interpreted as being due to a conducting carbonaceous shale sequence with a varying graphite content.

The contour map for $t = 15.3$ ms shows three well-defined anomalies which are caused by rocks of very high conductivity as evidenced by the decay curve for locality A, which has a higher amplitude and decays more slowly than

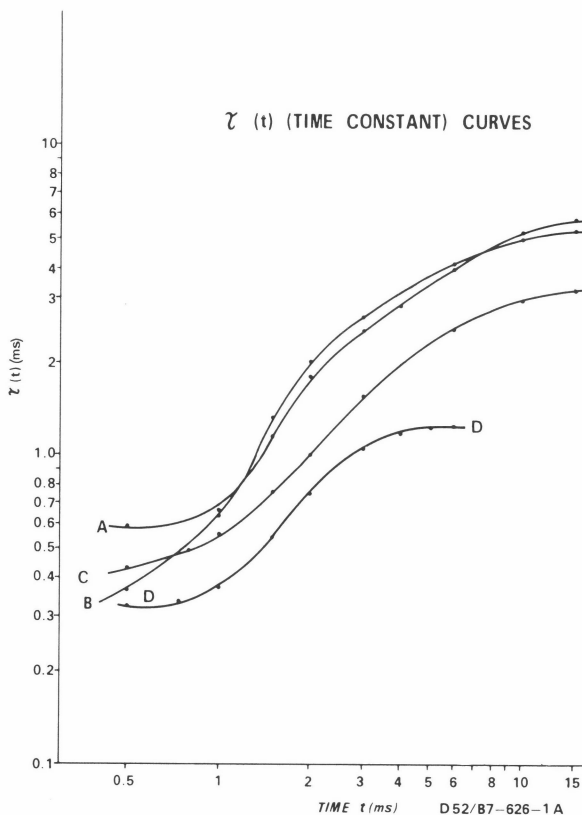
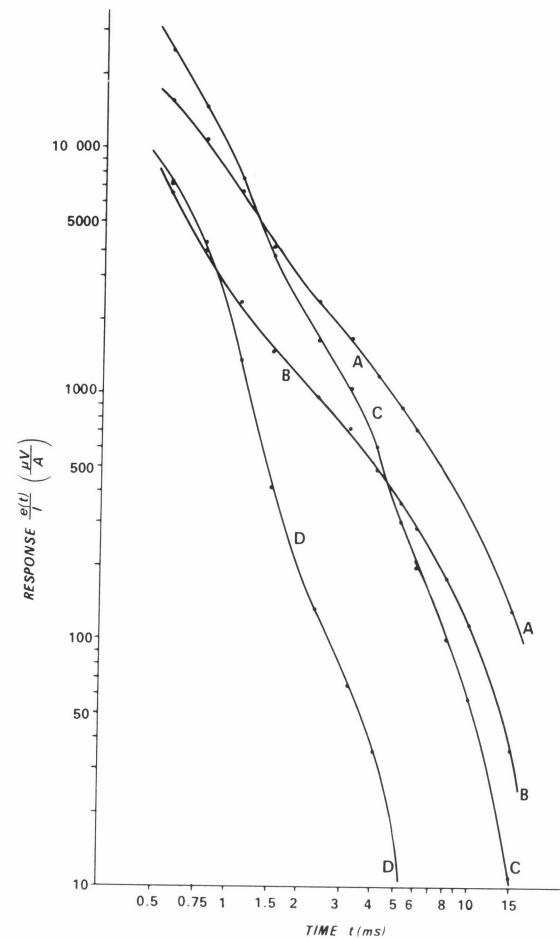


Figure 5. Mary River, transient decay curves

the curves at localities C and D.

The western anomaly was surveyed in more detail using 60 m loops (Fig. 4). At 1.1 ms the anomaly is still fairly broad whereas at later times it narrows to become a thin elongated feature indicative of a narrow and highly conducting source. Referring again to the transient decay curves it is interesting to note the similarity between the shape of the transient decay curves obtained at locality B using a 60 m loop and the shape at locality A using a 150 m loop. The curves have different amplitudes but have the same decay time constant, which at late times approaches 5.5 ms.

A vertical drill hole sited at B to test the TEM anomaly intersected pyrrhotitic carbonaceous shale underneath surficial deposits (I. Hone, pers. comm.).

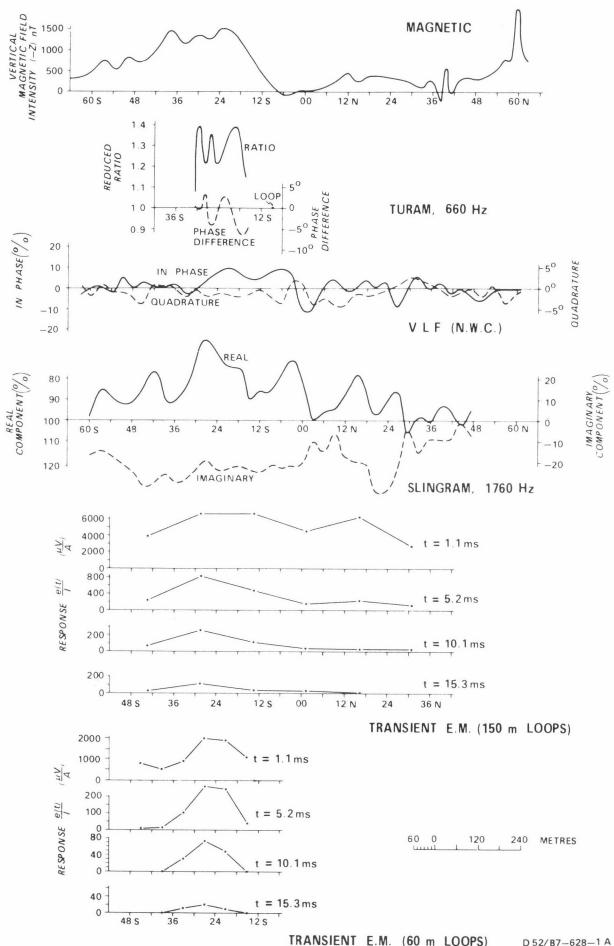


Figure 6. Mary River, comparison of geophysical methods

The results of TEM, magnetic, Slingram, Turam and VLF methods in this area are compared in Figure 6, which presents a north-south profile across the main anomaly. The association of a distinct magnetic high with the anomaly at 28S suggests rock alteration attributable to the nearby Cullen Granite intrusion.

The Slingram data reveal numerous complex anomalies which tend to be more pronounced in the real component than in the imaginary, indicating their sources to be moderate conductors. These conductors are considered to be within the zone of oxidation as the frequency used was fairly high (1760 Hz). The TEM anomaly is not reflected distinctly by the Slingram data, the latter probably representing only conductivity changes in the surficial layers.

The Turam profile was of limited length owing to very low

signal strength in the conducting environment at distances greater than 200 m from the primary loop. Results from the Turam work in general were similar to those from Slingram and did not contribute any additional information of significance.

Neither VLF, nor self-potential data (not presented) yielded distinctive anomalies or results which could be sensibly correlated between adjacent traverses or with other geophysical data.

It can be inferred from the results that surficial deposits of moderate conductivity represent the sources of the extensive EM anomalies recorded in the area. Greater resolution of conductor axes was possible from Turam and Slingram results than from TEM results. However, the Turam and Slingram data reflect near-surface conductors whereas TEM data recorded at late sample times highlight anomalies from unweathered conductive rock beneath surficial conducting material.

Tennant Creek

The next example comes from an area 10 km west of Tennant Creek, Northern Territory. The area contains Lower Proterozoic greywacke and shale of the Warramanga Group, intruded by quartz-feldspar porphyry and containing ironstone bodies which are often associated with gold or copper mineralization (Crohn & Oldershaw, 1965). The ironstone bodies are mostly quartz-magnetite bodies below the water-table but the magnetite has been altered either partially or completely to hematite in the oxidized zone; the depth of oxidation is usually greater than 70 m.

A TEM survey was made over a known hematitic

ironstone body which had been wagon-drilled (Hone, 1974). The body, which is in a shear zone, is within 2 to 8 m of the surface and extends to a depth of at least 70 m.

The TEM profiles presented in Figure 7 show a low over the body with peaks on either side. Double-peaked anomalies can be obtained over bodies at shallow depth, the distance between the peaks being approximately the size of the loop (Velikin & Bulgakov, 1967). However in this case the distance between the peaks is 600 m and the loop size is 100 m. It is more likely that the peaks reflect differences in thickness and/or conductivity of the overburden. The decay curve at 750N is presented in Figure 8 and appears as a straight line on a log-linear scale. This response is simple exponential and is typical of a thin horizontal conductive sheet (Velikin & Bulgakov, 1967; Becker, 1969). Velikin & Bulgakov have defined the product of the thickness and conductivity of a sheet as 'longitudinal conductance', S , where S , for early sample times (up to 2 ms), is given by the equation:

$$\frac{e(t)}{I} = \frac{3\pi}{16} \frac{1}{S} \left(\frac{\mu SR}{t} \right)^4 \quad \dots\dots(2)$$

where $e(t)/I$ is response, volts/amp
 t is time, seconds
 R is half loop size, metres
 μ is magnetic permeability, which is $4\pi \cdot 10^{-7}$ H/m in free space.

The response could be due to conductive surficial deposits or zones of saline water in the substratum. Making use of equation (2) S varies from 8 to 6 siemens across the profiles for $t = 1.1$ and 1.5 ms, so that if, for example,

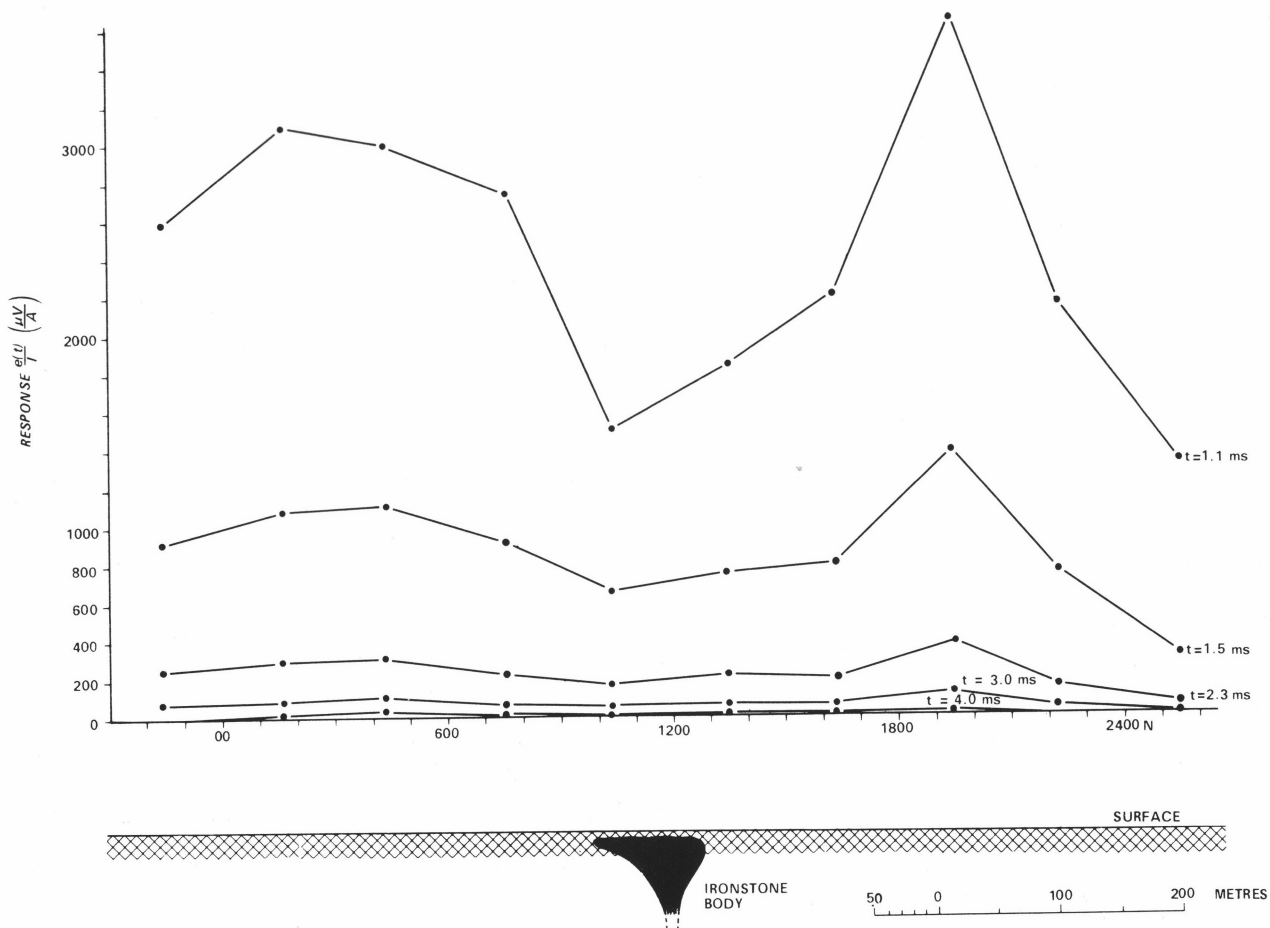


Figure 7. Tennant Creek, TEM profiles and cross-section of ironstone body

the conductive layer was 10 m thick, the conductivity would vary from 0.8 to 0.6 S/m. Conversely the thickness of the layer could change assuming a constant resistivity.

Laboratory tests on ironstone samples from the Tennant Creek area showed that ironstone often has conductivities less than 0.001 S/m which implies that surrounding strata should be more conducting. The low TEM readings over the ironstone body are interpreted as being due to thinning of the overburden.

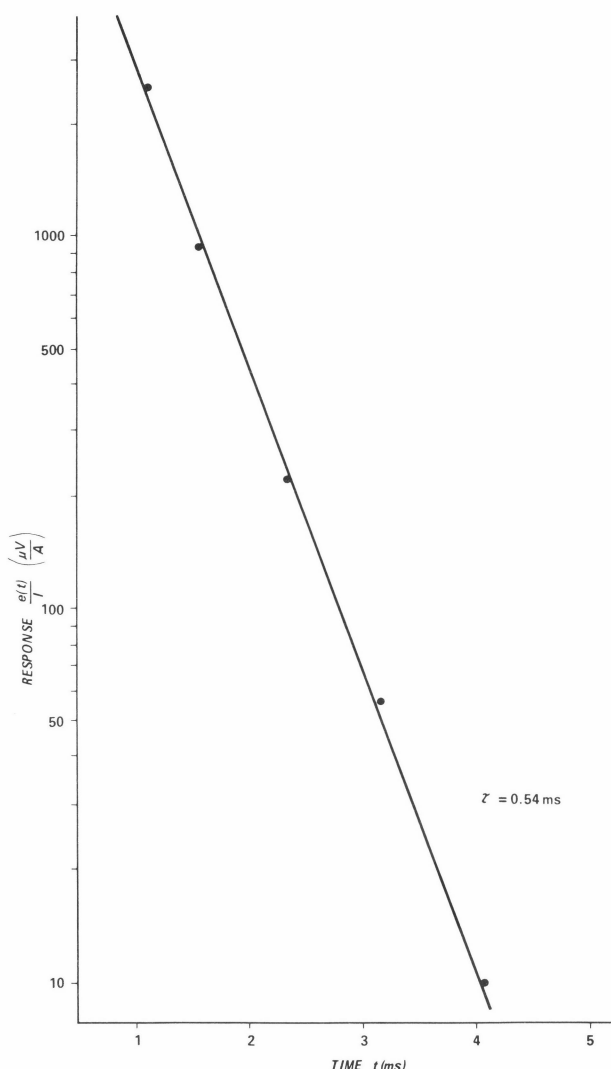


Figure 8. Tennant Creek, transient decay curve

Scale Model Studies

Scale model studies are often used to study the structure of electromagnetic fields when the numerical approach is unreasonably difficult. Mathematical expressions for TEM response are quite complicated and can only be applied to bodies of simple geometrical shape.

Model studies were useful in gaining an insight into responses produced by bodies of different size, shape and conductivity to aid interpretation of field results. References to TEM modelling are restricted to American workers who modelled the Input system (Becker, Gavreau & Collet, 1972) and Russian workers who used the MPPO-1 equipment (Velikin & Bulgakov, 1967; Bulgakov, 1971a &

b; Bulgakov & Zhirnova, 1971). In the model studies described in this paper the field equipment was used and only minor modifications were necessary. Models representative of various field situations were also studied and results compared with field data. This assisted interpretation and the design of follow-up surveys.

Theoretical Considerations

A description of the basic theory of scaling electromagnetic models is given by Frischknecht (1971). The general modelling relationship which enables similitude to be assumed between a field (full scale situation) and a laboratory model is

$$\sigma_m \mu_m \omega_m L_m^2 = \sigma_f \mu_f \omega_f L_f^2 \quad \dots (3)$$

where the subscript f indicates a quantity measured in the field situation, and the subscript m indicates a quantity measured in the model, and

- σ = conductivity (S/m)
- μ = magnetic permeability (H/m)
- ω = 2π frequency (Hz)
- L = linear dimensions (m)

For a time domain system time T can be substituted for $1/\omega$. The magnetic permeability is usually assumed to be that of free space for both the field situation and the model. Using equation (3) it is possible to describe the geometrical structure of electromagnetic fields and determine dimensionless parameters such as the ratio of secondary field amplitude to primary field amplitude, and field direction. However when modelling TEM fields it is also necessary to simulate the absolute dimensions of the measured quantity $e(t)/I$ in the model and an additional expression given by Spies (in press) must be used in conjunction with (3):

$$e(t)_m/e(t)_f = L_m T_f/L_f T_m \quad \dots (4)$$

The two examples which follow had a model of aluminium in air. Time was not scaled and loops of 50 turns were used. The approximation of infinite resistivity of the host rock was considered valid because of the very large conductivity contrasts encountered in the field and in laboratory measurements on drill core.

Woodlawn Copper-Lead-Zinc Deposit

The Woodlawn deposit is located 12 km west of Tarago, NSW, and is contained within the Silurian acid volcano-sedimentary succession of the Lachlan Geosyncline. The orebody is a concordant lens of bedded, high grade copper-lead-zinc sulphides which dips west at about 45° . The oxidized zone is approximately 12 m thick consisting mainly of ferruginous clay, and has a sharp contact with the sulphides (Malone et al., in press).

The model used was a tabular sheet of aluminium in air; the scaling factor used was 1300 and this gave a geological model with the following parameters: thickness 16.5 m, dip 45° , depth 12 m and conductivity 20 S/m. This model was only an approximation of the field situation because it was known from drill hole data that the orebody varied in thickness, dip and strike along its length. The value for conductivity was chosen on the basis of downhole resistivity measurements which indicated a conductivity contrast of over 10 000 between the orebody and the country rock and so justified the use of a metallic model in air to simulate the geological situation.

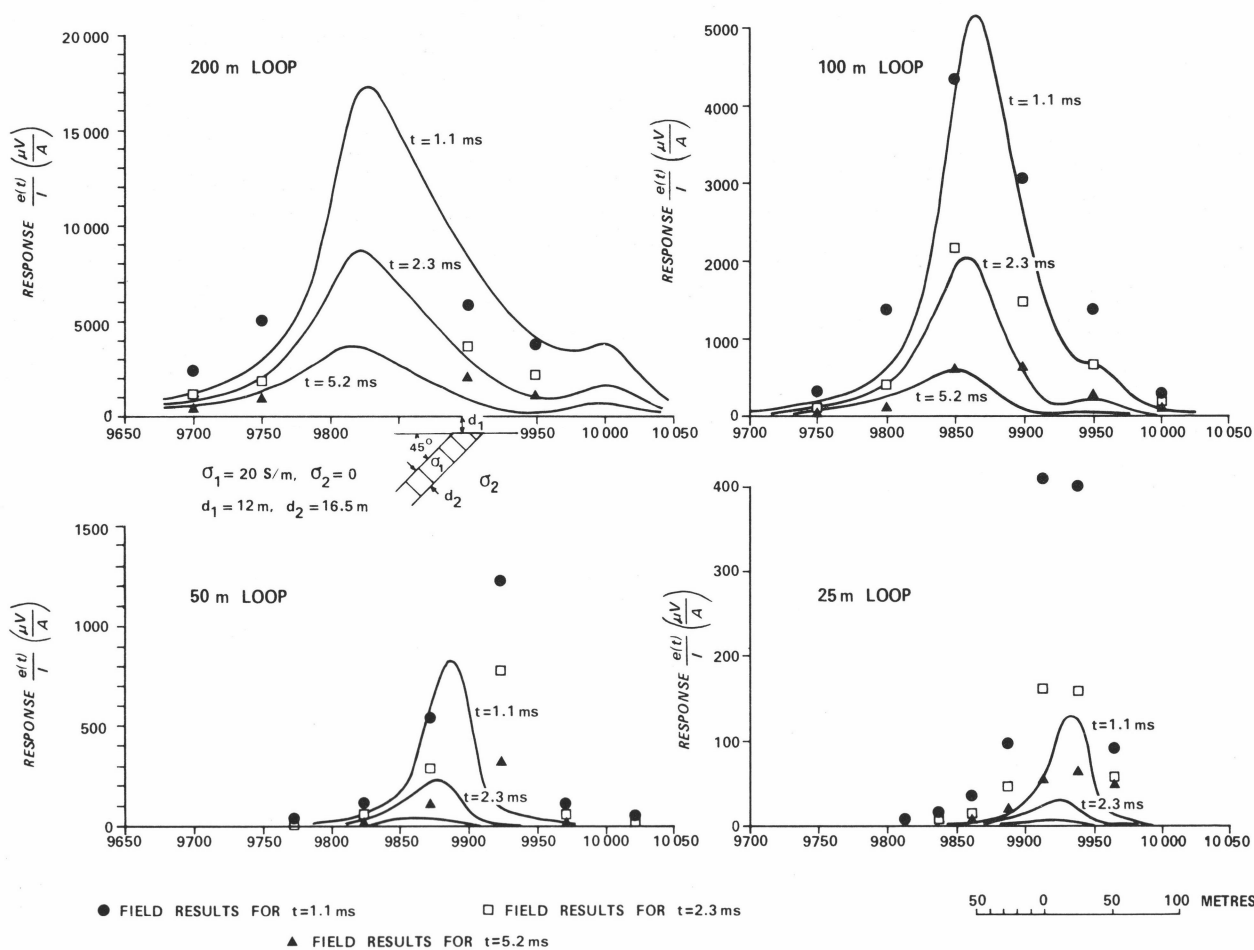


Figure 9. Woodlawn copper-lead-zinc deposit, comparison of field results and model study

Results of the model study are shown in Figure 9. Profiles are presented for 200, 100, 50 and 25 m loops for times $t = 1.1, 2.3$ and 5.2 ms. Field results from Young (in prep.) are shown as dots on the profiles. The model profiles have been reduced in amplitude by 25 percent to allow a better curve fit; this implies that the chosen conductivity of 20 S/m was somewhat too high or the model was too thick.

The best curve fit is for the 100 m loop, in which 50 percent loop-overlap was used. The results for the 200 m loop show that the loop-overlap was not sufficient to define the shape of the anomaly, the centre of which was missed entirely.

Results for the 50 m and 25 m loops show considerable scatter of field data from the model profiles. The tendency for field values to exceed model values can be explained by the model being too deep. If some conducting material was present closer to the surface (within the zone of oxidation) the response from the smaller loops would be increased without significantly changing the responses obtained from the larger loops.

In addition to amplitude differences, some loop sizes produced lateral displacement of the anomaly. The depth penetration of TEM is dependent on the size of the loop, so differences in curve fit can in part be explained by the non-uniform dip of the body.

Model profiles were also produced for different depths of burial of the orebody. The results are presented in Figure 10 for $t = 1.1$ ms. It is apparent that the larger the loop size, the greater is the depth penetration. The curve for the 100 m loop shows that if the threshold resolution of an anomaly is 50 microvolts/amp, the body can be detected to depths of

100 m. For a 200 m loop the range of detectability increases to 200 m.

The limits of threshold resolution involve geological noise, and loop size. The larger the loop size the greater is its response to electrical interference, and small amplitude readings become less reliable.

Several results emerge from this study:

1. The amount of loop-overlap necessary to define the anomaly form depends on both the loop size and the size of the target. In this example it would be necessary to use 75 percent loop-overlap for the 200 m loop, and 50 percent loop-overlap for the 100 m loop. For smaller loops no overlap is necessary.
2. The model chosen was an approximation, erring in either too high a conductivity being attributed to the orebody, or too great a thickness being used. The oxidized zone was assumed to be resistive but is probably fairly conductive and so contributes to the responses obtained with the smaller loops.
3. The results of the model study indicate that the orebody may have been detected at depths of up to 200 m. The results also show that large loops have a greater depth penetration than small loops.

Gubberah Gossan

The Gubberah Gossan is located 3 km northwest of the Mary River area described earlier (Fig. 1) and has been surveyed with the TEM method (Spies, 1974). The geology of the area (similar to that of Mary River) and drill hole data are given by Daly (1971). The main TEM feature observed was a discontinuous northwest-trending anomaly

which coincided with self-potential and Turam anomalies described by Michail (1974). The area is one of high topographic relief which rendered the other electromagnetic methods tried ineffective.

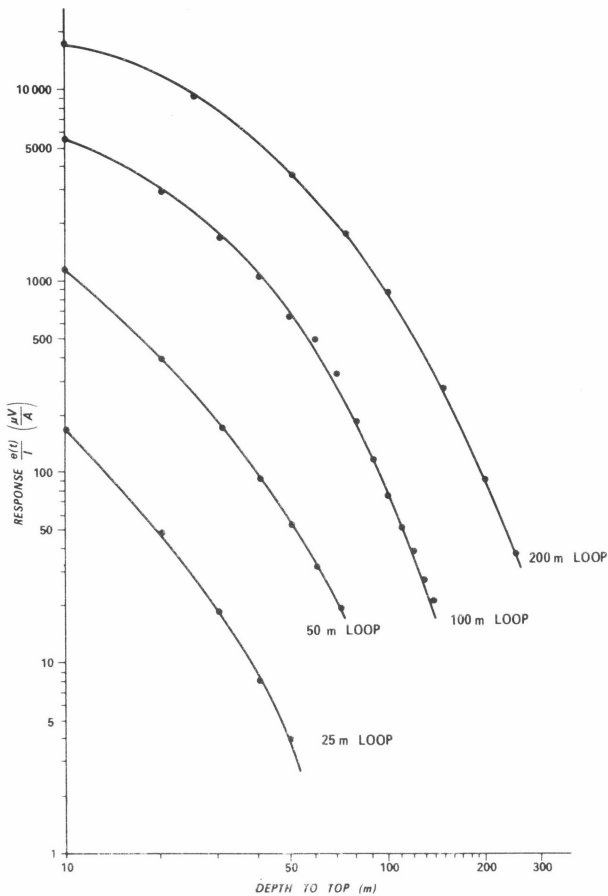


Figure 10. Woodlawn copper-lead-zinc deposit, model results for different depths of orebody, $t = 1.1$ ms

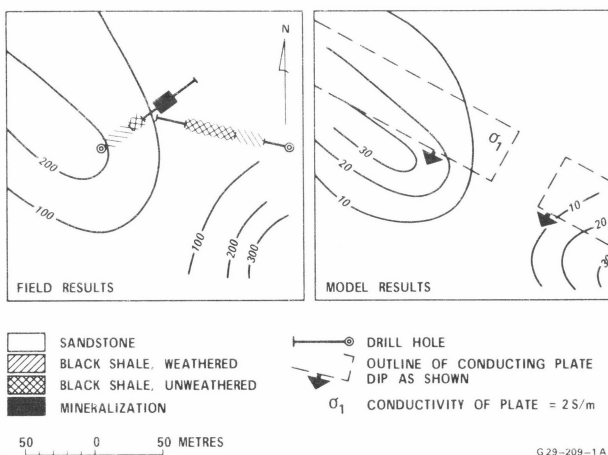


Figure 11. Gubberah Gossan, comparison of field results and model study, $t = 1.1$ ms

The anomaly was attributed to conducting carbonaceous shale. Laboratory measurements on drill core showed clearly the high conductivity of the carbonaceous shale in contrast to the low conductivity of the quartz-sphalerite mineralization which was intersected beneath the gossan. The discontinuity in the TEM anomaly (Fig. 11) was interpreted as due to a resistive fissure filling of quartz and/or sphalerite within the shale.

To test this interpretation a model study was made to determine the response of a 40 m thick bed, with 70° dip, 20 m depth, 2 S/m conductivity, intersected by a highly resistive unit 45 m wide. The results are shown in Figure 11 as contours of $e(t)/I$ for $t = 1.1$ ms. The anomaly patterns are similar for both the field and model results. The amplitudes of the model results are approximately one tenth those of the field results, which implies that the assumed conductivity of the geological model was too small. Nevertheless the model study showed that the anomaly pattern in the Gubberah Gossan area can be caused by a resistive break in a conductor.

Conclusions

The transient electromagnetic method offers considerable advantages over fixed-frequency electromagnetic systems in that the measurement of the response at different sample times is equivalent to measuring the response at a number of frequencies. An analysis of the shape of the received transient signal gives information on near-surface and underlying conductors, and provides an opportunity to overcome the problem, often encountered in Australia, presented by conductive near-surface rocks and saline water masking the response of an underlying conductor.

In the Rum Jungle area results show how the dip of a conductor can be inferred from the TEM response. In the Mary River area large loops used in a reconnaissance survey enabled a large area to be covered quickly. An anomalous area defined by surveying with large loops was resurveyed using smaller loops to delineate the anomaly more accurately. It was shown how the TEM response at various delay times can be used in interpretation. The advantages of the TEM method over other EM methods was demonstrated in this area of a conductor under a conductive overburden. In the Tennant Creek area it was again shown how the TEM response at various delay times can be used in interpretation; in this case the results indicated conductive surficial deposits with no underlying conductors.

Scale modelling programs made in conjunction with field surveys can be a quick, effective and inexpensive method of gaining an insight into TEM response. By modelling field examples the design of follow-up surveys can be significantly enhanced. Two examples of model studies demonstrate how individual problems relating to particular geological environments can be readily studied. Modelling of the Woodlawn copper-lead-zinc deposit showed that loop-overlap must be used with larger loops in order to define the anomaly form. The results indicated that the orebody would have been detected at depths of up to 200 m. A model study of the Gubberah Gossan demonstrated that the anomaly pattern could be caused by resistive quartz-sphalerite mineralization in a conductive carbonaceous shale unit.

References

- BECKER, A., 1969—Simulation of a time-domain airborne electromagnetic system response. *Geophysics* **34** (5), 739-752.
- BECKER, A., GAVREAU, C., & COLLET, L. S., 1972—Scale model studies of time domain electromagnetic response of tabular conductors. *Transactions of Canadian Mining Institute* **75** (725), 90-95.
- BONIWELL, J. B., 1967—Some recent results with the Input airborne EM system. *Canadian Mining and Metallurgical Bulletin* **60**, 325-332.

- BULGAKOV, Yu. I., 1971a—Interpreting surveyed results by the single loop transient process method. Paper 12 in papers on the transient process method in the search for sulphide orebodies. 'NEDRA', Leningrad.
- BULGAKOV, Yu. I., 1971b—An outline of the transient decay field due to cylindrical conductor in a uniform conducting half-space. Paper 6 in papers on the transient process method in the search for sulphide orebodies. 'NEDRA', Leningrad.
- BULGAKOV, Yu. I., & ZHIRNOVA, S. V., 1971—The transient process in common loops in the presence of several vertical conducting plates. Paper 7 in papers on the transient process method in the search for sulphide orebodies. 'NEDRA', Leningrad.
- CROHN, P. W., & OLDERSHAW, W. 1965—The geology of the Tennant Creek 1-mile Sheet area, NT. *Bureau of Mineral Resources, Australia—Report 83*.
- DALY, M. R., 1971—1970 Mary River Survey. *Northern Territory Geological Survey—Report*.
- DUCKWORTH, K., 1968—Mount Minza area experimental geophysical surveys, Northern Territory, 1966 and 1967. *Bureau of Mineral Resources, Australia—Record 1968/107* (unpublished).
- FARROW, B. B., 1967—Gould area (Mount Minza and Waterhouse No. 2) geophysical survey, NT, 1966. *Bureau of Mineral Resources, Australia—Record 1967/97* (unpublished).
- FRISCHKNECHT, F. C., 1971—Electromagnetic scale modelling; in Wait, J. R. (Editor) *ELECTROMAGNETIC PROBING IN GEOPHYSICS*, 265-320, Golem Press.
- HONE, I. G., 1974—Ground geophysical survey, Tennant Creek, NT, 1971. *Bureau of Mineral Resources, Australia—Record 1974/80* (unpublished).
- LEE, T. & LEWIS, R., 1974—Transient EM response of a large loop on a layered ground. *Geophysical Prospecting 22* (3), 430-444.
- MALONE, E. J., OLGERS, F., CUCCHI, F. G., NICHOLAS, T., & MACKAY, W. J., in press—The Woodlawn copper-lead-zinc deposit. In *ECONOMIC GEOLOGY OF AUSTRALIA AND PAPUA NEW GUINEA*, Editor, C. L. KNIGHT, *Australasian Institute of Mining and Metallurgy, Melbourne*.
- MICHAEL, F. N., 1974—Mary River geophysical survey, NT, 1972. *Bureau of Mineral Resources, Australia—Record 1974/66* (unpublished).
- MORRISON, H. F., PHILLIPS, R. J., O O'BRIEN, D. P., 1969—Quantitative interpretation of transient electromagnetic fields over a layered half space. *Geophysical Prospecting 17* (1), 82-101.
- NEGI, J. G., VERMA, S. K., 1972—Time domain electromagnetic response of a shielded conductor. *Geophysical Prospecting 20* (4), 901-9.
- SHATWELL, D. O. & DUCKWORTH, K., 1966—Gould area geochemical and geophysical surveys, Rum Jungle area, Northern Territory, 1965. *Bureau of Mineral Resources, Australia—Record 1966/154* (unpublished).
- SPIES, B. R., 1974—Transient electromagnetic field tests, NT and Qld, 1972. *Bureau of Mineral Resources, Australia—Record 1974/167* (unpublished).
- SPIES, B. R., in press—The derivation of absolute units in electromagnetic scale modelling. *Geophysics*.
- VELIKIN, A. B., & BULGAKOV, Yu. I., 1967—Transient method of electrical prospecting (one-loop version): International seminar on geophysical methods of prospecting for ore minerals. Moscow, 1967.
- WAIT, J. R., 1951—A conducting sphere in a time varying magnetic field. *Geophysics 16* (4), 666-672.
- WAIT, J. R., 1956—Shielding of a transient electromagnetic dipole field by a conducting sheet. *Canadian Journal of Physics, 34*, 890-893.
- YOUNG, G. A.,—Drill hole and transient electromagnetic test surveys, Woodlawn deposit, New South Wales, 1973. *Bureau of Mineral Resources, Australia—Record* (in prep.).

The Cretaceous of the Eromanga and Surat Basins

N. F. Exon and B. R. Senior

Little deformed Cretaceous sedimentary rocks underlie 1 500 000 km² of eastern Australia. Depositional environments in them range from freshwater to shallow marine. The Neocomian and Aptian sequences are quartz-rich, and the Albian and Cenomanian sequences are quartz-poor. The older sequences were derived largely from nearby basement rises, while the younger sequences were probably derived from Cretaceous volcanics forming a mountain range to the northeast. Glauconite is common in marine and paralic sequences.

An epicontinental sea, with seaways to the north and east, covered the basins in the late Aptian, but the eastern seaway closed during an early Albian regression. A second transgressive-regressive cycle, in the late Albian, was virtually confined to the Eromanga Basin. Collectively the two transgressions and regressions were spread over about 20 million years.

The present Baltic Sea is thought to provide a small-scale depositional model for the sequences under consideration: of an epicontinental sea in a cool climate, in which the salinity, the number of planktonic organisms, and the variety of benthonic organisms, decrease away from the ocean. The shallowness of the sea and its entrances mean that it is very susceptible to major environmental changes, caused by such factors as eustatic changes of sea level.

The area had a gentle northwesterly regional tilt during the Cretaceous, but mid-Tertiary movements changed this to southwesterly. Despite subsequent erosion, as much as 2000 m of Cretaceous sediment is preserved in the Eromanga Basin, and 700 m in the Surat Basin.

The Eromanga and Surat Basins occupy a wide but relatively shallow structural depression in eastern Australia, covering 1 500 000 km² (Fig. 1). The basins, which contain broadly similar sedimentary sequences, are separated by a subsurface basement rise. They contain up to 3500 m of Jurassic and Cretaceous rocks, in part mantled by Cainozoic stream sediments and sand dunes. The Cretaceous sequence is characterized by shallow marine sedimentation and is up to 2000 m thick.

The name 'Great Artesian Basin' is not used here. It has been applied in two senses: as a geological term to cover the Jurassic-Cretaceous Eromanga, Surat and Carpentaria Basins, and as a hydrological term to cover the sequences which yielded artesian water in the same general area. Whitehouse (1954), in his pioneering study, tended towards a hydrological usage. Although Jurassic and Cretaceous sediments yield most of the water in the Great Artesian Basin, Permian and Triassic sediments are also involved, so that the hydrological basin is different in detail from the geological basin. We believe that the name should no longer be used in a geological sense. Geologists of the Geological Survey of New South Wales now use the term 'Great Australian Basin' for the Jurassic-Cretaceous super-basin which corresponds to the former geological usage of Great Artesian Basin (Byrnes, Morgan & Scheibnerova, 1975), but we prefer to refer to the individual basins as appropriate.

Since the early 1960s geologists of the Bureau of Mineral Resources (BMR) and the Geological Survey of Queensland (GSQ) have systematically mapped the Queensland portions of the two basins. This paper synthesizes the Cretaceous geology of the basins in Queensland; the stratigraphy is related to that of the equivalent sequences in the Carpentaria Basin (Douch, Smart & Grimes, in prep.) and in South Australia and New South Wales. It is based on the reviews of Senior (in press), Senior, Harrison & Mond (in press), Mond & Harrison (pers. comm.), and Exon (in press).

The regional geological map (Fig. 2) and the palaeogeographic map (Fig. 5) result from the regional mapping and related palaeontological work. The first is a generalized reduction of constituent 1:1 000 000 geological maps, and

the second is compiled from stratigraphic and palaeontological information.

The structure contour map (Fig. 3) and the complementary structural trend map (Fig. 4) were compiled from several 1:1 000 000 scale maps (see Senior, in press; Senior, Harrison & Mond, in press; Exon in press). They use data from 260 petroleum exploration wells, 70 shallow stratigraphic bores drilled by BMR and GSQ, 800 wireline logs of water bores obtained by BMR, and about 160 seismic surveys. The density of information throughout the area was more than adequate for a reliable regional review. Suitable structure contour maps covering the whole area of Figure 2 were not available to us, and as a result the structural diagrams (Figs. 3 & 4) cover a somewhat smaller area than the geological map (Fig. 2).

The wireline logging of water bores carried out over the last 15 years has provided the most reliable stratigraphic data in much of the Eromanga Basin and in parts of the Surat Basin. The logging techniques used are described by Exon & Morrissey (1975). For stratigraphic purposes the gamma-ray logs are the most useful; typical log characteristics of most of the stratigraphic units are related to lithology in Figure 6. Several gamma-ray log correlations (Figs. 7-11) allow interpretation of stratigraphic relationships, lithological changes, and thickening and thinning of units across the basin; they are located on Figure 3.

This paper also considers in some detail the environment in which the Cretaceous rocks accumulated, and the relevant palaeogeography. Information sources are given in the body of the text.

The sandstone nomenclature used follows Crook (1960).

Stratigraphy

The stratigraphic nomenclature of the Eromanga and Surat Basins has evolved over more than a century, although the first regional synthesis was that of Whitehouse (1954). His Jurassic and Cretaceous nomenclature, and recent modifications to it, are shown in Table 1. Much of his nomenclature has been modified but his basic subdivisions are little changed.

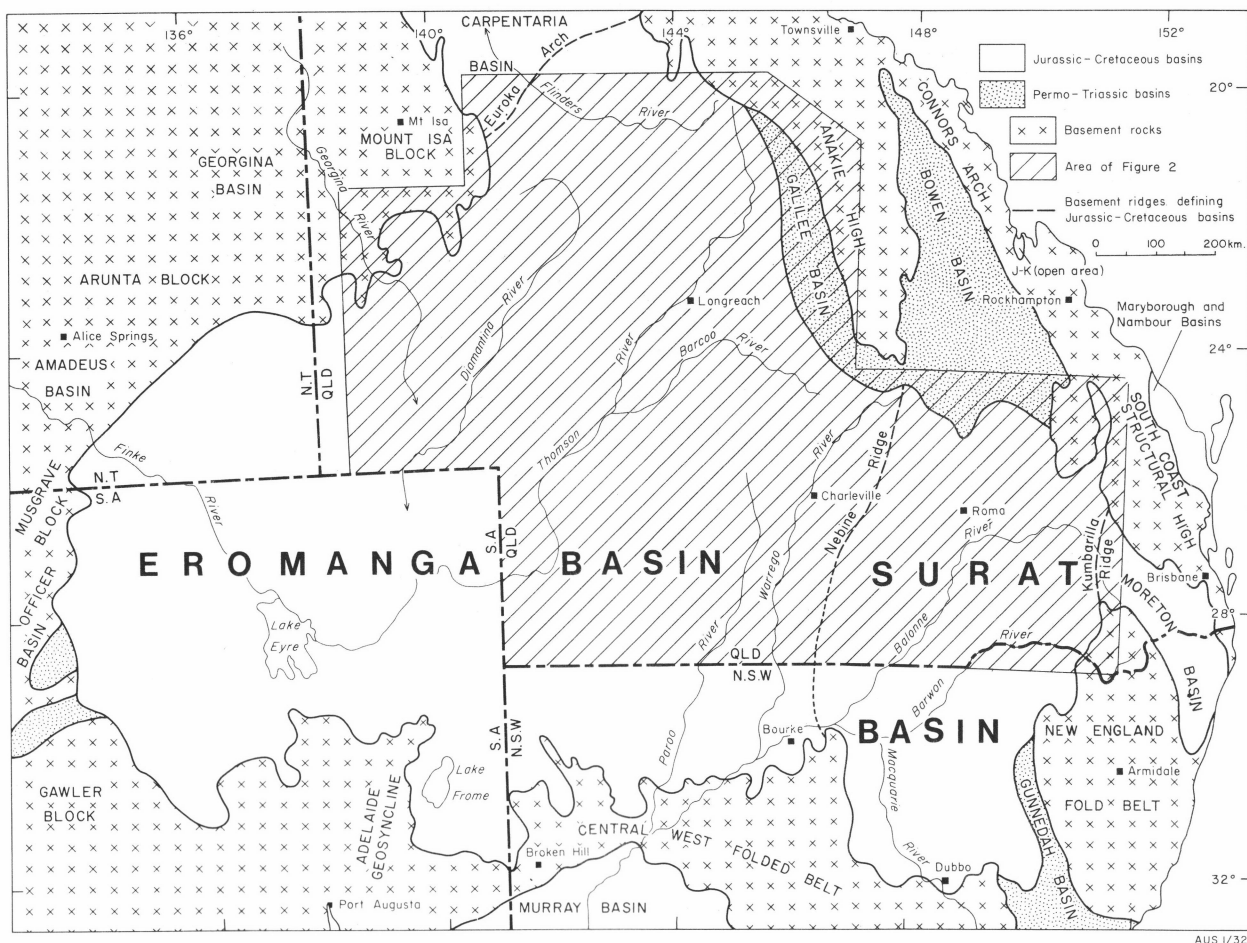


Figure 1. Regional setting

The nomenclature used for the Eromanga and Surat Basins in Queensland is compared with South Australian and Carpentaria Basin nomenclature in Table 2. Although the names vary from area to area, and although the stratigraphy changes in detail, the stratigraphic succession has marked similarities throughout. Eromanga Basin stratigraphy is summarized in Table 3, and Surat Basin stratigraphy in Table 4.

It has long been recognized (e.g. Whitehouse, 1954) that the Jurassic sequence is essentially non-marine, that much of the Cretaceous sequence is marine, and that there is a transitional sequence of mostly Neocomian age. Studies since 1960 have shown that quartz-rich clastic sediments predominate in the non-marine Jurassic sequence and through into the marine Aptian, but that andesitic debris characterizes the marine and non-marine clastic sediments of the Albian and Cenomanian. Glauconie* and montmorillonite characterize both the paralic and marine sequences.

In the Eromanga and Surat Basin there are early Neocomian fluvial sandstone sequences: the upper part of the Hooray Sandstone in the former, and the Mooga Sandstone in the latter. The overlying paralic (transitional) sequences, of late Neocomian and earliest Aptian age, are the Cadna-owie Formation and the Bungil Formation respectively. The fluvial sequence averages 150 m thick in the Eromanga and 100 m in the Surat Basin, and the

paralic sequence 60 m in the Eromanga and 150 m in the Surat Basin.

In both basins the paralic sequence is overlain by late Aptian and younger marine, paralic and fluvial, essentially clastic sequences, of the Rolling Downs Group. In the Eromanga Basin the group ranges up into the Cenomanian and averages 1000 m thick; in the Surat Basin it extends only into the late Albian and averages 400 m thick.

Structure

Major subsurface basement rises separate the Jurassic-Cretaceous basins of eastern Australia (Figs. 1 & 4); the Eureka Arch separates the Carpentaria and Eromanga Basins, the Nebine Ridge separates the Eromanga and Surat Basins, and the Kumbarella Ridge separates the Surat and Moreton Basins. The Nebine and Kumbarella Ridges rose spasmodically during the Cretaceous, and influenced sedimentation intermittently; the Eureka Arch came into existence in the Late Jurassic and remained static during the Cretaceous, so it had only a very limited effect on Cretaceous sedimentation (Smart, in press). The major downwarp in the Cretaceous sequence (Figs. 3 & 4) overlies the Permo-Triassic Cooper Basin and was a Cretaceous depocentre, and the Cretaceous sequence is generally thin where no Permo-Triassic sediments are preserved.

In most of the area structural movements affecting the Cretaceous sequence were of three types: epirogenic movements and tilting related to uplift in the north and east, which gave both basins their regional tilt to the southwest, readjustments on old fault lines which led to minor fault

* The term 'glauconie' is discussed under Data of Environmental Significance.

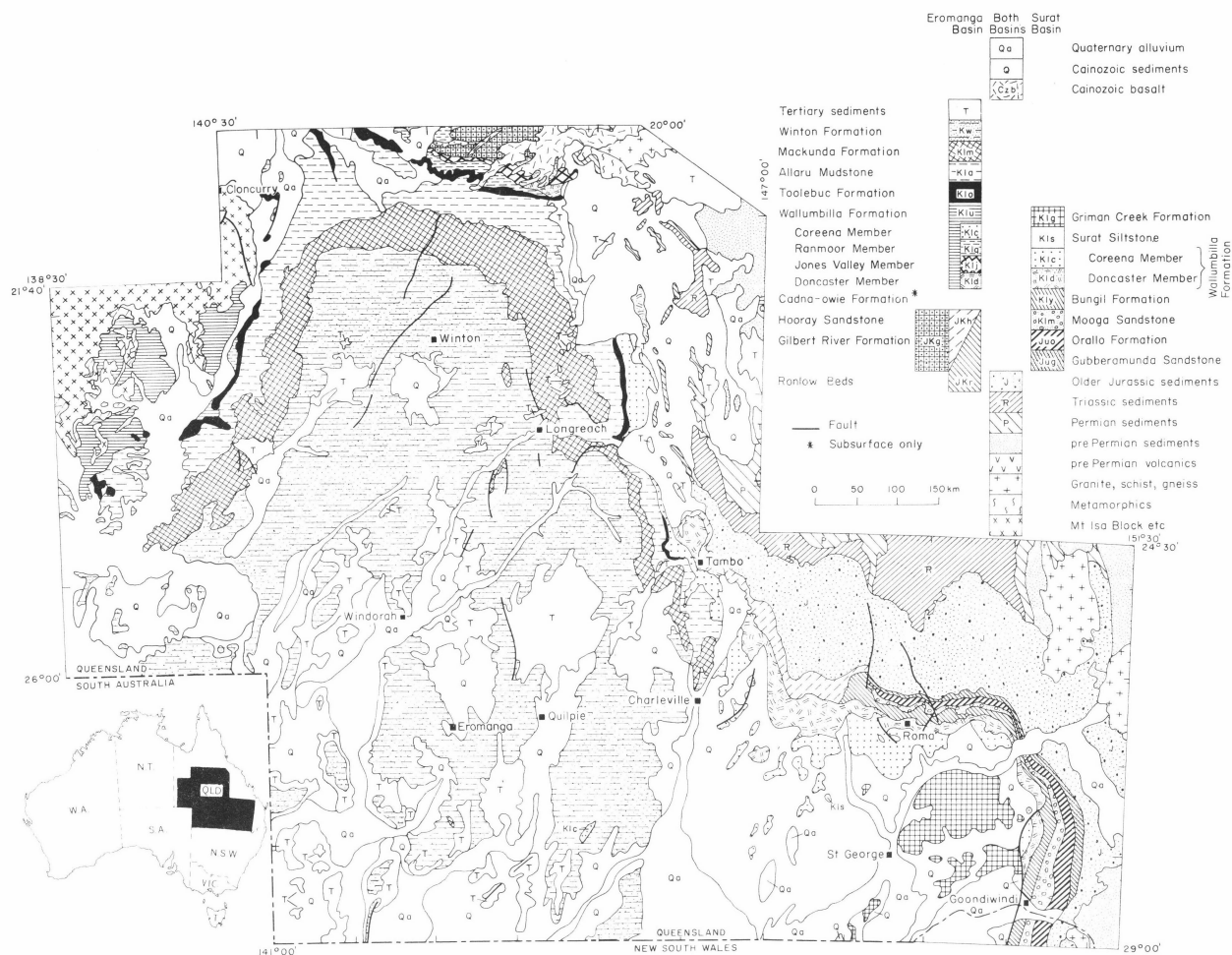


Figure 2. Geological map

displacements or monoclines near the surface, and broad warps related to compaction in the older sequences. Folds have a decreasing amplitude upwards in the Cretaceous sequence, and the displacement of faults becomes less. The overlying Tertiary sequences are also folded and displaced in some cases, so that there is evidence of movement both during and after Cretaceous times.

The structural pattern is dominated by normal faults and related anticlines. The anticlines are commonly drape folds over deeply buried basement fault blocks. Intermittent movement during sedimentation has resulted in some thinning over these blocks.

Eromanga Basin

In the northwest the Diamantina Slope (Fig. 4) falls regularly away from the Mount Isa Block (Fig. 1) and the Euroka Arch. Its eastern margin is defined by a north-northeasterly trending zone of faults, which includes the Wetherby Structure, the Cork Fault and the Holberton Structure.

East of this zone of faults, and both within and to the north of the extent of the Cooper Basin, are numerous anticlines, domes, synclines and faults (Figs. 3 & 4). These structures formed by compaction over basement ridges and troughs, and generally parallel the north-northeasterly trends of the basement and the Cooper Basin. Flank dips on some of the domes and anticlines above the Cooper Basin approach 30°. As there is only slight thinning of Cretaceous sediments across these structures, most of the movement must have taken place during the Late Cretaceous or Cainozoic. Oligocene and Miocene epeirogenic uplift to the

east occurred at the same time as rejuvenation of basement faults along the old lines of weakness marked by the Cooper Basin gave rise to anomalously intense structures.

The eastern edge of this folded zone is generally marked by a longitudinal zone of faults and anticlines including the Beryl Anticline, Stormhill Fault, Canaway Fault and Ridge, and the Dynevor Fault (Fig. 4). In the south the Thargomindah and Dynevor Shelves separate the folded zone of the Cooper Basin from the longitudinal zone of faulting.

Further east a zone of north-northeasterly trending folds such as the Pleasant Creek Arch separates relatively undeformed areas to the south (Cunnamulla Shelf) and to the north. These folds overlie basement ridges, many of which are anticlines traceable into the Drummond Basin. The Eromanga Basin is limited to the east by the Nebine Ridge, a basement rise whose surface expression is the Maranoa Anticline. The Nebine Ridge grades southward into the broad, undeformed Cunnamulla Shelf.

Surat Basin

The Cretaceous sequence of the Surat Basin is little deformed, although the structure of the pre-Jurassic rocks is quite complex (Exon, 1974). The larger, generally longitudinal faults, such as the Merivale, Arbroath, Hutton-Wallumbilla and Goondiwindi-Moonie Faults (Fig. 4) have displacements mostly less than 100 m. Displacement in the Cretaceous sequence is by normal faulting. Much of the deformation of the Surat Basin Cretaceous sequence is probably related to mid-Tertiary epeirogenic uplift around the basin margins.

36 N. F. EXON AND B. R. SENIOR

Age	Present Eromanga Basin Nomenclature (Vine et al., 1967; Senior et al., 1975).			Eromanga Basin Nomenclature (Vine & Day, 1965; Exon, 1966; Exon et al., 1972)		Eromanga—Surat Basin Nomenclature (Whitehouse, 1954)		Present Surat Basin Nomenclature (Vine et al., 1967; Exon & Vine, 1970; Reiser, 1970).		
Cenomanian	Winton Formation			Winton Formation		Winton Formation		<div>— ? — ? — ? — ? — ? — ? — ? —</div> <div>Griman Creek Formation</div> <div>Surat Siltstone</div> <div>Coreena Member</div> <div>Doncaster Member</div> <div>Minmi Member</div> <div>Nullawurt Sst. Member</div> <div>Kingull Member</div>		
Albian	Mackunda Formation			Mackunda Formation						
	Allaru Mudstone			Wilgunya Formation	Allaru Member					
	Toolebuc Formation				Toolebuc Member					
	Wallumbilla Formation	Ranmoor Member	Coreena Member		Ranmoor Member					
Jones Valley Member		Jones Valley Member								
Aptian	Doncaster Member			Doncaster Member		Roma Formation		Wallumbilla Formation	Doncaster Member	
Neocomian	Wyandra Sandstone Member			Hooray Sandstone		Blythesdale Group	Transition Beds			Bungil Formation
	Cadna-owie Formation						Mooga Sandstone		Nullawurt Sst. Member	
Midle and Late Jurassic	Hooray Sandstone						Hooray Sandstone		Fossil Wood Beds	
	Hooray Sandstone			Gubberamunda Sandstone					Orallo Formation	
	Gubberamunda Sandstone			Gubberamunda Sandstone		Gubberamunda Sandstone		Gubberamunda Sandstone		
Westbourne Formation			Westbourne Formation		Walloon Coal Measures		Westbourne Formation			

TABLE 3: EROMANGA BASIN ROCKS UNITS: LATE JURASSIC TO LATE CRETACEOUS

Age	Unit	Maximum Thickness (m) Average	Lithology and Palaeontology	Environment	Relationships
Cenomanian	Winton Formation	1100 500	Labile sandstone, siltstone, mudstone, calcareous in part; mudclast conglomerate, minor coal. Freshwater molluscs, plants, spores and pollen. Reptile tracks.	Plains: streams, swamps, lakes. Wide river flats and local development of short-lived streams.	Restricted to Eromanga Basin.
	Mackunda Formation	200 60	Labile sandstone, siltstone, mudstone, coquina limestone, mudclast conglomerate, cone-in-cone limestone. Glauconie-bearing. Marine molluscs, fish and sharks teeth, forams. Plant fragments, spores and pollen.	Marine regression. Deposition in paralic environments.	Restricted to Eromanga Basin.
Late Albian	Allaru Mudstone	270 200	Blue-grey mudstone, siltstone, minor fine labile sandstone, calcareous in part. Molluscs, with ammonites and pelecypods dominant, forams. Minor plant fragments, spores and pollen, microplankton.	Shallow seas, largely below wave base. Good connection with open sea.	Restricted to Eromanga and Carpentaria Basins.
	Toolebuc Formation	75 15	Bituminous and calcareous shale, black siltstone, fine grained limestone, coquinite, labile sandstone. Richly fossiliferous; relatively few genera of pelecypods, gastropods ammonites and belemnites. Fish remains, planktonic forams, spores, pollen and microplankton.	Shallow seas, with shoals. Good connection with open sea.	Restricted to Eromanga and Carpentaria Basins.
	Coreena Member	220 150	Siltstone, mudstone, labile sandstone, mudclast conglomerate. Glauconie-bearing and calcareous in part. Locally rich marine fauna of pelecypods, gastropods, belemnites, scaphopods, and rare ammonites; forams. Plant fragments, spores, pollen and microplankton.	Shallow marine and paralic gives way to coastal plain.	Continuous with Coreena Member of Surat Basin.
	Ranmoor Member	310 250	Grey to black mudstone, siltstone, carbonaceous in part. Upper part rich in kerogen (oil shale). Marine fossils, near Hughenden only, from near base and top. Fauna of ammonites, belemnites and pelecypods. Spores, pollen and microplankton.	Shallow marine, paralic (possibly enclosed basins or lagoons).	Northeastern marginal facies of Eromanga Basin. Correlate of Coreena Member.
Early and Middle Albian	Rolling Downs Group				
Late Aptian	Wallumbilla Formation	Jones Valley Member 10 5	Siltstone, calcareous siltstone, and limestone, and very fine labile sandstone. Minor glauconie. Fossils only at a few localities. Pelecypods, belemnites, scaphopods, burrows, crinoids, and brachiopods. Spores, pollen and microplankton.	Paralic (possibly lagoons and coastal plains)	Northeastern marginal facies of Eromanga Basin. Correlate of upper part of Doncaster Member.
		Doncaster Member 220 150	Blue-grey mudstone, siltstone, glauconie-bearing and calcareous in part. Minor sandstone. Minor limestone, some cone-in-cone. Fossiliferous concretions containing marine fauna. Pelecypods dominant; also ammonites, belemnites, gastropods, crinoids, brachiopods, decapods, crustacea and algae. Spores, pollen and varied microplankton.	Shallow seas, locally above wave base.	Continuous with Doncaster Member of Surat Basin.
Neocomian to Early Aptian	Wyandra Sandstone-Member	20 15	Medium to coarse quartzose sandstone with scattered quartz pebbles. No known fossils.	Beach deposits? May represent Lower Cretaceous marine transgression.	Restricted to subcrop, in central portion of Eromanga Basin.
	Cadna-owie Formation	80 60	Medium quartzose to sublabe sandstone with increasing siltstone towards base. Spores, pollen, and microplankton.	Dominantly stream deposits, grading to shallow marine in places. Littoral facies adjacent to granite inliers of Eulo Ridge.	Restricted to subcrop except in southwestern (South Australia) portion of Eromanga Basin.
	Hooray Sandstone	200 150	White quartzose to sublabe sandstone, with interbeds of siltstone, conglomerate and coal. Spores and pollen, plant fragments. Marine fossils in Boulia-Springvale area: pelecypods, gastropods, belemnites, starfish and arenaceous foraminifera.	Predominantly stream deposits; shallow marine in central west.	Laterally continuous with Gubberamunda and Mooga Sandstones of Surat Basin.
	Westbourne Formation	120 100	Brown micaceous siltstone and mudstone, minor quartzose to sublabe sandstone. Spores and pollen, worm casts, animal tracks, plant roots, and fragmentary plant material. Acritarchs.	Lakes and streams. Possibly shallow marine in Nebine Ridge area.	Laterally continuous with Westbourne Formation of Surat Basin.
Late Jurassic					

TABLE 4: SURAT ROCK UNITS: LATE JURASSIC AND EARLY CRETACEOUS

Age	Unit	Maximum Thickness (m) Average	Lithology and Palaeontology	Environment	Relationships
Albian	Griman Creek Formation	480 300	Lithic sandstone, siltstone, mudstone; some intraformational conglomerate. Glauconie-bearing. Marine and freshwater molluscs, plants, spores and pollen.	Marine regression; very shallow seas gave way to coastal plains.	Probably equivalent to upper Coreena, Toolebuc and Allaru in Eromanga Basin. No known lateral connection.
	Surat Siltstone	150 100	Siltstone, mudstone; some fine sandstone. Glauconie-bearing. Small marine molluscs, benthonic forams, spores and pollen, dinoflagellates.	Shallow marine below and above wave base; water shoaled with time.	Probably equivalent to part of Coreena in Eromanga Basin.
	Coreena Member (Wallumbilla Formation)	150 100	Siltstone, mudstone, fine labile sandstone. Glauconie-bearing. Marine molluscs including belemnites; benthonic forams, spores and pollen, dinoflagellates.	Marine regression; very shallow seas gave way to coastal plains.	Equivalent to lower Coreena in Eromanga Basin, with which it is in lateral continuity.
late Aptian	Doncaster Member (Wallumbilla Formation)	200 150	Mudstone, carbonaceous in part, siltstone; some fine labile sandstone. Glauconie-bearing. Marine molluscs including belemnites and rare ammonites; brachiopods, algal colonies, sponges, crinoids, benthonic forams, spores and pollen, dinoflagellates.	Shallow marine below and above wave base. Good connections with open sea on occasions.	Laterally continuous with Doncaster in Eromanga Basin. In part probably deeper water equivalent of Bungil Formation.
Neocomian to early Aptian	Bungil Formation	270 150	Sandstone, siltstone, mudstone. Glauconie-bearing. Marine and freshwater molluscs, brachiopods, arenaceous forams, spores and pollen, dinoflagellates.	Marine transgression: coastal plain gave way to shallow restricted seas.	Laterally continuous with Cadna-owie Formation in Eromanga Basin.
	Mooga Sandstone	200 100	Sandstone; some siltstone and mudstone. Spores and pollen, plants, <i>Unio</i> .	Stream deposition on plains.	Laterally continuous with upper Hooray Sandstone in Eromanga Basin.
Late Jurassic	Orallo Formation	270 200	Lithic sandstone, siltstone, mudstone, intraformational conglomerate, coal. Spores and pollen, <i>in situ</i> plants.	Stream, swamp and lake deposits on plains. Includes volcanic ash.	Pinches out westward; equivalents lie in middle Hooray Sandstone in Eromanga Basin.
	Gubberamunda Sandstone	200 100	Sandstone; some conglomerate, siltstone. Spores and pollen, plant debris.	Stream deposition on plains.	Laterally continuous with lower Hooray Sandstone in Eromanga Basin.
	Westbourne Formation	200 150	Siltstone, mudstone, carbonaceous in part; fine sandstone. Spores and pollen, plant debris, acritarchs.	Coastal plain; possibly shoreline and shallow marine.	Laterally continuous with Westbourne in Eromanga Basin.

Dips are radial into the depression of the Mimosa and Dirranbandi Synclines. Relatively steep dips near the Moonie and Goondiwindi Faults are probably related to the mid-Tertiary uplift of the Kumbarilla Ridge to the east.

Data of Environmental Significance

Some of the environmental evidence on which this paper is based is discussed below, and major characteristics are related to the stratigraphy in Table 5.

Petrology of detrital grains

The study of thin sections, especially of sandstone (e.g. Galloway, 1967; Byrnes, 1973), has shown that there is a marked change in lithology at the Aptian-Albian boundary. Sandstones of the Aptian Doncaster Member and the older Cretaceous sequences are mature, being dominated by quartz and resistant rock fragments, and appear to have been derived from basement rocks. On the other hand Albian and Cenomanian sandstones are very immature, being dominated by plagioclase and volcanic rock fragments, and these have been rapidly derived from contemporaneous volcanics, which were apparently largely andesitic.

Clay minerals

Clay mineral analyses of rocks from various levels in the Jurassic and Cretaceous sequences (Gregory & Vine, 1970; Exon, in press; E. Slansky, pers. comm.) show that montmorillonite predominates in the Rolling Downs Group and the underlying paralic sequences, whereas kaolinite is the dominant clay mineral in the earliest Neocomian and older fluvial sequences.

E. Slansky, who has studied several core holes in the Surat Basin in NSW, has suggested (pers. comm.) that the change from kaolinite to montmorillonite might possibly be related to the change from fluvial to marine or progressively more saline lacustrine environments. However, some non-marine sequences in the Jurassic and within the Rolling Downs Group are dominated by montmorillonite, so additional factors must be involved. Montmorillonite is commonly associated with immature volcanogenic sandstone, and kaolinite with mature quartz-rich sandstone, suggesting that montmorillonite was produced by contemporaneous volcanism, but this relationship does not apply to the Neocomian-early Aptian paralic sequences or the late Aptian marine sequence.

Because montmorillonite is associated with immature sequences characterized by labile sandstone, and kaolinite with mature sequences characterized by quartzose sandstone, one can suggest perhaps that clays from the source

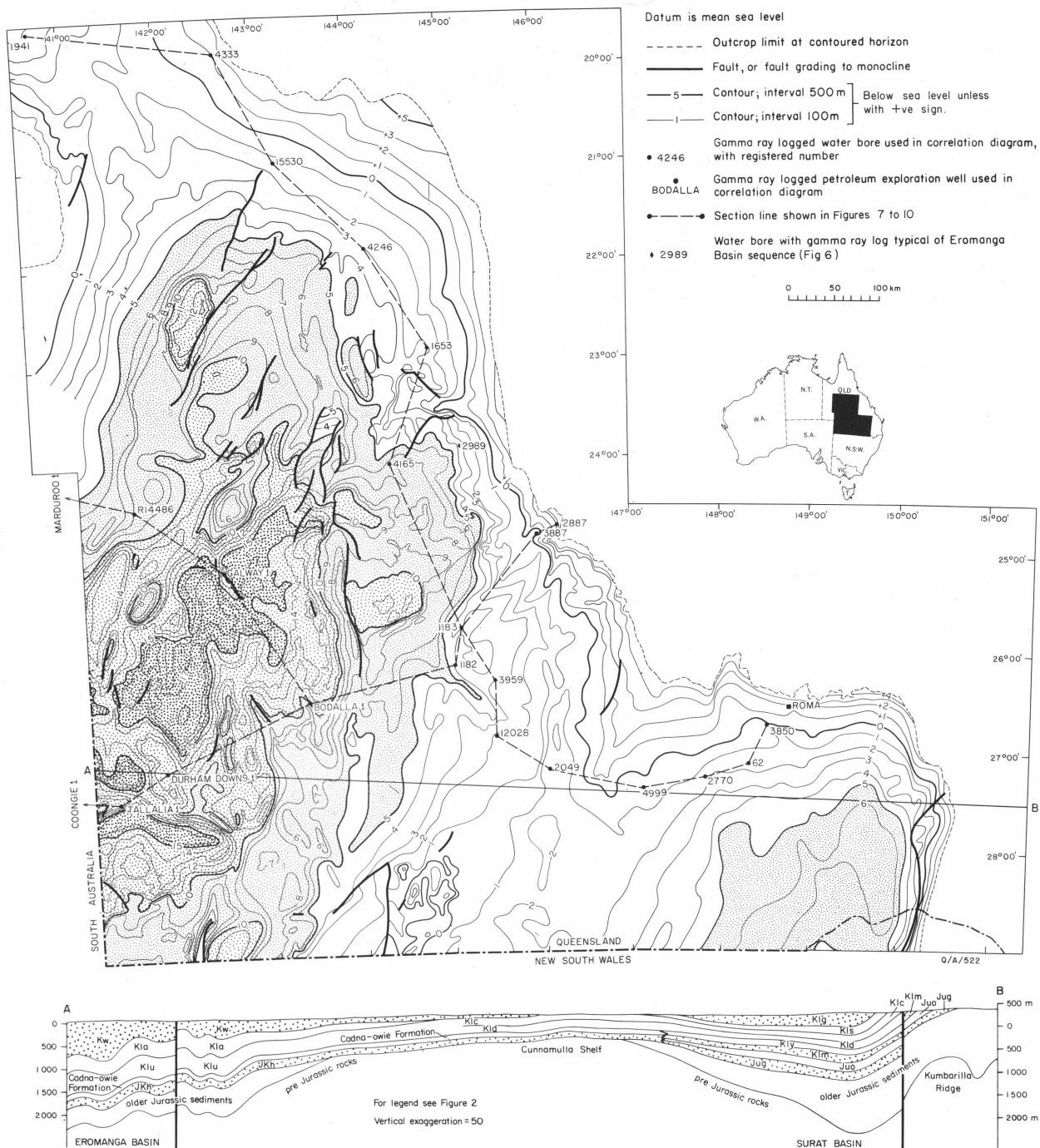


Figure 3. Structure Contours on the base of the Rolling Downs Group (top of Mooga Sandstone in Surat Basin).

areas were generally dominated by montmorillonite, which persisted in sequences that were rapidly buried and little reworked, but which broke down to kaolinite in sequences that were extensively reworked and weathered within the depositional basin.

Glaucconie

'Glaucconite' has long been recognized as characteristic of the marine Cretaceous sequence, the name having been used for any rounded green grains consisting of clay minerals ('morphological glauconite'). Within the Eromanga and Surat Basins such grains are generally restricted to the Cadna-owie Formation, Bungil Formation, and Rolling Downs Group (e.g. Galloway, 1967). The grains are seldom mineralogical glauconite (Exon, 1972a, in press;

E. Slansky, pers. comm.) so the term 'glaucconie'* (Millot, 1970) is more appropriate for them. The glauconie grains vary from dark green and well rounded, with a granular internal structure, to pale green and crystalline, with little or no rounding. Many of the non-rounded grains are apparently authigenic replacements of detrital mica, but the rounded grains are probably precursors of true glauconite. The rounded glauconie is most abundant in sequences which palaeontological evidence shows to be

* Millot (1970, p. 205) defined 'glaucconie' as 'A variable mixture of minerals in which illite, montmorillonite, chlorite or various mixed layers can be identified. The total aspect remains that of green clay minerals, but it is not known whether one part or another yet merits the name "glaucconite".'

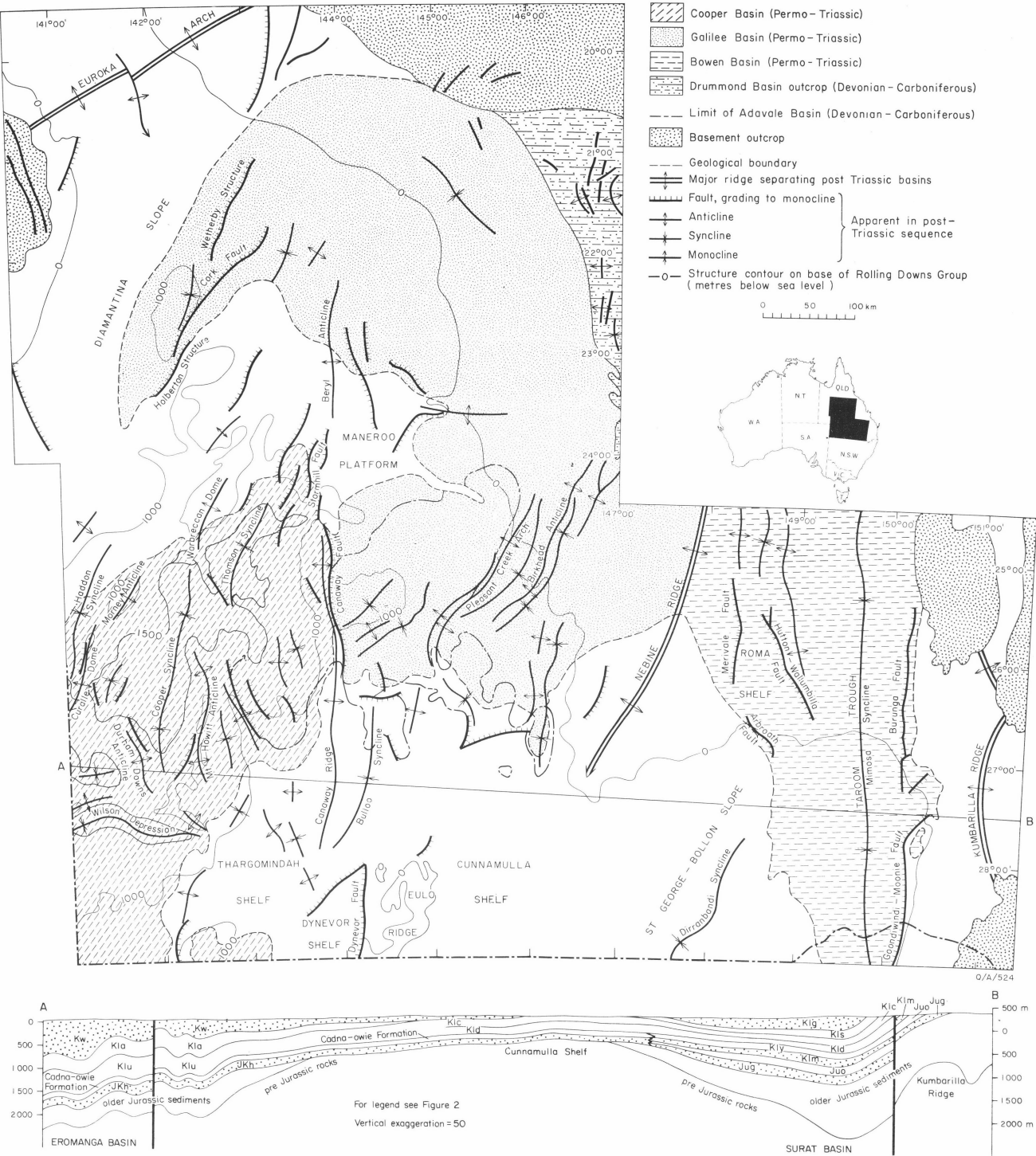


Figure 4. Structural trends and pre-Jurassic basins

TABLE 5 MAJOR ENVIRONMENTAL CHARACTERISTICS OF VARIOUS SEQUENCES

Sequence	Provenance	Dominant clay mineral	Glauconite	Marine fossils	Environment
Winton Formation (late Albian-Cenomanian)	Andesitic volcanics	Montmorillonite	Rare	None	Fluvial
Most of the Rolling Downs Group (Albian)	Andesitic volcanics	Montmorillonite	Abundant	Shelly fossils, planktonic and benthonic forams, microplankton	Shallow marine to coastal plain
Doncaster Member (late Aptian)	Siliceous basement rocks and sediments	Montmorillonite	Abundant	Shelly fossils, benthonic forams, microplankton	Shallow marine
Early Aptian and late Neocomian	Siliceous basement rocks	Montmorillonite	Fairly common	Shelly fossils, benthonic forams, microplankton	Paralic
Early Neocomian	Siliceous basement rocks	Kaolinite	Absent	Rare acritarchs	Fluvial

marine or paralic. Furthermore, glauconite usually forms only in salt or brackish water, and if glauconite is a true precursor it also is probably an indicator of saline conditions; we regard it as such.

Palaeontology

Shelly macrofossils, foraminifera, microplankton, and spore and pollen grains provide a wealth of environmental evidence. Details are given in Tables 3 and 4.

Day (1969) summarized the macropalaeontological evidence, which is of critical importance to an understanding of the two basins. Studies by Whitehouse (1926) showed that there are two major faunas, Tambo and Roma, which are best defined on the basis of ammonites, although these make up only a small part of the contained, largely molluscan, faunas. Day stated that the ammonites *Sanmartinoceras*, *Ailoceras*, *Australiceras*, *Tropaeum*, '*Toxoceratoides*' and *Lithancylus* are diagnostic of the upper Aptian Roma fauna, and *Prohysterocheras*, *Falciferella*, *Laboceras*, *Appurdiceras*, *Myloceras*, *Beudanticeras*, *Brewericeras* and *Boliteceras* are diagnostic of the Albian Tambo fauna. Both faunas suggest cool temperate conditions and some isolation of the basins from the open sea. The strength of marine connections at various times is indicated by the abundance of various fossil groups. Thus, abundant pelagic ammonites and belemnites suggest good connections, whereas a high proportion of benthonic freshwater or brackish molluscs suggests the reverse.

Foraminiferal studies include those of Crespin (1963), Ludbrook (1966) and Haig (1973). Abundant planktonic forms indicate marine conditions with nearly normal salinities, whereas their absence, allied with the presence of specialized benthonic forms, points to various brackish milieu. The evidence from the foraminifera corroborates that of the macrofauna.

Statistical studies of the abundance of various types of microplankton, such as that of Burger (1975) in the Surat Basin, yield valuable palaeoenvironmental information. In a shallow epicontinental sea abundance of dinoflagellates indicates high salinity, whereas acritarchs alone suggest low salinity. The two most abundant acritarch groups are *Michrystidium* and *Leiosphaeridia*, the former group generally indicating more saline conditions than the latter.

Palynological studies (see Dettman & Playford, 1969) tend to corroborate the macropalaeontological evidence (Day, 1969) and oxygen isotope evidence (Dorman & Gill, 1959), of cool Cretaceous climates.

Early Neocomian Fluvial Sequences

At the close of the Jurassic the area of the Eromanga and Surat Basins consisted of broad alluvial plains overlying about 1000 m of non-marine Jurassic sediments and probably draining to the north; the plains were surrounded by slopes and uplands of older sediments and basement rocks (see Fig. 1). The Jurassic sequence was generally thickest where it rested on the Permo-Triassic basins whose extent is shown in Figure 4.

Early Neocomian sequences were laid down in both basins and consist dominantly of quartzose sandstone. They are the product of the type of fluvial sedimentation that had prevailed in the Jurassic. The **Hooray Sandstone** was derived from uplands bordering the Eromanga Basin, and these consisted largely of acid igneous and metamorphic rocks. Drainage was probably northward. The **Mooga Sandstone** of the Surat Basin was also derived from nearby uplands consisting of siliceous basement rocks, and to some extent from Permian, Triassic and Jurassic sediments of the Bowen and northern Surat Basins. Palaeocurrent and

isopach information indicates that drainage was probably eastward into the Moreton Basin, through the Kumbarella Ridge via an antecedent drainage system (Exon, in press). The clay mineral assemblage in the fluvial sequences is dominated by kaolinite (Exon, op. cit.; E. Slansky, pers. comm.) and glauconite is not present.

The Hooray Sandstone averages 150 m thick and the Mooga Sandstone 100 m thick, and the rate of deposition of these sandstones was probably less than the average Jurassic rate of around 40 m/million years (Exon, in press).

Late Neocomian and Early Aptian Transitional Sequences

The first effects of the worldwide Cretaceous marine transgression were felt in this period. Sands, silts and muds were laid down to form the **Cadna-owie Formation** and its correlatives in the west, and the **Bungil Formation** in the Surat Basin.

In the Surat Basin sedimentological and microplankton evidence (Burger, 1975) suggests increasing marine influence with time in the Bungil Formation. The middle (Nullawurt Sandstone) member is a beach sand in places, and contains the oldest marine macrofauna recorded in the Surat, Eromanga or Carpentaria Basins. It consists largely of pelecypods (Day, 1969). On this basis Day suggested an early eastern seaway, probably from the vicinity of the Maryborough Basin. The uppermost (Minmi) member consists of littoral deposits and contains an abundant marine macrofauna, largely of pelecypods and gastropods (Day, 1969).

In the Eromanga Basin the sandy **Gilbert River Formation** in the northeast, and the upper part of the Hooray Sandstone in the northwest, contain marine macrofossils (e.g. Day, 1969) and microplankton (Burger, 1973) and are littoral and shallow, open marine sediments.

Further south in the Eromanga Basin siltstone and sandstone of the Cadna-owie Formation are present. Outcrops are largely confined to South Australia, but subsurface information is available throughout the basin. In South Australia in the southwestern Eromanga Basin paralic sandstone and siltstone containing benthonic foraminifera (Ludbrook, 1966) are overlain by fluvial sandstone, the **Mount Anna Sandstone Member**, which built northward across the paralic sediments (Wopfner et al., 1970). The Parabarana Sandstone north of Lake Frome (for general location see Fig. 1), an equivalent of the Cadna-owie Formation, contains *Lingula* and scattered molluscs (Ludbrook, 1966) and is a shallow marine sand.

In Queensland the Cadna-owie Formation is largely confined to the deeper parts of the Eromanga Basin, where shell fragments and glauconite have been recorded in petroleum exploration wells (Senior, Exon & Burger, 1975). The lower part of the formation consists of sandstone and siltstone which were probably deposited in various nearshore environments, and the upper (Wyandra Sandstone) member consists of well sorted quartzose sandstone which was probably a transgressive marine sand.

The development of paralic conditions throughout the Eromanga Basin and further north, in the Carpentaria Basin, suggest the formation of a northern seaway by the early Aptian (see Fig. 5a), and similar paralic conditions prevailed in the Surat Basin. Near the entrances of the depositional basin salinities were normal or nearly normal, but salinities decreased away from the open ocean.

The relationships of Neocomian and early Aptian formations are shown in Figures 7 to 11. The paralic sandstones, siltstones and mudstones of the Cadna-owie Formation of the deeper part of the Eromanga Basin grade

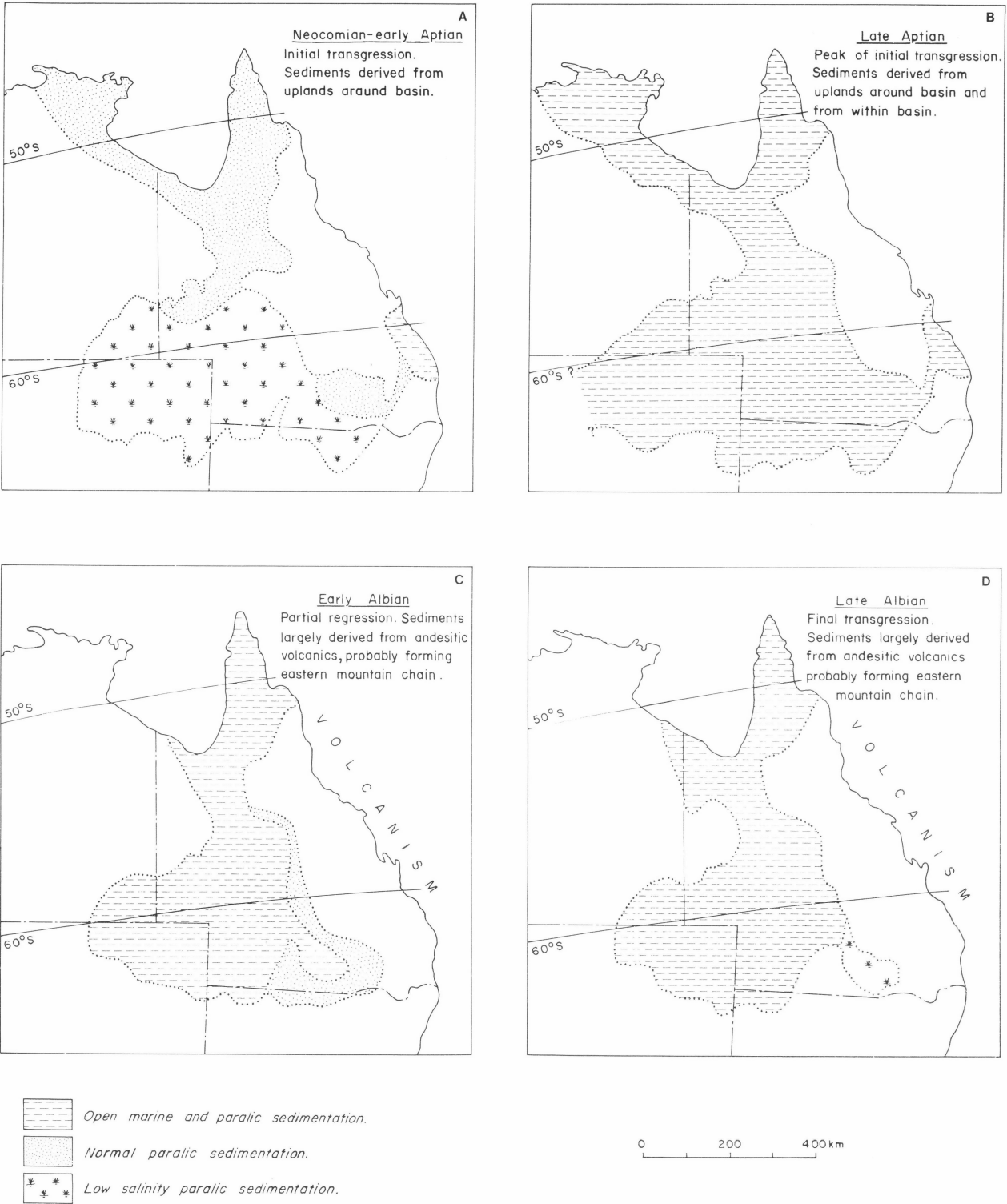


Figure 5. Cretaceous palaeogeography of Eromanga, Surat and Carpentaria Basins, showing known extent of Cretaceous Seas. Based in part on Day (1969) and unpublished information from D. Burger and J. Smart. Palaeolatitudes after Irving (1964)

westward into the sandstones of the upper part of the Hooray Sandstone (Fig. 10), which are marine in part, northward into the sandstones of the upper marine part of the Gilbert River Formation (Fig. 9), northeastward into the freshwater sandstones of the upper part of the Hooray Sandstone (Fig. 7), and eastward into the paralic sandstones, siltstones and

mudstones of the Bungil Formation of the Surat Basin (Fig. 8).

The sediments laid down during this period were largely transported by streams from quartz-rich upland areas, as quartzose and sublabe sandstone greatly predominate over labile sandstone. However wave erosion of Jurassic and

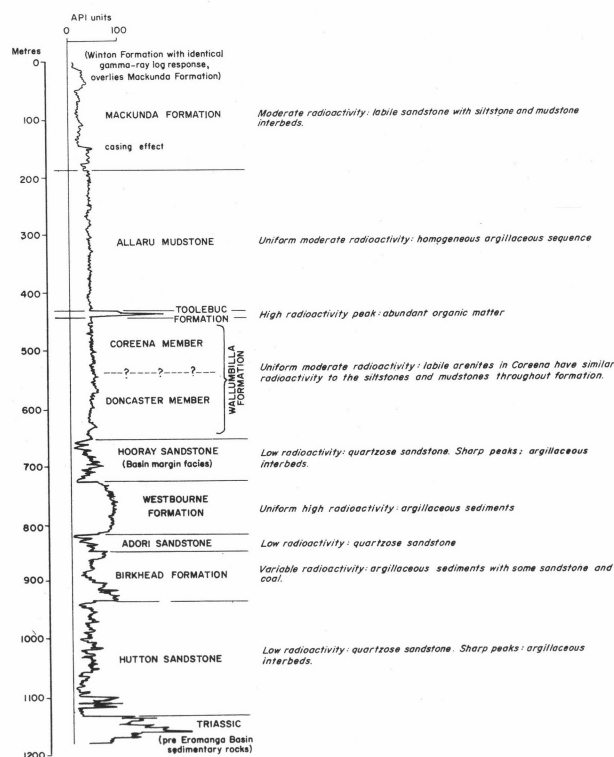


Figure 6. Bore 2989: Gamma-ray log illustrating typical Characteristics of Eromanga Basin Sequence

earlier Cretaceous sediments must also have contributed detritus. The dominant clay mineral is montmorillonite (Exon, in press; E. Slansky, pers. comm.), and glauconie is widespread and locally abundant (Galloway, 1967; Exon, 1972a and in press; Byrnes, 1973; E. Slansky, pers. comm.). The glauconie grains are most apparent in sandstone.

Nowhere does the thickness of this paralic sequence exceed 100 m, suggesting that, as in the early Neocomian, depositional rates were low.

Late Aptian to Cenomanian (Rolling Downs Group)

The Rolling Downs Group consists of several marine, paralic and freshwater units, whose relationships are shown in Table 2. Mineralogical and petrological conclusions in this section are drawn from Galloway (1967), Gregory & Vine (1970), Exon (1972a, in press), Byrnes (1973), and E. Slansky (pers. comm.). Glauconie is present in all units, although rare in the Winton Formation, and montmorillonite is the dominant clay mineral throughout. Average thicknesses for the group, of 1000 m in the Eromanga Basin and 400 m in the Surat Basin, suggest depositional rates of as much as 100 m/million years.

The oldest formation in the group in both basins is the **Wallumbilla Formation** of late Aptian to middle Albian age, which consists of carbonaceous mudstone, siltstone and some sandstone. It rests conformably on the underlying paralic sequences. Palynological evidence (D. Burger, pers. comm.) suggests that the upper part of the formation is younger in the Eromanga Basin than in the Surat Basin, where the Surat Siltstone and lowermost Griman Creek Formation are the time equivalents of the upper Wallumbilla Formation.

In much of the area studied the formation can be subdivided into the transgressive late Aptian Doncaster Member and the regressive early Albian Coreena Member.

However in the northwest, west and south of the Eromanga Basin, where there is less outcrop information and wireline logs suggest there is less lithological differentiation, these members have not been recognized (Figs. 7, 8, 10, 11). The Wallumbilla Formation is present in the Carpentaria Basin, and its time equivalent in part of South Australia (Table 2) is the Bulldog Shale.

The **Doncaster Member** consists predominantly of carbonaceous mudstone with abundant siltstone and minor sandstone. Glauconie is common in the mudstone in places. The Cretaceous transgression reached a peak in the late Aptian, when much of eastern Australia was inundated (Fig. 5b). The member averages 150 m in thickness, and seldom exceeds 200 m. In the extreme north of the Eromanga Basin the upper part of the unit grades laterally into the silty Jones Valley Member.

The Doncaster sediments were apparently derived largely from quartz-rich basement areas, as the few sandstones are generally sublabe. Laminated carbonaceous and commonly pyritic mudstones are characteristic, but these are thinly interbedded with siltstone and sandstone at some levels. The mudstones appear to have been laid down below normal wave base, with more silty intervals accumulating in somewhat shallower water. Thin cross-laminated sandstone beds were probably deposited during occasional storms.

Derivation was probably largely by wave erosion of older sediments, as is normally the case in an epicontinental sea in a temperate climate (Seibold *et al.*, 1971). However streams would have provided some detritus from the surrounding uplands of basement rocks. The depositional rate was around 70 m/million year (Exon, in press), and similar relatively rapid depositional rates applied to most of the Rolling Downs Group.

The shelly macrofauna, known as the Roma fauna, consists largely of molluscs, but sponges, brachiopods and crinoids are also present (Day, 1969). Day regarded the fauna as provincial and the climate as temperate. The macrofauna is concentrated in thin calcareous beds or bands of nodules, within a thick sequence of barren mudstone. Benthonic foraminifera (Haig, 1973) and dinoflagellates (Burger, 1975) are common. In the Surat Basin the microplankton suggest that the highest salinities were reached during deposition of the Doncaster Member (Burger, 1975).

Although seaways to both the east and north were probably open, and a southwestern seaway may possibly have existed, the type of sediment and the general lack of ammonites and planktonic foraminifera suggest that much of the Doncaster Member was deposited in a somewhat restricted sea.

By the early Albian the seaway to the east had closed, and a slight regression reduced the area of the shallow sea (Fig. 5c). Silts, muds and sands (Coreena Member, Surat Siltstone, early Griman Creek Formation) were laid down under decreasingly marine conditions. At first paralic sediments were confined to the east, but in the middle Albian marine sedimentation was virtually confined to the Ranmoor Member in the north.

The **Coreena Member** consists of interbedded mudstone, siltstone and sandstone with abundant glauconie. The silts and muds of the lower part of the member were laid down in shallow marine conditions, and the sands, silts and intraformational conglomerates of the upper part were laid down in paralic and fluvial environments. The regression was more marked in the east (Fig. 5c).

The member averages 150 m thick in the Eromanga Basin, but is thinner in the Surat Basin, where the younger part is replaced by the Surat Siltstone (see Fig. 8).

The shelly macrofauna, which is an early Tambo fauna, consists largely of molluscs and particularly pelecypods

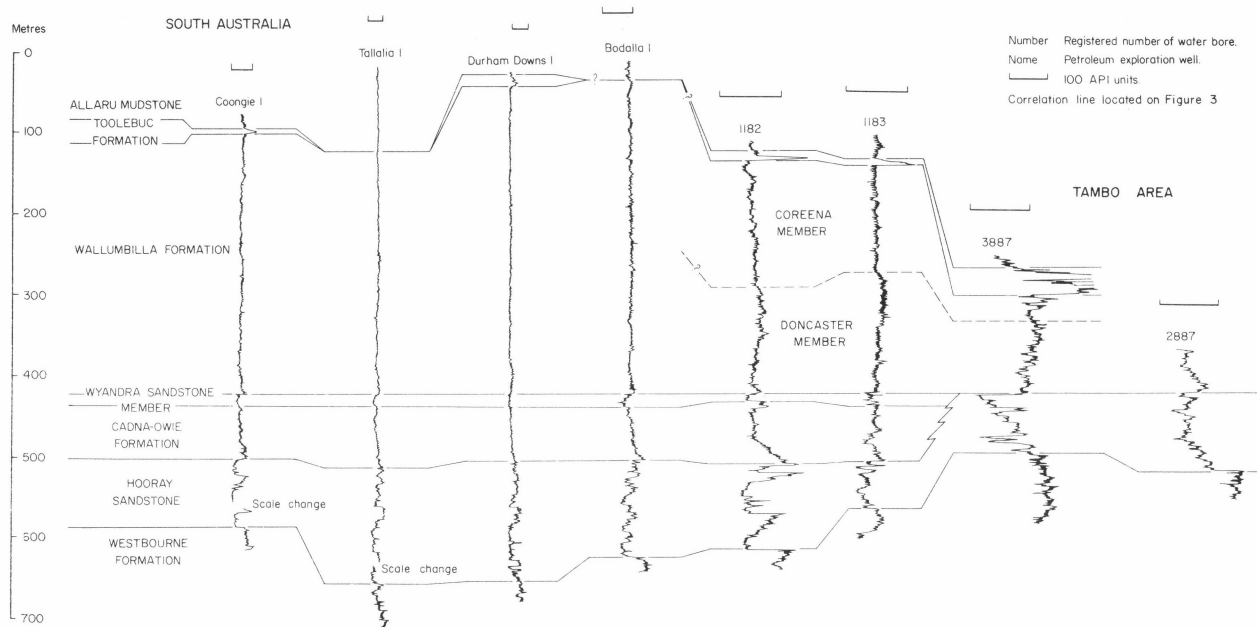


Figure 7. Gamma-ray log correlation from the Tambo area to north-east South Australia

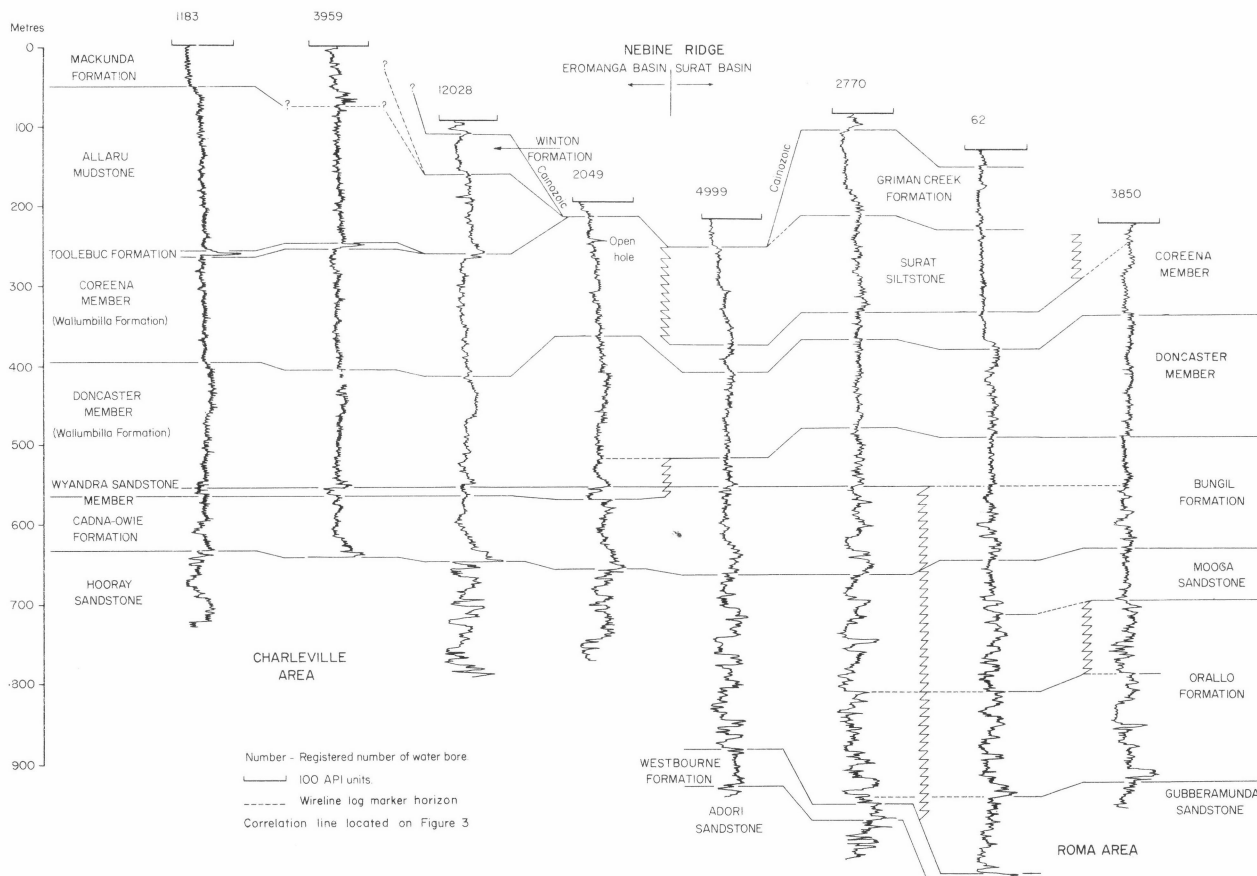


Figure 8. Gamma-ray log correlation line from the Charville area to the Roma area

(Day, 1969). Day regarded the Tambo fauna as more cosmopolitan than the Roma fauna, and the climate as temperate. Benthonic foraminifera are rare (Terpstra, 1969; Haig, 1973). Near the northern entrance to the open sea a variety of ammonites have been collected in the Ranmoor Member, but the eastern seaway had closed and elsewhere conditions were generally restricted, as evidenced

in particular by the lack of ammonites and planktonic foraminifera in the Coreena Member.

The Coreena Member is dominated by andesitic volcanic debris. This represents a major change in provenance from that prevailing earlier, and andesitic debris characterizes the remainder of the Rolling Downs Group (Galloway, 1967). As the western and southern margins of the area

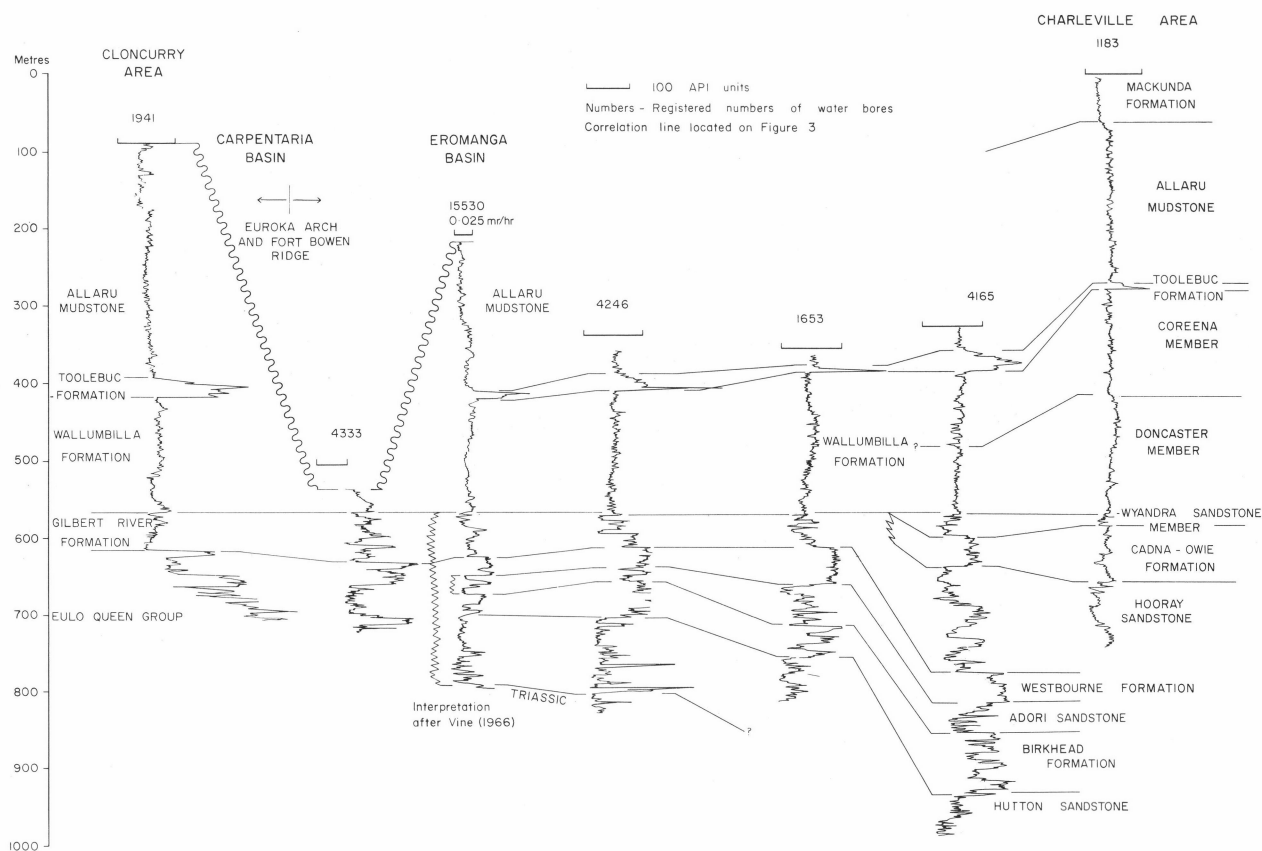


Figure 9. Gamma-ray log correlation line from the Charleville area to the Carpentarian Basin (Cloncurry area)

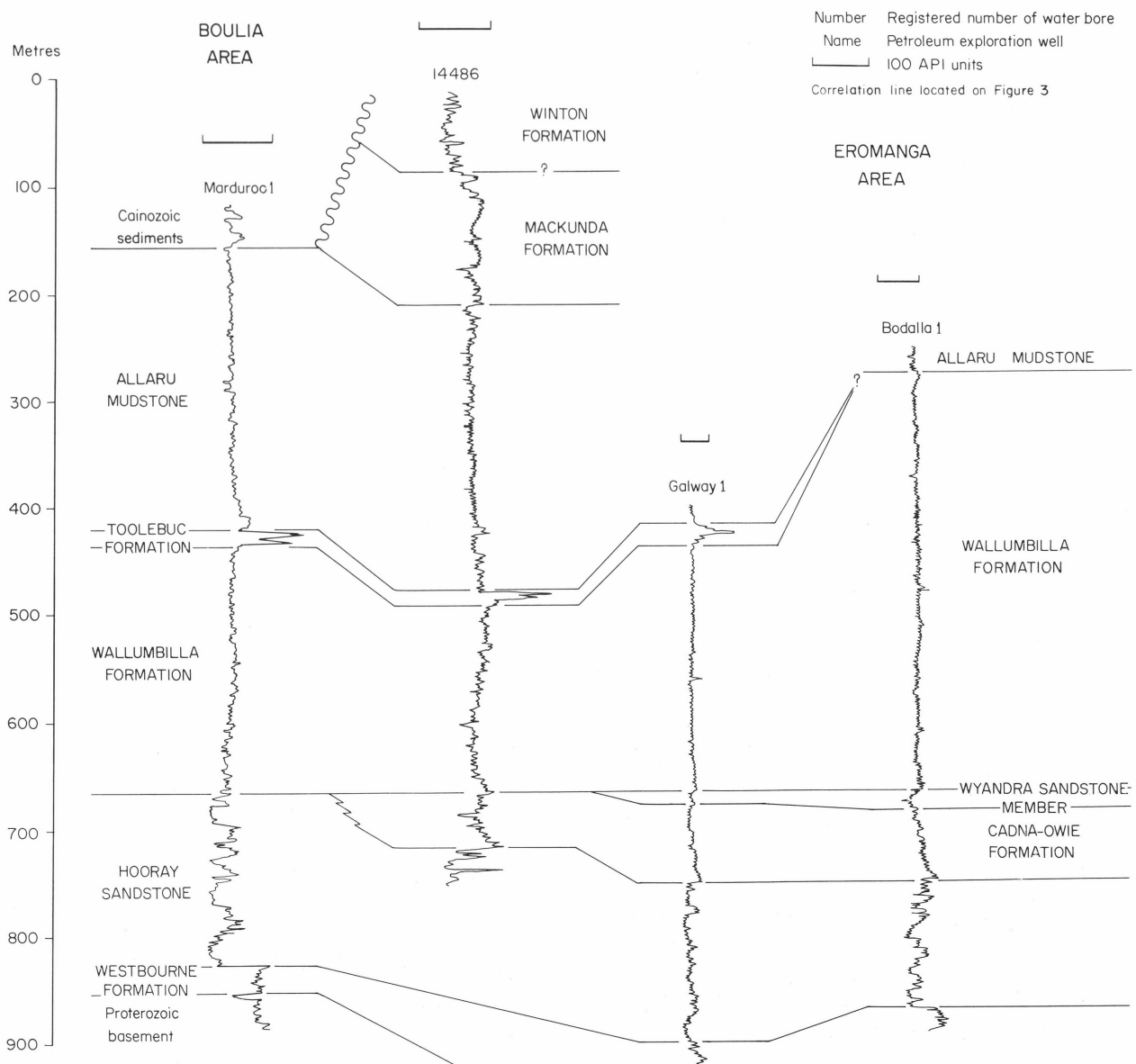


Figure 10. Gamma-ray log correlation line from the Eromanga area to the Boulia area

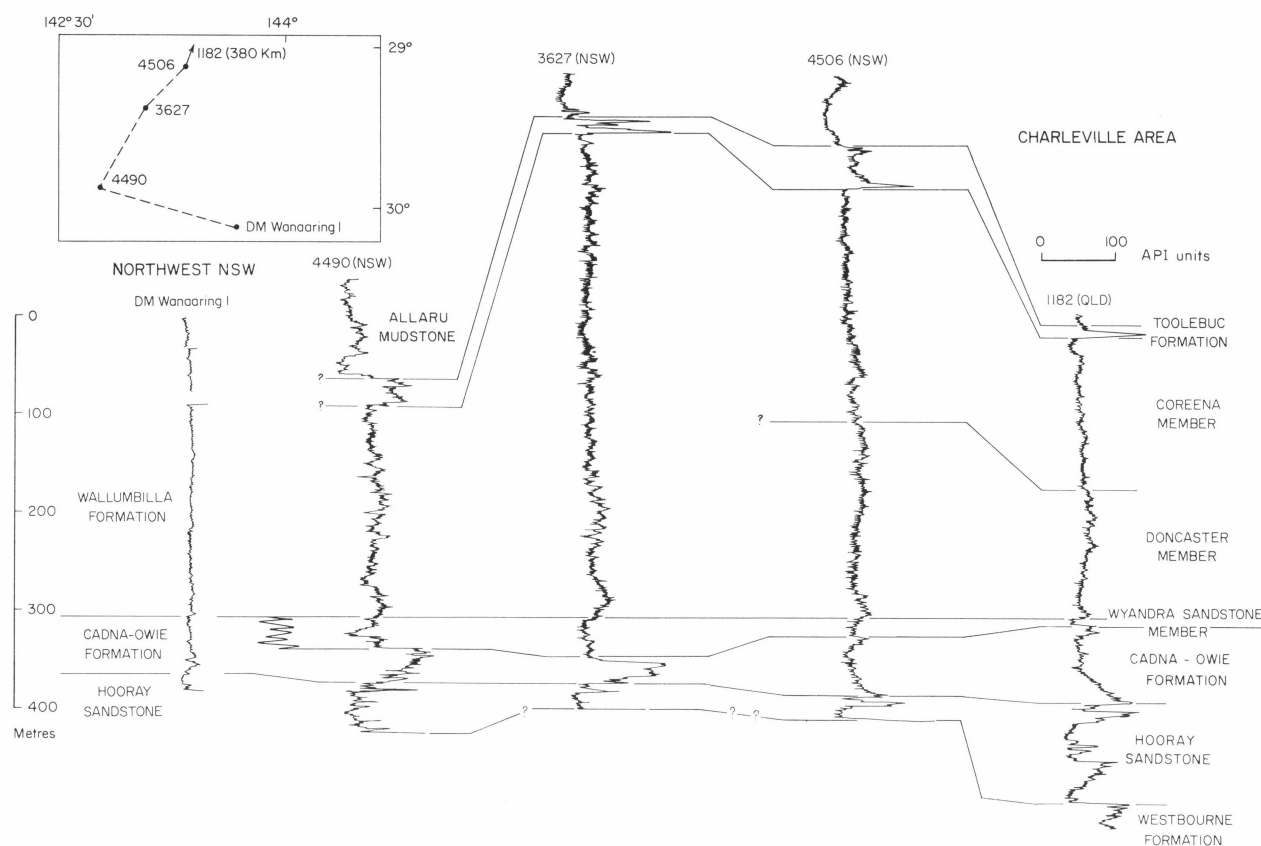


Figure 11. Gamma-ray log correlation line from the Charleville area to northwest New South Wales

were relatively stable, and no andesitic volcanics are present in those areas, it appears that the source of andesitic debris must have been to the east or northeast, where rifting prior to seafloor spreading may have commenced (Veevers & Evans, 1973). Spreading commenced in the Late Cretaceous in the Tasman Sea (Hayes & Ringis, 1973) and in the Eocene in the Coral Sea (Falvey & Taylor, 1974).

A suite of Albian dacitic to andesitic pyroclastics has been recorded off the present Queensland coast (Paine, 1969), and it is possible that a volcanic mountain chain extended for thousands of kilometres to the north-northwest from north of Brisbane. Largely volcanogenic sediments cover some 2 000 000 km² of the Eromanga, Surat and Carpentaria Basins to an average thickness of around 500 m. Assuming that Albian pyroclastics to the east were in fact the source, streams and wind must have carried more than 1 000 000 km³ of volcanic detritus to the southwest. If ranges 150 km wide and 3000 km long extended along and largely seaward of the present east coast, a thickness of about 2000 m of volcanics would have been required as the source of the sediments in the Cretaceous epicontinental sea.

How so much volcanic debris, much of it of sand-size, could have been eroded, transported more than 2000 km in some cases, and buried in an unweathered state remains an enigma. The cool climate would have meant that weathering was a slow process, and presumably the rate of erosion exceeded the rate of weathering. The lack of weathering of sediments deposited in subaerial environments is probably the most surprising feature of this model.

However, given the lack of volcanic vents within the basin, and the apparent lack of tectonic activity and volcanism around most of the basin, the tectonically and volcanically active northeastern margin is the only likely source for the basin sediments.

The **Surat Siltstone** of the Surat Basin rests on the Coreena Member and consists of shallow marine siltstone, mudstone and sandstone (Reiser, 1970), laid down largely above wave base. At some levels one or two species of small pelecypods are densely packed on bedding planes, and there are abundant benthonic foraminifera (Haig, 1973), but dinoflagellates and microplankton are uncommon (D. Burger, pers. comm.), suggesting that the formation was laid down under brackish conditions. It is generally around 100 m thick.

In the early part of the late Albian a shallow sea returned to the Eromanga Basin from the north, but did not cross the recently uplifted Nebine Ridge. The initial sediments were black organic muds with limestone lenses, laid down in a shallow sea and making up the Toolebuc Formation; at the same time fluvial sands, silts and muds of the Griman Creek Formation were probably being deposited in the east. When the transgression reached its peak much of the Eromanga Basin was covered by marine muds with a varied fauna (Day, 1969), while a thin paralic sequence (uppermost Griman Creek Formation) was laid down in the east (see Fig. 5d).

The sea finally withdrew northwards toward the end of the Albian, its withdrawal being marked by deposition of paralic sands and silts of the Mackunda Formation. Deposition of sands and silts of the Winton Formation, by meandering streams flowing northward in the late Albian and early Cenomanian, concluded Cretaceous deposition.

The late Albian **Toolebuc Formation** consists predominantly of black carbonaceous and bituminous shale and siltstone with limestone lenses and coquinites, and averages 15 m thick. Its carbonate content diminishes in a southwesterly direction, and limestones are absent throughout much of southwestern Queensland. The formation was deposited in a shallow sea, with a connection to the ocean in the north. The shales were laid down in

reducing conditions in sheltered areas, and the limestones probably developed as bioherms. Very probably algae extracted carbonate from the sea water producing a firm substrate which was heavily colonized by pelecypods.

The formation has a strong positive gamma-ray anomaly which makes it an excellent wireline-log marker (Fig. 6). This anomaly has been traced into South Australia (Fig. 7) and New South Wales (Fig. 11), and its character throughout the Eromanga Basin in Queensland was illustrated by Senior et al. (1975, Fig. 6).

The shelly macrofauna consists almost entirely of two sessile pelecypods (Day, 1969) for which environmental conditions must have been ideal. Swarms of the planktonic foraminifer *Globigerina* (Crespin, 1963) indicate periodic connection with the open sea, and some dinoflagellates also occur (Evans & Burger, 1972).

The **Allaru Mudstone** was laid down below wave base, and averages 200 m thick. It contains an abundant molluscan (Tambo) macrofauna including numerous ammonites (e.g. Day, 1969), foraminifera including *Globigerina* (Terpstra, 1968), and abundant microplankton (Burger, 1968). Planktonic organisms are more abundant and varied than in any other sequence in the Rolling Downs Group, suggesting that near-normal marine conditions prevailed during its deposition.

The late Albian **Mackunda Formation** consists of sandstone, siltstone and mudstone deposited in shallow marine and paralic environments, and averages 60 m thick. It contains a molluscan fauna dominated by pelecypods (Day, 1969) and common benthonic foraminifera (Crespin, 1963). The presence of coquinas and intraformational conglomerates, and the paucity of planktonic organisms, indicate shallowing and restriction of the sea.

The late Albian to Cenomanian **Winton Formation**, the youngest Cretaceous unit, consists largely of sandstone and siltstone and has a preserved average thickness of 500 m. The lack of marine fossils and the presence of intraformational conglomerate and peat suggest that it was deposited on a broad coastal plain as the sea withdrew.

The **Griman Creek Formation** of the Surat Basin overlies the Surat Siltstone, and palynological evidence (D. Burger, pers. comm.) suggests that it is probably an age-equivalent of the upper Coreena Member, the Toolebuc Formation, and perhaps the lowermost Allaru Mudstone of the Eromanga Basin. It is dominantly composed of siltstone, sandstone and mudstone and averages 300 m thick. Shell coquinas at the base of the sequence, which consist largely of brackish and non-marine forms, represent a regression and are overlain by non-marine sediments characterized by intraformational conglomerate and peat. At the top of the formation acritarchs are present in some areas, and D. Burger (pers. comm.) regards this sequence as brackish, and possibly equivalent to the Toolebuc Formation.

Rounded glauconie grains are most abundant in the sequences which palaeontological evidence shows to be marine or paralic. The presence of glauconie in regressive sequences such as the lower part of the Winton Formation near Tambo, and the Griman Creek Formation, probably indicates reworking of marine or paralic sediments by streams.

Later Events

The subsequent history of the basins has involved widespread weathering and erosion, tilting, and limited volcanism and deposition of sediment (Senior, in press; Exon, in press).

An erosional phase followed Cretaceous deposition and, as base level was neared, deep weathering of the Cretaceous

sequence took place. This led to an overall hardening of the parent rock, breakdown of less resistant fragments, and transformation of montmorillonite to kaolinite. Weathering profiles as much as 120 m thick have been preserved.

During the Cretaceous most of the area had a gently regional northwesterly tilt toward the present-day Gulf of Carpentaria, but mid-Tertiary epeirogenic uplift in the north and east, related to basic volcanism in those areas, altered the slope of the basins and established the present regional drainage toward the Darling River system and Lake Eyre. Cainozoic sands have been deposited by southwesterly-flowing streams, and the wind has formed dunes in the southwest.

Late Cretaceous and Tertiary erosion has removed a great deal of the Cretaceous sequence, especially around the basin margins. Nearshore sandstone, equivalent to the widely represented offshore siltstones and mudstones, have probably been selectively removed. However 2000 m of Cretaceous sediment is still preserved in the deepest part of the Eromanga Basin, where compaction of the underlying Cooper Basin sequence kept it largely below the base level of erosion. The early Tertiary weathering surface, being relatively resistant, forms extensive mesas in both basins.

A Depositional Model

The evidence of sediment grainsize, sedimentary structures, glauconie and contained fossils, suggests that Cretaceous deposition was in and near a broad shallow sea. Preserved sediments fall largely into four groups: non-marine sand bodies with derived glauconie but no marine fossils; near-shore marine sand bodies with a rich molluscan benthonic fauna and abundant glauconie; thinly interbedded sands and silts with glauconie, a molluscan fauna and abundant bioturbation, deposited above wave-base; and laminated carbonaceous and pyritic silts and muds deposited offshore and largely below wave base. The latter are generally barren and non-calcareous, but contain widely separated calcareous beds with an abundant molluscan fauna. Calcareous beds are, in contrast, relatively common in the first three sediment groups. Benthonic organisms generally predominate, but pelagic organisms are abundant at some levels.

Faunal evidence (Day, 1969) suggests that an easterly connection to the sea was open from late Neocomian to early Albian times, and a northerly connection from late Neocomian to late Albian times. Palaeotemperature and fossil evidence suggest a cool climate (Day, op. cit.).

A modern epicontinental sea in a cool climate, whose sedimentological features closely parallel those of the Cretaceous Eromanga and Surat Basins, is the Baltic Sea (Seibold et al., 1971; Exon, 1972b). Within the Baltic Sea the salinity, the number of planktonic organisms, and the variety of benthonic organisms, decrease away from the ocean. Tides are small, currents are unimportant, and waves are active erosive agents. The shallowness of the sea and its entrances cause drastic changes in environment with only slight changes in sea level.

The Baltic Sea at present is a typical adjacent sea in a humid climate, with outflow of brackish surface water and inflow of saline bottom water (Seibold et al., 1971). The two water bodies are separated by a density barrier which approximates to wave base. Solution of carbonate and calcareous organisms is characteristic of sediments laid down below wave base, because saltwater inflow from the open sea is very limited, and the deeper waters are oxygen-poor and have a low pH (Exon, 1972b). In the past, when inflow was greater, the density barrier disappeared, the bottom waters were oxygenated and the pH was normal,

there was no carbonate solution, and calcareous fossiliferous beds were laid down below wave base. Such fluctuations in inflow can explain the otherwise enigmatic occurrence of richly-fossiliferous beds within thick barren sequences in deeper water sediments of the Eromanga and Surat Basins.

The other major sediment groups in the Eromanga and Surat Basins also fit well with a Baltic Sea model: calcareous sand bodies containing some calcareous shelly remains near shore, and interbedded sand and silt developed offshore but above wave base, are characteristic of the Baltic Sea. Glauconie is, however, absent.

In the Eromanga and Surat Basins, as in the Baltic Sea (Exon, 1972b) the shallowness of the sea and its entrances would have meant drastic changes in environment with only slight changes in sea level. Changes in saltwater inflow through the seaways could have been related to changes in cross-section caused by eustatic sea level changes, isostatic movements or changing wind patterns. Even if the saltwater inflow did not vary, changes in the volume of the marine basin caused by sinking or infilling, or changes in freshwater inflow, could have tipped the balance of deepwater sedimentation from calcareous to non-calcareous muds or vice versa.

Acknowledgements

Numerous workers have helped us with field mapping and palaeontological identifications over the years. Among the field workers we owe a special debt of gratitude to R. R. Vine, D. J. Casey, M. C. Galloway, E. N. Milligan, A. Mond and J. Smart; among the palaeontologists, to R. W. Day and D. Burger, whose contributions were vital to an understanding of the palaeogeography.

References

- BURGER, D., 1968—Palynology of marine Lower Cretaceous strata in the northern and eastern Eromanga Basin, Queensland. *Bureau of Mineral Resources, Australia—Record* 1968/62 (unpublished).
- BURGER, D., 1973—Spore zonation and sedimentary history of the Neocomian, Great Artesian Basin, Queensland. *Geological Society of Australia—Special Publication* 4, 87-118.
- BURGER, D., 1975—Palynology of subsurface Lower Cretaceous strata in the Surat Basin, Queensland. *Palaeontological Papers* 1972, 27-42. *Bureau of Mineral Resources, Australia—Bulletin* 150.
- BYRNES, J. G., 1973—Lithological units from Great Artesian Basin cores D. M. Weilmoringle, Bellfield, Yantabulla, Wanaaring, NSW. *Geological Survey of New South Wales—Report* GS 1973/120 (unpublished).
- BYRNES, J. G., MORGAN, R., & SCHEIBNEROVA, V., 1975—Recent evidence for the age of Great Australian Basin sediments in New South Wales. *Quarterly Notes of the Geological Survey of New South Wales* 18, 2-13.
- CRISPIN, Irene, 1963—Lower Cretaceous arenaceous foraminifera of Australia. *Bureau of Mineral Resources, Australia—Bulletin* 66.
- CROOK, K. A. W., 1960—Classification of arenites. *American Journal of Science* 258, 419-28.
- DAY, R. W., 1969—The Lower Cretaceous of the Great Artesian Basin; in CAMPBELL, K. S. W. (Editor), STRATIGRAPHY AND PALAEOLOGY: ESSAYS IN HONOUR OF DOROTHY HILL, 140-173. *Australian National University Press*.
- DETTMAN, Mary E., & PLAYFORD, G., 1969—Palynology of the Australian Cretaceous; a review; in CAMPBELL, K. S. W. (Editor), STRATIGRAPHY AND PALAEOLOGY: ESSAYS IN HONOUR OF DOROTHY HILL, 174-210. *Australian National University Press*.
- DORMAN, F. H., & GILL, E. D., 1959—Oxygen isotope palaeotemperature measurements of Australian fossils. *Proceedings of the Royal Society of Victoria* 74, 73-98.
- DOUTCH, H. F., SMART, J., & GRIMES, K. G., in prep.—The geology of the Carpentaria and Karumba Basins, Queensland. *Bureau of Mineral Resources, Australia—Bulletin*.
- EVANS, P. R., & BURGER, D., 1972—Palynology of shallow stratigraphic boreholes and oil exploration wells. Appendix 1 in *Bureau of Mineral Resources, Australia—Report* 143.
- EXON, N. F., 1966—Revised Jurassic to Lower Cretaceous stratigraphy in the south-east Eromanga Basin, Queensland. *Queensland Government Mining Journal* 67, 232-238.
- EXON, N. F., 1972a—Shallow stratigraphic drilling in the eastern Surat Basin, Queensland, 1966, 1967 and 1968. *Bureau of Mineral Resources, Australia—Record* 1972/54 (unpublished).
- EXON, N. F., 1972b—Sedimentation in the outer Flensburg Fjord area (Baltic Sea) since the last glaciation. *Meyniana* 22, 5-62.
- EXON, N. F., 1974—The geological evolution of the southern Taroom Trough and the overlying Surat Basin. *APEA Journal* 14, 50-58.
- EXON, N. F., in press—The geology of the Surat Basin in Queensland. *Bureau of Mineral Resources, Australia—Bulletin* 166.
- EXON, N. F., GALLOWAY, M. C., CASEY, D. J., & KIRKEGAARD, A. G., 1972—Geology of the Tambo/Augathella area, Queensland. *Bureau of Mineral Resources, Australia—Report* 143.
- EXON, N. F., & MORRISSEY, Jean, 1975—Wireline logging of water bores in the Surat Basin, 1960 to 1974. *Bureau of Mineral Resources, Australia—Report* 188.
- EXON, N. F. & VINE, R. R., 1970—Revised nomenclature of the 'Blythesdale' sequence. *Queensland Government Mining Journal* 71, 48-52.
- FALVEY, D. A., & TAYLOR, D. W., 1974—Queensland Plateau and Coral Sea Basin: structural and time-stratigraphic patterns. *Australian Society of Exploration Geophysicists—Bulletin* 5, 123-126.
- GALLOWAY, M. C., 1967—The petrology of some sediments from the Tambo, Augathella, Eddystone, and Mitchell 1:250 000 Sheet areas—Queensland. *Bureau of Mineral Resources, Australia—Record* 1967/81 (unpublished).
- GREGORY, C. M., & VINE, R. R. 1970—Canterbury, Queensland, 1:250 000 Geological Series. *Bureau of Mineral Resources, Australia—explanatory Notes* SG/54-7.
- HAIG, D., 1973—Lower Cretaceous Foraminifera, Surat Basin, southern Queensland: a preliminary stratigraphic appraisal. *Queensland Government Mining Journal* 74, 44-52.
- HAYES, D. E., & RINGIS, J., 1973—Seafloor spreading in the Tasman Sea. *Nature* 243, 454-8.
- IRVING, E., 1964—PALAEOLOGY. Wiley, New York.
- LUDBROOK, N. H., 1966—Cretaceous biostratigraphy of the Great Artesian Basin in South Australia. *Geological Survey of South Australia—Bulletin* 40.
- MILLOT, G., 1970—GEOLOGY OF CLAYS. *Springer Verlag*.
- NUGENT, O., 1969—Sedimentation and petroleum potential of the Jurassic sequence in the southwestern Great Artesian Basin. *APEA Journal* 9, 97-106.
- PAINE, A. G. L., 1969—Palaeovolcanology of central eastern Queensland. *Geological Society of Australia—Special Publication* 2, 183-192.
- PARKIN, L. W., (Editor), 1969—HANDBOOK OF SOUTH AUSTRALIAN GEOLOGY. *Geological Survey of South Australia*.
- REISER, R. F., 1970—Stratigraphic nomenclature of the upper part of the Rolling Downs Group in the Surat area. *Queensland Government Mining Journal* 71, 301-3.
- SEIBOLD, E., EXON, N. F., HARTMANN, M., KÖGLER, F.-C., KRUMM, H., LUTZE, G. F., NEWTON, R. S., & WERNER, F., 1971—Marine geology of Kiel Bay. *VII International Sedimentological Congress 1971: Guidebook to sedimentology of parts of central Europe*, 209-35.
- SENIOR, B. R., in press—Notes on the geology of the central part of the Eromanga Basin. *Bureau of Mineral Resources, Australia—Bulletin* 167B.

- SENIOR, B. R., EXON, N. F., & BURGER, D., 1975—The Cadna-owie and Toolebuc Formations in the Eromanga Basin, Queensland. *Queensland Government Mining Journal*, 76, 445-55.
- SENIOR, B. R., HARRISON, P. L., & MOND, A., in press—Notes on the geology of the northern part of the Eromanga Basin. *Bureau of Mineral Resources, Australia—Bulletin* 167A.
- SMART, J., 1972—The terms Toolebuc Limestone and Kamileroi Limestone. *Queensland Government Mining Journal* 73, 280-6.
- SMART, J., in press—Stratigraphic correlations in the southern Carpentaria and northern Eromanga Basins. *Queensland Government Mining Journal*.
- SMART, J., GRIMES, K. G., & DOUTCH, H. F., 1972—New and revised stratigraphic names—Carpentaria Basin. *Queensland Government Mining Journal* 73, 190-210.
- SMART, J., INGRAM, J. A., DOUTCH, H. F., & GRIMES, K. G., 1971—Recent geological mapping in the Carpentaria Basin—new stratigraphic names. *Queensland Government Mining Journal* 72, 227-33.
- TERPSTRA, G. R. J., 1968—Micropalaeontological examination of BMR Jericho 9, Tambo 5, 6, Augathella, 1, 2, 3, and Adavale 1. *Bureau of Mineral Resources, Australia—Record* 1967/81 (unpublished).
- TERPSTRA, G. R. J., 1969—Micropalaeontological examination of cores from the Rolling Downs Group in G.S.Q. boreholes Surat 1, 2, and 3, Queensland. *Bureau of Mineral Resources, Australia—Record* 1969/114 (unpublished).
- VEEVERS, J. J., & EVANS, P. R., 1973—Sedimentary and magmatic events in Australia and the mechanism of world-wide Cretaceous transgressions. *Nature, Physical Science* 245, 33-36.
- VINE, R. R., 1966—Recent geological mapping in the northern Eromanga Basin, Queensland. *APEA Journal* 6, 110-15.
- VINE, R. R., & DAY, R. W., 1965—Nomenclature of the Rolling Downs Group, northern Eromanga Basin. *Queensland Government Mining Journal* 66, 416-21.
- VINE, R. R., DAY, R. W., MILLIGAN, E. N., CASEY, D. J., GALLOWAY, M. C., & EXON, N. F., 1967—Revision of the nomenclature of the Rolling Downs Group in the Eromanga and Surat Basins. *Queensland Government Mining Journal* 68, 144-51.
- WHITEHOUSE, F. W., 1926—The Cretaceous Ammonoidea of eastern Australia. *Queensland Museum—Memoir* 8, 195-242.
- WHITEHOUSE, F. W., 1954—The geology of the Queensland portion of the Great Artesian Basin. Appendix G in Artesian water supplies in Queensland. *Department of the Co-ordinator-General of Public Works, Queensland—Report A. 56*, 1955.
- WOPFNER, H., FREYTAG, I. B. & HEATH, G. R., 1970—Basal Jurassic-Cretaceous rocks of western Great Artesian Basin, South Australia: stratigraphy and environment. *American Association of Petroleum Geologists—Bulletin* 54, 383-416.

Significance of Middle Cambrian Trilobites from Elcho Island, Northern Territory

K. A. Plumb, J. H. Shergold, and M. Z. Stefanski*

A recently discovered Templetonian (Middle Cambrian) trilobite fauna, with affinity to that of the Beetle Creek Formation of western Queensland, is reported from pebbles derived from the Elcho Island Formation (Wessel Group) on Elcho Island, in the Arafura Basin, northern Australia. Consequently, a previously determined isotopic age of 790 m.y., on glauconite from the Elcho Island Formation, is now clearly much greater than the age of deposition of the formation, and the age of the occurrence of *Skolithos* at the base of the Wessel Group (Buckingham Bay Sandstone) can be reconsidered as Early or early Middle Cambrian, rather than late Proterozoic. Regional correlation of the Buckingham Bay Sandstone and Raiwalla Shale of the Arafura Basin with the Bukalara Sandstone and Cox Formation of the McArthur River region is reiterated on the basis of rock types and presence of the trace fossil *Skolithos*.

During the course of hydrogeological investigations by Stefanski on Elcho Island in June 1974, an occurrence of fossils near Ularnga Point (shown as Warnga Point on published maps), Elcho Island (Fig. 1), was pointed out by Mr. E. W. Parr of Elcho Island Mission. Samples collected by Stefanski were assigned an early Middle Cambrian age by Miss Joyce Gilbert-Tomlinson (BMR) (unpublished preliminary note). Further samples collected in August 1974 by M. J. Wiltshire on behalf of Champlin Philippines Inc., and S. K. Skwarko (BMR) were determined by Shergold and confirm the Middle Cambrian age.

The fossils were collected from angular blocks and rounded pebbles of fine-grained quartz sandstone and siliceous siltstone, in gravels along the strand line of 'Tembi' and 'Second' Beaches on Elcho Island; similar material occurs, but becomes progressively less abundant, for several kilometres to the northeast (M. J. Wiltshire, personal communication, September 1st, 1974). Although no fossiliferous material has been positively identified in situ, the similarity of the host rock to nearby exposures of Elcho Island Formation (Wessel Group, Fig. 2), the distribution and volume of material and its occurrence close to the wave-cut platform, and the obviously slight abrasion of the large angular slabs, leaves little doubt that the fossils are derived from the Elcho Island Formation in the vicinity of Ularnga Point. Wiltshire (pers. comm.) has postulated a source just below the tidal zone off the northwest shoreline of Ularnga Point (Fig. 1).⁽¹⁾

Outcrops of Elcho Island Formation are confined mainly to discontinuous weathered exposures beneath laterite, and to wave-cut platforms and low cliffs along the coasts of Howard, Elcho, and Drysdale Islands (Fig. 1). At Elcho Island Mission the basal beds of the formation consist of interbedded ferruginous sandstone, green micaceous and glauconitic fine-grained sandstone, and shale. These pass upwards into flaggy interbedded leached dolomitic and siliceous siltstone and chert, in discontinuous exposures along the coast to the north of the Mission (Dunnet, 1965; Plumb, 1965). The youngest beds of the Elcho Island Formation, and hence of the Wessel Group, preserved onshore were found at Ularnga Point.

The Fauna

The recovered fauna of the Elcho Island Formation is composed largely of trilobite remains—mostly fragmented, but occasionally articulated, xystridurid and eodiscid carapaces. Agnostina, Oryctocephalidae, and Ptychopariidae occur rarely, as do the non-trilobite elements of the fauna. The identified fauna includes:

Trilobita	<i>Lyriaspis</i> cf. <i>sigillum</i> Whitehouse, 1939
	<i>Oryctocephalites runcinatus</i> Shergold, 1969
	<i>Pagetia</i> cf. <i>significans</i> (Etheridge, 1902)
	<i>Pagetia</i> aff. <i>significans</i> (Etheridge, 1902)
	<i>Pagetia</i> sp. nov.
	<i>Peronopsis</i> cf. <i>normata</i> (Whitehouse, 1936)
	<i>Xystridura</i> cf. <i>templetonensis</i> (Chapman, 1929)
	xystridurid undet.
Bradoriida:—	aff. <i>Indota</i> sp. undet.
Hyalolitha:—	<i>Hyalolithes?</i> sp. undet.

Generically undetermined inarticulate Brachiopoda and sponge spicules also occur.

A conservative approach to the determinations is necessary pending the publication of a paper by A. A. Öpik (in preparation) dealing with some of the listed taxa, and continuing palaeontological investigations. Furthermore, specimens on weathered surfaces are often too badly abraded to permit precise specific determination.

The Elcho Island fauna has a Middle Cambrian age and belongs to the pre-*Ptychagnostus gibbus* portion of the Templetonian Stage as conceived by Öpik (1967, 136-7).

Similar generic associations occur widely in western Queensland and eastern Northern Territory, in the Arthur Creek Beds, Beetle Creek Formation, Border Waterhole Formation, Burton Beds, Sandover Beds and Wonarah Beds. The specific association determined here, however, is most similar to that occurring in the Beetle Creek Formation of western Queensland.

The fine grain size of the sediment and its fine lamination, coupled with a fauna having low species diversity but rich in individuals, often completely articulated, suggests a low energy, probably cool and/or deep water, ocean-facing depositional environment.

* M. Z. Stefanski publishes with the permission of the First Assistant Secretary (Resource Development), Water Resources Branch Department of the Northern Territory.

⁽¹⁾During a recent visit to Ularnga Point L. P. Black (BMR) located the fauna in situ on the wave-cut platform at low tide.

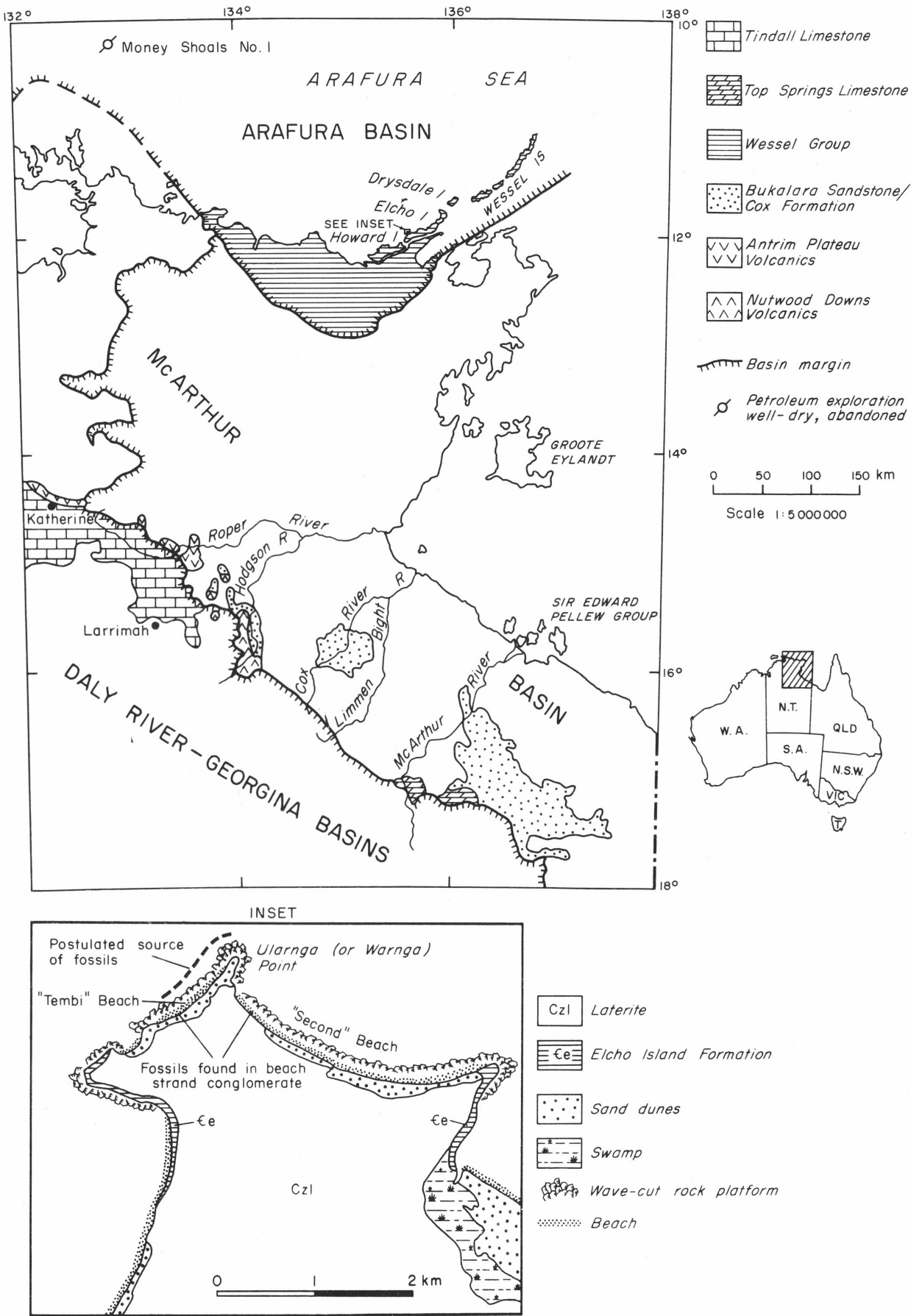


Figure 1. Locality maps

Previous Interpretation of Age

The Arafura Basin (Plumb, 1965; Plumb & Derrick, 1975) is a relatively undeformed epicratonic basin situated along the north coast of Arnhem Land, Northern Territory, and extending offshore beneath the Arafura Sea (Fig. 1). It overlies the Proterozoic McArthur Basin and older metamorphic rocks with strong angular unconformity and is unconformably overlain by Early Cretaceous rocks. Only the lowermost part of the basin succession, the 1450 m-thick Wessel Group (Fig. 2), is exposed onshore. Offshore the Wessel Group passes up into a largely unknown sequence, whose thickness, estimated by depths to aeromagnetic basement, is over 10 000 m.

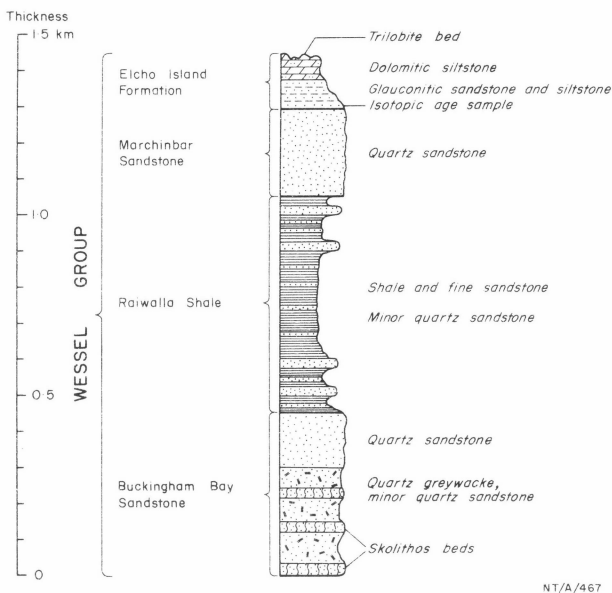


Figure 2. Schematic stratigraphic column

The assignment of the Wessel Group has been problematical: 'Permo-Carboniferous' (Brown, 1908; Jensen, 1914); Early Cambrian or Precambrian (Wade, 1924); Cambrian (?) (Plumb, 1963); Adelaidean or 'Upper Proterozoic' (Dunnet, 1965; McDougall, et al., 1965; Plumb, 1965; Dunn, Plumb & Roberts, 1966; BMR, 1967, 1974; GSA, 1971).

The tentative Cambrian age proposed by Plumb (1963) was based on the recognition of similar sequences in the Arafura Basin and unconformably overlying the McArthur Basin in the McArthur River region (Dunn, 1963; Plumb & Paine, 1964), and the occurrence of vertical tubes made by an unknown burrowing organism, *Skolithos*, in sandstones (Buckingham Bay and Bukalara) at the base of these sequences (Dunnet, 1965; Plumb, 1965; Plumb & Derrick, 1975).

However, isotopic dating of glauconite from the Elcho Island Formation, at the top of the Wessel Group in the Arafura Basin, produced ages of 770 m.y. by K-Ar and 790 m.y. by Rb-Sr methods (McDougall et al., 1965). Since this was regarded as a minimum age for deposition, the Wessel Group was subsequently thought to be Adelaidean (or 'Upper Proterozoic') (eg. Dunnet, 1965; Plumb, 1965; Dunn, Plumb & Roberts 1965; BMR 1967). The range of *Skolithos*, found in northern Australia and elsewhere in rocks of Early Palaeozoic ages, was thus extended down to about 800 m.y., as noted by Glaessner (1966, p. 42).

Significance of New Dating

A Middle Cambrian age for the Elcho Island Formation at the top of the Wessel Group has important implications for the regional stratigraphy and proposed correlation of rock units of northern Australia (Fig. 3).

Although poor outcrop obscures the precise stratigraphic relationships between the Elcho Island Formation and underlying units in the Wessel Group, the formations show regional structural concordance and boundaries between them are gradational. Since there is no evidence for any major break in the sequence, the whole of the Wessel Group can be reassigned to the Cambrian with some confidence, and an Early or early Middle Cambrian age postulated for the occurrence of *Skolithos* at its base.

The Buckingham Bay Sandstone and Raiwalla Shale of the Arafura Basin have previously been correlated with the Bukalara Sandstone and Cox Formation (Dunn, 1963; Plumb & Paine, 1964) of the McArthur River region (Fig. 3), because of their strong similarity in rock types and structural setting, and the presence of *Skolithos* in the Buckingham Bay and Bukalara Sandstones. The Bukalara Sandstone also unconformably overlies the McArthur Basin (Roberts, Rhodes & Yates, 1963; Smith, 1964), and itself is generally overlain with slight unconformity by the Middle Cambrian Tindall or Top Springs Limestones (Dunn, 1963; Plumb & Rhodes, 1964). However, in the Hodgson River area, the Bukalara Sandstone is overlain by and intertongued with the Nutwood Downs Volcanics, which are regarded as equivalent to the Antrim Plateau Volcanics (Dunn, 1963). These correlations would seem to support an Early Cambrian age for the Antrim Plateau Volcanics.

The prospectivity of the Arafura Basin for hydrocarbons, dependant on the presence of a thick section of Palaeozoic rocks beneath the Mesozoic and Cainozoic of the overlying Money Shoals Basin, was reduced when a Proterozoic age was postulated for the Wessel Group. Since the Wessel Group marks the base of the Arafura Basin onshore, and Silurian fossils (palynomorphs) were found in one horizon of the otherwise unfossiliferous section intersected by Money Shoals No. 1 Well (Blake, et al, 1973), it is reasonable to reassign the whole of the basin succession to the Palaeozoic. The new fossil discovery therefore enhances the petroleum potential of the Arafura Basin.

Care has always been needed in interpreting isotopic ages obtained from glauconite; the experience in Australia has generally been that glauconite ages tend to be too young. Although McDougall et al. (1965) analysed only one sample, the age was considered reliable because of the close agreement between the K-Ar (760 m.y.) and Rb-Sr (790 m.y.) data. These ages are now clearly much older than the age of deposition (550 m.y.) of the rocks. Another example where the glauconite age is apparently too old is the Vaughan Springs Quartzite (Cooper, Wells & Nicholas, 1971; Marjoribanks & Black, 1974; 1280 vs 1076 m.y.).

An explanation of the anomalously old isotopic age of the glauconite is not immediately apparent, and further samples are under investigation. The glauconite sample originally analysed was a very pure concentrate, excluding contamination (R. W. Page, pers. comm., 1974). One possible explanation is that detrital glauconite was derived by erosion of a Precambrian terrain. However, the nearest and youngest available sources are the 1300 m.y. old Malay Road and Roper Groups, which are much older than the determined age (790 m.y.). It seems unlikely that soft glauconite pellets would survive transportation over the 50 km distance from the nearest source area. Furthermore, some of the glauconite is intimately associated with, and has apparently formed from, detrital biotite. Thus, another

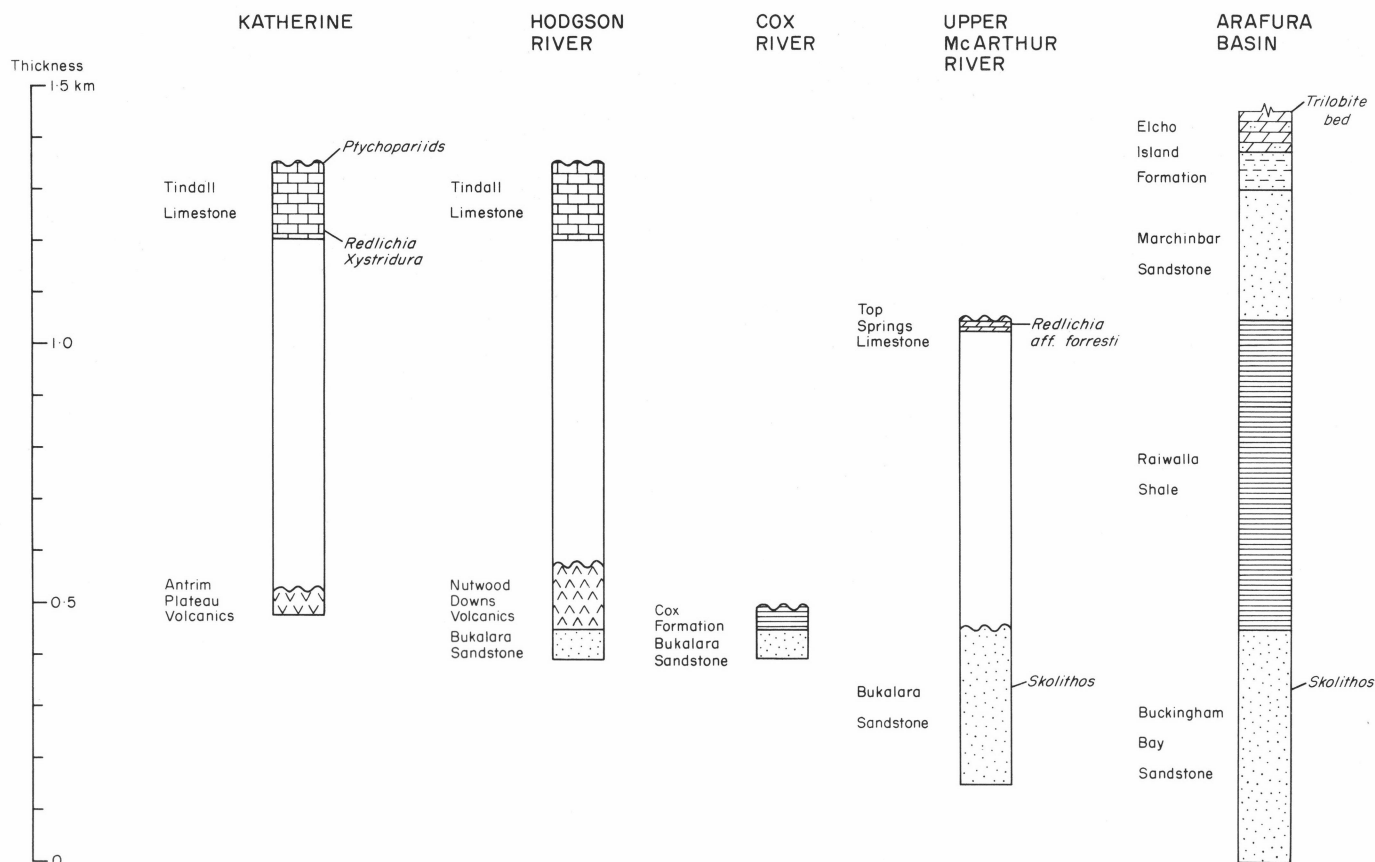


Figure 3. Regional correlation of Cambrian successions

explanation, favoured herein, is that the apparent age is partly inherited from the parent mica. The concordance of the original K-Ar and Rb-Sr data, however, still remains to be investigated.

Acknowledgements

The authors wish to thank Mr E. W. Parr (Elcho Island Mission) for initially drawing attention to the occurrence of the fossils; M. J. Wiltshire (Glenside, S.A.) and S. K. Skwarko (BMR) for providing additional materials; and W. Jauncey (Champlin Philippines Inc.) for permitting access to unpublished documentation. Miss J. Gilbert-Tomlinson and Drs I. McDougall and M. R. Walter critically read the manuscript.

References

- BALKE, B., PAGE, C., HARRISON, R., & ROUSSOPOULOS, G., 1973—Exploration in the Arafura Sea. *APEA Journal*, **13**, 9-12.
- BMR (Bureau of Mineral Resources), 1967—Geological Map, Arnhem Land, Northern Territory. Scale 1:500 000. *Canberra*.
- BMR (Bureau of Mineral Resources), 1974—Geology of the Kimberley to Mount Isa Region, Northern Australia. 1:2 500 000 Special Map. *Canberra*.
- BROWN, H. Y. L., 1908—Geological reconnaissance from Van Dieman Gulf to McArthur River by the Government Geologist, 1907. *South Australian Parliamentary Papers*, **25**.
- CHAPMAN, F., 1929—On some trilobites and brachiopods from the Mount Isa district, N.W. Queensland. *Proceedings of the Royal Society of Victoria*, (II), 206-216, pls XXI-XXII.
- COOPER, J. A., WELLS, A. T., & NICHOLAS, T., 1971—Dating of glauconite from the Ngalia Basin, Northern Territory, Australia. *Journal of the Geological Society of Australia*, **18**, 97-106.
- DUNN, P. R., 1963—Hodgson Downs, N.T.,—1:250 000 Geological Series. *Bureau of Mineral Resources, Australia—Explanatory Notes SD/53-14*.
- DUNN, P. R., PLUMB, K. A., & ROBERTS, H. G., 1966—A proposal for time-stratigraphic subdivision of the Australian Precambrian, *Journal of the Geological Society of Australia*, **13**, 593-608.
- DUNNET, D., 1965—Arnhem Bay/Gove, N.T.,—1:250 000 Geological Series. *Bureau of Mineral Resources, Australia—Explanatory Notes SD/53-3/4*.
- ETHERIDGE, R., Jnr, 1902—Official contributions to the palaeontology of South Australia, 13—Evidence of further Cambrian trilobites. *South Australian Parliamentary Papers* (1902), 3-4, pl. II.
- GLAESSNER, M. F., 1966—Precambrian palaeontology. *Earth-Science Reviews*, **1**, 29-50.
- GSA (Geological Society of Australia), 1971—Tectonic map of Australia and New Guinea, 1:5 000 000. *Sydney*.
- JENSEN, H. I., 1914—Geological report on the Darwin Mining District; McArthur River District; and the Barkly Tableland. *Bulletin of the Northern Territory of Australia*, **10**, 24 pls.
- MCDUGALL, I., DUNN, P. R., COMPSTON, W., WEBB, A. W., RICHARDS, J. R., & BOFINGER, V. M., 1965—Isotope age determination on Precambrian rocks of the Carpentaria Region, Northern Territory, Australia. *Journal of the Geological Society of Australia*, **12**, 67-90.
- MARJORIBANKS, R. W., & BLACK, L. P., 1974—Geology and geochronology of the Arunta Complex north of Ormiston Gorge, central Australia. *Journal of the Geological Society of Australia*, **21**, 291-299.
- ÖPIK, A. A., 1967—The Ordian Stage of the Cambrian and its Australian Metadoxidae. *Bureau of Mineral Resources, Australia—Bulletin* **92**, 133-168, pls. 19-20.
- ÖPIK, A. A., (in preparation)—Middle Cambrian Agnostacea. *Bureau of Mineral Resources, Australia—Bulletin* **172**.

- PLUMB, K. A., 1963—Explanatory notes on the Wessel Islands—Truant Island 1:250 000 geological series Sheet SC53-15/16. *Bureau of Mineral Resources, Australia—Record* 1963/134 (unpublished).
- PLUMB, K. A., 1965—Wessel Island/Truant Island, N.T.—1:250 000 Geological Series. *Bureau of Mineral Resources, Australia—Explanatory Notes* **SC/53-15/16**.
- PLUMB, K. A. & DERRICK, G. M., in press—Geology of the Proterozoic rocks of northern Australia: in KNIGHT, C. L. (editor), *ECONOMIC GEOLOGY OF AUSTRALIA AND PAPUA NEW GUINEA. Australasian Institute of Mining and Metallurgy, Melbourne*.
- PLUMB, K. A., & PAINE, A. G. L., 1964—Mount Young, N.T.—1:250 000 Geological Series. *Bureau of Mineral Resources, Australia—Explanatory Notes* **SD/53-15**.
- PLUMB, K. A. & RHODES, J. M., 1964—Wallhallow, N.T.—1:250 000 Geological Series. *Bureau of Mineral Resources, Australia—Explanatory Notes* **SE/53-7**.
- ROBERTS, H. G., RHODES, J. M., & YATES, K. R., 1963—Calvert Hills, N.T.—1:250 000 Geological Series. *Bureau of Mineral Resources, Australia—Explanatory Notes* **SE/53-8**.
- SHERGOLD, J. H., 1969—Oryctocephalidae (Trilobita: Middle Cambrian) of Australia. *Bureau of Mineral Resources, Australia—Bulletin* **104**, 12 pls.
- SMITH, J. W., 1964—Bauhinia Downs, N.T.—1:250 000 Geological Series. *Bureau of Mineral Resource, Australia—Explanatory Notes* **SE/53-3**.
- WADE, A., 1924—Petroleum prospects, Kimberley District of Western Australia, and Northern Territory. *Commonwealth of Australia Parliamentary Papers* **142**, 13 pls.
- WHITEHOUSE, F. W., 1936—The Cambrian faunas of northeastern Australia. Part 1—Stratigraphic outline. Part 2—Trilobita (Miomera). *Memoirs of the Queensland Museum*, **11** (1), 59-112, pls. VIII-X.
- WHITEHOUSE, F. W., 1939—The Cambrian faunas of northeastern Australia. Part 3—The Polymerid trilobites (with supplement 1). *Memoirs of the Queensland Museum* **21** (3), 179-282, pls. 19-25.

Automated Density Profiling over elongate topographic features

W. Anfiloff

Nettleton's concept of density profiling can be utilised to give useful estimates of the bulk density of topographic features. These estimates can be used to infer the composition of such topography, or to assist in the interpretation of local gravity anomalies.

Two methods that facilitate multiple density profiling over elongate topography are presented. One is a simulation reduction method utilising the two-dimensional line integral formula of Talwani, Worzel & Landisman (1959). It enables data from any detailed gravity traverse crossing an elongate topographic feature at right angles to be automatically reduced by computer to a set of multiple density Bouguer profiles. From these profiles, the bulk density of the topographic feature can be estimated by visual correlation. The other is a graphical method of converting a set of multiple density Bouguer profiles directly to point density estimates, without the need for visual correlation. Both methods are theoretically exact for the ideal case.

A visual correlation determination of $2.85 \pm 0.05 \text{ g cm}^{-3}$ is demonstrated for a traverse crossing the 300 m high Harts Range, Northern Territory, and three point determinations of 2.97, 2.97, and 2.99 g cm^{-3} , for a traverse crossing the 100 m high Fraser Range, Western Australia.

Nettleton's (1939) density profiling concept can be expressed thus: by seeking a minimum correlation between Bouguer anomaly and elevation over a topographic feature, a bulk density can be determined for the feature. Nettleton envisaged that density estimates determined from topographic features could be used for the Bouguer reduction of gravimeter observations in their vicinity. Naturally, such estimates can also be used to infer the overall composition of the millions of tonnes of rock in the vicinity of the gravity observations. Nettleton emphasised that terrain corrections have to be applied in areas of steep topography, and that steep geological boundaries, where density changes could complicate the profiles, should be avoided. Subsequent authors, (Parasnis, 1951; Dobrin, 1952; Vajk, 1956; Grant and West, 1965; Linsser, 1965; Beattie, 1975) have discussed the concept of density profiling, its applications, and complicating factors.

The main drawback to density profiling is the need to apply a separate terrain correction at every station if the topography is steep. Perhaps for this reason, its use has generally been restricted to low hills, for which the resolution is inherently poor. Poor resolution was probably the main reason why a recent profiling attempt (Beattie, 1975) failed to give conclusive results. The formula which Hubbert (1948) used to derive theoretical terrain effects over two-dimensional topography might have been applicable to density profiling, but presumably it was too cumbersome for use in a real situation. The advent of computers led to the use of numerical methods of cross-correlating gravity and elevation in three dimensions to obtain a regional density distribution, (Simpson 1954; Grant and Elsharty, 1962; Linsser, 1965), and facilitated the computation of terrain corrections. The use of terrain charts was partly automated (Bott, 1959), and the gravity attraction of actual two and three-dimensional topography was computed automatically (Takin & Talwani, 1966) using the exact line integral formula of Talwani, Worzel and Landisman (1959). However, in the Takin & Talwani case, the objective was to apply terrain corrections to gravity readings made near the base of topographic features, whereas for density profiling, gravity readings must be made at the top and on the flanks as well.

In this paper, the exact two-dimensional gravity simulation formula of Talwani *et al.* (1959) is used to compute the combined Bouguer and terrain corrections for gravity stations situated on a topographic cross-section of any height and shape. This enables data from gravity surveys which cross reasonably two-dimensional topography

at right angles to be automatically reduced to sea level, and thereby greatly facilitates the production of multiple density profiles from which bulk density can be determined. A graphical method of selecting a matching pair of Bouguer profiles to determine bulk density is also described. The latter will, in favourable cases, eliminate the need to visually cross-correlate gravity and elevation—which is a subjective procedure—thus improving the accuracy of a determination. These methods are demonstrated using gravity data from two surveys over the Harts and Fraser Ranges (Fig. 1). Neither of these surveys was intended specifically for density profiling, but both yielded reasonable density estimates nonetheless.



Figure 1. Location of the Harts and Fraser Ranges

Automated Reduction to Bouguer Anomaly

One way of calculating the Bouguer and terrain corrections for gravity observations made on a two-dimensional topographic feature is to simulate the gravity attraction of its cross-sectional shape down to the required datum, usually mean sea level, using a chosen Bouguer density as the density contrast. This is demonstrated using

detailed gravity data from a Bureau of Mineral Resources (BMR) survey across the Harts Range, Northern Territory. The elevation and gravity profiles across the Harts Range are shown in Figure 2. The gravity effect of the range on the observed gravity is about 60 m Gal. This is superimposed on a gradient associated with a regional anomaly to the north.

To apply the simulation reduction method, a model is constructed incorporating the elevation profile, extended sides, and a bottom at the datum. The gravity attraction of this model at each station along the elevation profile is equal to the combined Bouguer slab and terrain corrections for that station. However, computation of this model is not possible using the two-dimensional formula of Talwani et al. (1959) if any sections of the model are above the level of the reference point. This problem can be overcome by inverting all sections of the elevation profile that are above the level of the point for which the reduction is being carried out, forming the mirror image, as demonstrated for points P1 and P2 in Figure 2. The profile inversion technique is

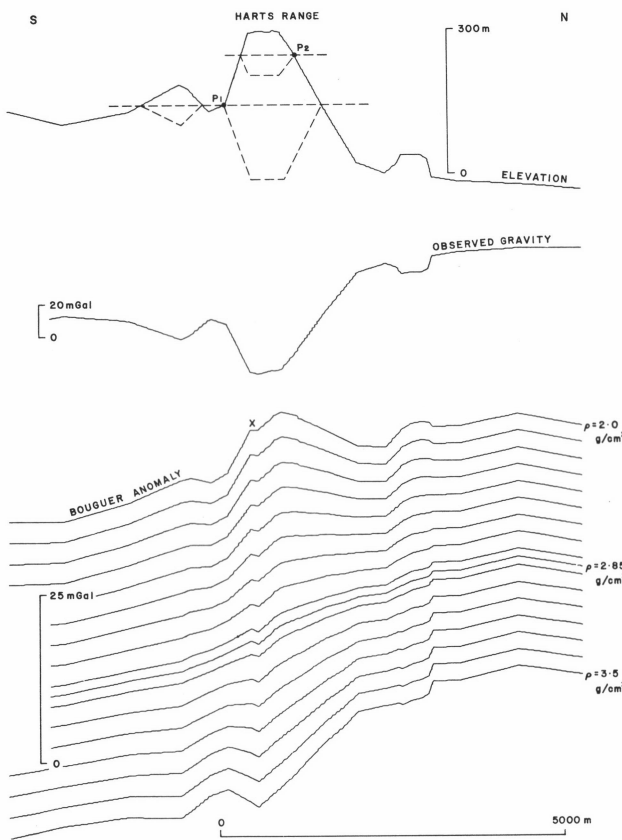


Figure 2. Harts Range—Derivation of multiple density Bouguer profiles

similar to the method of manipulating terrain masses used for geodetic calculations by Rudzki (1905). It is valid because at the level of inversion the gravity effect arising from the shape of the air-topography interface is the same as that arising from its mirror image. The method is therefore exact for the ideal case.

The computation for every point in the elevation profile, and the repetition of the process for a range of Bouguer densities can be done by computer, and will produce a set of multiple density Bouguer profiles. From these, the one with the minimum correlation with the elevation profile can be selected visually. For the Harts Range (Fig. 2), a choice of either 2.85 or 2.90 g cm⁻³ could be made. However, the effect of the regional gravity anomaly to the north requires consideration, and this can be done by constructing a model. A set of synthetic Bouguer profiles from a model

which generates a regional anomaly (Fig. 3) shows that for a 500 m ridge there is ample resolution to distinguish between the 2.80, 2.85, and 2.90 profiles, and that the required profile has a slight upward bulge over the ridge. This bump

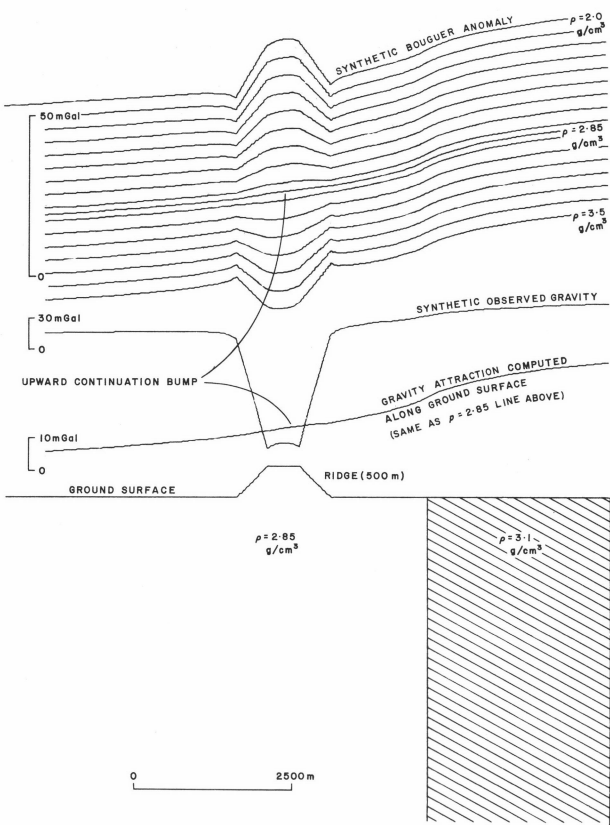


Figure 3. Model demonstrating upward continuation

is caused by the upward continuation of the regional anomaly as the ridge is traversed. For the Harts Range determination, the 2.85 g cm⁻³ profile is therefore the best selection as it has a slight upward bulge. From the shape of the profiles, the accuracy of this determination can be estimated at ± 0.05 g cm⁻³.

It can be seen in Figure 2 that the 2.85 selection holds fairly well for all the inflexions of the elevation profile in the vicinity of the main range, implying that the density determination is valid over a distance of about 3 km. This suggests that the bulk of the Arunta Complex in the vicinity of the Harts Range probably has a density of about 2.85 g cm⁻³, a value which reflects its composition and metamorphic grade. Furthermore, the body causing the positive anomaly just to the north of the range must have an even greater density, probably in excess of 3.0 g cm⁻³, and therefore be of mafic composition.

Profile Matching

The profile matching method is demonstrated using detailed gravity data from a BMR survey across the Fraser Range in Western Australia. Multiple density Bouguer gravity profiles across the range are shown in Figure 4. Although there is a regional gravity anomaly, upward continuation effects are small, because of the low relief. The smoothness of the minimum correlation Bouguer profiles suggests that the range has a fairly uniform density, and also that there is little lateral variation in density below it—an ideal situation for density profiling. However, the visual

selection resolution is poor, and the synthetic Bouguer profiles (Fig. 5) derived from the actual elevation profile, excluding the regional anomaly, confirm that the resolution will be poor for a ridge of only 100 m relief. The synthetic profiles also show that for a uniform topographic feature, and in the absence of deeper density variations, there is complete symmetry about the minimum correlation line. Consequently, given favourable circumstances, the desired minimum correlation density can be found by locating any pair of Bouguer profiles with an equal and opposite elevation effect, and taking the mean of their densities.

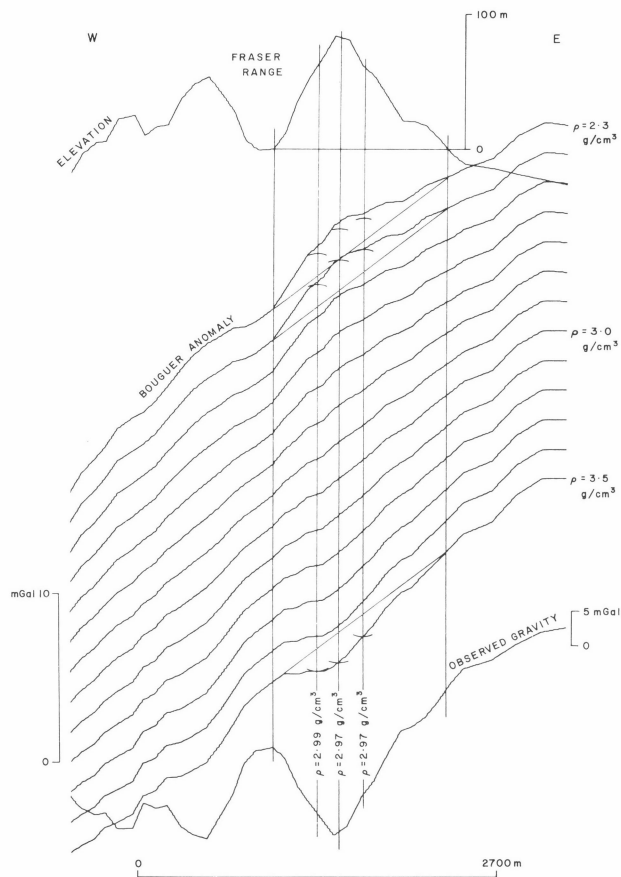


Figure 4. Fraser Range—Locating matching Bouguer profiles

A graphical method for separating the amplitude of the elevation effect from the regional gravity anomaly and locating equal and opposite amplitude matching profiles is shown in Figure 4. A horizontal line is drawn across the base of the ridge on the elevation profile, and two vertical lines are drawn through the Bouguer profiles. Lines drawn between these two verticals for each Bouguer profile isolate the elevation effect, which can then be measured along any number of verticals across the topographic feature. For each vertical, a match for any high density amplitude can be found amongst the low density amplitudes, and the mean of the two densities gives a point determination, which represents the integrated bulk density of the whole ridge.

The profile matching method exploits the linear relationship between Bouguer anomaly and terrain density for a given mass distribution, and in the ideal case is exact. Parasnis (1951) also used linearity in a graphical manner, but his work did not involve density profiles. Provided that there are no anomalous bodies below the reduction datum, profile matching can be utilised to convert multiple density Bouguer profiles directly to absolute density values. The method allows any number of point density determinations to be made across a topographic feature. All determinations

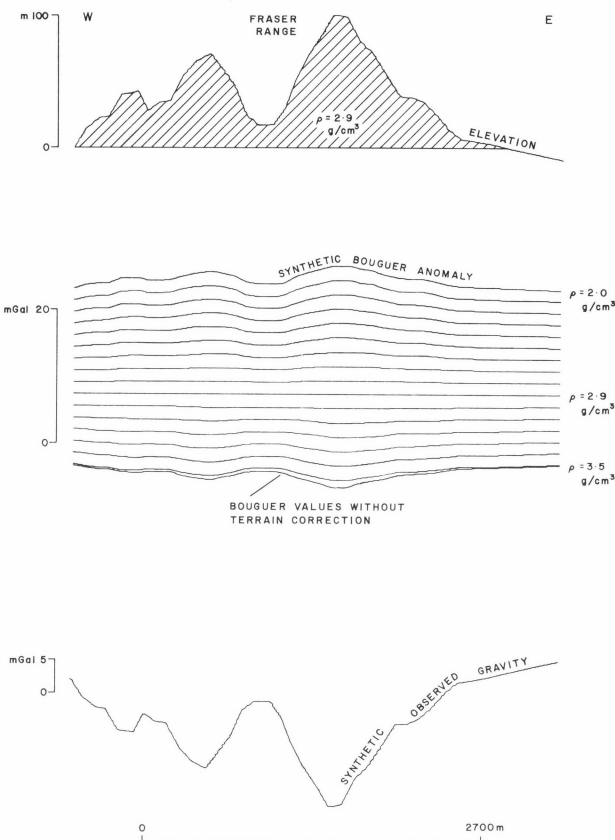


Figure 5. Fraser Range — Synthetic multiple density Bouguer profiles

made across a homogeneous feature will provide the same value, while with an inhomogeneous feature, determinations will indicate the integrated bulk density, at each point, and their variation across the feature will reflect changes in composition. The point determination precision is high: for 300 m and 100 m high ridges, there is about a 1.2 and 0.4 m Gal change in Bouguer anomaly for a 0.1 g cm⁻³ difference in density. Consequently, two such ridges could give point density determination precisions of ± 0.004 and ± 0.012 g cm⁻³ respectively if surveys were carried out across them to an accuracy of ± 0.05 m Gal.

For the Fraser Range, three point determinations of 2.97, 2.97 and 2.99 g cm⁻³ were made (Fig. 4). These values have not been corrected for departure from two-dimensionality, but are likely to be accurate because the minimum correlation Bouguer profile is reasonably smooth and straight. The high density values suggest that the range must have a predominantly mafic composition, and the straightness of the minimum correlation profile indicates that the range is not of an anomalous density with respect to the Fraser Complex which surrounds it. It is therefore possible to use these determinations as a guide to the density of the Fraser Complex in interpreting the 140 m Gal anomaly that is associated with it.

Discussion

Density profiling can, in principle, be carried out over topography of any shape or size, in two or three dimensions, but in the past, the need to apply terrain corrections from charts has curtailed experimental work. The problem has now been greatly reduced—the simulation reduction method described here enables the profiling reductions to be carried out by computer for elongate features which can be adequately represented in two dimensions by a cross-

section. Partly elongate features can also be used if the density is to be applied only for the reduction to Bouguer anomaly, when an approximate value is usually sufficient.

The ideal topographic feature for density profiling is one which is homogeneous, has steep sides and a simple shape, and is underlain by homogeneous rock. A detailed gravity survey with optically levelled stations and using an accurately calibrated gravity meter would then give a precise density determination. In practice, however, several types of complications capable of reducing the precision can be anticipated. Erratic changes in density will become apparent as bumps in the minimum correlation Bouguer profile, and density values will then require averaging to obtain an overall estimate. Systematic changes in density will affect the overall estimate. However, point density determinations can be plotted to indicate changes in rock type. In the presence of a regional gravity anomaly, for a large topographic feature, there will be a substantial bump in the minimum correlation Bouguer profile (Fig. 3). The bump is caused by the upward continuation of the anomaly, and results in an asymmetry between matching profiles. In all cases, the upward continuation effect can be evaluated by reconstructing the anomaly in a model, and the bump can then be removed from the Bouguer profiles.

Uneven topography can have a serious effect on density profiling. The bump in the Harts Range Bouguer profiles at point X (Fig. 2) was caused by a large gully situated within 100 m of the traverse. Less noticeable systematic errors can arise when the simulation reduction method is used for an elongate feature which is not adequately represented by the cross-section established along the traverse. The amount of departure from two-dimensionality which can be tolerated should be the subject of further study. Fortunately, the magnitude of the systematic errors is limited by the fact that the gravitational attraction is inversely proportional to the distance squared, and that only the vertical component of the attraction is measured. Furthermore, a simulation reduction determination can be upgraded by applying terrain corrections for the departure from two-dimensionality directly to the observed gravity, using the apparent density of the terrain.

Some authors (Dobrin, 1952, Grant & West, 1965) have emphasised that since topography is usually an erosional feature it can be correlated with subsurface geology. Where a topographic feature has an anomalous density root, the density profiles will be complicated by a gravity anomaly with a width of about the same as that of the feature. However, since slight changes in lithology with hardly any density changes can lead to differential erosion, many topographic features need not necessarily have an anomalous density root. The Fraser Range appears to be an example of this. If there is no anomalous root, the minimum correlation Bouguer profile will be straight (Fig. 5), whereas if there is a root, none of the profiles will be straight (Fig. 6). There is thus little likelihood of subsurface density contrasts affecting a determination subtly. Furthermore, the density contrast caused by the terrain effect is much greater than that resulting from subsurface changes. Large ridges can therefore give good results, even if major subsurface anomalies occur—as shown in Figure 6, where the ratio of density contrasts is 28.5:1.

Conclusions

The Harts and Fraser Range examples demonstrate how standard gravity survey data over elongate topography can be processed by computer using a simulation reduction method, to give Nettleton's density profiles, from which bulk density can be determined. Such density determinations can be used to derive the composition of topographic features, and are

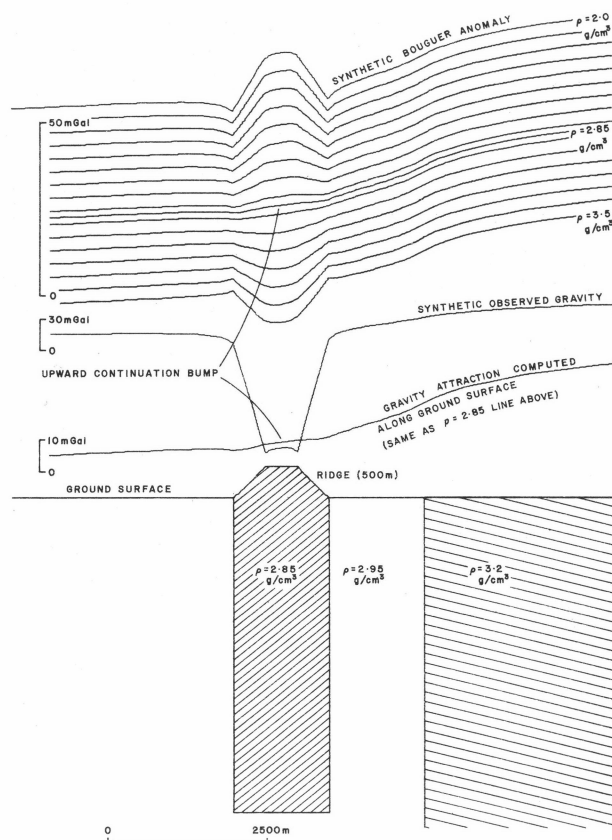


Figure 6. Model of a ridge with an anomalous density root.

particularly useful in the interpretation of gravity anomalies. With rigidly controlled surveys carried out over selected topography, density profiling can be expected to yield highly accurate and reliable absolute determinations for millions of tonnes of rock. Features over about 300 m in relief can be expected to give a good determination even with geological complications. Smaller features of about 100 m relief, will yield accurate results through the use of the profile matching method, but this method cannot be used if there are geological complications.

References

- BEATTIE, R. D., 1975—A Fortran program for calculating rock densities from gravity survey data. *CSIRO Minerals Research Laboratory. Division of Mineral Physics. Technical Communication* 56.
- BOTT, M. P. H., 1959—The use of electronic computers for the evaluation of gravimetric terrain corrections. *Geophysical Prospecting*, **7**, 45-54.
- DOBRIN, M. B., 1952—INTRODUCTION TO GEOPHYSICAL PROSPECTING. *McGraw-Hill*.
- GRANT, F. S., & ELSAHARTY, A. F., 1962—Bouguer gravity corrections using a variable density. *Geophysics*, **28**, 616-626.
- GRANT, F. S., & WEST, G. F., 1965—INTERPRETATION THEORY IN APPLIED GEOPHYSICS. *McGraw-Hill*.
- HUBBERT, M. K., 1948—Gravitational terrain effects of two-dimensional topographic features. *Geophysics*, **13**, 226-254.
- LINSSER, H., 1965—A generalized form of Nettleton's density determination. *Geophysical Prospecting*, **13**, 247-258.
- NETTLETON, L. L., 1939—Determination of density for the reduction of gravimeter observations. *Geophysics*, **4**, 176-183.
- PARASNIS, D. S., 1951—A study of rock densities in the English Midlands. *Royal Astronomical Society, Geophysical Supplements to Monthly Notices*, **6**, 252-271.

- RUDZKI, M. P., 1905—Sur la détermination de la figure de la terre d'après les mesures de la gravité, *Bulletin astronomique service B*, **22**.
- SIMPSON, S. M., 1954—Least squares polynomial fitting to gravitational data and density plotting by digital computers. *Geophysics*, **19**, 255-269.
- TAKIN, M. & TALWANI, M., 1966—Rapid computation of the gravitational attraction of topography on a spherical earth. *Geophysical Prospecting*, **14**, 119-142.
- TALWANI, M., WORZEL, J. L., & LANDISMAN, M., 1959—Rapid computations for two-dimensional bodies with application to the Mendocino Submarine Fracture Zone, *Journal of Geophysical Research*, **64**, 49-59.
- VAJK, R., 1956—Bouguer corrections with varying surface density. *Geophysics*, **21**, 1004-1020.

Hierarchical classification and vector ordination in the distinction of limestones in the Fairfield Group Canning Basin, Western Australia

B. M. Radke

The existence of two Formations, the Laurel and Gumhole, in the Upper Devonian to Lower Carboniferous Fairfield Group from the Lennard Shelf in the Canning Basin has been established during field studies and confirmed using a multivariate analysis based on petrographic and geochemical data. Limestones of the Gumhole Formation are generally characterised by a dominance of either ooids or brachiopods, or the presences of bryozoa, as well as higher levels of Mn, Fe, Pb, Zn and the ratio Ca/Mg than are present in the limestones of the Laurel Formation, which are characterised by the presence of either pelecypods or silt, and higher levels of Mg, Sr, and the ratio Sr/Ca. For the study, two representative groups of limestones from these formations were analysed. The analysis involved a taxonomic technique incorporating classification, ordination and diagnostic programs, and utilized in all 19 petrographic and 14 geochemical attributes. In both groups, at least 74 per cent of the samples were successfully differentiated on the criteria presented.

The Fairfield Group is an Upper Devonian to Lower Carboniferous sequence of carbonates, with some interbedded clastics, in the Canning Basin. The group is poorly exposed along the Lennard Shelf to the north-east of the Fitzroy Trough (Fig. 1). It overlies a Middle to Upper

Devonian reef complex (Playford and Lowry, 1966), and is in turn overlain by continental sands of the Anderson Formation.

The sequence is composed of about 550 m of limestone, with some siltstone, sandstone, dolomite and shale, and is

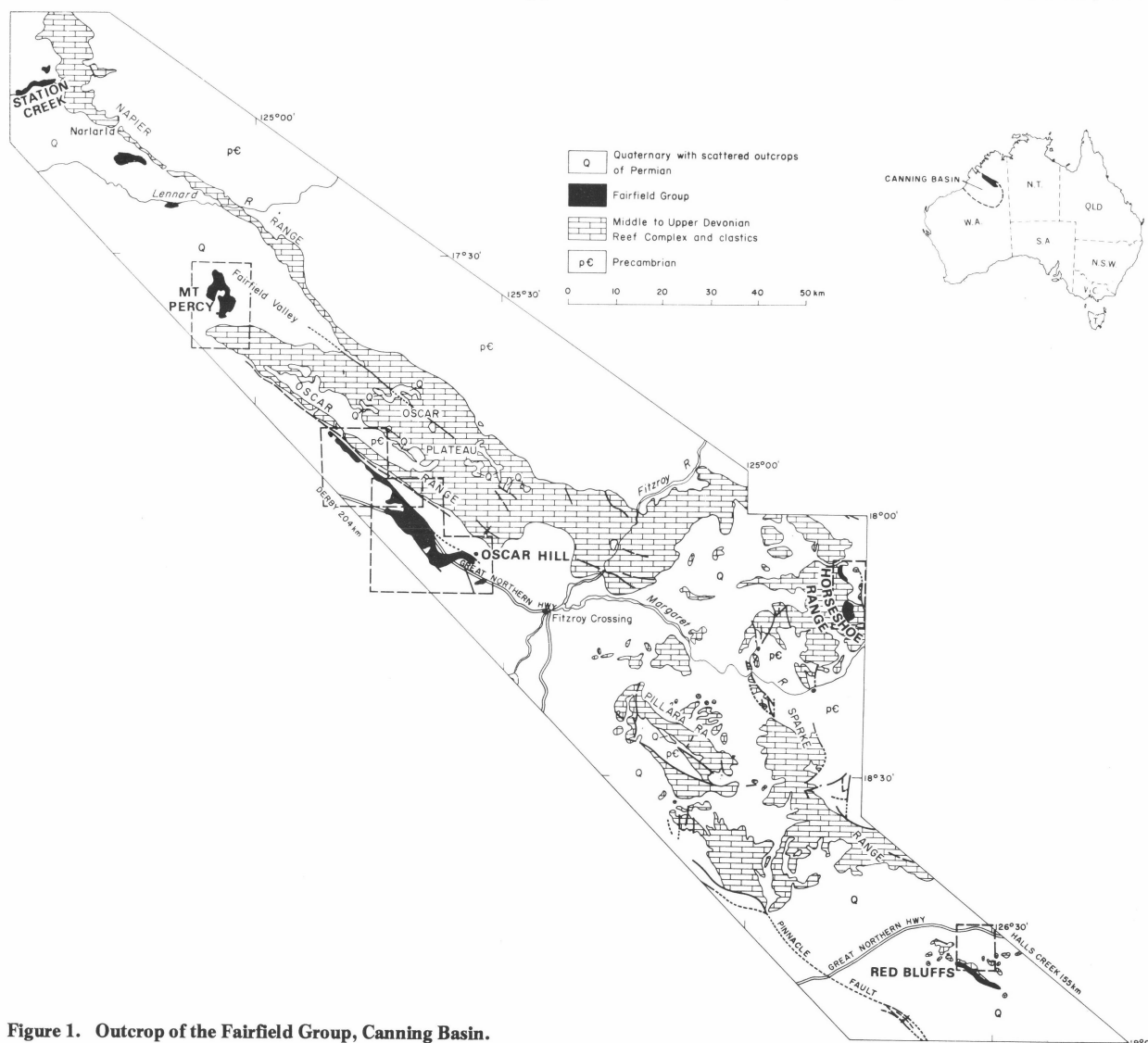


Figure 1. Outcrop of the Fairfield Group, Canning Basin.

characterised by both lateral and vertical variability. Differing views have been expressed on whether one or two carbonate formations could be distinguished in the group: Williams and McKellar (1958) considered that the Gumhole and Laurel Formations could be distinguished by the presence of a sandy carbonate horizon in the basal Laurel, by colour differences between the fossiliferous limestones of each unit, and also by the age of the fauna. However Playford and Lowry (1966) stated that 'it has not been practicable to differentiate the two units in mapping'.

Stratigraphic drilling by the BMR, during regional mapping undertaken jointly by the BMR and the Western Australian Geological Survey during 1972 led to the recognition of an intermediate unit, the Yellow Drum Sandstone, between the two carbonate formations (Druce & Radke, in prep.). This formation is, however, poorly exposed, and thus is of little use in distinguishing between actual exposures of the two carbonate units. Identification of these in the field was based on differences in surface colour, weathering characteristics and some skeletal characteristics. However the viability of these criteria was uncertain and this study was initiated to establish statistically diagnostic criteria and to confirm the subdivision made. Petrographic attributes and geochemical parameters of limestones from the two formations are treated statistically in an attempt to define such characteristics. 229 samples were used from sixteen measured stratigraphic sections. To establish whether the results were reproducible, the samples were split into two groups: Group I with 111 samples, and Group II with 118. Each group represents the full stratigraphic range but was taken from different sections. The representative limestone through a thickness of 1.5 m was selected for analysis. Chemical analyses of all these samples were available, but it is necessary to describe the petrography of the carbonates before treating the samples statistically.

The basic strategy of the taxonomic technique adopted in this treatment is to produce an agglomerative hierarchical classification in the form of a dendrogram as well as ordinating the same data using principal co-ordinate analysis. 'Diagnostic' programs were then used to evaluate the significance of the attributes in each fusion of the groups involved in the dendrogram: and also the influence or weighting of each attribute in the vectors used for ordination. The results of both agglomerative hierarchical classification and ordination methods are then compared. The 3600 and, later, the Cyber 76 Control Data Computers of the Division of Computing Research, CSIRO, Canberra, were used in this study. The following programs, available in the Division of Computing Research, were used: classification—MULTBET, MULCLAS; ordination—GOWER, MAXGOWER; diagnostic—GROUPE, GOWECOR. These programs are discussed in Lance and Williams (1967a, b) and Lance *et al* (1968).

Taxonomic programs have been used in carbonate classification and facies identification: by Imbrie and Purdy (1962), and Van Andel and Veevers (1967) on modern carbonates; and by Bonham-Carter (1956), Harbaugh and Demirmen (1964), Veevers (1969) and others on ancient carbonates.

Petrography

By definition limestones are carbonate rocks which contain less than 50 per cent terrigenous matter. Dunham's limestone classification, which is based primarily on textural maturity, is followed (Dunham, 1962). In this, mud-supported carbonates with less than 10 percent grains are mudstones; those with more than this are wackestones.

Grain-supported carbonates containing mud are packstones; those without mud are grainstones. Two further types cannot be related to maturity: the crystalline carbonates; and boundstone, in which an organic framework binds and modifies the sediment irrespective of its textural maturity.

The Fairfield limestones are dominantly grainstone (78 percent), with minor packstone (12 percent), crystalline (7 percent), boundstone (2 percent) and wackestone (1 percent). Examples of this classification are figured as follows: grainstone (Fig. 7A), packstone (Fig. 7B), wackestone (Fig. 7C), boundstone (Fig. 7D), and crystalline carbonates (Fig. 10E).

Limestones contain both allochemical and orthochemical constituents (Folk 1968). Many of the allochems are used here as attributes in the classification of the limestones. These and terrigenous grains in the limestones, are described below. Thin sections, polished sections and

DATA TYPE	ATTRIBUTE	NUMBER & TYPE OF STATES
QUALITATIVE	DOLOMITIC (dol)	YES / NO
	SILTY (silt)	YES / NO
DISORDERED MULTISTATE	LIMESTONE TYPE	GRAINSTONE (G) PACKSTONE (P) BOUNDSTONE (B) CRYSTALLINE (C)
ORDERED MULTISTATE	PELLETS (p)	ABSENT / PRESENT / DOMINANT (d)
	OOIDS (o)	
	INTRACLASTS (i)	
	BRACHIOPODS (b)	
	PELECYPODS (p)	
	GASTROPODS (g)	
	CEPHALOPODS (c)	
	CRINOIDS (cr)	
	BRYOZOANS (y)	
	OSTRACODS (o)	
	FISH FRAGMENTS (f)	
	CORALS (c)	ABSENT / PRESENT
	RUGOSE (SOLITARY) RS	
	RUGOSE (COLONIAL) RC	
	TABULATE T	0 / 0-10 / 10-20 / 20-30 / >30%
	SAND %	
	SAND - GRAIN SIZE *	
		VERY FINE (vf)
		FINE (f)
		MEDIUM (m)
		COARSE (c)

Symbols are recorded where appropriate.
* Only sand ranges recorded in diagrams are listed.

TABLE 1 Petrographic attributes used in the classification of the limestones.

stained acetate peels were used for the petrographic studies. The staining technique used for the identification of carbonate minerals on the peels (Dickson 1966) involved the use of Alizarin red-S and potassium ferricyanide (Davies and Till, 1968). The petrographic data were recorded in qualitative and semi-quantitative form, outlined in Table 1.

Attributes

Pellets

Pellets are the dominant constituent when present. They are usually spherical to elongate in shape (Fig. 7E), and have a diameter less than 0.25 mm. A clotted appearance, the structure grumeleuse of Cayeux (1935) is a common feature in the pelletal limestones. No internal fabric was observed in the pellets; this rules out a faecal origin as described by Scoffin (1973) and the pellets are regarded as being of either inorganic or algal origin.

Ooids

Ooids are also the dominant constituent when present

and are commonly 0.25 to 0.5 mm in diameter. They are spherical to slightly elongate in shape and display prominent concentric growth lines and a coarse mottled radial fabric. The nuclei, which consist of terrigenous sand or small, well abraded skeletal grains (Fig. 7A) influence the shape in immature ooids.

Intraclasts

Intraclasts are usually present in the grainstones. Mud lumps which incorporate terrigenous silt grains (Fig. 7F) were probably rounded prior to lithification. Other types such as reworked lithified lumps (Fig. 8A) and crystalline grains are also present.

Brachiopods

Brachiopods are an abundant skeletal constituent and occur in all states of preservation. Articulated, non-abraded forms with intact spiralia (Fig. 8B) are more common in muddy rocks. Disarticulated, fragmented or abraded pieces are recognised by their shell microstructure, which is relatively resistant to recrystallization. Productid brachiopods constitute a considerable proportion of the fauna and as a result accumulations of their spines are common (Fig. 8C). Algal boring is frequently seen on brachiopod valves; it is usually present only on the outer surface, a fact that suggests algal colonization on living forms.

Pelecypods

Pelecypods, like brachiopods, are abundant in some horizons. The shells are usually disarticulated, and individual valves and fragments are frequently recrystallized, with micritized or algal-bored margins. Often the shell structure has been removed by solution, leaving only the outer micritic envelope (Fig. 8D). In this state it is difficult to distinguish the shell from some forms of thallic algae.

Gastropods

Like the pelecypods, the gastropods are usually recrystallized and these forms are preserved as micritized outlines. Size, shape and shell thickness are variable: from thick, high-spined to thin, low-spined shells (Fig. 8E). The latter are probably encrusting forms (Fig. 8F).

Cephalopods

Straight and curved nautiloids occur in some silty horizons as solid carbonate casts, but they have not been observed within limestone beds. Small ammonoids such as the goniatite *Imitoceras rotatorium* are, however, preserved in the limestone, they lie flat and have thin shells that are ovate in section, shells that are infilled by a drusy cement.

Crinoids

Ossicles of all sizes are common constituents in some limestones. Each ossicle is a single calcite crystal with a complex internal pore structure. Frequently these pores are infilled by calcite in optical continuity with the ossicles which are then solid forms (Figs. 9A, 7B). Syntaxial overgrowths of calcite may also form in optical continuity with the ossicle. Finely disseminated pyrite in the pore cement imparts a dusty appearance to it. Limonite may be the infilling cement; a circumstance that inhibits the development of syntaxial cement. The ossicles may be up to 2 cm long but are variable in size and shape. Delicate echinoid spines are preserved in association with the crinoids, and can be recognized by the radial pattern of their symmetrical cross-sections.

Bryozoans

Three morphological forms of bryozoa are observed. Most common is an encrusting form in which thin, broad colonies cover a host skeletal fragment (Fig. 9B). In thin section the branching form has a central core from which individual zooecia diverge to a surface where the apertures are constricted by a thickening of the zooecial wall (Fig. 9C). Silt, sand or limey mud is sometimes trapped in the zooaria and the remaining pores are infilled by several phases of calcite cement (Fig. 9D). Fenestrate forms are less robust and fragments are only preserved in the muddier limestones.

Ostracods

Ostracods are present in most of the limestones, and appear in thin section as bivalved oval bodies which may be infilled with mud and/or a drusy cement (Figs. 9E, 8A). The valves may be thick, thin or ornamented; and may be disarticulated, but only rarely do they show signs of abrasion. Eridostracans are valved crustaceans with close affinities to ostracods (Jones 1962, 1968); *Cryptophyllus* (Fig. 9F) is common in many limestones and in some cases is the dominant constituent. The bivalved test may be complete, but commonly is disarticulated (Fig. 10C). It has a characteristic microstructure of fused plates which are lobed anteriorly.

Corals

Corals constitute only a minor skeletal contribution to the rocks but have been subdivided into three categories:

1. Solitary rugose corals. *Catactotoechus*, a small solitary coral (Fig. 10A), often shows rejuvenescence and is commonly internally filled with cement.
2. Colonial rugose corals.
3. Tabulate corals. Encrusting auloporid corals are rare (Fig. 10B).

Syringopora sp. occurs both as a framework of boundstones (Fig. 7D), or more commonly as a fragmented component, where silicification of both the calyx and the infilling cement has been observed.

Fish

Fish fragments are usually abundant in the sequence. Lung fish teeth and scales, fragmented Arthrodiran plates, Acanthodian spines, cladodont and bradyodont shark teeth have been determined (G. C. Young, pers. comm.). These components are composed of fluorapatite which has a very low birefringence and a deep yellowish colour. In section the fragments have outer and inner lamellar layers which enclose a thicker cellular zone mottled with frequent vascular spaces (Fig. 10C).

Terrigenous sand and silt

The siliciclastic component of the limestones is dominated by sand and silt-sized particles. Grain size and abundance were selected as attributes for this study.

Grain size categories are as defined by Wentworth (1922) and sand abundance is recorded as weight percent of the sample (Table 1). The presence of silt is a qualitative observation. The dominant minerals occurring are quartz, feldspar, and mica as well as lithic fragments and these are outlined below.

Quartz. Quartz occurs in the size range from silt to very coarse sand. Generally the maturity of particle morphology increases proportionately with the grain size (Fig. 10D). Most of the grains are monocrystalline with undulose extinction. Some of the larger grains are pitted,

the larger pits being caused by interpenetration of other mineral grains in the original source rock.

Feldspar. Grains of orthoclase, microcline and some plagioclase are abundant, varying in size and morphology in a similar manner to the quartz grains. Some orthoclase grains have prominent abraded syntaxial overgrowths; such feldspars have been reworked from an arenite that was deposited in a marine environment.

Mica. Muscovite and biotite flakes are present only as a minor constituent in those limestones in which the quartz and feldspar fragments are of medium-grained sand size or finer. The flakes usually parallel the bedding, but may be distorted by compaction.

Lithic fragments. Chert, shaly siltstone, quartzite and claystone are rare constituents of the limestones. The quartzite and chert grains have similar morphological properties to the quartz grains, and probably have a similar provenance terrain. The shaly siltstone and claystone clasts are often larger than the host sediment grain size. The claystone clasts are light green in colour, friable, lath-shaped, and are often deformed by compaction.

Dolomite

Although a diagenetic product in these limestones (Figs. 10E, 10F), dolomite was considered to be of probable value if its distribution was controlled stratigraphically. Determinations were made from stained peels (Davies and Till, 1968) and in some cases, confirmed with X-ray Diffraction.

Analysis of Petrographic Data

The 19 petrographic attributes used in this study are listed in Table 1. It will be recalled that the 229 samples were divided into two groups: Group I with 111 samples, and Group II with 118; and that each of these groups represents the full stratigraphic range of the two formations but was taken from different sections.

With the hierarchical agglomerative classification, 13 groups were produced at an information gain level of 24 in a dendrogram of the samples from Group I (Fig. 2A): four groups (e, h, i and j) are of Gumhole samples, four groups (b, k, l and m) of Laurel samples, while the remaining five groups were mixed, i.e. containing samples from both formations. The first division separated a group of Laurel samples from mixed samples which were then subdivided into a Gumhole group and a remaining mixed group. In considering the dendrogram classification of Group II, an information gain level of 21 was selected where a comparable number of groups existed: five groups (γ , κ , λ , μ and ν) are of Gumhole samples, a further five (β , δ , ϵ , η and θ) from the Laurel, while the remaining three groups (α , ζ and ι) are mixed (Fig. 2B).

Thus for both sample populations the dendrograms comprise not only Laurel and Gumhole groups, but also mixed groups. The structures of the two dendrograms were dissimilar, and so too was the significance of each attribute in the subdivisions into the groups of the Laurel and Gumhole Formations. It is considered that this can be related to the small size of the sample used for such a diversity of limestone types, and a larger group sample will be required for more consistent results.

Ordination and supporting diagnostic methods proved to be more definitive. In group I a good separation of Laurel and Gumhole samples was produced (Fig. 3A) with 26 per cent of the samples in an intermediate mixed zone (Fig. 3B). Vector 1 alone was responsible for the polarization of the samples. In Group II the separation produced a mixed zone of 22 percent, but in this instance the attitude of this zone is

such that both vectors 1 and 2 influence the separation (Fig. 4). For a comparison between ordination and dendrogram presentation, the groupings derived from the dendrogram classifications were plotted in the ordination vector diagrams (Fig. 3, 4A), showing the spatial separation of the groups. The mixed groups (α , ζ , δ , ϵ and ι of Group I; α , ζ and ι of Group II) have not been included as these overlap both Laurel and Gumhole fields.

In Group I the most diagnostic attributes of the Laurel samples are those significant in the negative direction of vector I, namely: the presence of ostracods, intraclasts, sand, pellets and pelecypods. The positive direction of vector I defines the Gumhole samples characteristically containing bryozoans, medium sand, solitary rugose corals, and/or ooids (Fig. 3B). The significance of vector I in this group is such that these attributes are considered to be diagnostic of the respective formations. It will be recalled that the attitude of the mixed zone in Group II is such that both vectors influence the separation: the first quadrant (Fig. 4B) has mostly Laurel samples, and gastropod, pelecypod, brachiopod, fish, ostracod, intraclast, silt, and crinoid grain types are typical. The third quadrant contains Gumhole samples almost exclusively and brachiopod dominant, ostracod, bryozoan and ooid dominant assemblages are extremes. It is difficult to differentiate the mixed populations of the second and fourth quarters.

It can be seen from Table 2 that criteria for the differentiation of the two formations differs in the two ordinations, and here too a larger group sample will be required to produce more consistent results. However, the following criteria are common to both ordinations: Gumhole—dominance of ooids or brachiopods, or the presence of bryozoans. Laurel—the presence of pelecypods or silt.

Analysis of Geochemical Data

The following attributes were used in a similar analysis of geochemical data: Ca, Mg, Sr, Fe, Mn, insoluble residue, the trace elements Cu, Pb, Zn, Cd, Ba, P, and the ratios Ca/Mg and Sr/Ca. The carbonate mineralogy of the limestones is simple. Low magnesium calcite and dolomite are the only significant species and thus the Ca/Mg ratio is an inverse expression of dolomite abundance. Sr/Ca ratios are indicative of strontium levels in the carbonate fraction. Details of the sampling and analytical methods are discussed in Druce and Radke (in prep.).

The dendrogram constructed from the samples of Group I shows an almost complete separation into two larger groupings, one composed of seven Gumhole groups and the other of six Laurel (Fig. 5A). 90 percent of the samples in Group I were classified as expected into each grouping of the respective formations, the remaining samples being misclassified according to the stratigraphic interpretation. Vector ordination (Fig. 5A) shows that the Laurel Formation samples were largely restricted to the positive end of vector Y, but are widespread along vector X. The Laurel samples are well separated within the field, and tend to envelop the more clustered Gumhole group. The latter occupies a field defined by negative to low positive vector Y values, and positive to low negative values for vector X.

The dendrogram from the samples of Group II (Fig. 5B) dichotomizes initially into a larger assemblage of 8 groups of Gumhole samples from a second containing 5 Laurel groups. The diagnostic elements and their concentration in each formation is tabulated in Figure 5B. In this classification, 93 percent of the samples were categorised as expected from stratigraphic information. Vector ordination shows that the two can be virtually separated with reference

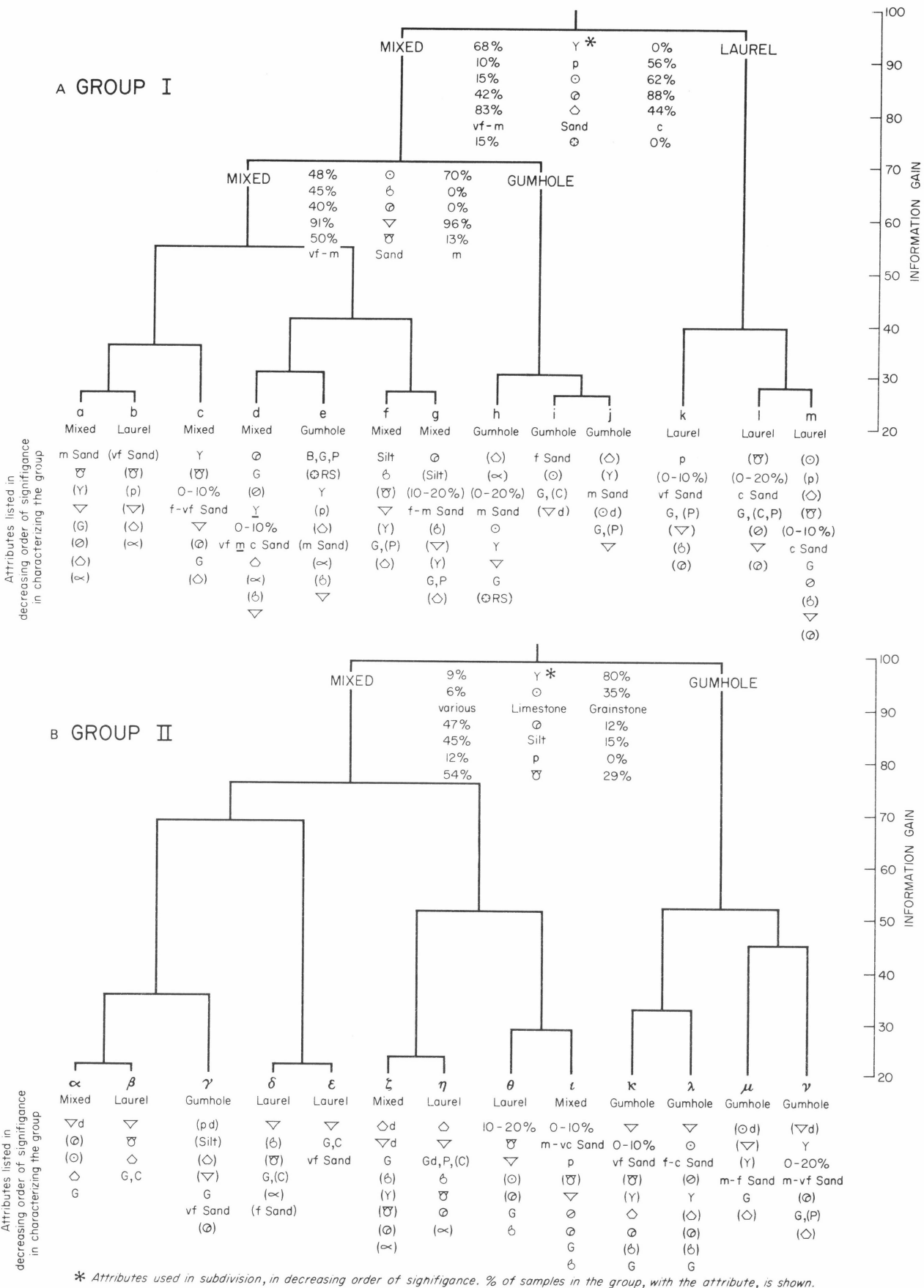


Figure 2. Dendrogram classifications of limestones using petrographic data

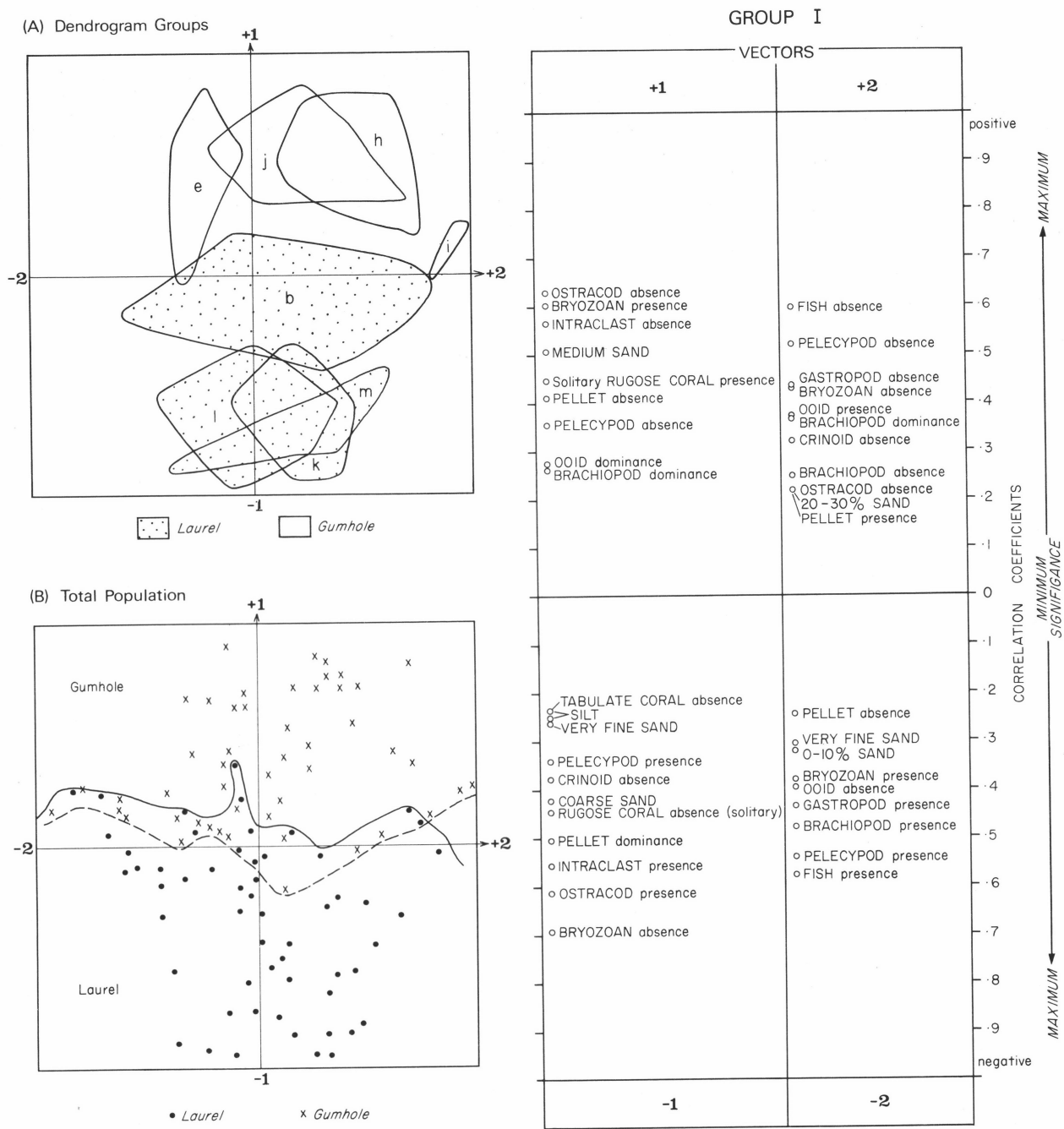


Figure 3. Vector ordination of Group I petrographic data.

to vector Y (Fig. 6B). An overlap of populations along vector X involves 9 percent of the individual samples.

The results from dendrograms for the two groups (Fig. 5) are very similar. That for group I shows that the major differences between the Gumhole and Laurel groupings are that the former is characterized by higher levels of Mn, Fe, Pb and Zn, and had a higher Ca/Mg ratio; and that the latter has higher Mg. The mean values of diagnostic elements are tabulated on the dendrogram (Fig. 5). In group II the Gumhole grouping has higher Mn, Fe, Pb and Zn, and also a greater Ca/Mg ratio; while the Laurel has characteristically higher Sr values and Sr/Ca ratios. Criteria common to both groups then are that the Gumhole

Formation contains higher values of Mn (mean 0.17 percent cf. 0.03 percent, Laurel), Fe (mean 0.16 percent cf. 0.05 percent Laurel), Pb (mean 31 ppm cf. 8 ppm Laurel), Zn (mean 24 ppm cf. 10 ppm Laurel), and higher Ca/Mg ratio (mean 204 cf. 121 Laurel). The Laurel limestones have higher but varied levels of Mg and Sr. From both groups of data, these hierarchical dendrograms produced similar groupings which were a significant differentiation between Gumhole and Laurel limestones.

Ordination and supplementary diagnostic programs also proved definitive (Fig. 6). Using the two principal vectors, ordination in each group sample gave a good spatial separation of fields; each with less than 10 percent overlap.

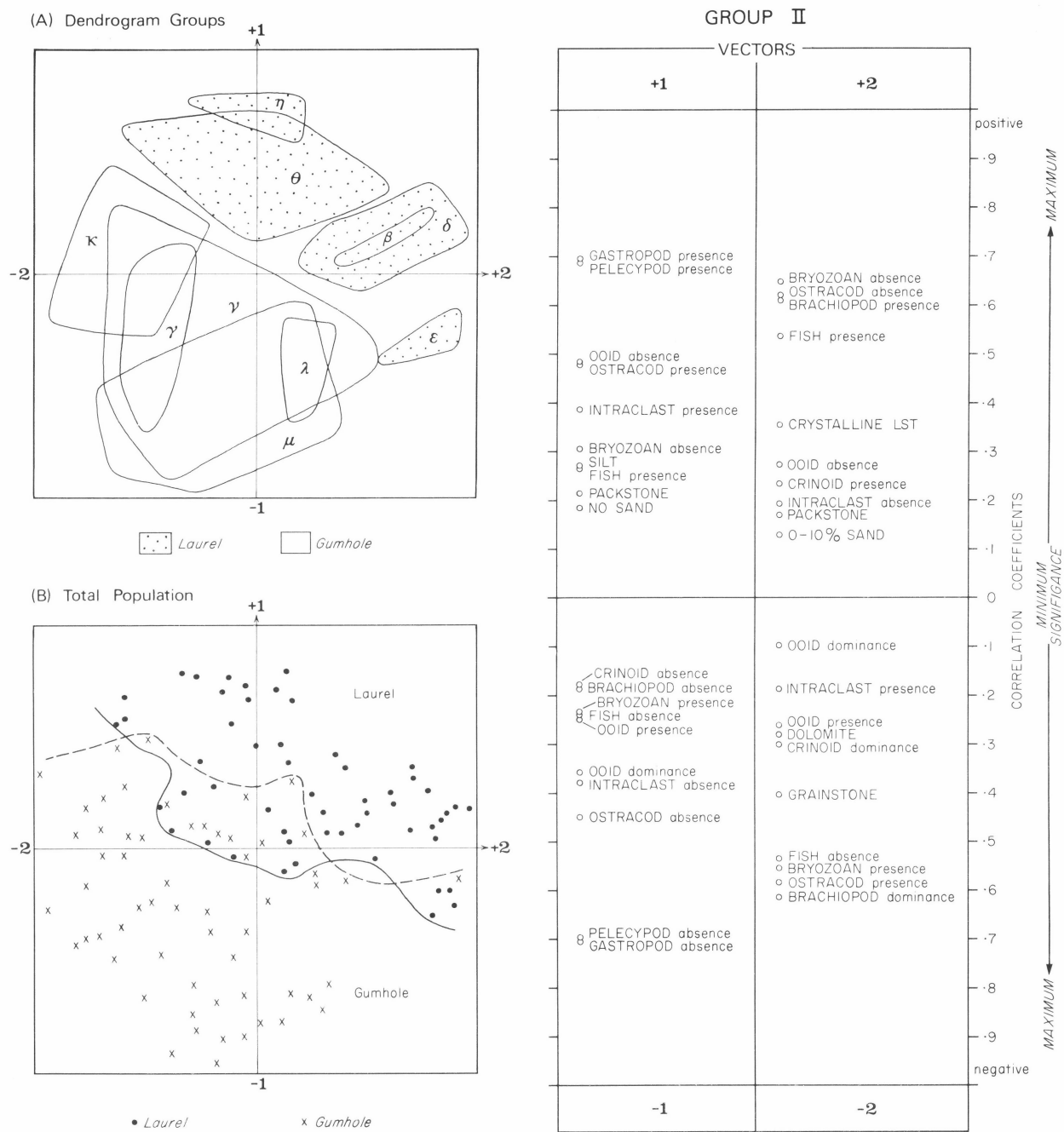


Figure 4. Vector ordination of Group II petrographic data

The significant attributes of Group I samples (Table 3) were—Gumhole: higher values for Fe, Mn, P, Pb, Cu and Zn, and of the Ca/Mg ratio; and Laurel: higher values for Mg, Ca, and a higher Sr/Ca ratio. Although it is encouraging that the Gumhole attributes are almost identical in both the dendrogram and in vector ordination, it must be reiterated that both vectors were required to differentiate the Gumhole samples. In Group II, on the other hand, the significance of vector Y alone should be noted. In this group the Laurel Formation, with positive Y values (Table 3), has higher values for Mg, P, Sr, and the ratio Sr/Ca; while the Gumhole, with negative Y values, has higher values for Fe, Pb, Mn and Zn, and for the ratio

Ca/Mg. These results agree closely with the dendrogram for this group. Elements that are significant for both groups are that the Gumhole Formation has higher values for Fe, Mn, Pb, and Zn, and for the ratio Ca/Mg, in the carbonates than found in Laurel Formation (Table 2).

Conclusions

Limestones of the Laurel and Gumhole Formations can be differentiated on the basis of geochemical and petrographic characteristics. In the Gumhole Formation, limestones are characterized by relatively higher levels of Mn, Fe, Pb, Zn

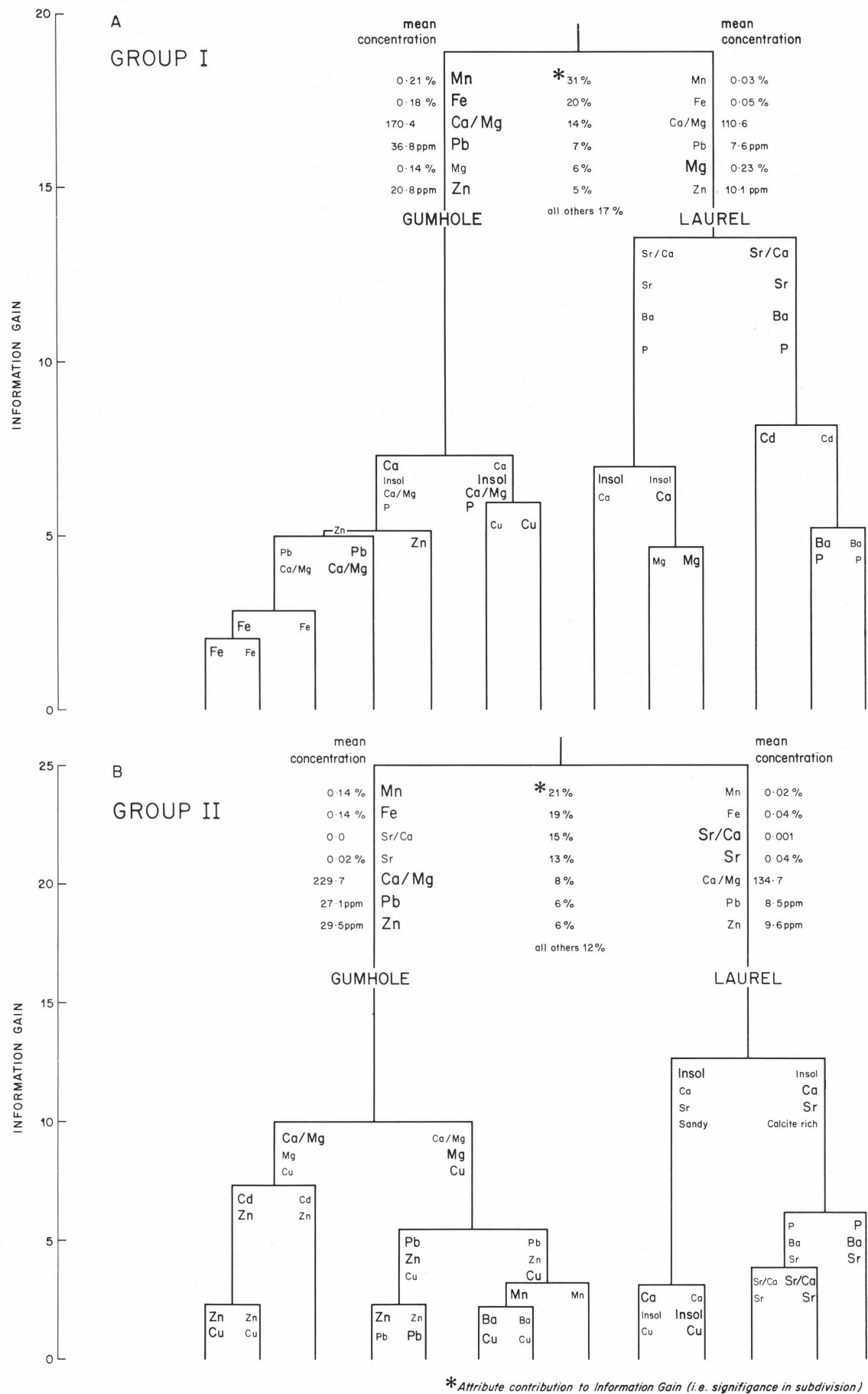


Figure 5. Dendrogram classification of limestones using geochemical data.

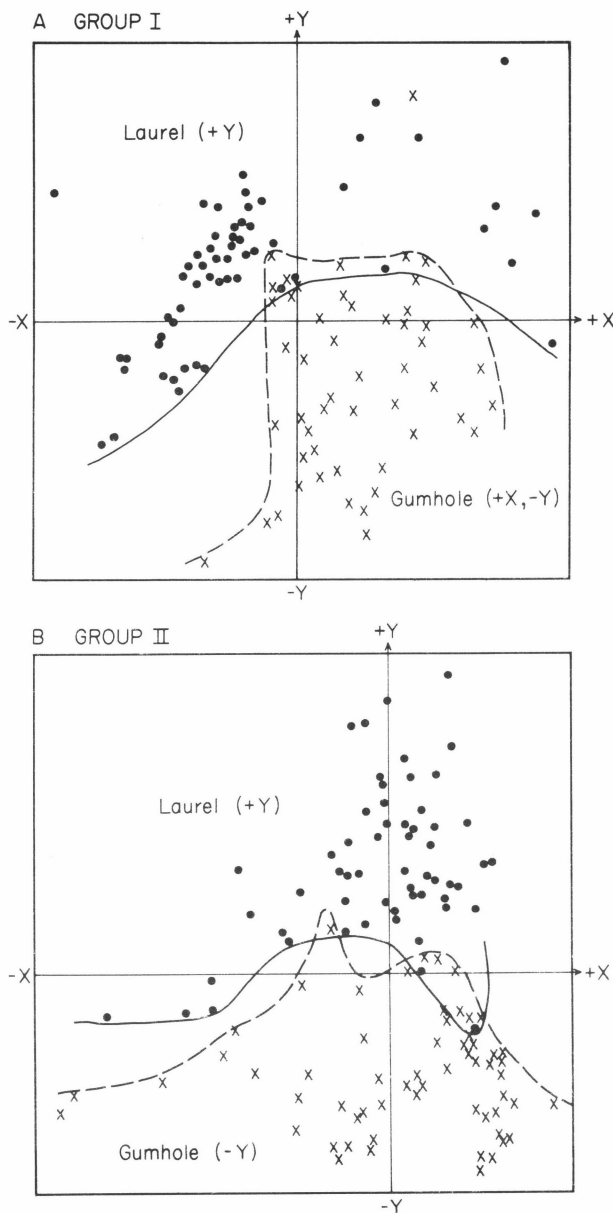


Figure 6. Vector ordination using geochemical attributes.

and Ca/Mg ratio (compare in Fig. 5), and a dominance of brachiopods or ooids, or the presence of bryozoans; compared to limestones in the Laurel Formation, with higher levels of Mg, Sr, Sr/Ca ratio, and the characteristic presence of pelecypods or silt.

Both classification techniques showed this with varying degrees of success.

Using petrographic data, results of the agglomerative hierarchical classification were not reproducible and a larger group sample is necessary. The ordination method produced more consistent results.

With geochemical data, dendrogram classifications differentiated the formations clearly and ordination methods were equally successful, producing the same criteria for differentiation.

Overall, the use of geochemical data is more significant in the limestone differentiation than petrography, probably because the chemistry of all carbonate rock types in one formation is relatively consistent and therefore geochemical differences between the formations are readily detected.

	LIMESTONES			
	GUMHOLE		LAUREL	
Group Sample	GROUP I	GROUP II	GROUP I	GROUP II
PETROGRAPHIC				
bryozoans	●	●	○	○
medium sand	●			
solitary rugose corals	●		○	
ooids	●	●		○
brachiopods	●	●		●
ostracods	○		●	
intraclasts	○		●	
pellets	○		●	
coarse sand			●	
pelecypods	○	○		●
very fine sand			●	
silt			○	●
crinoids		●		
dolomite		●		
fish		○		●
gastropods		○		●
grainstone		●		
GEOCHEMICAL				
Sr			X	X
Sr/Ca			X	X
Mg			X	X
Ca			X	
P	X			X
Mn	X	X		
Fe	X	X		
Pb	X	X		
Ca/Mg	X	X		
Zn	X	X		
Ba		X		

○ absence of attribute is diagnostic ● dominance of attribute is diagnostic
● presence of attribute is diagnostic x higher levels of attribute are diagnostic

TABLE 2 Comparison of diagnostic criteria used in ordination classification.

GROUP I		Correlation Coefficients	GROUP II		significance
+X	+Y		+X	+Y	
VECTORS		positive	VECTORS		MAXIMUM
		+9	Ca	Sr/Ca	
		+8			
		+7	Ca/Mg		
		+6		Mg	
Fe	Sr/Ca	+5			
Ba	Mg	+4			
P	Sr/Ca	+3	P	P	
Mn	Ca	+2	Ba	Ca	
Sr		+1			
Sr/Ca		0	Cd		
Ca		-1	Sr		
		-2	Mn		
		-3			
		-4			
		-5			
		-6			
		-7			
		-8			
		-9			
		negative			MINIMUM
-X	-Y		-X	-Y	

TABLE 3 Correlation coefficients of attribute significance in vector ordination (geochemical data).

Acknowledgements

This paper is one of several publications to result from the BMR West Canning Basin Project and my thanks are due to Drs E. C. Druce and R. S. Nicoll for their contribution of samples and stratigraphic information used in this study. I thank Messrs. A. Adams, D. Felsh, J. Gorter and A. T. Wilson for their assistance with the field work.

I am indebted to Peter Milne, Division of Computing Research, CSIRO, for his advice and guidance with the programs used in this study.

Finally I thank Drs E. C. Druce and A. R. Jensen for useful suggestions offered throughout this study, and Dr J. Truswell for his suggestions for the improvement of the text.

References

- BONHAM-CARTER, G. F., 1956—A numerical method of classification using qualitative and semi-qualitative data, as applied to the facies analyses of limestones. *Bulletin of Canadian Petroleum Geology*, **13**, 482-502.
- CAYEUX, L., 1935—LES ROCHES SEDIMENTAIRES DE FRANCE—ROCHE CARBONATES, (CALCAIRES ET DOLOMITES): Masson & Cie, Paris.
- DAVIES, P. J. & TILL, R. 1968—Stained dry cellulose peels of ancient and recent impregnated carbonate sediments. *Journal of Sedimentary Petrology*, **38**, 234-237.
- DICKSON, J. A. D., 1966—Carbonate identification and genesis as revealed by staining. *Journal of Sedimentary Petrology*, **36**, 491-505.
- DRUCE, E. C., & RADKE, B. M., in prep.—The Late Devonian and Early Carboniferous Geology of the Lennard Shelf, Canning Basin, Western Australia *Bureau of Mineral Resources, Australia—Bulletin*.
- DRUCE, E. C., & RADKE, B. M., in prep.—Geochemistry of the Fairfield Group, Canning Basin. *Bureau of Mineral Resources, Australia—Report*.
- DUNHAM, R. J., 1962—Classification of carbonate rocks according to depositional texture. In: W. E. HAM (Editor), CLASSIFICATION OF CARBONATE ROCKS. *American Association of Petroleum Geologists—Memoir* **1**, 108-121.
- FOLK, R. L., 1968—PETROLOGY OF SEDIMENTARY ROCKS. *Hemphills, Texas*.
- HARBAUGH, J. W., and DEMIRMEN, F., 1964—Application of factor analysis to petrologic variations of Americus Limestone (Lower Permian), Kansas and Oklahoma. *Geological Survey of Kansas—Special Publication* **15**.
- IMBRIE, J., and PURDY, E. G., 1962—Classification of modern Bahamian carbonate sediments. In: W. E. HAM (Editor), CLASSIFICATION OF CARBONATE ROCKS. *American Association of Petroleum Geologists Memoir* **1**, 253-272.
- JONES, P. J., 1962—The ostracod genus *Cryptophyllus* in the Upper Devonian and Carboniferous of Western Australia. *Bureau of Mineral Resources, Australia—Bulletin* **62** (3).
- JONES, P. J., 1968—Upper Devonian Ostracoda and Eridostraca from the Bonaparte Gulf Basin, northwestern Australia. *Bureau of Mineral Resources, Australia—Bulletin* **99**.
- LANCE, G. N., & WILLIAMS, W. T., 1967a—Mixed-data classificatory programs. 1. Agglomerative systems. *The Computer Journal*, **9** (4), 373-380.
- LANCE, G. N., & WILLIAMS, W. T., 1967b—A general theory of classificatory sorting strategies. 1. Hierarchical systems. *The Computer Journal*, **9** (4), 373-380.
- LANCE, G. N., MILNE, P. W., & WILLIAMS, W. T., 1968—Mixed-Data Classificatory Programs III. Diagnostic systems. *The Australian Computer Journal*, **1**, 178-181.
- PLAYFORD, P. E., and LOWRY, D. C., 1966—Devonian reef complexes of the Canning Basin, Western Australia. *Geological Survey of Western Australia—Bulletin* **118**.
- SCOFFIN, T. P., 1973—Crustacean faecal pellets, *Favreina*, from the Middle Jurassic of Eigg, Inner Hebrides. *Scottish Journal of Geology*, **9**, 145-146.
- VAN ANDEL, T. H., & VEEVERS, J. J., 1967—Morphology and sediments of the Timor sea. *Bureau of Mineral Resources, Australia—Bulletin* **83**.
- VEEVERS, J. J., 1969—Sedimentology of the Upper Devonian and Carboniferous Platform Sequence of the Bonaparte Gulf Basin. *Bureau of Mineral Resources, Australia—Bulletin* **109**.
- WENTWORTH, C. K., 1922—A scale of grade and class terms for clastic sediments. *Journal of Geology*, **30**, 377-392.
- WILLIAMS, F. B., & MCKELLAR, M. G., 1958—The uppermost Devonian and lowermost Carboniferous sediments of the Canning Basin, Kimberley district. *West Australian Petroleum Pty. Ltd.*, (Unpublished Company Report.)

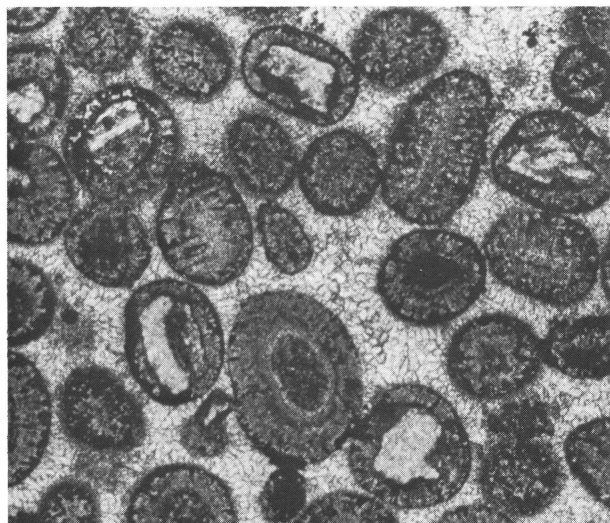
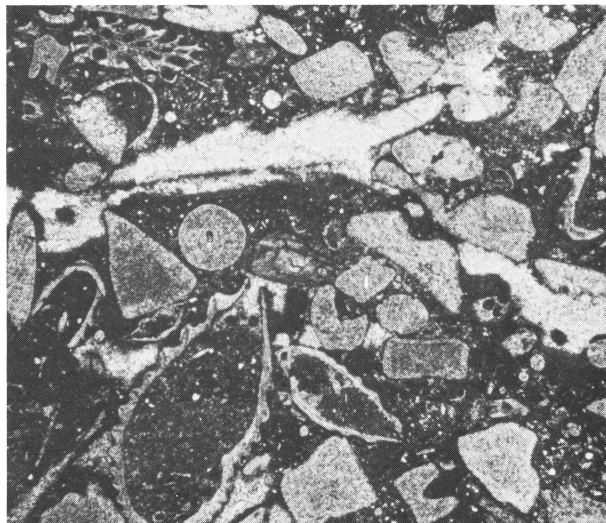
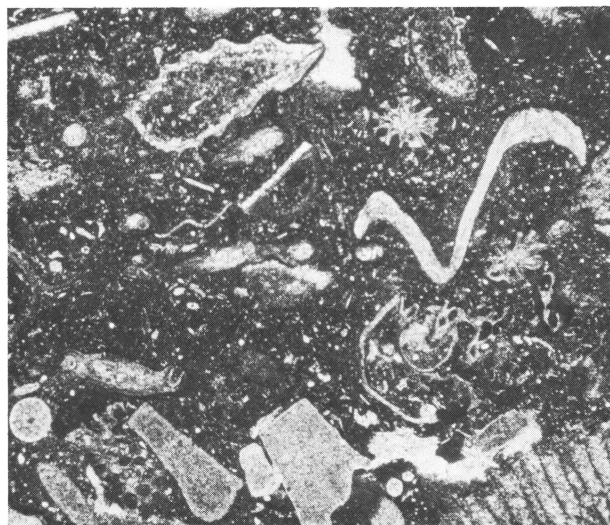


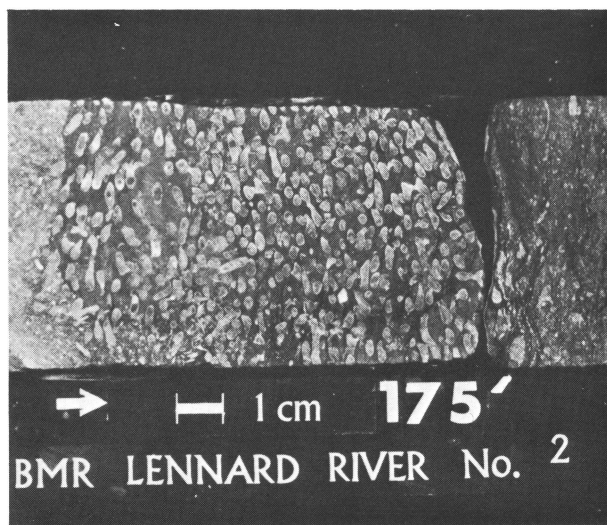
Figure 7. A. Ooid grainstone with drusy cement, Gumhole Formation, Oscar Hill. $\times 37$.



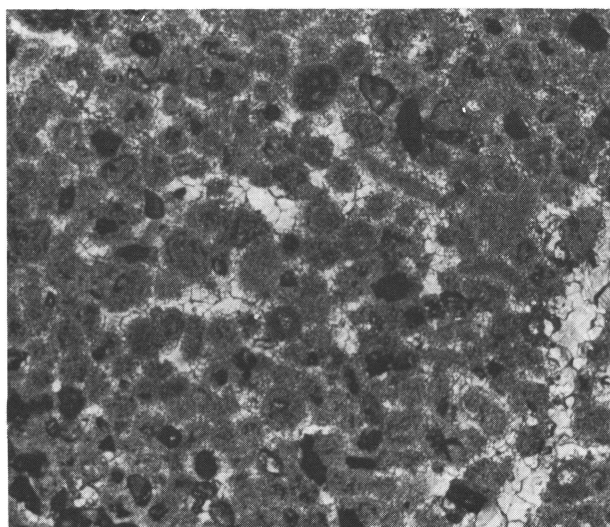
B. Skeletal packstone with brachiopod, crinoid and bryozoan fragments, Gumhole Formation, Gumhole Bore. $\times 24$.



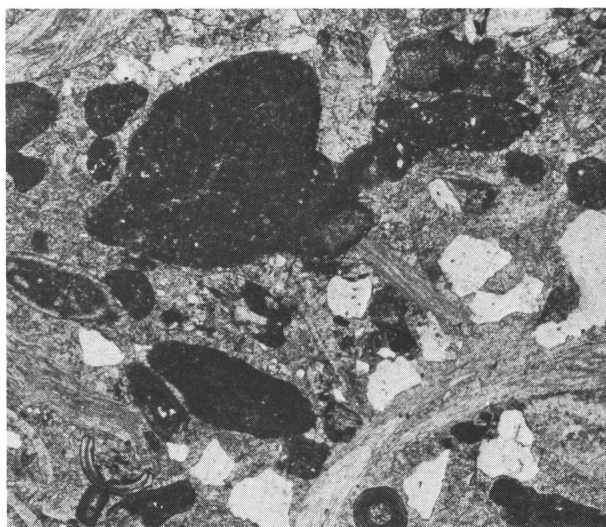
C. Skeletal wackestone with crinoid plates, brachiopods and bryozoans, Gumhole Formation, Gumhole Bore. $\times 26$.



D. Coralline boundstone with interconnected *Syringopora* tubes, Laurel Formation, BMR Lennard River 2 Stratigraphic Hole. $\times 0.6$.



E. Sandy pelletal grainstone. Small angular dark grains are sand. In patches the pellets have coalesced, forming a grumuleuse texture. Laurel Formation, type section. $\times 34$.



F. Rounded mud lumps incorporating terrigenous silt particles. Gumhole Formation, Horseshoe Range. $\times 30$.

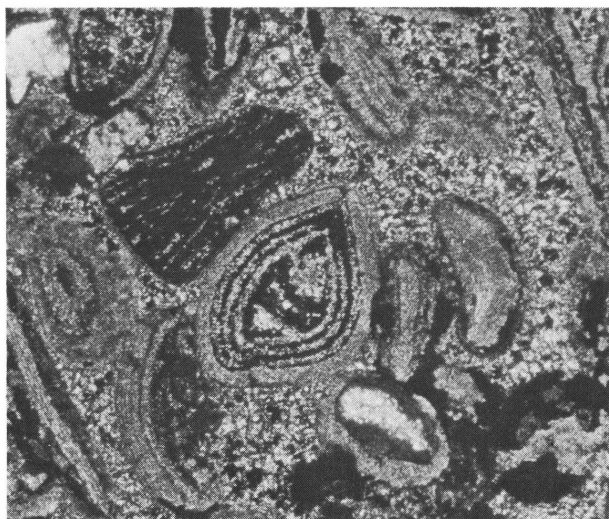
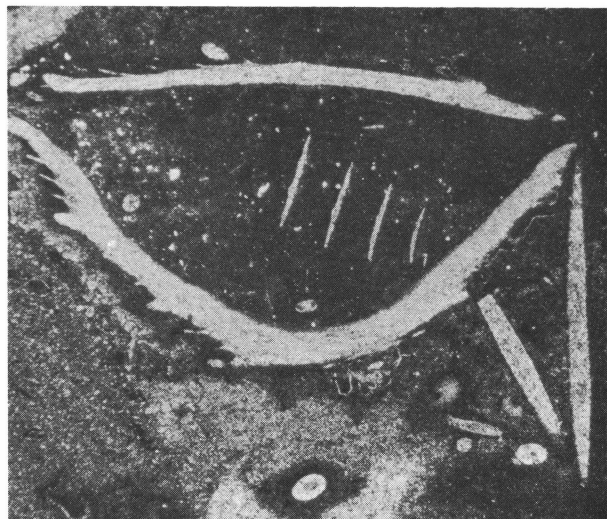
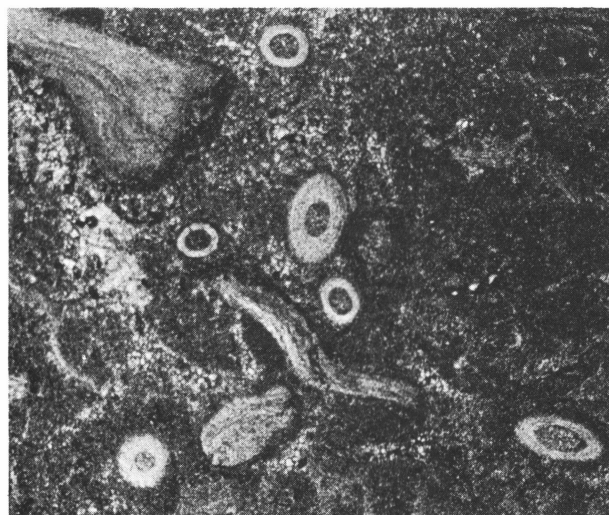


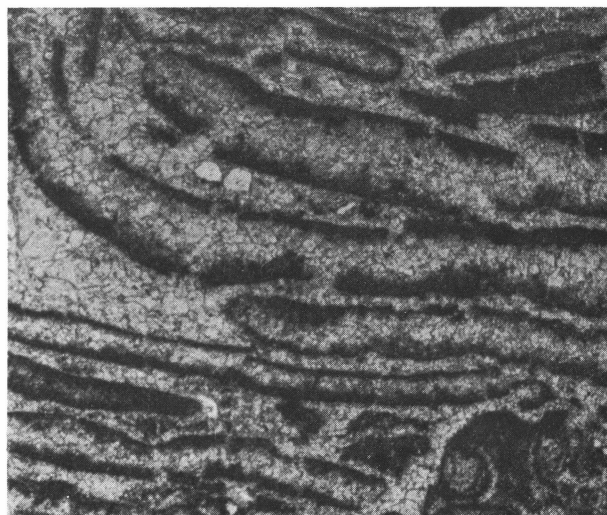
Figure 8. A. Rounded lithified lump intraclast (dark striated grain), and complete ostracods which are infilled with several phases of calcite and pyrite cement. Gumhole Formation, type section. $\times 44$.



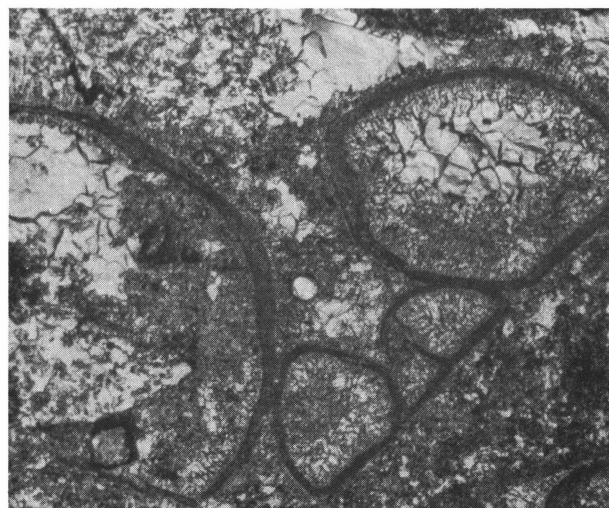
B. Cross section of a complete brachiopod with the enclosed spiralia intact. Gumhole Formation, type section. $\times 31$.



C. Section through brachiopod spines, externally coated with micrite. Gumhole Formation, type section. $\times 31$.



D. Micritic envelopes preserving the form of pelecypod or thallic calcereous algal fragments. Laurel Formation, type section. $\times 33$.



E. Pseudo-planispiral thin-shelled gastropod in partly recrystallised cement and matrix. Laurel Formation, BMR Lennard River 2. $\times 54$.



F. Syringoporiid coral with attached small gastropods. Gumhole Formation, type section. $\times 13$.

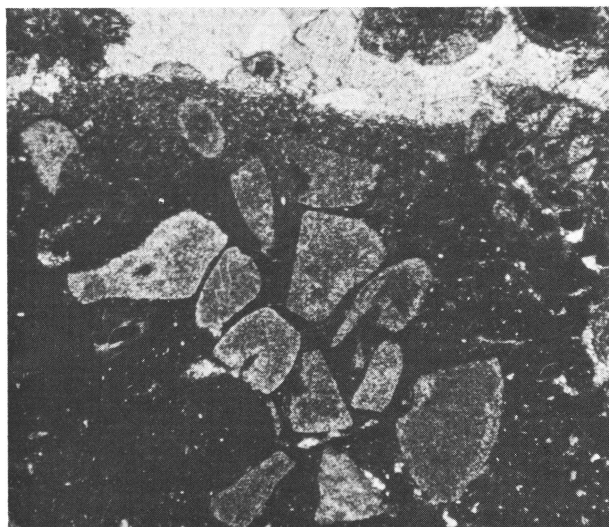
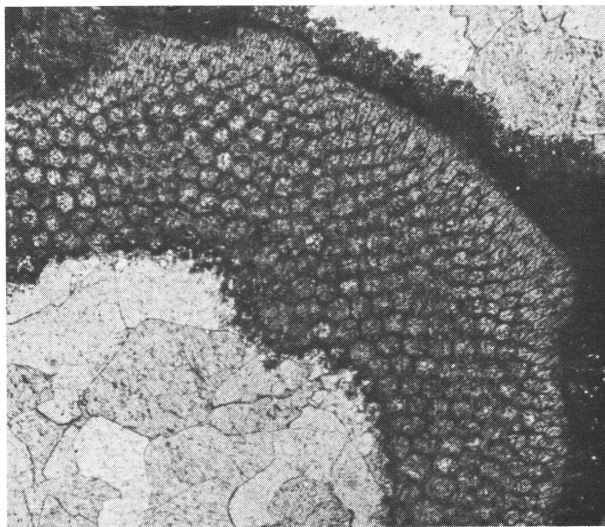
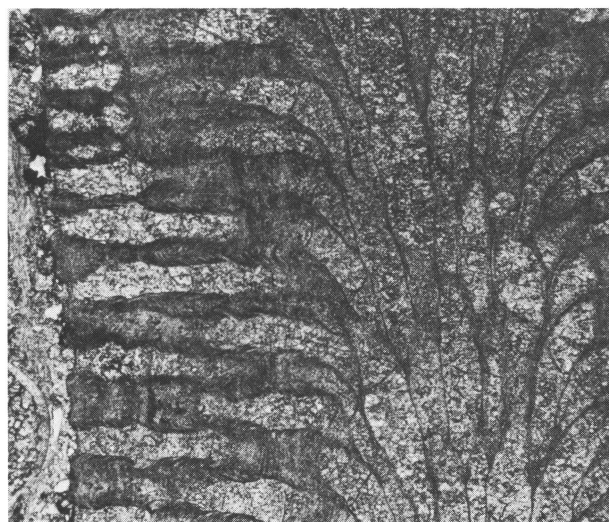


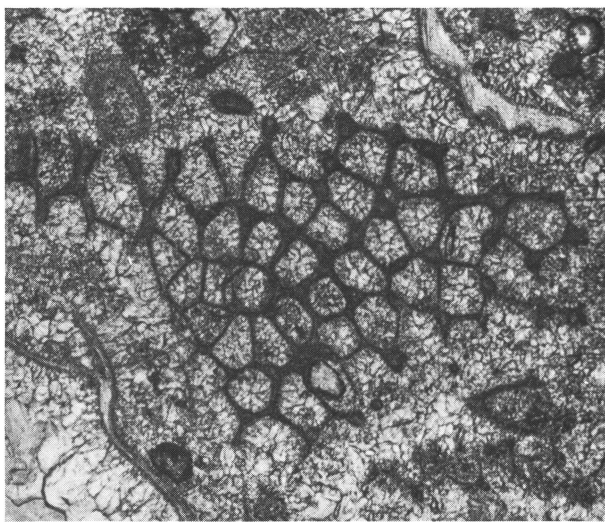
Figure 9. A. Disarticulated crinoid plates with fine limonite infill of pores. Gumhole Formation, type section. $\times 15$.



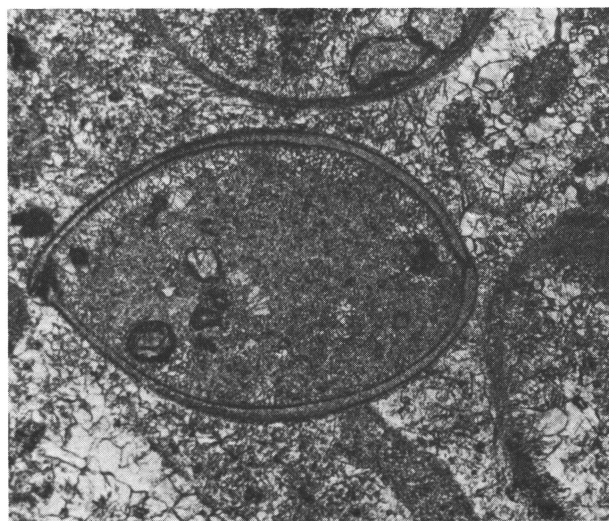
B. Bryozoan encrustation with the initial substrate removed by solution and replaced by a vadose geopetal structure. Gumhole Formation, type section. $\times 15$.



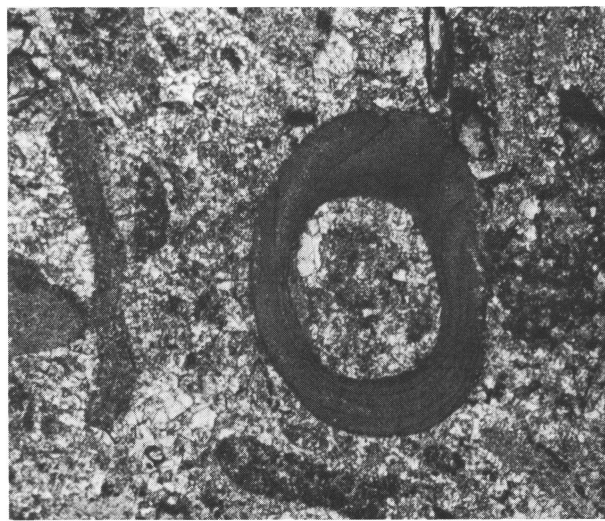
C. Longitudinal section of a trepostome bryozoan. Note the thickening of zooecial walls near the apertures. Gumhole Formation, Horseshoe Range. $\times 31$.



D. Fragment of a colonial bryozoan, with drussy cement infilling zooecial pores. Laurel Formation, type section. $\times 34$.



E. Articulated ostrocod valves enclosing carbonate mud and quartz sand. Laurel Formation, BMR Lennard River 2. $\times 14$.



F. Cryptophyllid valve in cross section. Laurel Formation, BMR Lennard River 2. $\times 54$.

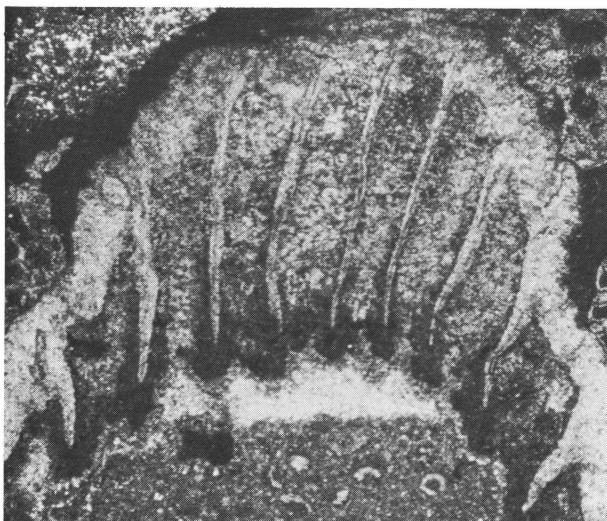
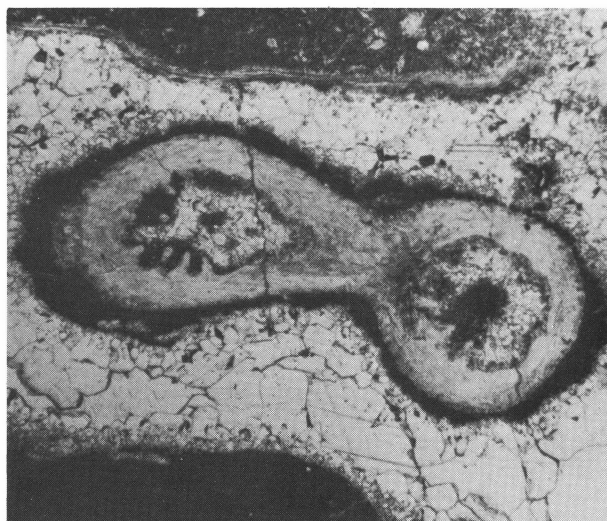
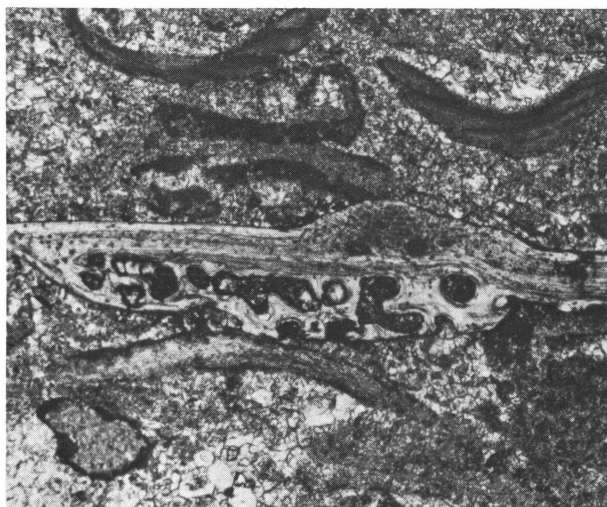


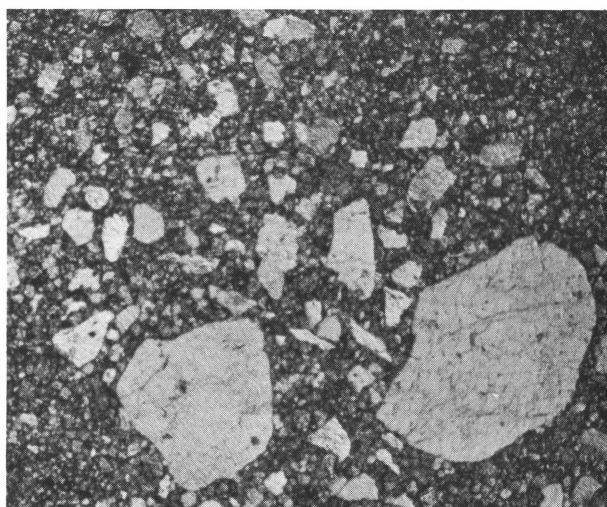
Figure 10. A. Calyx of a solitary rugose coral on oblique cross section. The coral is encrusted internally by algae and externally by bryozoa and algae. Gumhole Formation, type section. $\times 15$.



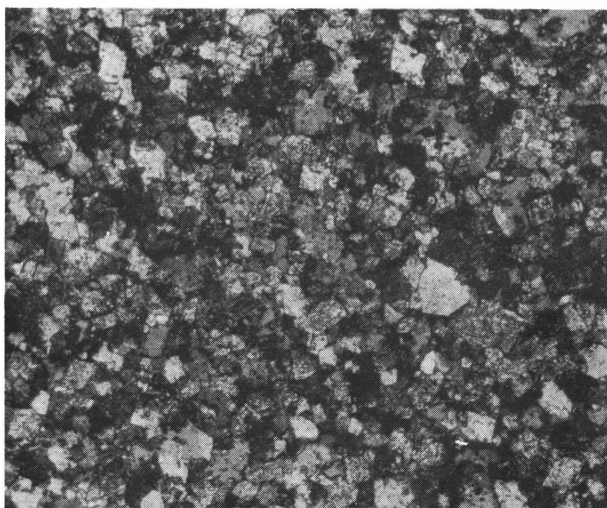
B. Auloporid (?) coral in cross section, with a thin irregular algal micrite coating. Gumhole Formation, Gumhole Bore. $\times 20$.



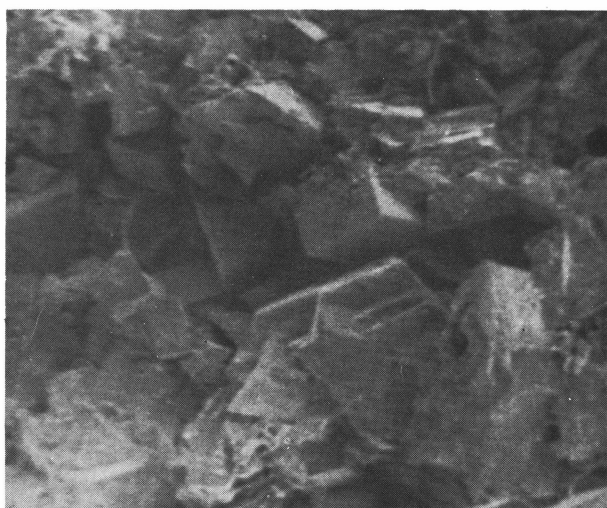
C. Cryptophyllic valves and a fish fragment. Note the diagnostic large vascular spaces in the latter. Laurel Formation, BMR Lennard River 2. $\times 42$.



D. Mixed coarse and fine sand grains in a matrix of sucrosic dolomite. Yellow Drum Sandstone. BMR Noonkanbah 4. $\times 32$.



E. Sucrosic dolomite, note subhedral dolomite and interstitial anhedral calcite. Yellow Drum Sandstone, type section. $\times 55$.



F. Dolomite rhombs lining a micropore in a calcareous dolomite. Yellow Drum Sandstone, BMR Noonkanbah 4. $\times 3300$, SEM.

The Veevers Crater: a possible meteoritic feature

A. N. Yeates, R. W. A. Crowe and R. R. Towner*

A new crater was discovered in July, 1975 during reconnaissance geological mapping by a joint Bureau of Mineral Resources and Geological Survey of Western Australia field party in the southern part of the Canning Basin, Western Australia.

The crater is located at 22°58'06", 125°22'07"E in the south of the Ural 1:250 000 Sheet area, Western Australia, between the Great Sandy and Gibson Deserts (Fig. 1). It (Fig. 2) has a diameter of 80 m and the deepest point of its depression is 7 m below the 20 m wide rim. The crater is symmetrical and is floored mainly by aeolian sand. The rim, which rises 1.5 m above the surrounding sand plain, slopes outward at 10-15°, the dip of exposed sheets of pisolitic laterite near its crest. The sand is probably no thicker than 5 m. Fresh bedrock is not exposed nearby but regional evidence suggests the laterite is probably developed on horizontally bedded Cretaceous rocks. The laterite is no older than Late Cretaceous. The well preserved physiographic expression suggests the age of the crater is relatively recent.

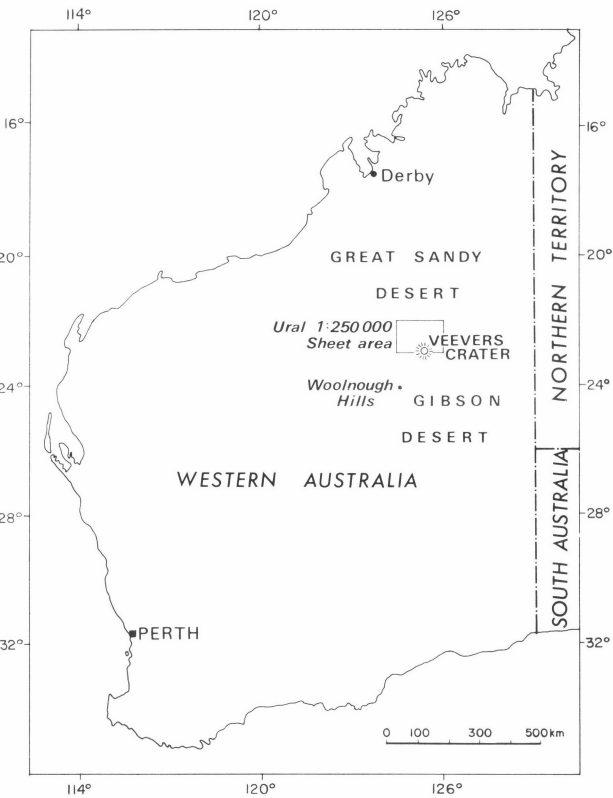


Figure 1: Locality map

The origin of the crater remains speculative. The possible alternatives are: a diapiric structure, a structure produced from a man-made explosion, a cryptovolcanic structure or a meteorite crater.

Although an evaporite sequence known from WAPET Kidson No 1 petroleum exploration well 53 km to the north-west revealed about 700 m of halite within the Upper

Ordovician to Lower Devonian Carribuddy Formation (West Australian Petroleum Pty Ltd, 1966) and which is probably present 3000 m below the surface, there is no supporting physiographic, geologic or geophysical evidence for the presence of diapirs at or near the crater. At Woolnough Hills, two hundred kilometres to the southwest, diapirs of uncertain age were observed by the authors. They reach the surface through similar but thinner rock successions (Van de Graaff, 1974; Kennewell, in press); they are larger, less regular and have central rises quite unlike the feature described here. These diapirs also coincide with a gentle regional topographic high.

There is no evidence that the crater was formed by an exploding rocket from the Woomera Rocket Range in South Australia: no fragments were found, while the age of the trees in the crater appears to pre-date that of these rockets.

No volcanic rocks, igneous intrusions, or carbonatites are known in the southern part of the Canning Basin, and as a result a cryptovolcanic or subsurface explosive origin is also discounted. There is a zone of recent earthquake epicentres 150 km northeast of the crater (Denham et al., 1974) but craters are not generally associated with epicentres without actual volcanism. An aerial reconnaissance over this area in 1973 did not reveal any surface traces of structures that might have been produced by these earthquakes.



Figure 2. Veevers Crater viewed westwards showing slightly raised rim and central depression with a few trees. The surrounding sand plain is colonised by clumps of spinifex grass and scattered low shrubs.

An area of about 200 m around the crater was examined but yielded no meteoritic material. Three samples of the pisolitic laterite rim did not yield anomalous values of nickel nor did three thin sections reveal evidence of shock metamorphism. However, the crater is similar in size and depth to some of the Henbury Meteorite Craters described by Milton (1968) some of which have associated meteoritic

* R. W. A. Crowe publishes with the permission of the Director, Geological Survey of Western Australia.

fragments, and which are unquestionably of meteoritic origin.

No unequivocal evidence for any origin is thus available, but it is considered most likely that the crater results from meteorite impact. A more thorough search may lead to the finding of meteoritic material at the Veevers Crater.

The crater is named after Associated Professor J. J. Veevers, now of Macquarie University, Ryde, N.S.W., in recognition of his contribution to reconnaissance geological mapping of the Canning Basin in the late 1950s while a member of BMR. The name has the approval of the Division of National Mapping, Canberra, and the Lands Department, Western Australia.

References

- DENHAM, D. H., EVERINGHAM, I. B., & GREGSON, P. J., 1974—East Canning Basin Earthquake, March, 1970. *Journal of the Geological Society of Australia*, **21** (3), 353-358.
- KENNEWELL, P. J., in press—Madley, W.A., 1:250 000 Geological Series. *Bureau of Mineral Resources, Australia—Explanatory Notes SG51-3*.
- MILTON, D. J., 1968—Structural geology of the Henbury Meteorite Craters, Northern Territory, Australia. *United States Geological Survey Professional Paper 599-C*.
- VAN DE GRAAFF, W. J. E., 1974—Warri, W. A., 1:250 000 Geological Series. *Bureau of Mineral Resources, Australia—Explanatory Notes SG51-4*.
- WEST AUSTRALIAN PETROLEUM PTY LTD., 1966—Kidson Number 1 Well Completion Report (*Unpublished Company Report*).

The occurrence of *Thylacinus* in Tertiary Rocks from Papua New Guinea

M. Plane

Collecting at the Pliocene Awe fauna type locality (Plane 1967) on the west bank of the Watut River, in the Morobe District of Papua New Guinea during 1962 and 1963 produced a number of fine mandibles and maxillae of *Protemnodon otibandus*. Although these were the highlights of the collecting in this quarry the bulk of the collections were isolated teeth of *P. otibandus*, *Kolopsoides cultridens* and lesser number of *Kolopsis rotundus*. Among the collection a half tooth passed unnoticed during the sorting and subsequent study of the fauna. This tooth has now, thanks to L. Marshall of the Department of Palaeontology, University of California, Berkeley, been brought to my attention. It is the posterior half of a *Thylacinus* lower second premolar. The specimen documents the earliest record of this genus beyond the mainland of Australia.

The problem of dealing with a fragmentary premolar of the rather nondescript morphology such as possessed by larger marsupial carnivores is not as complex as would be imagined. The fragment clearly belongs in the size range of the living genera *Sarcophilus*, *Thylacinus* and the largest species of *Dasyurus*. It was accordingly compared with both neontological and palaeontological specimens of *Sarcophilus harisii*, *Thylacinus cynocephalus* and *Dasyurus maculatus* in the Palaeontology and Mammal Departments of the Australian Museum, Sydney.

A brief examination of the largest individuals of *Dasyurus maculatus* eliminated this genus from consideration on the basis of size and morphology.

The two upper and lower premolars of *Sarcophilus* are robust, conical and low crowned. They lack a distinctive posterior cingular shelf and are in close contact.

The three upper and lower thylacine premolars are well spaced and increase in size posteriorly. The development of a distinctive posterior cingular shelf also increases backwards, being almost unrecognizable on P_1 , a little developed on P_2 and strong on P_3 . The upper premolars have a well marked median crest but lack a well defined basin on the lingual side of the posterior cingular shelf and have a rather simple heel. The diastems between P_1 , P_2 and P_3 are evenly spaced but P_3 is close to M_1 . P_1 , P_2 and P_3 are evenly spaced and P_3 is separated from M_1 . The ridge from the apex of the tooth des-

cends posteriorly in a curve to the labial side of the tooth, then swings back to the centre line at the posterior edge of the tooth. There is a marked lingual basin on the posterior cingular shelf—not deep but distinctive.

P_1 , P_2 and P_3 all have a distinctive profile and the curve of the ridge from the top of the crown backwards to the posterior edge of the tooth enables differentiation between isolated premolars.

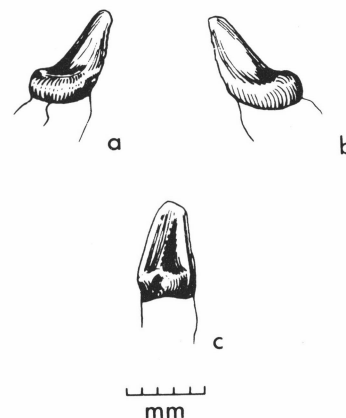


Fig. 1 *Thylacinus* sp. x 2, UCMP 107737

a. Lingual view b. labial view c. posterior view

The fossil fragment UCMP 107737/V6234 (Fig. 1) is the posterior half of a left P_2 complete with posterior root. The root, which is broken near its tip, is slightly tapered, broad and robust. A fine crest descends from the apex of the crown posterolabially and turns lingually to end on the posterior cingular shelf. This crest defines the labial edge of a slight but distinct lingual basin. The crown is 5.5 mm high from the base of the enamel between the roots to the apex. From the same point to the back of the tooth, at the base of the enamel, is 4.3 mm and the crown is 3.9 mm wide.

Both the morphology and the dimensions of the fossil fragment accord closely with a series of twenty five recent thylacine lower premolars which were measured and examined. Measurements were made on left P_2 's from the

base of the enamel, between the roots, to the tip of the crown; from the base of the enamel, between the roots, to the posterior edge of the tooth at the base of the enamel; and across the width of the tooth at the broadest point. They averaged 5.5 mm, 5.4 mm, and 3.5 mm respectively. The fossil is the posterior half of a thylacine left P_2 of a species whose P_2 is very close to that of *Thylacinus cynocephalus*.

The occurrence of the thylacine in Papua New Guinea was first recorded by Van Deusen (1963). He reported a specimen recovered from an archaeological dig at Kiowa, 3 miles south east of Chuave in the Eastern Highlands, at an elevation of 1525 m. This mandible (AMNH 160284) was found in level nine of the dig; it was associated with fire ash which was dated using the C_{14} method at 9920 ± 200 years before 1950 (Bulmer 1964). A later paper (Bulmer 1974), again refers to the thylacine and assigns it an age of between 6 and 9 000 years before present.

Thylacines have again been found in New Guinea in 1975. M. Mountain of the Department of Anthropology, University of Papua New Guinea, working at a site previously called Niobe by J. P. White (1972), but which is now called Nombe and which is located 2 miles south of the Kiowa site, has found several specimens throughout the human occupation levels.

That thylacines should have roamed New Guinea during the late Tertiary is not surprising for although the animal is extinct, or almost so, in Tasmania, it certainly ranged widely over the Australian continent during the Pleistocene and is found, albeit as a somewhat rare item, in widely separated assemblages of fossil mammals. (Ride, 1964; Archer, 1974).

The similarities between animals found in Tertiary fossil mammal localities in central Australia and in later deposits or even among the living fauna of Papua New Guinea has been noted by several workers. Woodburne (1967) records,

Crocodylus porosus, *Kolopsis torus* and *Dorcopsoides fossilus*, from a late Miocene site at Alcoota in central Australia, all of which have their nearest descendants in Pliocene and later faunas of Papua New Guinea. The meagre thylacine material from the Awe fauna, reported here does not allow a statement about possible relationships with *Thylacinus potens* from Alcoota, however it does add to the list of genera shared by the Alcoota and Awe faunas and once again underlines their similarities.

The text figure was drawn by R. W. Brown.

References

- ARCHER, M., 1974—New information about the Quaternary distribution of the thylacine (Marsupialia, Thylacinidae) in Australia. *Journal of the Royal Society of Western Australia*, **57**, (2), 43-50.
- BULMER, S., 1964—Radio Carbon dates from New Guinea. *Journal of the Polynesian Society* **73** (3), 327-8.
- BULMER, S., 1974—Working paper in Anthropology & Archaeology. Linguistics and Maori Studies No. 30, Archaeology. *Unpublished Report, Department of Anthropology, University of Auckland*.
- PLANE, M. D., 1967—Stratigraphy and vertebrate fauna of the Otibanda formation, Morobe district, New Guinea. *Bureau of Mineral Resources, Australia—Bulletin* **86**.
- RIDE, W. D. L., 1964. A Review of Australian Fossil Marsupials. *Journal of the Royal Society of Western Australia*, **47**, 97-131.
- VAN DEUSEN, H. M., 1963—First New Guinea record of *Thylacinus*. *Journal of Mammalogy*, **44** (2), 279-280.
- WHITE, J. P., 1972—01 Tumbuna. *Terra Australis*, **2**, 1-176.
- WOODBURNE, M. O., 1967—The Alcoota Fauna, Central Australia, an integrated Palaeontological and Geological study. *Bureau of Mineral Resources, Australia—Bulletin* **87**.

Reinterpretation of Isotopic Ages from The Halls Creek Mobile Zone, Northwestern Australia

R. W. Page

Data presented elsewhere in this issue (Page, Blake, & Mahon, 1976) provide some of the first ages from The Granites-Tanami Block. Unfortunately it did not prove possible to date or even adequately sample the weathered low grade metasediments and metavolcanics of the Tanami complex, clearly the oldest exposed component of the block. For this reason age data pertaining to the Halls Creek Group, the suggested correlative of the Tanami complex in the Kimberley region to the northwest (Page *et al.*, this volume, Fig. 1), are now reinterpreted in an attempt to arrive at a reasonable estimate of the age of these old rocks. In considering the available information on the geochronology of this part of Australia it is also pertinent to review the age of the Whitewater Volcanics, Castlereagh Hill Porphyry and Bow River Granite, which form a Lower Proterozoic comagmatic suite overlying and intruding the Halls Creek Group in the Halls Creek Mobile Zone.

The Age of the Halls Creek Group

This group is the basement throughout much of the east

Kimberley region and crops out extensively in the Halls Creek Mobile Zone. It consists of tightly folded and complexly faulted low grade metasediments and metavolcanics, and was subdivided by Dow & Gemuts (1969) into four separate formations. The similarities in lithology, regional metamorphism and deformation between the Halls Creek Group and the Tanami complex suggest that these units are stratigraphically equivalent (Blake *et al.*, 1975).

Rb-Sr studies on the Halls Creek Group and later intrusions were undertaken by Bofinger (1967a), and subsequently some of these results have been quoted (Bofinger, 1967b; Compston & Arriens, 1968; Dow & Gemuts, 1969; Gellatly, 1971), leading to the now widely held belief that the Group may be older than 2700 m.y., i.e. Archaean in age. The data are examined here to assess the validity of this age.

Limited Rb-Sr data obtained from three formations in the Halls Creek Group by Bofinger (1967a) yield the following anomalous age pattern:

Ding Dong Downs Volcanics—one intrusive or extrusive acid volcanic sample has a model Rb-Sr age of 2050 m.y.

Biscay Formation—two intrusive or extrusive acid volcanic samples have model ages of 1540 m.y. and 1490 m.y.

Olympio Formation—three shale samples lie on a 1705 m.y. isochron, regarded as the time of faulting; the three point isochron has a high initial $\text{Sr}^{87}/\text{Sr}^{86}$ of 0.725, and the oldest model age of any of the three samples is 2010 m.y.

Although these results are equivocal, they do provide a likely maximum Lower Proterozoic estimate for the age of the Halls Creek Group. There is no evidence from these data to suggest that the rocks could be as old as Archaean.

Samples from the Tickalara Metamorphics and the concordant gneissic Mabel Downs Granodiorite, which are regarded as the metamorphosed equivalents of the Halls Creek Group (Dow & Gemuts, 1969), define an isochron of 1960 ± 30 m.y. with a low initial $\text{Sr}^{87}/\text{Sr}^{86}$ of 0.701 ± 0.001 . Bofinger (1967a) considered that this low value could only be explained by complete loss of radiogenic Sr^{87} from all the rocks at 1960 m.y., the time of metamorphism. This view was partly based on the belief that the Halls Creek Group must be much older than 1960 m.y., i.e. that the group is Archaean. Another view to be considered, however, is that the metamorphics and gneissic granites had little or no crustal prehistory; that is, that the Halls Creek Group may not be much older than the 1960 m.y. metamorphism. Even if the 1960 m.y. isochron is the result of a mixing line giving an age that is too old and an initial ratio too low, it is unlikely the Tickalara metamorphics could have been derived from rocks much older than 2100 to 2200 m.y.

In summary, the available data on the Halls Creek Group and on its metamorphosed equivalents do not show any signs of an Archaean prehistory; if anything they suggest that the group has a maximum age of 2200 m.y. and is possibly as young as 2050 m.y.

The most oft-quoted isotopic evidence for the age of the Halls Creek Group is based not on data from the group itself, but on an Rb-Sr analysis by Bofinger (1967a) of a pegmatite intruding the group. Duplicate model ages on this one pegmatite total rock sample are 2750 and 2720 m.y., but the highly radiogenically enriched muscovite from this rock gives an isochron age of only 1755 m.y. Another pegmatite with the same intrusive relationships has a model age of 2250 m.y. yet the granites with which these pegmatites are at least spatially associated have a maximum model age of about 2100 m.y. These large discordances render the data extremely difficult to interpret, but certainly the single 2700 m.y. pegmatite result cannot be accepted at this stage as providing an adequate minimum age for the Halls Creek Group.

In conclusion it is considered that the available geochronological evidence points to a Lower Proterozoic rather than an Archaean age for the Halls Creek Group. Given the suggested correlation, a similar age, of greater than 1960 m.y. but less than 2200 m.y., is inferred for the Tanami complex, the basement rocks in The Granites-Tanami region.

The Age of the Whitewater Volcanics, Castlereagh Hill Porphyry and Bow River Granite

Acid volcanics and intrusives of possibly similar Lower Proterozoic age to the Mount Winnecke Formation (1808 ± 15 m.y.) and Winnecke Granophyre (1802 ± 15 m.y.) of The Granites-Tanami region (Page *et al.*, this volume) crop out in the Halls Creek Mobile Zone of the Kimberley region, 300 km west of the Mount Winnecke area. The Kimberley

units are the Whitewater Volcanics, Castlereagh Hill Porphyry, and Bow River Granite, all three of which are considered to have been comagmatic (Dow & Gemuts, 1969).

The Whitewater Volcanics consist of porphyritic rhyolitic ignimbrites, minor andesitic lavas, and, near the top, some interbedded volcanic conglomerate, sandstone, chert, and lapilli tuff. They have been isotopically dated by the Rb-Sr total rock method at 1823 ± 17 m.y. by Bofinger (1967a) and 1940 ± 110 m.y. by Bennett & Gellatly (1970). These ages are experimentally indistinguishable from each other at the stated 95 percent confidence levels using the statistical 't' test. The validity of the two isochrons needs to be carefully assessed, however, as some of the samples used came from sites more than 100 km apart. Both isochrons also include samples from associated high-level intrusive rocks. Because of these uncertainties, two additional statistical regressions of the earlier reported data have been made. The first regression involves only the volcanic samples collected from the Halls Creek Mobile Zone and dated by Bofinger; this gives an age of 1802 ± 35 m.y., and an initial $\text{Sr}^{87}/\text{Sr}^{86}$ of 0.7165 ± 0.0050 . The second involves seven volcanic samples from the Whitewater Volcanics cropping out in the King Leopold Mobile Zone further west in the Kimberley region, and yields an age of 1953 ± 109 m.y. and an initial $\text{Sr}^{87}/\text{Sr}^{86}$ of 0.7065 ± 0.0059 . The difference in apparent ages is now further enhanced, but it is unlikely to be geologically meaningful, as both sets of rocks are mapped as part of the same formation.

Bennett & Gellatly (1970) noted that all the west Kimberley samples that make up the older isochron have relatively low $\text{Rb}^{87}/\text{Sr}^{86}$ ratios (less than 10), whereas the east Kimberley samples have ratios of 14 to 104. If both sets of samples are combined, the resulting isochron shows an apparent curvature accompanied by an increase in extrapolated initial $\text{Sr}^{87}/\text{Sr}^{86}$. This phenomenon has been cited previously by Fairbairn *et al.* (1966) and has been found in other Rb-Sr age studies of Precambrian acid volcanic rocks in New Brunswick, Canada (Cormier, 1969), in southeastern Missouri (Bickford & Mose, 1975) and in the Mount Isa province of northwestern Queensland (R. W. Page, unpublished data). The lavas of the Mount Winnecke Formation (Page *et al.*, this volume) do not show this effect, probably because there has been no geological disturbance in this area since the time of emplacement of this igneous suite, 1800 m.y. ago. In the New Brunswick example, however, fossiliferous control demands acceptance of the oldest isochron given by volcanic rocks with the lowest Rb/Sr values. In the other two studies, comparison of the Rb-Sr data with U-Pb zircon data shows that the oldest Rb-Sr isochron that can be generated is, in these instances, only a minimum age for the time of crystallization. There is therefore good evidence to show that the Rb-Sr system in acid lavas is easily disturbed under mild metamorphic conditions, probably as a result of bulk loss of strontium. The extent to which individual samples are affected depends not only on the grade and duration of the event, but also most importantly on Sr content, as found by Bickford & Mose (1975). High-Sr, less alkali-rich samples are less affected by such geochemical changes than samples with a high Rb/Sr ratio. Given these analogies of open-system behaviour in acid lavas, it is likely that the steeper of the two Whitewater Volcanics Rb-Sr isochrons (1953 ± 109 m.y.) from samples with lower Rb/Sr ratios, is the better age determination for this unit. However, this age could still represent only a minimum value for the age of crystallization.

A reappraisal of field data (K. A. Plumb, pers. comm. 1975) shows that, without exception, the Sophie Downs and Bow River Granites of the east Kimberley region, and

similar granites in the west Kimberleys, intrude the Whitewater Volcanics or their high-level equivalents, and that the report of a dyke of Castlereagh Hill Porphyry intruding Bow River Granite (Dow & Gemuts, 1967, 1969; Plumb, 1968) was incorrect. The presently preferred age for the Whitewater Volcanics, 1953 ± 109 m.y., would therefore now be in accord with Bofinger's (1967a) age of 1854 ± 14 m.y. for the pooled Rb-Sr data from the Sophie Downs and Bow River Granites, and with Bennett & Gellatly's (1970) age of 1880 ± 50 m.y. for the similar west Kimberley granites.

From the available evidence it is concluded that, in spite of the present uncertainties regarding the isotopic data, the Whitewater Volcanics are older than the acid volcanics in the Mount Winnecke Formation. Clearly, further work, possibly employing U-Pb geochronology on zircons, needs to be done to adequately test this conclusion.

The author is grateful to D. H. Blake, L. P. Black, K. A. Plumb and V. M. Bofinger for their comments on an earlier version of the manuscript.

References

- BENNETT, R. & GELLATLY, D. C., 1970—Rb-Sr age determinations of some rocks from the west Kimberley region. *Bureau of Mineral Resources, Australia—Record* 1970/20 (unpublished).
- BLAKE, D. H., HODGSON, I. M., & SMITH, P. A. 1975—Geology of the Birrindudu and Tanami 1:250 000 Sheet areas, Northern Territory. *Bureau of Mineral Resources, Australia—Report* 174.
- BICKFORD, M. E., & MOSE, D. G., 1975—Geochronology of Precambrian rocks in the St. Francois Mountains, southeastern Missouri. *Geology*, **3**, 537-540.
- BOFINGER, V. M., 1967a—Geochronology in the east Kimberley area of Western Australia. *Ph.D. Thesis, Australian National University* (unpublished).
- BOFINGER, V. M., 1967b—Geochronology in the east Kimberley area of Western Australia. *ANZAAS, 39th Congress*, (Abstract).
- CORMIER, R. F., 1969—Radiometric dating of the Coldbrook group of southern New Brunswick, Canada. *Canadian Journal of Earth Science*, **6**, 393-398.
- DOW, D. B., & GEMUTS, I., 1967—Dixon Range, W. A.—1:250 000 Geological Series. *Bureau of Mineral Resources, Australia—Explanatory Notes* SE/52-6.
- DOW, D. B., & GEMUTS, I., 1969—Geology of the Kimberley region, Western Australia: the east Kimberley. *Bureau of Mineral Resources, Australia—Bulletin* 106.
- FAIRBAIRN, H. W., BOTTINO, M. L., PINSON, W. H., & HURLEY, P. M., 1966—Whole-rock age and initial $\text{Sr}^{87}/\text{Sr}^{86}$ of volcanics underlying fossiliferous Lower Cambrian in the Atlantic provinces of Canada. *Canadian Journal of Earth Science*, **3**, 509-521.
- GELLATLY, D. C., 1971—Possible Archaean rocks of the Kimberley region, Western Australia. *Geological Society of Australia—Special Publications*, **3**, 93-101.
- PAGE, R. W., BLAKE, D. H., & MAHON, M. W., 1976—Geochronology and related aspects of acid volcanics, associated granites and other Proterozoic rocks from The Granites-Tanami region, northwestern Australia. *BMR Journal of Australian Geology and Geophysics*, **1**.
- PLUMB, K. A., 1968—Lissadell, W.A.—1:250 000 Geological Series. *Bureau of Mineral Resources, Australia—Explanatory Notes* SE/52-2.

BMR Publications

Publications issued in 1975 include the following:

BULLETINS

- 121 Templetonian and Ordian Xystridurid trilobites of Australia by A. A. Opik (\$6.50).
- 146 Chemical analyses of Australian rocks: Part III, by G. A. Joplin (\$6.50).
- 148 (Papua New Guinea Bulletin 8) Explanatory notes on the 1:2 500 000 mineral deposits map of Papua New Guinea, by D. J. and R. L. Grainer (\$8.75 with map).
- 150 Palaeontological Papers 1972-1973 (Papers by D. J. Belford, D. Burger, S. K. Skwarko and B. Kummel) (\$8.25).
- 152 Standard curves for interpretation of magnetic anomalies due to thin finite dykes, by J. E. Haigh and M. J. Smith (\$3.50).
- 153 Late Cambrian and Early Ordovician trilobites from the Burke River Structural belt, by J. H. Shergold (\$15.75).
- 154 Permo-Triassic stratigraphy and sedimentation in the Bowen Basin, Queensland, by A. R. Jenson (\$9.50).
- 157 Marine geology of the Arafura Sea, by D. Jongsma (\$7.25).

REPORTS

- 152 Geology of the Landsdown 1:250 000 Sheet SE52-5, W.A., by D. C. Gellatly, G. M. Derrick and K. A. Plumb (\$7.00).
- 153 The older Precambrian geology of the Lennard River Sheet area, W.A., by D. C. Gellatly, J. Sofoulis, G. M. Derrick and C. M. Morgan (\$19.00).
- 167 The geology of the southern Victoria region, N.T., by I. P. Sweet, J. R. Mendum, R. J. Bultitude and C. M. Morgan (\$19.00).
- 171 Environmental significance of folds in the Rangal Coal Measures at Blackwater, Queensland, by W. A. Burgis (\$2.50).
- 174 Geology of the Birrindudu and Tanami 1:250 000 Sheet Areas, Northern Territory, by D. H. Blake, I. M. Hodgson, and P. A. Smith (\$8.25).
- 175 Galilee Basin seismic and gravity survey, Queensland by P. L. Harrison, W. Anfiloff and F. J. Moss (\$8.25).
- 176 (Papua New Guinea Report 7) Seismological report on the Mandang earthquake of 31 October 1971 and aftershocks, by I. B. Everingham (\$2.00).
- 177 Burdekin delta underground water investigation, north Queensland 1962-1963, by W. A. Weibanga, E. J. Polak, J. T. G. Andrew, M. Wainwright and L. Kevi (\$6.00).
- 178 (Papua New Guinea Report 8) Some earthquake focal mechanisms in the New Guinea/Solomon Islands region, 1963-1970, by I. D. Ripper (\$3.75).
- 179 A structural analysis of the Gulf of Papua and northwest Coral Sea region, by J. C. Mutter (\$3.50).
- 189 Geological Branch Summary of activities 1974 (\$4.50).

AUSTRALIAN MINERAL INDUSTRY

ANNUAL REVIEW 1972 (\$6.00); and preprint chapters for 1973 (\$0.40 each) and 1974 (\$1.00 each).

QUARTERLY REVIEWS, Vol. 26, No. 4, Vol. 27, Nos 1, 2 & 3 (\$1.50 per issue). Mineral Resources Report 6, Uranium (\$0.50).

PETROLEUM TITLES MAP AND KEY for 1 July 1974 (\$1.00).

1:250 000 GEOLOGICAL MAPS AND EXPLANATORY NOTES

Dalby, Goondiwindi, Port Clinton, Rockhampton, Warwick (Queensland); Alcoota (Northern Territory); Herbert, Mason, Cobb, Dongara-Hill River, Malcolm-Cape Arid, Murgoo, Warri, Seemore (Western Australia); Karimui, Tufi-Cape Nelson, Wau, Blucker Range, Huon-Sag Sag, Ramu (Papua New Guinea) (\$3.00 each).

GRAVITY MAPS AND AEROMAGNETIC MAPS

Those issued in 1975 are not listed here, but maps are now available of individual sheet areas to cover most of the continent.

PICTORIAL INDEX OF ACTIVITIES

To December 1974 (\$7.50).

Contents

	Page
L. C. Noakes	
Preface	iii
R. W. Page, D. H. Blake, and M. W. Mahon	
Geochronology and related aspects of acid volcanics, associated granites and other Proterozoic rocks in The Granites-Tanami region, northwestern Australia.	1-13
A. McEwin, R. Underwood, and D. Denham	
Earthquake risk in Australia.	15-21
B. R. Spies	
The Transient Electromagnetic Method in Australia	23-32
N. F. Exon and B. R. Senior	
The Cretaceous of the Eromanga and Surat Basins.	33-50
K. A. Plumb, J. H. Shergold, and M. Z. Stefanski	
Significance of Middle Cambrian trilobites from Elcho Island, Northern Territory . . .	51-55
W. Anfiloff	
Automated density profiling over elongate topographic features.	57-61
B. M. Radke	
Hierarchical classification and vector ordination in the distinction of limestones in the Fairfield Group, Canning Basin, Western Australia.	63-76
Notes	
A. N. Yeates, R. W. A. Crowe, and R. R. Towner	
The Veevers Crater: a possible meteoritic feature.	77-78
M. Plane	
The occurrence of <i>Thylacinus</i> in Tertiary rocks from Papua New Guinea.	78-79
Discussion	
R. W. Page	
Reinterpretation of isotopic ages from the Halls Creek Mobile Zone, northwestern Australia.	79-81